UNIVERSITY OF CALIFORNIA, SAN DIEGO

Macroevolutionary Patterns in Planktonic Foraminifera and the Recovery of Pelagic Ecosystems from the Cretaceous-Paleogene Mass Extinction

A dissertation submitted in partial satisfaction of the
requirements for the degree Doctor of Philosophy

in

Oceanography

by

Pincelli Marie Hull

Committee in charge:

Professor Richard D. Norris, Co-Chair
Professor Mark D. Ohman, Co-Chair
Professor Peter J. S. Franks
Professor Jeremy B. C. Jackson
Professor George Sugihara
Professor Lawrence Saul

2010

UMI Number: 3398253

All rights reserved

INFORMATION TO ALL USERS
The quality of this reproduction is dependent upon the quality of the copy submitted.

In the unlikely event that the author did not send a complete manuscript
and there are missing pages, these will be noted. Also, if material had to be removed,
a note will indicate the deletion.

UMI 3398253
Copyright 2010 by ProQuest LLC.
All rights reserved. This edition of the work is protected against
unauthorized copying under Title 17, United States Code.

ProQuest LLC
789 East Eisenhower Parkway
P.O. Box 1346
Ann Arbor, MI 48106-1346

Copyright

Pincelli Marie Hull, 2010

All rights reserved.

The Dissertation of Pincelli Marie Hull is approved, and it is acceptable in quality and form for publication on microfilm and electronically:

_____

_____

_____

_____

_____

_____

Co-Chair

_____

Co-Chair

University of California, San Diego

2010

TABLE OF CONTENTS

LIST OF FIGURES

LIST OF TABLES

ACKNOWLEDGEMENTS

It is hard to even know where to begin with such a momentous task as acknowledging the generous support, guidance and kindness of those who have help me along the path of becoming an oceanographer. Each step in its own time was as important as the last or the next and so too was the delightful presence of those around me.

I must thank my advisors, Dick Norris and Mark Ohman, first and foremost, for being fantastic mentors each in their own way. Dick has an unending enthusiasm and curiosity into the natural world, and a joyful approach to science, teaching and mentoring, not to mention a formidable knowledge of living and ancient ecosystems on land and in the sea. Dick always has time for those he mentors and our scientific discussions and endeavors over the years were both fascinating and formative for me as a scientist, not to mention a lot of fun. Mark grounded me in the oceans of our modern world, while imparting a rigorous scientific ethic and idealism and an exacting standard for scientific writing and presentation. His commitment to his graduate students and graduate student education is unwavering and I am fortunate to have benefited from both.

I was lucky to have a thesis committee that was both involved and supportive of my scientific endeavors. Peter Franks has been both a mentor in science and in life, not to mention a wonderful professor in the classroom as well. I thank Jeremy Jackson in part for my education as a paleontologist and for his mentorship beginning in the Center for Marine Biodiversity and Conservation's summer course and spanning

through my dissertation research. From George Sugihara I first learned the fundamentals and theoretical underpinnings of ecology, and his insight and understanding into the dynamical behavior of natural systems was always fascinating and greatly appreciated. Lawrence Saul was a wonderful mentor in unsupervised machine learning; he enthusiastically collaborated on problems from the natural world, providing both ideas and technical guidance.

Beyond my advisors and committee, I thank the Scripps Community for their support; it is hard to imagine a better environment in which to be a graduate student. I have rather wide-ranging interests and my initial inquiries in various fields always met with useful guidance from graduate students and professors alike, who were generous with both their time and ideas. As a testament to this fact, I cannot even begin to list those who have helped me in this manner as these acknowledgements would begin to look like the SIO phone directory and I would feel quite awful when I later on remembered those whom I had previously forgotten.

As graduate students at the Scripps Institution of Oceanography, we are lucky enough to be supported by our own Graduate Department whose technical guidance as well financial support smooth the bumps of graduate life in enumerable ways. For this, I cannot thank Denise Darling, Josh Reeves, Dawn Huffman, Alice Zheng, Becky Burrola, and everyone else enough for their time and patience with me over the years. I also would like to thank those in the GRD, IOD, and MBRD business office for their help in accomplishing all the tasks I seem most inept at doing. Finally, I would like to thank Penny Dockry of the Center for Marine Biodiversity and Conservation (CMBC)

for taking care of me over the years and always finding an innovative solution for my innovative problems. For those of us within the CMBC, it is impossible to imagine our graduate life without Penny.

My friends have been my teachers and my joy. To my fellow CMBC cohort, Octavio Aburto, Kate Hanson, Melissa Roth, Katie Cramer, and Kristen Marhaver, thank you for all the dinners, parties, debates, and for all the fun chasing fish around in Mexico. Octavio, thank you for teaching me not only how to be an underwater scientist, but how to be a scientist and expedition leader as well. My cohort of Biological Oceanography students, Pete Davison, Kate Hanson, Jenny Prairie, Mike Stukel, and Moira Decima, were my stalwarts as we faced the first year exam and now as we head into TGs filled with the next generation of graduate students. Many friends helped me scientifically over the years, but when it came to computing and statistics I pestered Christian Anderson more than others. My labmates have had much to teach me and special thanks go to Sandy Kirtland and Phil Sexton for my education in paleoceanography and paleoclimatolgy; to my fellow paleontologists, Jill Leonard-Pingel and Katie Cramer; and to Jess Carilli, Flavia Nunes, Zac Hsieh, Dave Field, and Erica Goetze for setting high standards to live up to within my respective labs and for being wonderful examples of how to go about being a young scientist. My apologies to all the friends left off this SIO list; I'm not forgetting, I'm just running out of time here.

For life at and beyond Scripps, special thanks to Emily Kelly and Monique Measures. Emily is the one friend who has been by my side from the beginning of

college to the very end of my PhD; thank you for so many happy years and for helping out endlessly over the past two months of my PhD. I couldn't have wrapped it without you. Thank you Monique for always insisting that I, along with all my nerdy friends, be sure to enjoy the rest of life with 'real people'.

Before, during and after graduate school there has always been my family and they more than anyone else have been my support, my friends, and my life. My mom taught me the most important skills for graduate school and life: be happy, be curious, work hard, and look it up. My family has loved and encouraged me in all my endeavors and I feel beyond fortunate to be a part of such an amazing group of individuals. Thank you, Walter, for always insisting that I take time to enjoy life while it is happening and for being such a wonderful partner through it all.

MATERIAL SUBMITTED FOR PUBLICATION IN THE DISSERTATION

The data chapters of this dissertation are in preparation or have been submitted for publication. Chapter II was submitted for publication as "The relative importance of environment and dispersal to global pelagic community similarity". I was the sole author and primary investigator this paper. Chapter III was published as "Evidence for abrupt speciation in a classic case of gradual evolution" in the *Proceedings of the National Academy of Sciences USA* 106 (50): 21224-21229. Copyright 2009 National Academy of Sciences, U.S.A. I co-authored this paper with Richard Norris, and was the primary investigator and author. Chapter V is in preparation for publication as "Using mixing models and iridium anomalies to quantify sediment mixing at the Cretaceous-Paleogene boundary". This study is in collaboration with Peter Franks and Richard Norris, and I am the primary investigator and author of this work. Chapter VI is in preparation for publication as: "Geographically and temporally heterogeneous changes in ocean export productivity at the Cretaceous-Paleogene boundary". This chapter is co-authored with Richard Norris and I am primary investigator and author. Chapter VII is in preparation for publication as: "Rapid recovery of pelagic ecosystem function following the end-Cretaceous extinction". I am the primary investigator and author of this paper in collaboration with Richard Norris, Timothy Bralower, and Atreyee Bhattacharya.

VITAE

2003	B.S. Duke University
2004-2005	Regents Fellowship, University of California, San Diego
2004-2008	Chancellor's Fellowship, University of California, San Diego
2005-2008	NSF Pre-doctoral Fellowship
2008	Teaching Assistant, Paleoecology, University of California, San Diego
2008-2010	Research Assistant, University of California, San Diego
2010	Ph.D., Scripps Institution of Oceanography, University of California, San Diego

PUBLICATIONS

Hull P.M. and Norris R.D. 2009. Evidence for abrupt speciation in a classic case of gradual evolution. *Proceedings of the National Academy of Sciences USA* 106 (50): 21224-21229

Lewis J.M., Hull P.M., Weinberger K., Saul L. 2008. Mapping Uncharted Waters: Exploratory Analysis, Visualization and Clustering of Oceanographic Data. *Proceedings of the 7th International Conference on Machine Learning and Applications (ICMLA-08)*, pages 388-395. San Diego, California. doi: 10.1109/ICMLA.2008.125

Aburto-Oropeza O. and Hull P.M. 2008. A probable spawning aggregation of leather bass, *Dermatolepis dermatolepis*, in the Revillagigedo Archipelago, Mexico. *Journal of Fish Biology* 73 (1): 288-295

ABSTRACT OF THE DISSERTATION

Macroevolutionary Patterns in Planktonic Foraminifera and the Recovery of Pelagic Ecosystems from the Cretaceous-Paleogene Mass Extinction

by

Pincelli Marie Hull

Doctor of Philosophy in Oceanography

University of California, San Diego, 2010

Professor Richard D. Norris, Co-Chair
Professor Mark D. Ohman, Co-Chair

In this dissertation, I investigate macroevolutionary patterns and dynamics in planktonic foraminifera and accompanying changes in their pelagic environment. My research focuses on processes that structure diversity in the open sea, including the response of oceanic ecosystems to the largest biotic disturbance of the Cenozoic, the Cretaceous-Paleogene mass extinction.

I begin by investigating the determinants of community similarity in modern planktonic foraminiferal communities. Here, I find that community similarity is primarily determined by the environmental similarity between communities, and not geographic distance. On a global scale, planktonic foraminifera provide an exception to the rule that geographic proximity is the strongest predictor of community similarity.

Patterns of morphological evolution in planktonic foraminifera also suggest that different evolutionary processes may predominate in the open ocean. I investigate a classic case of gradual evolution in the *Globorotalia plesiotumida-G. tumida* lineage of planktonic foraminifera using more sensitive numerical techniques and find evidence for a cryptic speciation event and a more rapid evolution of *G. tumida* than previously hypothesized.

New analytical approaches were also developed in order to ask questions at a higher stratigraphic resolution at the Cretaceous-Paleogene (KPg) boundary than is currently possible. To this end, Lagrangian advection-diffusion models were modified to fit iridium anomalies deposited by the KPg impactor.

Insights into the recovery of pelagic ecosystems from the KPg mass extinction were obtained from high-resolution geochemical, grain size, and taxonomic records of the early post-extinction interval. Barium proxy records were used to investigate boundary-related changes in export productivity, and supported inferences from benthic foraminifera in describing geographically and temporally heterogeneous changes in export productivity following the KPg impact. When productivity was

considered along with planktonic foraminifera community composition and relative flux, this evidence suggested that an alternative pelagic ecosystem may have thrived in some locales in a post-extinction world.

CHAPTER I

Introduction to the dissertation

INTRODUCTION

The deep time record of pelagic ecosystems provides a means for understanding ecological and evolutionary processes that occur over time scales longer than those spanned by modern observations. The history of the open ocean is recorded in the fossil-rich sediments that carpet much of the ocean floor (Phleger 1954; Vincent and Berger 1981). Deep-sea cores of ocean sediment spanning 10's to 100's of meters provide a relatively highly resolved record of the ecological and evolutionary history of fossil algae like coccolithophorids and diatoms, of consumers like planktonic foramininifera and radiolarians, of environmental variables like temperature, ocean circulation, and productivity, and of the feedbacks between biogeochemical systems. Over the last 50 years, deep-sea cores have been collected throughout the world ocean, providing a spatially and temporally resolved record of the past 150 million years of ocean history (http://www-odp.tamu.edu/). These records provide evidence of past global disturbances like global deep sea anoxic events in the Cretaceous (Jenkyns 1980), an extraterrestrial impact caused extinction at the Cretaceous-Paleogene boundary (Alvarez et al. 1980; Hildebrand et al. 1991), rapid climate change and ocean acidification at the Paleocene-Eocene boundary (Kennett and Stott 1991; Thomas 1990), complete desiccation of the Mediterranean in the Miocene followed by catastrophic flooding (Garcia-Castellanos et al. 2009; Hsu et al. 1973), and the transformation of the world from a greenhouse climate with ice-free poles to the ice-capped, glacial-interglacial world of today (Zachos et al. 2001). Similarly, these records document the ecological and evolutionary changes in oceanic species and ecosystems

following these global events (e.g., D'Hondt 2005; Jiang et al. in press), and provide a perspective that cannot be obtained by simply scaling up short-term ecological or evolutionary studies in the modern ocean. Thus, this deep-time perspective has the potential to inform our expectations for how species and ecosystems will respond to modern perturbations like global warming, ocean acidification, or the extinction of species, beyond what we can infer from studies of today's ocean.

Large spatial and temporal scales provide key vantage points for the two primary questions addressed in my thesis: 1) What were the dominant processes that structured the diversity of the modern ocean? and 2) How have oceanic ecosystems responded to global perturbations in the past? In both ecology and evolution, there is a well-known problem of scale. The spatial and temporal scales of ecological studies only capture a small range of the scales important for understanding evolutionary and ecological processes (e.g., Levin 1992), and predicting the patterns and dynamics of future change (e.g., Scheffer et al. 2009; Scheffer et al. 2001). A similar issue exists in trying to scale microevolutionary inferences up to macroevolutionary scales. Although we have a growing, highly detailed knowledge of molecular evolution (e.g., Coyne and Orr 2004), the bacterium *Escherichia coli* provides one of the only systems where the processes of speciation and evolutionary innovation have been observed first hand (Lenski and Travisano 1994). In contrast, speciation and extinction are recorded in abundance in the fossil record (Jackson and Cheetham 1999).

Along with the advantages of studying ecological and evolutionary patterns on large temporal and spatial scales, are corresponding losses in acuity that impede

mechanistic interpretations and hypothesis testing. For instance, very few taxa are actually well fossilized, and those that are have a disproportionate influence on our understanding of past oceanic ecosystems. While it is possible to recover fish teeth, shark denticles, and other remains from open ocean sediments, the number of these fossils is quite small as compared to the abundance of foraminifera, coccolithophorids, radiolarians, diatoms, and even ostracods. As a result, most studies in the open ocean have tended to focus on the more abundant fossils, in particular planktonic foraminifera and coccolithophorids (Giraudeau and Luc 2007; Kucera 2007; Phleger 1954; Vincent and Berger 1981). My research focuses on planktonic foraminifera, single-celled eukaryotes with a calcareous test ($CaCO_4$) that first arose from a benthic foraminiferal ancestor in the Jurassic (Lipps 1979). Similarities in the distributions of many zooplankton taxa in the modern ocean, like planktonic foraminifera (Bé and Tolderlund 1971; Bradshaw 1959), euphausiids (Brinton 1962), and chaetognaths (Bieri 1959), suggests that planktonic foraminifera may provide a good proxy for past changes in zooplankton in general. While comforting, this does not mean that planktonic foraminifera provide an equally valid proxy at all times. For instance, evidence from terrestrial plants suggests that taxa respond individualistically to climatic perturbations (e.g., Jackson and Williams 2004), although the opposite appears to be true of mammalian assemblages (McGill et al. 2005). Without cross-taxa records in the ocean, it is difficult to anticipate whether the response of planktonic foraminifera to major perturbations is representative of zooplankton in general.

In addition to the loss of taxonomic scope, fine-scale temporal resolution is typically lost in deep sea sedimentary records as well. In my chapters to follow, I investigate ecological and evolutionary changes over millions of years. In these studies, the amount of time averaged into a single sample and the spacing between subsequent samples is on the scale of 1,000 – 10,000 years. Ecological and evolutionary processes operate over much shorter time scales from days to years to decades, and leave a fossil record that is mixed with other sediments that differ in age by hundreds to thousands of years. In short, the record of any given change is simply not preserved at the temporal resolution that is ecologically relevant in most sedimentary environments. In addition to the loss of the temporal resolution necessary to understand ecological mechanisms, even within a well-fossilized group like planktonic foraminifera, preferential preservation of some taxa will result in a sedimentary assemblage not entirely like that which produced it (Berger 1967; Berger 1971).

Finally, there are disadvantages in studying planktonic foraminifera in particular as we have only a limited understanding of the basic life history of most extant species or the selective advantages of most morphological traits, although some species have been described in more detail (Bé 1982; Brummer and Kroon 1988). This is problematic in evolutionary studies as it is often not clear which, if any, traits are under selection and why. Similarly, from an ecological perspective, there is little information on the determinants of relative or absolute population size. Furthermore, genetic studies of a number of modern studies have uncovered cryptic species complexes comprising every planktonic morphospecies studied to date (Darling and Wade 2008). Together, these

issues seriously impede studies of speciation and evolution in ancient lineages, and minimize the complexity of ecological inferences that can be made from fossil planktonic foraminiferal assemblages.

In large part, the scientific contributions of my dissertation arise from seeking to increase the methodological, temporal, taxonomic, stratigraphic, and/or environmental resolution in a number of long-standing questions.

OUTLINE OF THE DISSERTATION

Understanding evolution and ecology in past oceanic ecosystems is an inherently interdisciplinary undertaking. For instance, in **Chapter III** I revisit a classic case of gradual evolution in planktonic foraminifera. In order to interpret the patterns of morphological evolution in terms of speciation (the primary focus of the study), I needed to consider issues pertaining to biogeography, confounding sedimentary processes, and paleoceanographic proxies. While my thesis appears similarly topically wide ranging, it can be divided into the chapters that primarily investigate a specific process or mechanism in ecology, evolution, or geology (**Chapters II, III, V**), and those chapters that apply multidisciplinary approaches to understand past oceanic ecosystems (**Chapters VI-VII**).

In **Chapter II**, I study the biogeography of modern planktonic foraminifera in order to investigate the determinants of community similarity in the modern ocean. In terrestrial ecosystems, the similarity between the species composition of communities in two different locations is determined, in large part, by the distance between them

(Nekola and White 1999). This is due to the relative importance of dispersal limitation in these environments. Although San Diego and Sydney may have similar climates, a wallaby is limited by its dispersal from establishing populations in San Diego County. In contrast, there is abundant evidence from species distributions in the open ocean that dispersal limitation may be less important in determining species distributions. For instance, the same genetic species of planktonic foraminifera appears to inhabit both the Antarctic and the Arctic (Darling et al. 2007). I therefore directly test the relative importance of environmental similarity versus geographic separation in structuring the community composition of planktonic foraminifera. The major conclusion of this study, that environmental similarity is the more important driver of community similarity, provides context for my later chapters on speciation (**Chapter III**) and community change following the Cretaceous-Paleogene mass extinction (**Chapter VII**).

In **Chapter III** I investigate a classic case of gradual evolution in the *Globorotalia plesiotumida*-*G. tumida* lineage of planktonic foraminifera. At issue here is how well we can morphometrically measure speciation in a group like planktonic foraminifera, where it can be difficult to quantitatively separate species that appear genetically distinct. In **Chapter III**, I conclude that the morphometric method employed can strongly influence the perceived evolutionary pattern. While this is just one case study, these results imply that we may be misinterpreting the mode and underestimating the frequency of speciation in the fossil record and/or the standing diversity at a given time. I address the morphological limitations in planktonic foraminifera in **Chapter II**, by considering limited genetic information along with

community patterns, and in **Chapter VII**, by identifying foraminifera at a subspecific level. Both approaches fall short of solving the problem, but do provide a test for the conclusions reached using traditional species-level taxonomy.

In **Chapters IV-VII,** I focus on the recovery from the Cretaceous-Paleogene mass extinction as a case study for better understanding the response of the open ocean to biotic crises. **Chapter IV** provides a short introduction to this extinction event, as all subsequent chapters focus on the events that followed. **Appendix 1** provides details beyond the purview of the chapters themselves, and describes in geological detail all the sites studied in **Chapters V-VII**.

Chapter V is the last of the process-focused chapters. Here, I investigate sediment mixing at the Cretaceous-Paleogene (KPg) boundary by fitting a Lagrangian advection-diffusion model to a highly resolved iridium anomaly. This chapter describes a new approach for quantitatively understanding the effect of mixing on the fossil record at the KPg boundary. As a test and a description of a new approach, this chapter questions the fidelity of iridium as a tracer of sediment mixing, describes the mixing model, and then examines mixing in a number of theoretical cases and at one site in the North Pacific. Sediment mixing is an important and pervasive feature of the records used in my other chapters (**Chapter II, III, VI,VII**) and this research informs my understanding of the overprint of sediment mixing in general. However, in the future, I hope to specifically apply this method to quantitatively improve stratigraphic inferences at the KPg boundary.

In **Chapter VI** and **VII**, I investigate the recovery of pelagic ecosystems from the KPg mass extinction. In **Chapter VI**, I investigate the magnitude and duration of export productivity change at the KPg boundary using barium proxies in sites in the Atlantic, Pacific and Indian Oceans. While it is clear the KPg mass extinction led to the extinction of many pelagic organisms including ~95% of planktonic foraminifera (D'Hondt et al. 1996; Smit 1982) and ~88% of coccolithophorids (Thierstein 1982), and the complete extinction of groups like ammonites and large marine reptiles (Norris 2001), the effects of the extinction on oceanic export productivity are less clear. Some productivity proxies like surface-to-deep water $\delta^{13}C$ gradients, sedimentation rates, and interocean basin deep water aging (D'Hondt 2005; Hsu et al. 1982; Zachos et al. 1989) indicate large, global declines in export production. In contrast, benthic foraminiferal productivity proxies suggest some oceanic regions may have had export fluxes equal to or in excess of those preceding the mass extinction (Alegret and Thomas 2007; Alegret and Thomas 2009). The barium proxies I use have the advantage of providing a third, independent proxy for export productivity, one that may provide a higher fidelity tracer at a time where many of the species used in traditional proxies went extinct. Intriguingly, I find that the barium proxies support the benthic proxies in describing geographically heterogeneous effects of the KPg boundary mass extinction on export production. Some low diversity ecosystems may have had comparable or elevated levels of export production in spite of a major turnover in species at the KPg boundary.

Chapter VII investigates the structure of ecosystems for approximately 500,000 years following the mass extinction. This interval has been traditionally

understood as a very early recovery ecosystem: one that is depauperate in terms of species and characterized by either low total productivity and/or low export productivity (D'Hondt 2005). Here, I use grain size analysis to investigate changes in the relative abundance of calcareous nannoplankton and planktonic foraminifera, trends in community faunal composition, and changes in primary productivity and temperature in the North Pacific and in the South Atlantic. Surprisingly, I find an increased abundance of planktonic foraminifera in the earliest Danian relative to pre-impact communities in the North Pacific, suggesting that some species of foraminifera actually thrived in a post-impact world.

Finally, in **Chapter VIII**, I conclude by synthesizing the cross-chapter themes of my dissertation.

REFERENCES

http://www-odp.tamu.edu/. Ocean Drilling Program.

ALEGRET, L., and E. THOMAS. 2007. Deep-sea environments across the Cretaceous/Paleogene boundary in the eastern South Atlantic Ocean (ODP leg 208, Walvis ridge). Marine Micropaleontology **64:** 1-17.

---. 2009. Food supply to the seafloor in the Pacific Ocean after the Cretaceous/Paleogene boundary event. Marine Micropaleontology **73:** 105-116.

ALVAREZ, L. W., W. ALVAREZ, F. ASARO, and H. V. MICHEL. 1980. Extraterrestrial cause for the Cretaceous-Tertiary Extinction - experimental results and theoretical interpretation. Science **208:** 1095-1108.

BÉ, A. W. H. 1982. Biology of planktonic foraminifera, p. 51-92. *In* T. W. Broadhead [ed.], Foraminifera: notes for a short course. Department of Geological Sciences, Knoxville, Tennessee.

BÉ, A. W. H., and D. S. TOLDERLUND. 1971. Distribution and ecology of living planktonic foraminifera in surface waters of the Atlantic and Indian Oceans, p. 105-149. *In* B. M. Funnell and W. K. Riedel [eds.], Micropaleontology of marine bottom sediments. Cambridge University Press, Cambridge.

BERGER, W. H. 1967. Foraminiferal ooze - solution at depths. Science **156:** 383-385.

---. 1971. Sedimentation of planktonic foraminifera. Marine Geology **11:** 325-358.

BIERI, R. 1959. The distribution of the planktonic Chaetognatha in the Pacific and their relationship to the mater masses. Limnology and Oceanography **4:** 1-28.

BRADSHAW, J. S. 1959. Ecology of living planktonic foraminifera in the North and Equatorial Pacific Ocean. Contributions to the Cushman Foundation for Foraminiferal Research **10:** 25-64.

BRINTON, E. 1962. The distribution of Pacific euphausiids. Bulletin of the Scripps Institution of Oceanography **8:** 51-269.

BRUMMER, G. J. A., and D. KROON. 1988. Planktonic foraminifers as tracers of ocean-climate history. VU Uitgeverij, Amsterdam.

COYNE, J. A., and H. A. ORR. 2004. Speciation. Sinauer Associates, Sunderland.

D'HONDT, S. 2005. Consequences of the Cretaceous/Paleogene mass extinction for marine ecosystems. Annual Review of Ecology Evolution and Systematics **36:** 295-317.

D'HONDT, S. L., T. D. HERBERT, J. KING, and C. GIBSON. 1996. Planktic foraminifera, asteroids and marine production: Death and recovery at the Cretaceous-Tertiary boundary, p. 303–317. *In* G. Ryder, D. Fastovsky and S. Gartner [eds.], The Cretaceous-Tertiary event and other catastrophes in Earth history: Geological Society of America Special Paper 307.

DARLING, K. F., M. KUCERA, and C. M. WADE. 2007. Global molecular phylogeography reveals persistent Arctic circumpolar isolation in a marine planktonic protist. Proceedings of the National Academy of Sciences of the United States of America **104:** 5002-5007.

DARLING, K. F., and C. A. WADE. 2008. The genetic diversity of planktic foraminifera and the global distribution of ribosomal RNA genotypes. Marine Micropaleontology **67:** 216-238.

GARCIA-CASTELLANOS, D. and others 2009. Catastrophic flood of the Mediterranean after the Messinian salinity crisis. Nature **462:** 778-U796.

GIRAUDEAU, J., and B. LUC. 2007. Coccolithophores: From extant populations to fossil assemblages. *In* C. Hillaire-Marcel and A. de Vernal [eds.], Proxies in late Cenozoic paleoceanography. Elsevier, Oxford.

HILDEBRAND, A. R. and others 1991. Chicxulub crater - a possible Cretaceous Tertiary Boundary impact crater on the Yucatan Peninsula, Mexico. Geology **19:** 867-871.

HSU, K. J., Q. X. HE, and A. MCKENZIE. 1982. Terminal Cretaceous environmental and evolutionary changes, p. 317–328. *In* L. T. Silver and P. H. Schultz [eds.], Geological implications of impacts of large asteroid and comets on the Earth: Geological Society of America Special Paper 190.

HSU, K. J., W. B. F. RYAN, and M. B. CITA. 1973. Late Miocene desiccation of Mediterranean. Nature **242:** 240-244.

JACKSON, J. B. C., and A. H. CHEETHAM. 1999. Tempo and mode of speciation in the sea. Trends in Ecology & Evolution **14:** 72-77.

JACKSON, S. T., and J. W. WILLIAMS. 2004. Modern analogs in Quaternary paleoecology: Here today, gone yesterday, gone tomorrow? Annual Review of Earth and Planetary Sciences **32:** 495-537.

JENKYNS, H. C. 1980. Cretaceous anoxic events - from continents to oceans. Journal of the Geological Society **137:** 171-188.

JIANG, S., T. BRALOWER, M. E. PATZKOWSKY, L. R. KUMP, and J. D. SCHUETH. *in press*. Geographic controls on nannoplankton extinction across the Cretaceous-Paleogene boundary. Nature Geoscience.

KENNETT, J. P., and L. D. STOTT. 1991. Abrupt deep-sea warming, palaeoceanographic changes and benthic extinctions at the end of the Paleocene. Nature **353:** 225-229.

KUCERA, M. 2007. Planktonic foraminifera as tracers of past oceanic environments. *In* C. Hillaire-Marcel and A. de Vernal [eds.], Proxies in late Cenozoic paleoceanography. Developments in Marine Geology. Elsevier, Oxford.

LENSKI, R. E., and M. TRAVISANO. 1994. Dynamics of adaptation and diversification - a 10,000-generation experiment with bacterial-populations. Proceedings of the National Academy of Sciences of the United States of America **91:** 6808-6814.

LEVIN, S. A. 1992. The problem of pattern and scale in ecology. Ecology **73:** 1943-1967.

LIPPS, J. H. 1979. Ecology and paleoecology of planktic foraminifera. *In* J. H. Lipps, W. H. Berger, M. A. Buzas, R. G. Douglas and C. A. Ross [eds.], Foraminiferal ecology and paleoecology. SEP Short Course #6, Houston.

MCGILL, B. J., E. A. HADLY, and B. A. MAURER. 2005. Community inertia of quaternary small mammal assemblages in North America. Proceedings of the National Academy of Sciences of the United States of America **102:** 16701-16706.

NEKOLA, J. C., and P. S. WHITE. 1999. The distance decay of similarity in biogeography and ecology. Journal of Biogeography **26:** 867-878.

NORRIS, R. D. 2001. Impact of K-T Boundary events on marine life p. 229-231. *In* D. E. G. Briggs and P. G. Crowther [eds.], Palaeobiology II. Blackwell Science Ltd., Oxford.

PHLEGER, F. B. 1954. Foraminifera and deep-sea research. Deep-Sea Research **2:** 1-23.

SCHEFFER, M. and others 2009. Early-warning signals for critical transitions. Nature **461:** 53-59.

SCHEFFER, M., S. CARPENTER, J. A. FOLEY, C. FOLKE, and B. WALKER. 2001. Catastrophic shifts in ecosystems. Nature **413:** 591-596.

SMIT, J. 1982. Extinction and evolution of planktonic foraminifera at the Cretaceous/Tertiary boundary after a major impact, p. 329 –352. *In* L. T. Silver

and P. H. Schultz [eds.], Geological implications of impacts of large asteroids and comets on the Earth: Geological Society of America Special Paper 190.

THIERSTEIN, H. R. 1982. Terminal Cretaceous plankton extinctions: A critical assessment, p. 385–399. *In* L. T. Silver and P. H. Schultz [eds.], Geological implications of impacts of large asteroids and comets on the Earth: Geological Society of America Special Paper 190.

THOMAS, E. 1990. Late Cretacous-early Eocene mass extinctions in the deep sea, p. 481-496, Global catastrophes in earth history: An interdisciplinary conference on impacts, volcanism and mass mortality: Geological Society of America Special Paper 247.

VINCENT, E., and W. H. BERGER. 1981. Planktonic foraminifera and their use in paleoceanography, p. 1025-1119. *In* C. Emiliani [ed.], The Oceanic Lithosphere. The Sea: Ideas and observations on progress in the study of the seas. John Wiley & Sons, Inc., New York.

ZACHOS, J., M. PAGANI, L. SLOAN, E. THOMAS, and K. BILLUPS. 2001. Trends, rhythms, and aberrations in global climate 65 Ma to present. Science **292:** 686-693.

ZACHOS, J. C., M. A. ARTHUR, and W. E. DEAN. 1989. Geochemical evidence for suppression of pelagic marine productivity at the Cretaceous/Tertiary boundary. Nature **337:** 61-64.

CHAPTER II

The relative importance of environment and dispersal to global pelagic community similarity

ABSTRACT

Geographic proximity is the dominant determinant of community similarity on a global scale in ecosystems studied to date. However, open ocean species often occur in several disjunct, widely dispersed locations, calling into question the role of geographic proximity in structuring pelagic communities. Here, I investigate the relative importance of geographic proximity versus habitat characteristics in determining community similarity in the open ocean. I compare the distributions of objectively-defined biomes with planktonic foraminifera communities, and investigate the relationship between foraminifera community similarity and (i) geographic distance, or (ii) environmental similarity. The effect of cryptic speciation on perceived trends is also considered for two cryptic species complexes. Using unsupervised clustering, I find that global ocean biomes and planktonic foraminifera communities both have disjunct geographic distributions, with no evidence of dispersal limitation. Environmental similarity is found to predict up to 61% of planktonic foraminifera community similarity globally, while no significant correlation exists between geographic distance and community similarity. Consequently, planktonic foraminifera provide the first exception to the rule that geographic proximity determines community similarity on global scales. In contrast to most terrestrial and benthic marine ecosystems, community similarity in open ocean planktonic foraminifera appears to be primarily related to environmental similarity.

INTRODUCTION

Classic ecological theory predicts that, over large spatial scales, the relative similarity between two communities will be determined by the geographic distance between them (Nekola and White 1999). This pattern, a distance-decay relationship, is described by the adage "everything is related to everything else, but near things are more related than distant things" (Tobler 1970). For instance, neighboring communities in the Amazonian plant family Melastomataceae have an average community similarity of approximately 50%, while communities separated by 1000 km have less than a 10% similarity (logarithmic fit; Tuomisto *et al.* 2003). Over long periods of time, the geographic isolation of communities leads to divergent evolutionary histories. Global biogeographic realms in terrestrial and coastal marine environments delineate regions where historic geographic isolation has resulted in the phylogenetic divergence of the biota (Briggs 1974; Olson et al. 2001; Spalding et al. 2007). While the Neotropics and Afrotropics (both terrestrial biogeographic realms) contain regions with similar climates and vegetation structure, distinctly different taxonomic assemblages exist in the two realms as a result of a long history of geographic isolation. The empirical importance of geographic proximity and dispersal limitation in determining species' distributions has led to the incorporation of finite dispersal into a number of ecological and evolutionary theories, such as Hubbell's unified neutral theory of biodiversity and biogeography (Hubbell 2001) and the theory of island biogeography (MacArthur and Wilson 1967).

The generality of the distance-decay relationship has been challenged by microbial ecologists. Recent work has shown that community similarity is correlated to

habitat similarity more than geographic distance in soil and lake bacteria on continental scales (Fierer and Jackson 2006; Van der Gucht et al. 2007). These studies support the dispersal-unlimited, microbial hypothesis that "everything is everywhere, but, the environment selects" [Baas Becking 1934, translated in (de Wit and Bouvier 2006)]. However, there is also abundant evidence for dispersal limitation in microbial communities, with well documented cases in bacterial (Papke et al. 2003; Reche et al. 2005), archaeal (Whitaker et al. 2003), fungal (Green et al. 2004), and freshwater diatom communities (Soininen 2007; Vyverman et al. 2007). Despite evidence for both habitat selection and dispersal limitation in structuring microbial communities, Finlay and Fenchel hypothesize that microbial communities lack biogeographies altogether (Fenchel and Finlay 2004; Finlay 2002; Finlay et al. 1999). Thus, debates over the determinants of microbial biogeography and community similarity continue, particularly in regards to the universality and scaling of principles developed in macroorganismal terrestrial and benthic marine ecosystems (Dolan 2005; Green and Bohannan 2006; Martiny et al. 2006; Prosser et al. 2007).

The open ocean provides an interesting case study for investigating the generality of biogeographical principles. Unlike most species in biogeographic realms in terrestrial and shallow benthic environments, open ocean pelagic fauna often exhibit disjunct distributions with similar species being found in opposite hemispheres (antitropical distributions) and in different ocean basins (panoceanic distributions). Biogeographers have recognized five main faunal patterns both in the Pacific Ocean and globally based on the fragmented distributions of zooplankton species (Bradshaw 1959;

McGowan 1974; McGowan and Walker 1993). While the determinants of open ocean community similarity on a global scale have yet to be directly tested, there is a long history of pelagic biogeography indicating that global open ocean communities may be structured by habitat selection rather than dispersal limitation (see *Appendix 1* for a brief historical review). At a species level, pelagic species occur in habitats with similar environmental characteristics (de Vargas et al. 1999; Goetze 2005; McGowan and Walker 1993). At a community level, marine bacterial communities are predictable on the basis of environmental and biotic factors (Fuhrman et al. 2006; Fuhrman and Steele 2008), with distinct communities being found in similar oceanographic environments throughout the world (Rusch et al. 2007; Zwirglmaier et al. 2008). Furthermore, marine bacteria have a flat distance-decay relationships across open ocean gyres suggesting little dispersal limitation on that scale (Hewson et al. 2006).

Two recent developments in pelagic biogeography question the dominance of habitat selection in determining global pelagic species distributions and community assembly. First, Longhurst (1998) recently subdivided the world's ocean into 51 geographically contiguous provinces on the basis of environmental characteristics, species range boundaries and expert opinion. While this classification is more finely subdivided than the 5 faunal groupings mentioned above, it is notable that no open ocean province in Longhurst's classification has a disjunct distribution. Geographically contiguous provinces are consistent with an open ocean in which community similarity is determined by geographic proximity. Second, molecular studies are revealing that traditional morphological species in the ocean are often cryptic species complexes

(Goetze 2003; Knowlton 1993; Norris and de Vargas 2000). Taxonomic resolution can affect the perceived importance of dispersal limitation; generally, genetic species have greater endemism and dispersal limitation than morphospecies (Fontaneto et al. 2008; Taylor et al. 2006; Vanormelingen et al. 2008).

However, increased taxonomic resolution may not have this effect in the open ocean. A single genetic species can have a fragmented distribution and reoccur in multiple discontinuous geographic locations with similar environmental characteristics. This pattern has been observed in planktonic foraminifera (Darling et al. 2007; de Vargas et al. 1999), copepods (Goetze 2005), coccolithophores (Saez et al. 2003) and cyanobacteria (Ferris and Palenik 1998). Furthermore, there has been limited support for cryptic speciation in pelagic environments due to vicariant boundaries or dispersal limitation (Darling et al. 2007; Goetze 2003), although population genetics has revealed evidence of ecologically-mediated dispersal limitation among haplotypes (Goetze 2005).

The mixed evidence from pelagic species' distributions, Longhurst's provinces, and cryptic species complexes, raises several questions on the determinants of open ocean community similarity. Namely, can isolated open ocean biomes contain highly similar communities? And what is the relative importance of environmental similarity versus geographic distance in determining global community similarity?

In this study, I examine community similarity in relation to geographic distance and environmental similarity in the open ocean. I focus on planktonic foraminifera as they are a pelagic group for which the global distribution of species is known

(Rutherford et al. 1999), in addition to billfish and tuna (Worm et al. 2005). Planktonic foraminifera are considered a good open ocean model organism: their biogeographic patterns are representative of other pelagic fauna (Worm et al. 2005), genetic studies have resolved multiple cryptic complexes (Darling et al. 2004; Darling et al. 2007; de Vargas et al. 1999; de Vargas et al. 2001), and their fossils are found throughout the world ocean allowing for high-resolution studies of paleoceanography, paleoclimate, and macroevolution in addition to modern ecology and biogeography (Norris 2000; Phleger 1954; Vincent and Berger 1981).

First, I investigate the geographic continuity of both oceanic biomes and pelagic communities unconstrained by geographic proximity using unsupervised clustering. In this study, the term biome refers to regions with similar physical oceanographic (temperature, salinity, stratification, etc) and primary productivity characteristics. If dispersal limitation determines community similarity, clustered communities are predicted to be geographically contiguous regardless of the geographic continuity of biomes. Second, I compare global pelagic community similarity against environmental similarity and geographic distance using planktonic foraminifera. A decrease in community similarity with increasing geographic distance (a distance-decay relationship) is indicative of the dominance of dispersal limitation in structuring communities (Nekola and White 1999), while a decrease in community similarity with decreasing environmental similarity (an environmental-decay relationship) is indicative of the dominance of habitat selection. Finally, given concerns with the morphological species concept in planktonic foraminifera, the correlation of phylogenetic relatedness

with environmental and geographic similarity is examined within two well-studied cryptic species complexes of planktonic foraminifera, *Globigerina bulloides* and *Neogloboquadrina pachyderma* (Darling et al. 2004; Darling et al. 2007; Darling et al. 2003). These two case studies provide insight into the potential effect of cryptic speciation on the general inferences drawn from the morphologically-defined planktonic foraminifera communities.

MATERIAL AND METHODS

Environmental Factors

I classified open ocean biomes and investigated environmental similarity using both the long-term annual mean and annual range of seven variables (Figure 2-5 in the supplementary material). Four factors (temperature (SST, C°), salinity (practical salinity scale, PSS), phosphate (μmol/L), and dissolved oxygen (ml/L)) come from the World Ocean Atlas (WOA05) and were included as objectively analyzed annual and monthly climatologies in a 1° by 1° resolution at 10 meters depth (Antonov et al. 2006; Garcia et al. 2006a; Garcia et al. 2006b; Locarnini et al. 2006). The calculated 10-to-200 meter density difference, an index of water column stratification (Behrenfeld et al. 2006), was derived from WOA05 temperature and salinity climatologies at each depth (10 and 200 meters). The final two variables (photosynthetically active radiation (PAR, mol quanta/m^2/day) and net primary productivity (NPP, mg C/m^2/day)) were obtained from the Ocean Productivity website (http://www.science.oregonstate.edu/ocean.productivity/) as monthly averages from

1998-2005 at a 1/6 ° by 1/6° resolution, and NPP was calculated with the standard Vertically Generalized Production Model (VGPM) (Behrenfeld and Falkowski 1997) from Sea-viewing Wide Field-of-view Sensor (SeaWiFs) ocean color and PAR measurements, and Advanced Very High Resolution Radiometer (AVHRR) and Moderate Resolution Imaging Spectroradiometer (MODIS) sea surface temperature measurements. The long-term annual mean NPP and PAR is the mean of the available months (96 in total) from the Ocean Productivity site.

Annual range (a metric of environmental variability) was determined for all environmental factors (Figure 2-5). The annual range for all WOA05 variables (temperature, salinity, phosphate, dissolved oxygen and water column stratification) was determined by calculating the range across all monthly climatologies. For NPP and PAR, annual variability was calculated as the maximum range over a 12-month composite, with each monthly composite equal to the eight-year median value for that month. Additional data preparation details and considerations are described in *Appendix 1* in the supplementary material.

Global Planktonic Foraminifera

A trimmed version of the Brown Foraminiferal Database (BFD) was used to cluster foraminiferal communities for the biome comparison and to investigate the correlation between community similarity and geographic distance versus environmental similarity. The BFD includes 33 species and 6 subspecies, all morphologically defined, identified in the >150μm size fraction (Prell et al. 1999). The

planktonic foraminifera in the BFD come from surface sediments and represent recently dead assemblages. BFD assemblages are affected by the water depth of the surface sediments (increased water depth results in the selective dissolution and loss of some species) and the sedimentary depth of the sample (increased sedimentary depth includes individuals from relatively ancient communities). In this study, I investigated two subsets of the BFD database. The first subset (standard time control) included more samples (855 of the 1265 BFD samples) but also had relatively more time averaging of communities due to the range of sedimentary depths included (0-2.5 meters). The second subset (strict time control) included fewer samples (507 of the 1265 BFD samples) due to the exclusion of samples from any sediment depth greater than 0 meters on average. Both subsets were similarly controlled for the sample water depth (see details in *Appendix 1* in the supplementary material). The standard time control dataset was used to cluster foraminiferal communities, as it included a greater number of locations in the data-sparse Pacific and Indian Oceans. The effect of time averaging on the correlates of community similarity were considered by analyzing trends in both the standard and strict time control BFD datasets.

Community similarity, environmental similarity, and geographic distance was calculated pairwise between all eight foraminiferal clusters (foraminiferal clustering described below) in both BFD datasets (standard and strict time control). Geographic distance was calculated as the great-circle distance in kilometers between the geographic centers of the foraminiferal clusters (median latitude and longitude). Environmental similarity was calculated pairwise as the Euclidean distance between the

median of all environmental variables within the foraminiferal clusters (environmental variables normalized to a zero mean and a unit standard deviation before calculating median value). Although I use the term "environmental similarity" in this study, the Euclidean distance is actually a metric of environmental dissimilarity. A Euclidean distance of zero indicates two identical environments (perfectly similar) and a large Euclidean distance indicates two dissimilar environments. Community similarity was calculated by Morisita's Index of Similarity between all foraminiferal cluster pairs using the median abundance of species within each cluster (site abundances were normalized relative to the total sample size before calculating the median value). Correlations were investigated using a Mantel test with the Pearson product-moment correlation coefficient and 10,000 permutations.

Morisita's Index of Similarity was used as it includes the relative abundance of species in the calculation of community similarity (calculation in *Appendix 1*); the conclusions of this study were unchanged by the use of presence/absence metrics like Jaccard's and Sorensens's similarity coefficients (results not shown). The results of this study were also unchanged by the direct pairwise consideration of all 855 BFD sites (Figure 2-7 and *Appendix 4*), indicating that the relationships are not an artifact of the foraminiferal community clustering.

Cryptic Species

The correlation between genetic relatedness and geographic separation versus environmental similarity is investigated in two well-studied morphospecies of

planktonic foraminifera, *Neogloboquadrina pachyderma* and *Globigerina bulloides* (Darling et al. 2004; Darling et al. 2007; Darling et al. 2003). Both morphospecies have been genetically examined across most of their range and are considered to be cryptic species complexes (with 7-genetic species in each complex). These subpolar-to-polar species (with bi-polar distributions), provide an extreme test of dispersal limitation (Darling *et al.* 2007). Unlike several subtropical cryptic species complexes, neither *N. pachyderma* nor *G. bulloides* appears to subdivide the water column vertically by genotype (Darling et al. 2004; Darling et al. 2007; Stewart et al. 2001), although seasonal variation in the numerically dominant genotype is known in a small portion of the range of *G. bulloides* (Darling et al. 2003). Genetic distance among *N. pachyderma* and *G. bulloides* genotypes (7 and 5 genotypes analyzed respectively) was calculated pairwise as the mean number of nucleotide changes per 100 nucleotides (small-subunit ribosomal DNA, SSU rDNA, and SSU rRNA respectively) since the last common ancestor (see *Appendix 2* in the supplementary material for the published references used, methodological details, and an extended discussion). Environmental similarity and geographic distance were calculated pairwise among genotypes using all sites with confirmed genotypic presence (methodological details as described in the above section, *Global planktonic foraminifera).*

Biome and Community Clustering

K-means clustering, a basic unsupervised classification algorithm that seeks to minimize within cluster variance (MacQueen 1967), was used to cluster oceanic regions

based either on environmental characteristics or planktonic foraminifera communities. In spite of several well-known limitations with basic *k-means* clustering (Hartigan 1975), a comparison of multiple methods determined that basic *k-means* clustering performs as well or better than more sophisticated methods in identifying global ocean biomes (on regional scales, dimensionality reduction may improve *k-means* clustering performance) (Lewis et al. 2008). *K-means* clustering was run until convergence in Matlab (MathWorks, version 7.2.0.0283 R2006a), with the most variable cluster at *k*-1 seeded randomly to determine the k^{th} cluster. Each cluster level (from 2 to *k*) was reseeded 40 times, with the lowest intra-cluster variance cluster assignment saved at each level. The entire clustering routine looped 10-times to ensure that *k-means* clustering converges on the same, optimal cluster assignment (cluster assignments converged in 9 out of 10 environmental trials and in 10 out of 10 BFD trials). Before clustering, all environmental variables were normalized to a zero mean and a unit standard deviation and percent abundance was calculated for the planktonic foraminifera from the BFD.

One shortcoming of *k-means* clustering is that it does not provide a method for choosing *k*, the number of clusters (e.g., the number of biomes or foraminiferal communities). Statistical methods exist for informing the choice of *k*; however, these methods have a number of assumptions that appear to be violated by the environmental data in this study (see *Appendix 1* for details). Critically, methods like optimizing the Bayesian Information Criterion (BIC) or Akaike Information Criterion (AIC) assume a Gaussian distribution of points around centroids (Pelleg and Moore 2000), while other

methods used in spectral clustering and agglomerative clustering require regions of low density parameter space in order to identify significant clusters (Ng *et al.* 2001). When these criteria are not satisfied (non-Gaussian data distributions and/or continuous occupancy of parameter space), then the use of the statistical methods for informing *k* may not be justified. In this study, I failed to statistically find a best *k* for clustering open ocean biomes as was previously predicted (Longhurst 2007). As a result, I clustered biomes at *k*=10 as a compromise between the five global and basinal faunal groupings (Bradshaw 1959; McGowan 1974) and the 15 to 16 oceanic provinces recognized in the Pacific and Atlantic (Longhurst 2007). A comparable *k*=8 was used for the foraminiferal community clusters, as two biomes (the Subpolar-North Pacific and Polar-Arctic Coastal biomes) were effectively absent in the trimmed BFD database.

RESULTS

Open Ocean Surface Biomes

This study finds a geographically disjunct distribution of global surface ocean biomes (Figure 2-2a) as determined by *k-means* clustering of environmental variables and, independently, of pelagic communities by *k-means* clustering of planktonic foraminifera communities (Figure 2-2b). Major features of both classifications are similar. Three foraminiferal groups (see table in Figure 2-2) correspond to unique oceanic biomes (*FG II*, *V*, and *VI* correspond by 86% to the Tropical-Upwelling biome, by 72% to the Subtropical-East biome, and by 77% to the Coastal biome respectively). Four foraminiferal groups (*FG I*, *III*, *VII*, and *VIII*) correspond to oceanic biomes with

conflicts arising from the correspondence of an additional foraminiferal group with the same biome. In the first conflict, 65% of all *FG I* sites occur in the Tropical-Open biome, while *FG III* corresponds to the Tropical-Open biome by 52% and the Subtropical-Central biome by 49%. In the second conflict, 61% of *FG VII* sites correspond to the Subpolar-Antipodal biome, while *FG VIII* corresponds by 67% to the Subpolar-Antipodal biome and 37% to the Polar-Southern Ocean biome. Finally, one foraminiferal group (*FG IV*) and one biome (Subtropical-West) do not correspond well between the two classifications (see grey bars in the Figure 2-2b table). This difference in regions included in a biome and a community cluster (Subtropical-West and Subtropical-East are split relative to *FG V*), the potential causes of the lone foraminiferal cluster (*FG IV*), and a discussion of the conflicts in aligning the biomes and foraminiferal groups is provided in the supporting information along with an environmental characterization and discussion of the biomes (*Appendix 3* and Table 2-2).

Planktonic Foraminifera Community Similarity

Planktonic foraminifera community similarity among the eight foraminiferal community clusters is significantly correlated with environmental similarity but not geographic distance (Figure 2-3). Consistent with an environmental-decay relationship, an increase in environmental similarity (e.g., a decrease in Euclidean distance) is correlated by an increase in community similarity (Figure 2-3a; Pearson's r = -0.58 and p=0.005). The correlation between environmental similarity and community similarity

increases when time averaging is minimized within the BFD database (Figure 2-3c; r= -0.78 and $p<0.001$). In contrast, community similarity among foraminiferal groups is not significantly correlated to geographic distance in the standard or the strict time controlled communities ($p=0.689$ and $p=0.637$ respectively) and, in both cases, there is a weak increase in community similarity with increasing geographic distance (Pearson's r=0.10 and r=0.08 respectively).

A pairwise comparison of all 855 BFD sites reveals similar trends (Figure 2-7; see results and discussion *Appendix 4* in the supplementary material). Community similarity among all BFD sites in the global ocean is better predicted by environmental similarity than geographic distance. When individual BFD sites are considered within ocean basins, community similarity is better predicted by environmental similarity in the Atlantic and Pacific Oceans and by geographic distance in the Indian Ocean. This difference between ocean basins may be due the presence (Atlantic Ocean and Pacific Ocean) or absence (Indian Ocean) of species with antitropical distributions, which account for the existence of highly similar communities in remote geographic locations within basins.

Planktonic Foraminifera Genetic Similarity

The potential effect of cryptic speciation within planktonic foraminifera on inferences based on community composition is considered with an investigation of the correlates of genotypic similarity within two cryptic complexes, *Globigerina bulloides* and *Neogloboquadrina pachyderma* (Darling et al. 2004; Darling et al. 2007; Darling et

al. 2003). Genetic distance within the cryptic species complex *Globigerina bulloides* (5 genotypes, 36 locations) is significantly correlated to environmental similarity (Figure 2-4a; Pearson's r= 0.66 and *p*=0.065) but not geographic distance (Figure 2-4b; r= 0.14 and p=0.396). I interpret a p-value of 0.065 as significant in the *G. bulloides* analysis due to the distribution of possible correlation coefficients in the *G. bulloides* complex using a permuted Mantel test. The small size and structure of the *G. bulloides* matrices (5 genotypes compared) results in a limited number of possible correlation coefficients between genetic distance and environmental similarity (Figure 2-1). While a perfect correlation between genetic distance and environmental similarity would have a p-value of 0.033, the measured correlation (Pearson's r= 0.66) is the next highest possible correlation coefficient for this comparison.

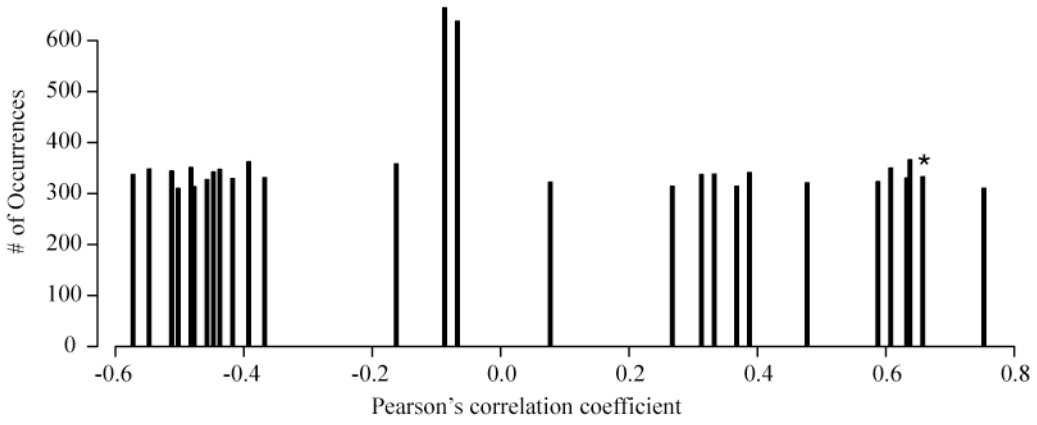

Figure 2-1. Permuted correlation coefficients for the comparison of genetic distance and environmental similarity within the G. bulloides complex. Pearson's correlation coefficients observed in 10,000 random permutations of the *G. bulloides* genetic distance matrix. Star indicates the empirical correlation from the original matrices.

In contrast, genetic similarity within the species complex *Neogloboquadrina pachyderma* (7 genotypes, 89 locations) is better predicted by geographic distance (Figure 2-4d; Pearson's r=0.22 and p=0.25) than environmental similarity (Figure 2-4c, Pearson's r = 0.05 and p=0.278), although neither correlation is significant. The determination of significance or non-significance was unchanged by the use of Spearman's rank correlation with the Mantel test for both species complexes.

DISCUSSION

Open Ocean Surface Biomes

Through an unsupervised classification of open ocean biomes and of planktonic foraminifera communities, I find that pelagic communities in two geographically isolated regions can be more similar than those found in adjacent regions (Figure 2-2b), thereby confirming classic biogeographic subdivisions (Bé and Tolderlund 1971; Bradshaw 1959) and corresponding with the overall distribution of pelagic biomes (Figure 2-2a). This result is robust to the number of biomes classified; disjunct environmental biome distributions were identified regardless of the number of biomes specified (k = 2-16; Figure 2-6). Furthermore, the biomes identified with the 14-environmental variables are similar in location and extent to those determined in past studies of species distributions (McGowan and Walker 1993) and environmental characteristics (Longhurst 1998) (additional details in *Appendix 3* in the supplementary material). Major geographic features (location, extent and membership) are broadly similar between the biomes and the foraminiferal community clusters; three of the eight

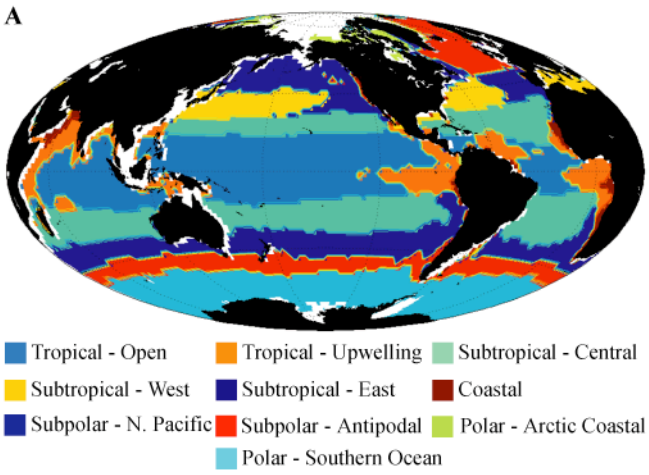

		percent of BFD sites in each biome							
FG	*N*	Trop-O	Trop-U	Subtr-C	Subtr-W	Subtr-E	Coast	Subp-A	Polar-S
I	68	65	35	3	6	1	3	0	0
II	22	23	86	0	0	0	5	0	0
III	258	52	15	49*	3	2	1	0	0
IV	154	51	25	23	7	8	1	0	0
V	109	0	0	18	13	72	9	7	1
VI	116	1	33	0	4	0	77	10	4
VII	61	0	0	0	8	21	18	61	0
VIII	67	0	0	0	0	0	0	67	37*

Figure 2-2. Global surface ocean biomes and community clusters. Unsupervised *k-means* clustering of (A) environmental variables and (B) planktonic foraminifera communities (Brown Foraminiferal Database, 855 locations) at k=10 & k=8 respectively. White indicates excluded areas (either shelf environments or areas with insufficient information); black indicates landmasses. Color-coded biome names listed for environmentally determined biomes (A). Coloring of the 8 BFD clusters (*FG I-VIII*) reflects the best match between the foraminiferal clusters and the biomes as determined by the percent geographical correspondence. The table (B*)* highlights the best biome match for the foraminiferal groups (with a matching color square), and lists the relative correspondence of each biome and foraminiferal group. In two instances, a foraminiferal group was colored according to the second best biome match and is identified by a star. The BFD cluster (*FG IV*) without a clear biome match is highlighted in grey in the table and mapped in yellow (by default).

foraminiferal clusters coincide with one predominant biome, and an additional four foraminiferal clusters match biomes with offsets (Figure 2-2b table).

Most geographical discrepancies between clustered communities and biomes are likely due to limitations of the foraminiferal data, since the foraminiferal assemblages from surface sediments average together several thousand years of communities and the environmental biomes have a greater correspondence to known range boundaries of living species. Temporal averaging in planktonic foraminiferal assemblages may combine individuals from spatially as well as temporally non-contemporaneous communities, as oceanographic fronts move geographically on a variety of time scales (from seasonal to millennial scales). Although quantitative approaches have been suggested on regional (Gregr and Bodtker 2007; Oliver et al. 2004) and global (Oliver and Irwin 2008; Sarmiento et al. 2004) scales to identify biogeochemical provinces, this study is the first to quantitatively correlate global biomes and pelagic communities preserved in surface sediments. These results support the use of objectively defined biomes for identifying, tracking and investigating pelagic communities.

Planktonic Foraminifera Community Similarity

At a global scale, environmental conditions explain more of the variance in planktonic foraminifera community similarity than does geographic proximity (Figure 2-3; Figure 2-7). Although the relative importance of environment is well known from pelagic species distributions (de Vargas et al. 1999; McGowan and Walker 1993; Norris 2000), this finding is noteworthy in several regards. Distance-decay relationships are

widespread in terrestrial and benthic environments (Nekola and White 1999), although the relative explanatory power of environmental characteristics and geographic separation is strongly scale dependent. For example, environmental constraints have

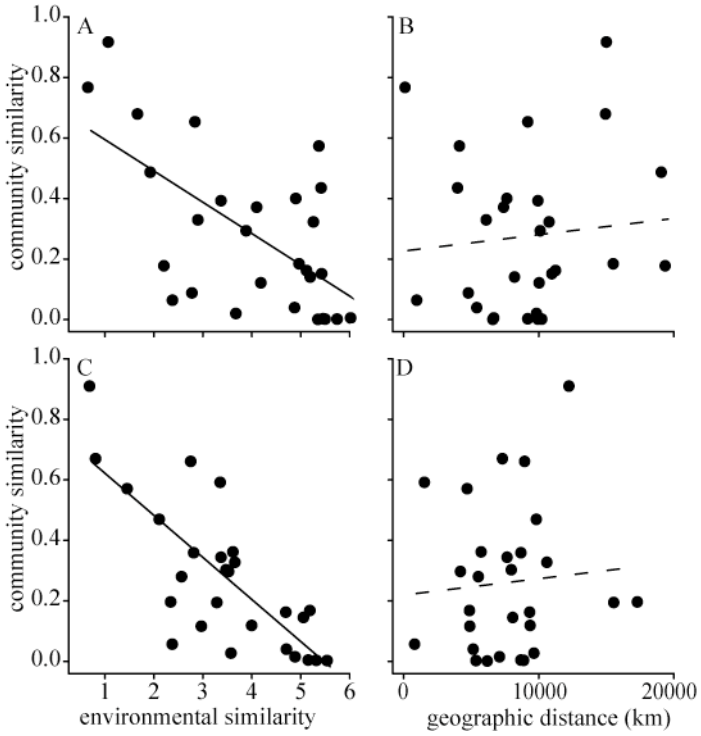

Figure 2-3. Community similarity versus environmental similarity and geographic distance. Planktonic foraminifera community similarity (Morisita's Index) considered pairwise among the 8-foraminiferal community clusters and (left column) environmental similarity (Euclidean distance between environmental variables, 0 = most similar), and (right column) geographic distance (great-circle distance, kilometers). The top row contains results from the 855-site analysis with standard time control for community similarity versus (A*)* environmental similarity (Pearson's r = -0.62) and (B) geographic distance (Pearson's r= 0.10). The bottom row contains results from the 507-site time controlled analysis with community similarity versus (C*)* environmental similarity (Pearson's r = -0.78) and (D) geographic distance (Pearson's r= 0.08). Significant correlations (<0.01) as determined with a Mantel test indicated by solid linear regression lines; insignificant correlations indicated with a dashed linear regression line.

been shown to be more important than dispersal limitation on certain scales in forests (Jones et al. 2006; Tuomisto et al. 2003), mammalian parasites (Vinarski et al. 2007), and marine benthic environments (Becking et al. 2006; Ellingsen 2002). In general, geographic distance is the primary determinant of community similarity on broad spatial scales while environmental factors can dominate on smaller scales (Freestone and Inouye 2006; Parmentier et al. 2005).

Open ocean community similarity in planktonic foraminifera is atypical by comparison, with open-ocean communities on a global scale best described as having an environmental-decay relationship (Figure 2-3). Geographic distance is not significantly correlated with community similarity at this scale and the directionality of the relationship is the opposite of that expected for a distance-decay relationship. The relative importance of environmental similarity among the 8-foraminiferal groups is not an artifact of clustering; environmental similarity is a better predictor of community similarity in a pairwise consideration of all 855 BFD locations (see Figure 2-7 and *Appendix 4* in the supplementary material). Additionally, decreasing time averaging of planktonic foraminiferal communities in the BFD by restricting included sites to those sampled in the uppermost sediments increases the correlation between environmental similarity and community similarity from a correlation coefficient of -0.62 to -0.78 (Figure 2-3a,c). The increased correlation with greater time control suggests that environmental similarity may be a stronger determinant of pelagic community similarity than is measured in this study with the use of assemblages from surface sediments. Finally, the correlation between community similarity and environmental similarity

reveals clear biogeographic structure in planktonic foraminiferal communities and provides further evidence against the hypothesis that protist morphospecies lack biogeographies (Finlay 2002; Finlay et al. 1999).

The relative importance of environmental similarity on a global scale for planktonic foraminifera embodies a key difference between non-bacterial terrestrial, benthic, and near-coastal ecosystems and open ocean ecosystems. While geographic distance dictates community similarity on the largest spatial scales in most other ecosystems, similarity among open-ocean foraminiferal communities appears to be driven by environmental similarity and habitat selection.

It is unclear if environmental similarity is the dominant determinant of community similarity for other pelagic taxa with potentially differing dispersal capabilities. As with some planktonic foraminifera (de Vargas et al. 1999), genetic similarity is not related to geographic proximity in the cryptic complex of the copepod, *Rhincalanus nasutus* (Goetze 2003). For instance, the *R. nasutus* southwest Pacific genotype is most closely related to the North Atlantic genotype and not the adjacent Peru Current genotype. In contrast, biogeographic distributions of euphausiids suggest dispersal limitation; euphausiids lack any truly bipolar species and tropical species in the Atlantic Ocean are endemic (Brinton 1962).

Planktonic Foraminifera Genetic Similarity

Given the widespread presence of cryptic diversity in pelagic species, I investigated the degree to which the current conclusions about the relative importance of environmental similarity versus geographic distance might change with increasing

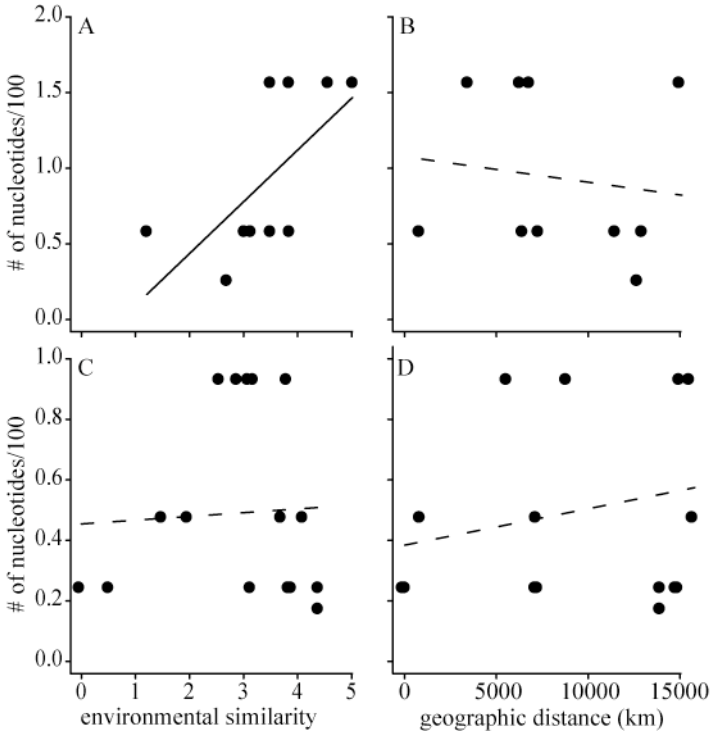

Figure 2-4. Genetic distance in *Neogloboquadrina pachyderma* and *Globigerina bulloides* versus environmental similarity and geographic distance. Genetic similarity within the species complex *G. bulloides* against (A) environmental similarity (Pearson's r= 0.66) and (B*)* geographic distance (Pearson's r= 0.14). Genetic similarity within the species complex *N. pachyderma* against (C) environmental similarity (Pearson's r= 0.05) and (D*)* geographic distance (Pearson's r= 0.22). Significant correlations as determined with a Mantel test indicated by solid linear regression lines; insignificant correlations indicated with a dashed linear regression line.

phylogenetic information about planktonic foraminifera. The correlation between genotypic similarity and environmental similarity versus geographic distance was

examined in two cryptic species complexes, *Globigerina bulloides* and *Neogloboquadrina pachyderma*. Although both come from comparable environments (predominately subpolar/polar), they differ in their correlation to environmental similarity and geographic isolation (Darling et al. 2007). Genetic distance within the *G. bulloides* complex is significantly explained by environmental similarity (Pearson's r=0.66) but not geographic distance (Figure 2-4a-b). Neither environmental similarity or geographic distance are significantly correlated with genetic distance in *N. pachyderma*, although the relative correlation of geographic distance is greater (Figure 2-4c-d). The difference between correlates of genetic distance in *G. bulloides* and *N. pachyderma* could result from interspecific variation in the degree of environmental specialization and dispersal limitation. For the environmental characteristics and timescales measured, genotypes of *N. pachyderma* are environmental generalists compared to *G. bulloides*, with genotypes spanning environmental distances as great as ~6 in *G. bulloides* and ~11 in *N. pachyderma*. Complementing this scenario, genotypes within the *G. bulloides* complex appear to be less dispersal limited; a given genotype of *N. pachyderma* has a geographic range of up to 4,000 km compared to 14,500 km in *G. bulloides*. However, the contrast between *G. bulloides* and *N. pachyderma* may be caused or exacerbated by a number of factors including: differences in the geographic coverage of the genotypes included, the number of locations sampled per genotype, the geographic distance calculation, and/or the presence of poorly resolved branches within the *N. pachyderma* complex (see discussion in *Appendix 2* in the supplementary material).

Globigerina bulloides and *Neogloboquadrina pachyderma* provide three main insights into how the perception of dispersal-limitation may change with phylogeographic studies of pelagic species. First, the geographic distribution of genotypes within the polar to subpolar *G. bulloides* complex confirms that it is possible for environmentally conservative species in the open ocean to occur in similar environments regardless of their geographic proximity (Darling *et al.* 2007). On a regional scale, comparable results led authors to evoke habitat choice and niche conservatism as the likely mechanism for population divergence in Galapagos warbler finches unconstrained by dispersal (Tonnis *et al.* 2005). Similarly, cryptic speciation in the case of *G. bulloides* may occur as a result of wide dispersal to similar environments globally, followed by regional environmental adaptations, genetic isolation, and speciation. Phylogenetic niche conservatism describes the isolation of populations (leading to speciation) due to the retention of ancestral characteristics (Wiens 2004); cryptic speciation within *G. bulloides* appears to be a globe-spanning example of the importance of phylogenetic niche conservatism in pelagic speciation. Second, the importance of dispersal limitation and environmental constraints to speciation within ecologically similar species complexes may vary substantially. Interspecific variation in dispersal limitation is not limited to planktonic foraminifera; differences in dispersal-limitation have been found among species within a family of copepods (Goetze 2003) and among haplotypes in two sibling-species of copepods (Goetze 2005). Third, considered together, an increase in taxonomic resolution (to a genetic species concept) is likely to increase the correlation of geographic proximity with community similarity.

To what extent is unclear and habitat selection could remain the dominant determinant of global community similarity in planktonic foraminifera.

CONCLUSIONS

Environmental similarity and habitat selection are more important than geographic proximity in determining foraminiferal community similarity on the largest spatial scales, in sharp contrast to most terrestrial biota. The empirical support for the dominance of environmental selection is of interest for macroecological and macroevolutionary research in the open ocean, since dispersal limitation should not be assumed. Notably, pelagic species richness patterns in opposite hemispheres may be driven by the occurrence of the same species in two ecologically similar but geographically isolated regions, and speciation may arise more commonly due to phylogenetic niche conservatism rather than vicariance. Finally, the evidence for habitat specificity in planktonic foraminifera supports the hypothesis that pelagic species are vulnerable to global environmental perturbations in spite of vast ranges and large populations (Norris 2000).

SUPPLEMENT

Appendix 1 : Additional background on the environmental correlates of species' distributions

Pelagic species' distributions have historically been correlated to a small subset of environmental parameters. Initial studies of open ocean biogeography linked species

distributions with variability in light and temperature (Giesbrecht 1892; Steuer 1933) and nutrient availability (Ekman 1953). Western biogeographers in the 1950s-70s attributed biogeographic distributions primarily to water mass distributions (Bé and Tolderlund 1971; Ekman 1953; Fager and McGowan 1963; Kanaya and Koizumi 1966; McGowan 1974), and one or more additional "physical-chemical" characteristics, such as dissolved nutrients, oxygen, or surface currents (Bieri 1959; Bradshaw 1959; Brinton 1962). Contemporaneous Russian biogeographers correlated "homologous pelagic biotopes" with physical processes and current patterns (Beklemishev 1969), as well as chemical factors, primary productivity and ecological interactions (Bogdanov 1961; Bogorov 1969). Supporting earlier findings, a recent analysis of planktonic foraminifera assemblages from surface sediments with 35 environmental and preservation factors found faunal variance to be primarily correlated with mean annual sea-surface temperature followed by environmental variability (Morey *et al.* 2005). In other studies, temperature is the primary correlate of species richness patterns globally in planktonic foraminifera (Rutherford *et al.* 1999) and tuna and billfish (Worm *et al.* 2005).

Environmental data preparation. Additional environmental data preparation included averaging annual mean and mean annual range of net primary productivity (NPP) and photosynthetically active radiation (PAR) from a 1/6 ° by 1/6° to a 1° by 1° resolution to match the initial resolution of the WOA05 climatologies. Neritic zones (Ekman 1953) were excluded for all variables using a 200-meter depth mask from WOA05. The resulting dataset was then trimmed to exclude all locations lacking any of the 14-

variables (annual mean and variability of temperature, salinity, phosphate, dissolved oxygen, stratification, NPP, and PAR). Finally, all variables were averaged to a 2° by 2°

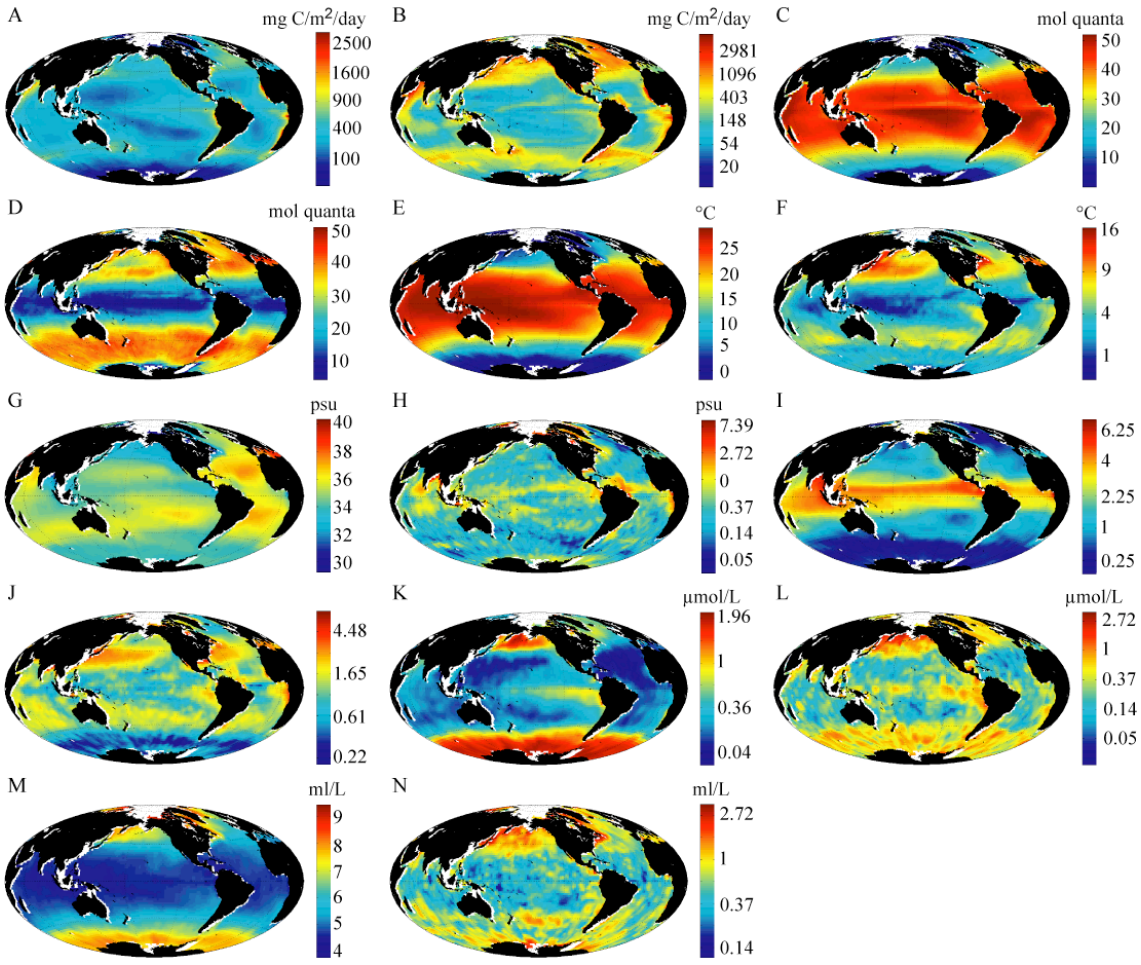

Figure 2-5. Environmental variables. Environmental variables used to determine environmental similarity and surface ocean biomes include the annual mean and mean annual variation of 7 physical, chemical and biological variables at a 2° by 2° resolution (9105 locations). Annual mean and mean annual variation respectively in (A, B) net primary productivity (NPP, mg C/m^2/day), (C, D) photosynthetically active radiation (PAR, mol quanta/m^2/day), (E, F) temperature (°C), (G, H) salinity (PSS), (I, G) water column stratification (10-200-meter density difference), (K, L) phosphate (µmol/L), and (M, N) dissolved oxygen (ml/L).

resolution to minimize the effect of low data density in the most sparsely sampled WOA05 factors (phosphate and dissolved oxygen) on the resulting analyses. The complete environmental dataset includes 14 variables at a 2° by 2° resolution for 9105 locations (see Figure 2-5 for data coverage, excluded and missing regions indicated in white).

Environmental variable selection. The variables included span many of the biologically relevant environmental parameters in the open ocean. Although nitrate climatologies were available from WOA05, the global coverage was less extensive then that for phosphate. As concentrations of nitrate and phosphate in surface ocean waters have a well-known linear relationship (Redfield 1958), I choose to use the phosphate climatologies as representative of nitrate, the more limiting macronutrient in the open ocean (Chester 2000). Although global datasets were available for mixed layer depth and sea surface height (a proxy for surface currents) (Montegut et al. 2004; Niiler et al. 2003), these were deliberately excluded parameters in spite of their importance in structuring oceanic ecosystems. Both factors were included in the initial analyses but were found to impair biome classification. When mixed layer depth was included, mixed layer depth variation within highly variable regions (like the Southern Ocean) dominated the subsequent clustering while the rest of the ocean remained classified into a few main regions. A similar problem was encountered when sea surface height was included. The first difference of sea surface height was included as a proxy for surface ocean currents. When included in the biome analysis, clusters predominately defined

the boundaries between the biomes, rather than the biomes proper. Increased clustering simply lead to finer subdivisions within these boundary regions.

K-means clustering. One shortcoming of *k-means* clustering is that it does not provide a method for choosing *k*, the number of clusters (or biomes, in this case). An attempt to determine *k* based on a recent method proposed for spectral clustering (Azran and Ghahramani 2006) failed to produce sensible results (per. comm. J. Lewis and P.M. Hull). This approach potentially failed because the oceanic environmental variables violate the principle assumption of the method, namely, that clusters are separated in the environmental parameter space by regions with few observations. For this spectral clustering method to work, there cannot be many cases of sites which could be equally well classified into more than one cluster. Additional statistical approaches were investigated to determine *k* (plotting of intra-cluster residual variance vs. k and optimizing the Bayesian Information Criterion) and similarly failed to provide strong support for a single best *k*, perhaps due to the expectation of a Gaussian data distributions for these methods (Pelleg and Moore 2000). The failure to find a single "best" *k* using automated methods confirms a well know feature of oceanic ecosystems: oceanic environments are known to be divisible at a variety of scales (Longhurst 2007).

In order to investigate the utility of *k-means* clustering to identify oceanic biomes, a cluster number of k=10 was selected for the environmental biomes as a compromise between the 5 main faunal distribution types (Bradshaw 1959; McGowan 1974) and the 15 and 16 oceanic provinces recognized by Longhurst in the Pacific and

Atlantic respectively (Longhurst 1998). I choose this biome number as suitable to the working hypothesis that regions within different ocean basins might comprise the same biome and support similarly communities; support for this hypothesis was found within biomes for *k's* ranging from 2-16 (Figure 2-6). If the *k-means* clustering had instead

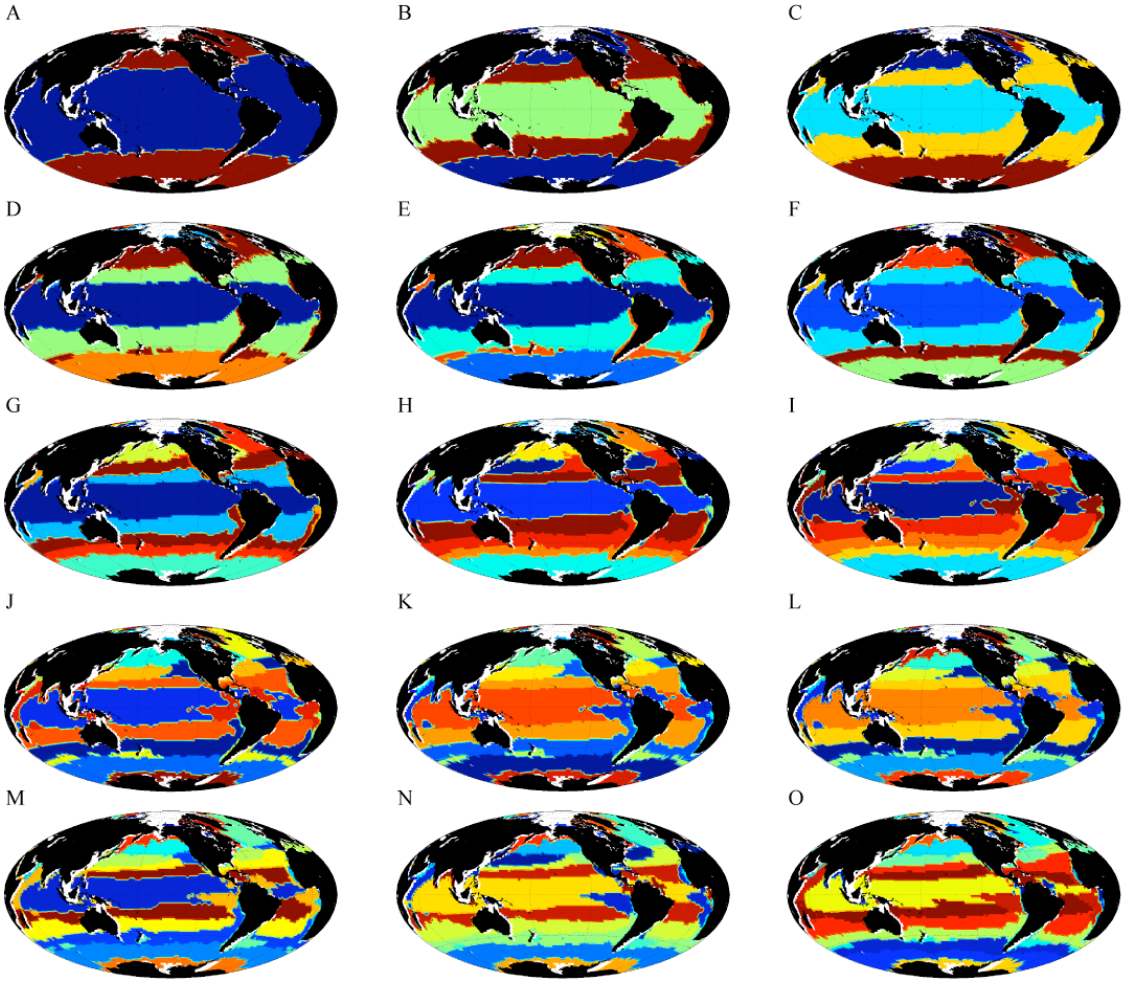

Figure 2-6. Global surface ocean biomes for 2 to 16 clusters. Unsupervised *k-means* clustering of environmental variables for k = 2-16 (A-O). Colors assigned based on the order of clustering and do not have ecological significance. White indicates excluded areas (either shelf environments or areas with insufficient information); black indicates landmasses.

identified geographically contiguous biomes or communities, *k* would have been increased to higher levels in keeping with that scenario.

Relative species abundances from the Brown Foraminiferal Database were similarly clustered with *k-means* clustering to compare with the biome classification. In order to investigate comparable cluster results, a lower *k* for the BFD clusters was chosen due to the limited geographic coverage of the BFD. Two biomes identified in the environmental clustering, the Subpolar-North Pacific and Polar-Arctic Coastal biomes, are represented by 1 and 0 BFD sites respectively, effectively lowering the appropriate *k* for comparisons to *k*=8. The similarity of the BFD clustering results to the environmental biome classification is determined by the percent of BFD sites within each environmental biome (Figure 2-2). The total percent of BFD clusters across all environmental biomes can add up to more than 100% because of the resolution of the BFD site locations (1°) versus the environmental variables (2°). When a BFD site fell on the boundary between two biomes, it was considered as being present at both surrounding cells (+/- 1°) resulting in the effective double counting of some BFD sites.

A recent objective classification of surface ocean provinces (using a combination of *k-means* clustering and Ward's linkage agglomerative clustering), used a Figure of Merit to automatically halt clustering when further subdivision failed to improved the predictive nature of the cluster centroid (Oliver and Irwin 2008). The number of ocean provinces identified by this method (81) is much higher than what is used in the present study, in part because the classification includes a number of coastal areas deliberately excluded from this analysis and in part due to biases introduced by

the reliance on remote sensing in Oliver *et al*. and the reliance on temporally and spatially average data in the current study. The topology of the 17 main clusters identified by Oliver *et al.* is comparable to those found in this study, with the additional biomes in Oliver *et al.* appearing to occur primarily along hydrographic boundaries. As methods develop in regards to objective ocean classification, promising approaches – like Oliver *et al*.'s – should be fully tested in future studies in regards to the ecological relevance of province divisions. Investigating the correlation between community clusters and biomes (or oceanic provinces), provides one such test.

Table 2-1. Correlation coefficient (r) among environmental variables. Linear correlations among all 14 environmental variables included in biome clustering and environmental analyses. All variable abbreviations are described in ***Materials and methods*** except for the following: Sal. = salinity, Strat.= index of water column stratification, Phos. = Phosphate, and Dis. O_2 = dissolved oxygen. Italicized "m" and "v" indicate long-term annual mean and average annual variability, respectively. Values in bold have an absolute r greater than or equal to 0.90, values italicized and in bold have an absolute r greater than or equal to 0.70 and less than 0.90, and italicized values have an absolute r greater than or equal to 0.50 and less than 0.70.

		SST	**SST**	**PAR**	**PAR**	**Sal.**	**Sal.**	**Strat.**	**Strat.**	**Phos.**	**Phos.**	**Dis. O_2**	**Dis. O_2**	**NPP**	**NPP**
		m	*v*	*m*	*v*	*m*	*v*	*m*	*v*	*m*	*v*	*m*	*v*	*m*	*v*
SST	*v*	-0.06	-												
PAR	*m*	**0.96**	-0.03	-											
PAR	*v*	*-0.50*	*0.51*	-0.40	-										
Sal.	*m*	*0.56*	0.04	*0.58*	-0.05	-									
Sal.	*v*	-0.06	-0.11	-0.17	-0.30	-0.39	-								
Strat.	*m*	***0.74***	-0.27	*0.64*	***-0.77***	0.01	0.34	-							
Strat.	***v***	0.32	*0.62*	0.25	-0.03	0.07	*0.51*	0.28	-						
Phos.	*m*	***-0.83***	-0.16	***-0.77***	0.26	*-0.50*	-0.11	*-0.55*	*-0.54*	-					
Phos.	*v*	*-0.57*	0.19	*-0.54*	0.24	*-0.50*	0.09	-0.34	-0.12	*0.56*	-				
Dis. O_2	*m*	**-0.99**	0.03	**-0.95**	0.44	*-0.61*	0.14	-0.67	-0.30	***0.81***	*0.57*	-			
Dis. O_2	*v*	*-0.59*	0.41	*-0.61*	0.26	-0.45	0.21	-0.35	0.16	0.37	*0.56*	*0.59*	-		
NPP	*m*	0.31	0.42	0.34	0.09	0.19	-0.04	0.14	0.36	-0.35	0.10	-0.35	0.01	-	

In the present study, one concern in including multiple variables in a *k-means* analysis is that covariance among variables could lead to an overemphasis of certain

features of the data. Of the 14-environmental variables (Figure 2-5), only 3 variables were highly covariable; annual mean temperature has an correlation coefficient of r = -0.99 and 0.96 with annual mean dissolved oxygen and PAR respectively (see Table 2-1 for the covariance among all environmental variables). Likewise, annual mean dissolved oxygen and PAR have an r = -0.95. Although all 14-variables were included in the biome analysis, the exclusion of annual mean dissolved oxygen and PAR has little effect on the resulting biome classification at k=10.

Appendix 2 : **Planktonic foraminifera community similarity**

In the Brown Foraminiferal Database (BFD) sites from more than 4500 meters water depth in the Atlantic and 3500 meters water depth in the Pacific and Indian Ocean (excluding the Southern Ocean) were excluded to minimize the effects of calcium carbonate dissolution on faunal assemblages (Broecker 1974).

Morisita's Index of Similarity was used as the metric of community similarity, as it is relatively robust to sample size and includes abundance information (not just species presence/absence) (Krebs 1999). Morisita's Index of Similarity between samples j and k (C_λ) is defined as

$$C_\lambda = \frac{2 \Sigma X_{ij} X_{ik}}{(\lambda_1 + \lambda_2) N_j N_k}$$

where X_{ij} and X_{ik} represent the number of individuals of species i in sample j and k and N_j and N_k represent the total number of individuals in samples j and k respectively. λ_1 and λ_2 are respectively defined as

$$\lambda_1 = \frac{\Sigma [X_{ij}(X_{ij} - 1)]}{N_j (N_j - 1)}$$

$$\lambda_2 = \frac{\Sigma [X_{ik}(X_{ik} - 1)]}{N_k (N_k - 1)}$$

Morisita's Index of Similarity was calculated using the raw abundances from the BFD sites.

Cryptic species. Genetic distance among *Neogloboquadrina pachyderma* and *Globigerina bulloides* genotypes is calculated for each genotype pair as the mean number of nucleotide changes per 100 nucleotides since the last common ancestor. The number of nucleotide changes were estimated from maximum-likelihood phylogenetic trees in published papers: *N. pachyderma* (Darling et al. 2004; Darling et al. 2007) and *G. bulloides* (Darling et al. 2007; Darling et al. 2003), where the phylogenetic trees were determined using partial SSU rDNA at 840 sites for *N. pachyderma* and partial SSU rRNA at 729 for *G. bulloides* (Darling et al. 2007). Given the large genetic distance between *G. bulloides* genotypes I and II, I restricted the analyses to the 5 genotypes within the complex *G. bulloides* Type II. The most recent maximum-likelihood phylogenetic tree for *N. pachyderma* failed to resolve the relationship between Type II and III; therefore, in this analysis the genotypes Type II and Type III are treated as having a nucleotide difference of 0 changes per 100 nucleotides. Furthermore, evolutionary relationship for *N. pachyderma* Type V is also poorly resolved, resulting in a polytomy.

To calculate genetic distance versus geographic or environmental distance, I included all geographic locations with confirmed genotypic presence estimated from published papers for *Neogloboquadrina pachyderma* (Darling et al. 2004; Darling et al. 2007) and *Globigerina bulloides* (Darling et al. 2007; Darling et al. 2003; Darling et al. 2000) respectively. While both species complexes have been sampled globally, greater geographic coverage and sampling effort (within the data-sparse upwelling regions and in the Indian Ocean, in particular) could affect the outcome of this analysis. Additionally, given the bipolar distribution of some genotypes, the use of median latitude and longitude in this analysis will capture the geographic distances relative to more sampled region.

While *G. bulloides* and *N. pachyderma* provide a geographically extreme test of dispersal limitation, they provide little insight into speciation in tropical and subtropical species. Biological characteristics of species within certain environments may serve as a pre-adaptation for (or against) long-distance dispersal. For example, many polar and subpolar zooplankton species have highly seasonal life histories including diapause during the winter months and rapid growth during spring blooms (Broms and Melle 2007; Pasternak and Schnack-Schiel 2001); such life history characteristics might pre-adapt species for long distance dispersal through unfavorable environments. Furthermore, depth parapatry could be a relatively more important mechanism of speciation in subtropical and tropical species living in environments with well-developed vertical gradients in habitat; indeed, genotypes from the subtropics are

known to co-occur in a single geographic region (Huber et al. 1997) and to respond differentially to light intensity variation in laboratory manipulations (Faber et al. 1989).

Appendix 3 : Biome descriptions at k = 10

Biomes were named according to their correspondence to 4-latitudinal bands (Tropical, Subtropical, Subpolar, Polar) followed by a descriptive locator (e.g., open, upwelling, east, west). Biome names do not fully describe the geographic location of all subregions within a biome, but rather act as an indicator to help readers locate and identify the oceanic biomes.

Low latitude biomes. Latitudinally speaking, *k-means* clustering identifies two predominately tropical biomes (Tropical-Open and Tropical-Upwelling) and one tropical-subtropical biome (Subtropical-Central). The Tropical-Upwelling biome contains low latitude regions affected by boundary currents and coastal upwelling: the Somali Current region, coastal Indonesian and the South China Sea, coastal Pacific Mexico and Central America, coastal Columbia, Ecuador and northern Peru with an off-shore extension, the Angola and Guinea Domes with a large westward extension south of the Ivory Coast, and the Guyana and Caribbean Countercurrent regions. In contrast, the Tropical-Open biome typically includes equatorial regions removed from the continents, including large regions in the tropical Atlantic, Pacific, and Indian Oceans. Although both biomes (Tropical-Open and Tropical-Upwelling) have comparable annual mean physical conditions (Table 2-2), Tropical-Upwelling has more than 1.5

times the mean annual range in temperature (3.90°C versus 1.98 °C), salinity (1.03 versus 0.57) and stratification (stratification ratios of 1.70 versus 0.96). The biomes are further differentiated by phosphate and primary productivity; Tropical-Upwelling has approximately 1.5 times the mean and annual range of phosphate and mean primary productivity, with more than 3 times the mean annual range in NPP (Table 2-2).

Mid latitude biomes. In addition to the Subtropical-Central biome, there are three predominately mid-latitude biomes: Subtropical-West, Subtropical-East, and Coastal. Subtropical-Central is the most unproductive of this group (263.78 mg C/m^2/day), boasting the warmest SST (24.17°C), the highest PAR (43.45 mol quanta/m^2/day), and the lowest concentrations of phosphate (0.16 μmol/L). Additionally, the Subtropical-Central biome has the lowest intra-annual variability in temperature (4.33°C) and NPP (151.87 mg C/m^2/day). The Subtropical-Central, Subtropical-East, and Coastal biomes have antitropical distributions and occur in both the subtropical North and South Atlantic and North and South Pacific. The Subtropical-West biome, in contrast, is restricted to the northern hemisphere and includes the Kuroshio Current and Extension, the Gulf Stream and Extension, and the Mediterranean. With annual mean NPP of 473.13 mg C/m^2/day and mean annual range NPP of 523.31 mg C/m^2/day, the Subtropical-West biome has more than 1.5 times the annual mean and nearly 3.5 times the intra-annual variability of the Subtropical-Central biome. Additional characteristics

Table 2-2. Environmental characterization of biomes in a 10-biome ocean. The mean (μ), standard deviation (σ), and coefficient of variation (CV) within each of the 10 biomes are listed for all 14 environmental variables. Environmental variable abbreviations described in Table 2-1 caption.

			Tropical-Open	*Tropical-Upwelling*	*Subtropical-Central*	*Subtropical-West*	*Subtropical-East*	*Coastal*	*Subpolar-N. Pacific*	*Subpolar-Antipodal*	*Polar-Arctic Coastal*	*Polar-S. Ocean*
SST (°C)	*m*	**μ**	27.74	26.54	24.17	19.58	17.41	20.53	6.46	9.46	-0.03	1.37
		σ	1.14	1.61	2.15	3.54	2.63	5.82	3.40	3.25	4.13	2.66
		CV	0.04	0.06	0.09	0.18	0.15	0.28	0.53	0.34	-127.01	1.94
SST (°C)	*v*	**μ**	1.98	3.90	4.33	9.42	5.81	6.07	8.69	4.40	3.24	2.91
		σ	0.80	1.31	1.17	1.59	0.96	2.23	2.73	1.15	1.55	0.77
		CV	0.41	0.34	0.27	0.17	0.16	0.37	0.31	0.26	0.48	0.26
PAR (mol quanta/m^2/day)	*m*	**μ**	45.85	45.39	43.45	33.91	35.13	37.67	21.05	23.78	4.77	13.43
		σ	3.00	4.87	3.41	4.64	3.93	8.90	5.37	5.59	5.11	7.20
		CV	0.07	0.11	0.08	0.14	0.11	0.24	0.26	0.23	1.07	0.54
PAR (mol quanta/m^2/day)	*v*	**μ**	13.61	14.26	27.65	36.54	37.95	26.62	34.34	38.95	23.45	32.21
		σ	4.09	5.00	5.39	4.15	3.75	11.70	4.70	2.85	8.39	8.52
		CV	0.30	0.35	0.19	0.11	0.10	0.44	0.14	0.07	0.36	0.26
Sal. PSS	*m*	**μ**	34.73	34.89	35.80	35.35	35.08	34.88	32.93	34.59	31.88	33.95
		σ	0.66	1.03	0.80	1.42	0.80	1.53	0.67	0.46	1.28	0.27
		CV	0.02	0.03	0.02	0.04	0.02	0.04	0.02	0.01	0.04	0.01
Sal. PSS	*v*	**μ**	0.57	1.03	0.35	0.42	0.26	0.86	0.56	0.30	3.12	0.37
		σ	0.26	0.71	0.16	0.32	0.15	0.88	0.41	0.23	1.53	0.24
		CV	0.45	0.69	0.46	0.78	0.59	1.02	0.74	0.76	0.49	0.65
Strat.	*m*	**μ**	3.69	3.53	1.60	1.42	0.99	2.14	1.04	0.41	2.00	0.34
		σ	0.74	0.90	0.56	0.42	0.37	1.08	0.45	0.22	1.09	0.21
		CV	0.20	0.25	0.35	0.30	0.37	0.50	0.43	0.55	0.55	0.63
Strat.	***v***	**μ**	0.96	1.70	1.36	2.61	1.36	1.91	1.56	0.81	2.54	0.45
		σ	0.26	0.45	0.34	0.42	0.25	0.91	0.50	0.26	1.21	0.16
		CV	0.27	0.26	0.25	0.16	0.19	0.48	0.32	0.33	0.48	0.36
Phos. (μmol/L)	*m*	**μ**	0.24	0.33	0.16	0.19	0.31	0.53	1.09	0.76	0.54	1.65
		σ	0.14	0.23	0.10	0.14	0.18	0.28	0.45	0.28	0.27	0.28
		CV	0.60	0.69	0.61	0.74	0.56	0.53	0.41	0.37	0.49	0.17
Phos. (μmol/L)	*v*	**μ**	0.27	0.43	0.19	0.31	0.34	0.59	1.06	0.63	0.63	0.57
		σ	0.13	0.23	0.10	0.17	0.15	0.27	0.48	0.17	0.22	0.19
		CV	0.48	0.54	0.51	0.56	0.44	0.45	0.45	0.27	0.35	0.33
Dis. O_2 (ml/L)	*m*	**μ**	4.62	4.65	4.89	5.33	5.55	5.18	7.13	6.51	8.35	7.55
		σ	0.12	0.14	0.19	0.40	0.30	0.70	0.55	0.48	0.70	0.37
		CV	0.03	0.03	0.04	0.08	0.05	0.14	0.08	0.07	0.08	0.05
Dis. O_2 (ml/L)	*v*	**μ**	0.42	0.58	0.49	0.97	0.73	0.90	1.58	0.80	1.39	0.90
		σ	0.13	0.24	0.17	0.30	0.21	0.34	0.49	0.28	0.54	0.38
		CV	0.32	0.40	0.34	0.31	0.29	0.37	0.31	0.36	0.39	0.42
NPP (mg C/m^2/day)	*m*	**μ**	291.47	537.21	263.78	473.13	441.12	1373.34	463.56	446.59	63.42	111.60
		σ	86.41	171.55	92.05	134.09	154.04	471.25	163.56	168.35	112.59	74.41
		CV	0.30	0.32	0.35	0.28	0.35	0.34	0.35	0.38	1.78	0.67
NPP (mg C/m^2/day)	*v*	**μ**	143.83	490.63	151.87	523.31	352.73	2194.10	946.66	793.21	406.97	259.62
		σ	82.95	317.52	80.11	255.54	214.25	1031.98	482.80	420.55	266.36	133.22
		CV	0.58	0.65	0.53	0.49	0.61	0.47	0.51	0.53	0.65	0.51

of the Subtropical-West biome include the highest intra-annual variability of SST (9.42°C) and of stratification (stratification ratio of 2.61) of the mid-latitude biomes. The Subtropical-East biome includes three main geographic regions: the eastern North Pacific offshore of the California Current, the eastern North Atlantic offshore of the Iberian Peninsula, and circumglobally in the Subtropical Convergence (ringing the Southern Ocean). The Subtropical-East biome has the coolest waters (17.41°C), low PAR (35.13 mol quanta/m^2/day), relatively low salinity (35.08 PSS), and the lowest stratification index of any mid-latitude biome (stratification ratio of 0.99). In spite of higher phosphate (0.31 versus 0.19 μmol/L) levels, the Subtropical-East biome is less productive than the Subtropical-West biome (with mean NPP of 441.12 versus 473.13 mg C/m^2/day) and has lower intra-annual variability (352.73 versus 523.31 mg C/m^2/day). Finally, the Coastal biome is found in both tropical and subtropical latitudes often lying inshore of the Tropical-Upwelling biome, including the west coast of Africa inshore of the Tropical-Upwelling biome, the Humboldt Current inshore and south of the Tropical-Upwelling biome, the southern Brazil Current, the near-coastal Guyana Current, in the near-coastal region California Current, the Sea of Cortez, and in the East Arabian Current inshore of the Tropical-Upwelling biome, as well as a few scattered locations in the Caribbean and off the east coast of the United States. Like Polar-Arctic Coastal, the Coastal biome includes coastal regions beyond the original purview of this study but captured nonetheless by the geographic coverage of the environmental variables. Coastal is characterized by the highest productivity of any biome (1373.34 mg C/m^2/day) with 2.5 to 5 times the productivity of other mid and low latitude biomes,

which include the second most productive global biome (Tropical-Upwelling). Additional characteristics of the Coastal include relatively warm annual SST (20.53°C), high PAR (37.67 mol quanta/m^2/day), and a well-stratified water column (stratification ratio of 2.14).

High latitude biomes. *K-means* clustering at k=10 identifies four high latitude biomes (Subpolar-North Pacific, Subpolar-Antipodal, Polar-Arctic Coastal, and Polar-Southern Ocean). The Subpolar- Antipodal biome includes the subantarctic zone of the Southern Ocean (bounded by the Subantarctic and Subtropical Fronts) and the subpolar North Atlantic. The Subpolar-North Pacific biome includes the subpolar North Pacific and the Labrador Current along the coast of Newfoundland. Compared to Subpolar-Antipodal, Subpolar-North Pacific is characterized by a higher mean and intra-annual variability in NPP (mean: 463.56 versus 446.59 mg C/m^2/day, range: 946.66 versus 793.21 mg C/m^2/day), in stratification (mean: 1.04 versus 0.41, range: 1.56 versus 0.81), and phosphate (mean: 1.09 versus 0.76 μmol/L, range: 1.06 versus 0.63 μmol/L). The Subpolar-Antipodal biome is generally warmer (9.46°C versus 6.46°C) and saltier (34.59 versus 32.93 PSS) than the Subpolar-North Pacific biome, with slightly more than half the intra-annual variability in temperature and salinity. It is notable, that while both of the predominately subpolar biomes' (Subpolar-North Pacific and Subpolar-Antipodal) mean annual NPP is only slightly greater than the Subtropical-Central and Subtropical-West biomes, the intra-annual variability of Subpolar-North Pacific and Subpolar-Antipodal is 2-3 times greater.

A single biome was identified in the Antarctic (Polar-Southern Ocean) and Arctic (Polar-Arctic Coastal) respectively. The Polar-Southern Ocean biome ranges from the Subantarctic Front to the Antarctic continent. It is characterized by consistently cold temperatures (mean: 1.37°C, intra-annual range: 2.91°C), a mean annual salinity of 33.95, and the lowest stratification index (0.34) and highest phosphate concentrations (1.65 μmol/L) of any biome. Satellite derived NPP is low (111.60 mg C/m^2/day) and seasonal (mean annual range: 259.62 mg C/m^2/day).

Due to a lack of data throughout much of the Arctic, the single Arctic biome, Polar-Arctic Coastal, is restricted to coastal locations, including Baffin Bay, the Northwest Passage (excluding Hudson Bay), the East Greenland Current, and a few scattered locations along the coast in the Kara and Beaufort Seas. The Polar-Arctic Coastal biome has the coldest mean annual SST (-0.03°C) and lowest PAR (4.77 mol quanta/m^2/day), the freshest and most variable salinities (mean: 31.88, range: 3.12), and the lowest NPP (63.42 mg C/m^2/day) with the relatively greatest annual range in productivity (406.97 mg C/m^2/day) of any biome. Phosphate concentrations in Polar-Arctic Coastal are comparable to Coastal (mean: 0.54 μmol/L, range: 0.63 μmol/L).

Validity of environmentally identified biomes. The general concordance of the 10-biome subdivision with known physical and biological features suggests that *k-means* clustering provides a simple and effective means of identifying open ocean biomes. The Southern Ocean biome, Polar-Southern Ocean, is divided along the Subantarctic Front from the subpolar Subpolar-Antipodal biome to the north, which is divided along

the Subtropical Front from subtropical Subtropical-East biome. These biome boundaries correspond with the major fronts in the Southern Ocean (with the exception of the Polar Front, which is a line of division at $k = 11$) and coincide with major biogeographic transitions. Among krill, Subtropical-East is inhabited by subtropical gyre species like *Euphausia recurva,* Subpolar-Antipodal by subantarctic species like *E. lucens, E. longirostris,* and *E. vallentini*, Polar-Southern Ocean by species (from north to south) like *E. similis*, *E. frigida,* and *E. superba* (Brinton 1962), with biogeographic patterns supported by many other Antarctic organisms (for example, see (Hunt and Hosie 2005)).

There are a number of differences between the biomes and Brown Foraminiferal Database clusters (BFD clusters), although most discrepancies are likely due to limitations of the foraminiferal data. Many BFD clusters have range boundaries that are offset latitudinally from the biome boundaries. As the biome boundaries have a greater correspondence to known range distributions of species collected in the water column (McGowan and Walker 1993) and biome boundaries (Longhurst 1998), I hypothesize that the offset of the BFD clusters may reflect the temporal averaging of foraminiferal assemblages in sediments from several thousand years of latitudinal variation in the location of the overlying planktonic ecosystems (due to seasonal and climatic forcing). The correlation of *FG I* with the Tropical-Open biome and *FG III* with the Subtropical-Central biome requires a latitudinally contracted and expanded range for the respective communities, and provides the best example of cluster boundary offsets. Similarly, inconsistent BFD cluster assignment in the tropical Pacific (resulting in the non-

analogous cluster, *FG IV*, interspersed with *FG I* and *FG II*) may also be a sedimentary artifact reflecting the post-depositional alteration of foraminifera community assemblages in the acidic bottom waters of the Pacific Ocean.

The southern subtropical gyres in the Atlantic, Pacific and Indian Ocean contain one dominant biome (Subtropical-Central) and are bounded by the Subtropical-East and Tropical-Open to the south and north, respectively. In contrast, the northern hemisphere subtropical gyres in the Pacific and Atlantic are both divided into the 3-biomes: Subtropical-Central , Subtropical-West, and Subtropical-East. The existence of two biomes (as in the southern hemisphere) is well supported by pelagic species distributions of "Pacific Central" and "Transitional" species groups as described by biogeographers (Brinton 1962; Fager and McGowan 1963; McGowan 1971). However, there is only weak evidence for east-west subdivision in species distributions corresponding with the Subtropical-West and Subtropical-East biomes. This east-west division was noted by Longhurst, who argued for an east-west subdivision predominately on the grounds of relative species abundance and primary productivity (Longhurst 2007). Exceptional species ranges do correspond with the Subtropical-West and Subtropical-East subdivision; for example, the distribution of the euphausiid *Thysanopoda acutifrons* corresponds with Subtropical-East biome in the California Current and in the South Pacific (Brinton 1962). At eight clusters, foraminiferal communities from the Brown Foraminiferal Database (BFD) did not cluster along this subtropical east-west divide (*FG V* spans the region). Indeed, even at higher numbers of clusters, *k-means* clustering of the BFD failed to reproduce this subdivision. It is

possible that the east-west environmental difference in the subtropical gyre can only be exploited by species with complex behaviors or greater locomotory powers, which could allow them to move against the surface current in order to stay within a single environment. This east-west environmental difference is likely not exploited by the majority of phytoplankton and zooplankton, and maybe over-split relative to species and community distributions. In contrast, the subdivision of the tropics into the Tropical-Open and Tropical-Upwelling biomes is well-supported by species distributions (e.g. for krill see *E. distinguenda*, *E. eximia, Stylocheiron microphthalma* [Brinton 1962] and for chaetognaths see *Sagitta bedoti, S. robusta, S. neglecta, and S. pulchra* [Bieri 1959]).

One of the strengths of the *k-means* clustering is being able to isolate the relative importance of one biome separation relative to the next. For instance, at k=11 the Southern Ocean is subdivided along the Polar Front, separating the Antarctic and Polar Frontal zones of the Southern Ocean (Tomczak and Godfrey 2003). In the increase in cluster number from 12 to 13, the Bering Sea and Sea of Okhotsk are separated from the rest of the subpolar Pacific. The lower priority of this split is reflected by the decisions of past biogeographers: 1) Longhurst separated this region on the basis of basin depth, seasonal ice cover, water stratification, environmental variability, and the community structure (Longhurst 2007), and 2) Pacific biogeographers did not divide it because of the continuous ranges of most species (Bieri 1959; Brinton 1962; McGowan 1971). Notably, increasing the number of biome clusters from 12 all the way to 16 does not result in a subdivision of the North Pacific by the North Atlantic Current, a classic

physical and biogeographic boundary (Barnard et al. 2004; Tomczak and Godfrey 2003) supported by the division of BFD communities (at *k*=8,foraminiferal groups *VII* and *VIII* share the geographic boundary). The failure of the 10-biome environmental assessment to identify a clear biogeographic boundary in the subpolar North Atlantic highlights a key shortcoming of this analysis, due potentially to the use of *k-means* clustering or the linear combination of 14-environmental variables, the lack of inclusion of an important environmental variable, the correlation of multiple environmental variables, or the metric and scale of environmental variability included. Further modifications to the *k-means* clustering algorithm (like those used by Oliver *et al*. 2008) to fully address the biogeographic concerns raised by this initial investigation (concerning to the split between Subtropical-West and Subtropical-East, and the missed biogeographic break at the North Atlantic Current), and to incorporate variables that are poorly sampled (e.g., community composition, micronutrient availability), difficult to integrate (e.g., sea surface height, current strength, seasonal ice cover), or hard to quantify (e.g., connectivity), will increase the robustness this bioinformatic approaches to biome classification and community clustering.

Appendix 4 : Pairwise investigation of community similarity among individual BFD locations

I investigated pairwise all 855 BDF sites in order to i) test the possibility that the correlation between community similarity in the 8-foraminiferal clusters and environmental similarity was an artifact of the community clustering, and ii) to examine

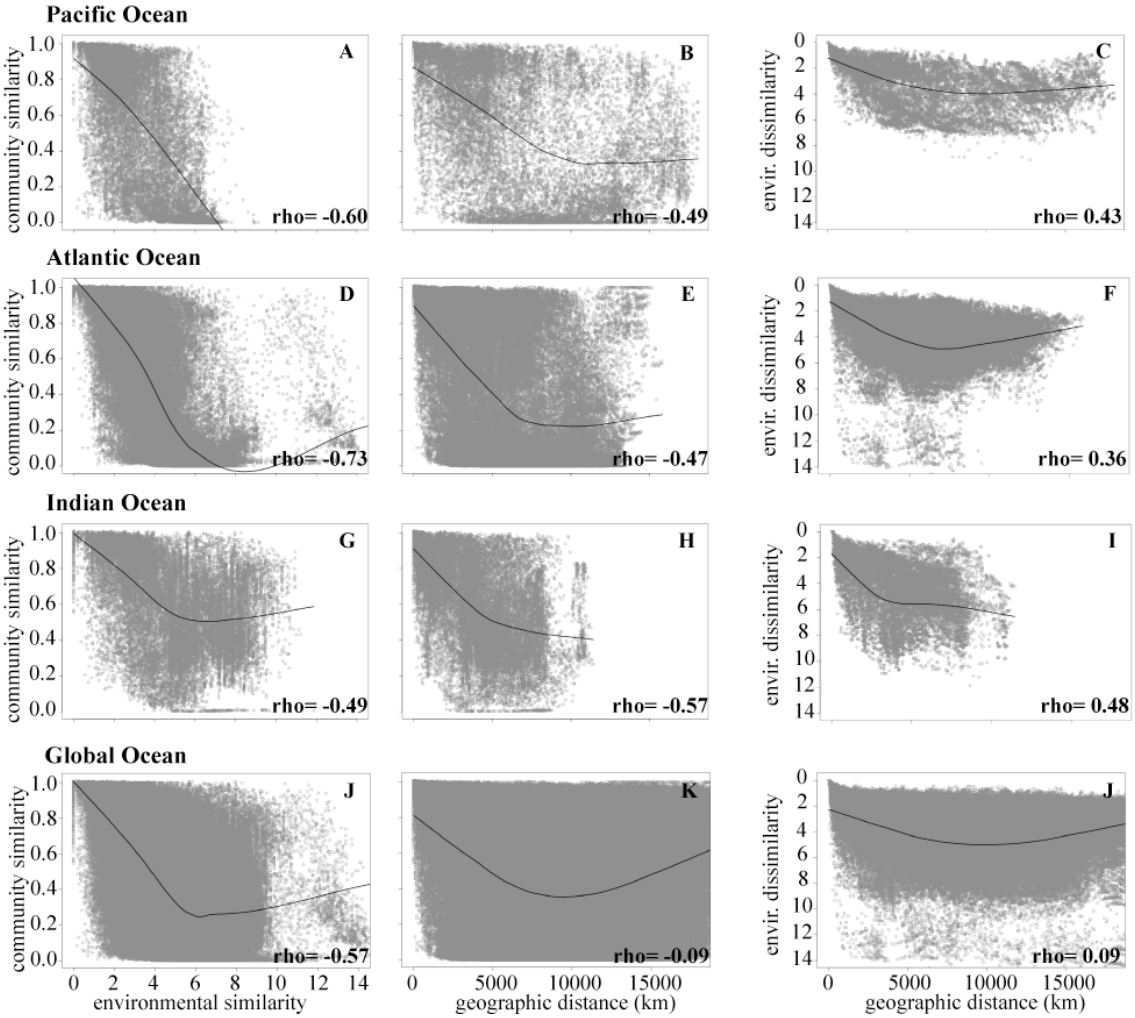

Figure 2-7. Community similarity versus environmental similarity and geographic distance among BFD sites. Planktonic foraminifera community similarity (Morisita's Index) versus environmental similarity (Euclidean distance between environmental variables, identical communities have a distance of zero) and geographic distance (great-circle distance, kilometers) in the (A, B) Pacific, (D, E) Atlantic, and (G, H) Indian Oceans and (J, K) globally. The correlation between geographic distance and environmental similarity is shown for the respective regional comparisons (C,F,I,L); note, the axis for environmental similarity is inverted in these comparisons. Loess regression lines (span = 0.75) and Spearman Rank Correlations (rho) displayed for all relationships. All correlations were significant (< 0.001) as determined with a Mantel test.

distance-decay and environment decay relationships within ocean basins (Atlantic, Pacific and Indian, including adjacent sections of the Southern Ocean). The within-

ocean basin comparisons minimize improbable great circle paths, like cross continental connections, in the calculation of geographic distance, thus removing one potential bias against detecting dispersal limitation from this study. As these comparisons lack clear linear relationships, I test for correlations using a Mantel test with a Spearman's rank correlation (rho) and I visualize correlations using a Loess regression. All correlations were significant (< 0.001) as determined with a Mantel test.

Planktonic foraminifera community similarity is better predicted by environmental similarity than geographic distance in the Pacific and Atlantic Oceans (Figure 2-7a-b,d-e, rho = -0.60 and -0.49 in the Pacific and -0.73 and -0.46 in the Atlantic for environmental and geographic comparisons respectively). The converse is true in the Indian Ocean; community similarity is better predicted by geographic distance rather than environmental similarity (Figure 2-7*g*-h, rho = -0.57 and -0.49 respectively). Environmental similarity is correlated with geographic distance for distances of less than ~10,000 km in the Pacific, less than ~7,000 km in the Atlantic, and less than ~4,000 km in the Indian Ocean (Figure 2-7c,f,i). Considering all ocean basins together, variance in community similarity is predicted predominately by environmental similarity rather than by geographic distance (Figure 2-7j-l, rho = -0.52 and -0.09 respectively).

Importantly, this comparison of all 855 BFD sites indicates that the conclusions of this study are not an artifact of considering relationships among the eight planktonic foraminiferal community groups identified by cluster analysis. While all relationships are significant given the greater sample size, environmental similarity explains more

than 25% of the global variation in community similarity while geographic distance explains less than 1% (Figure 2-7j-k).

The relative importance of environmental similarity is reflected within most ocean basins as well. While the distance-decay relationship can describe the decrease in community similarity at spatial scales of approximately less than 10,000 km in the Pacific Ocean or 7000 km in the Atlantic Ocean (Figure 2-7b,e), above the respective thresholds there is no relationship between community similarity and geographic separation. In contrast, the correlation between environmental and community similarity persists throughout the range of environmental distances (excepting a small upwelling region in the Atlantic accounting for the scatter between environmental distances of 11-14, Figure 2-7a,d). The relatively small environmental range of communities within the Pacific Ocean does not necessarily imply a greater uniformity of environments across the basin; there are simply relative few BFD sites in the Pacific as a result of bottom water conditions.

One exception to the finding that community similarity is primarily correlated with environmental similarity is found in the Indian Ocean. Communities in the Indian Ocean are better correlated with geographic distance rather than environmental similarity (Figure 2-7g-i). This contrary result may primarily arise from the unique geography of the basin; the Indian Ocean is restricted primarily to a single hemisphere and therefore lacks species and biomes with antitropical distributions. Furthermore, upwelling along the extensive coastlines and a monsoonal climate are potentially suboptimally captured by the environmental variables included in this analysis.

ACKNOWLEDGEMENTS

I would like to thank Christian Anderson, Sarah T. Gille, Neil D. Gordon, Aurélien Ponte, Gino A. Passalacqua, and Janet Sprintall for technical suggestions and guidance, Lawrence K. Saul, Joshua Lewis, and Kilian Weinberger for the methodological collaboration that strengthened the foundations of the biome clustering, Holger Kreft, Dov F. Sax, Miriam Goldstein, and Katherine M. Hanson for insightful suggestions and encouragement, and Mark D. Ohman and Richard D. Norris for numerous conversations and extensive comments which considerably improved this manuscript. I was supported by a National Science Foundation Graduate Research Fellowship and obtained additional PAGES travel funds (thanks to Michael N. Dawson) to present my initial results at the International Biogeography Society meeting.

REFERENCES

ANTONOV, J. I., R. A. LOCARNINI, T. P. BOYER, A. V. MISHONOV, and H. E. GARCIA. 2006. World ocean atlas 2005. Volume 2: Salinity. NOAA Atlas NESDIS 62. U.S. Government Printing Office, Washington, D.C.

AZRAN, A., and A. Z. GHAHRAMANI. 2006. Spectral methods for automatic multiscale data clustering 2006 IEEE Computer Society Conference on Computer Vision and Pattern Recognition **1:** 190-197.

BARNARD, R. and others 2004. Continuous plankton records: plankton atlas of the North Atlantic Ocean (1958-1999). II. Biogeographical charts. Marine Ecology-Progress Series **Suppl. S:** 11-75.

BÉ, A. W. H., and D. S. TOLDERLUND. 1971. Distribution and ecology of living planktonic foraminifera in surface waters of the Atlantic and Indian Oceans, p. 105-149. *In* B. M. Funnell and W. K. Riedel [eds.], Micropaleontology of marine bottom sediments. Cambridge University Press, Cambridge.

BECKING, L. E. and others 2006. Beta diversity of tropical marine benthic assemblages in the Spermonde Archipelago, Indonesia. Marine Ecology-An Evolutionary Perspective **27:** 76-88.

BEHRENFELD, M. J., and P. G. FALKOWSKI. 1997. Photosynthetic rates derived from satellite-based chlorophyll concentration. Limnology and Oceanography **42:** 1-20.

BEHRENFELD, M. J. and others 2006. Climate-driven trends in contemporary ocean productivity. Nature **444:** 752-755.

BEKLEMISHEV, K. V. 1969. Pelagic ecology and biogeography [Russian]. Nauka, Moscow.

BIERI, R. 1959. The distribution of the planktonic Chaetognatha in the Pacific and their relationship to the mater masses. Limnology and Oceanography **4:** 1-28.

BOGDANOV, D. V. 1961. Map of the natural zones of the ocean. Okeanologiya **1:** 941-943.

BOGOROV, V. G. 1969. Biology of the Pacific Ocean. Part I. Plankton. U.S. Naval Oceanographic Office, Washington.

BRADSHAW, J. S. 1959. Ecology of living planktonic foraminifera in the North and Equatorial Pacific Ocean. Contributions to the Cushman Foundation for Foraminiferal Research **10:** 25-64.

BRIGGS, J. C. 1974. Marine zoogeography. McGraw-Hill, New York,.

BRINTON, E. 1962. The distribution of Pacific euphausiids. Bulletin of the Scripps Institution of Oceanography **8:** 51-269.

BROECKER, W. S. 1974. Chemical oceanography. Harcourt Brace Jovanovich, Inc., New York.

BROMS, C., and W. MELLE. 2007. Seasonal development of *Calanus finmarchicus* in relation to phytoplankton bloom dynamics in the Norwegian Sea. Deep-Sea Research Part II-Topical Studies in Oceanography **54:** 2760-2775.

CHESTER, R. 2000. Marine geochemistry, 2nd ed. Blackwell Science, Oxford.

DARLING, K. F., M. KUCERA, C. J. PUDSEY, and C. M. WADE. 2004. Molecular evidence links cryptic diversification in polar planktonic protists to quaternary climate dynamics. Proceedings of the National Academy of Sciences of the United States of America **101:** 7657-7662.

DARLING, K. F., M. KUCERA, and C. M. WADE. 2007. Global molecular phylogeography reveals persistent Arctic circumpolar isolation in a marine planktonic protist. Proceedings of the National Academy of Sciences of the United States of America **104:** 5002-5007.

DARLING, K. F., M. KUCERA, C. M. WADE, P. VON LANGEN, and D. PAK. 2003. Seasonal distribution of genetic types of planktonic foraminifer morphospecies in the Santa Barbara Channel and its paleoceanographic implications. Paleoceanography **18:** 1-11.

DARLING, K. F., C. M. WADE, I. A. STEWART, D. KROON, R. DINGLE, and A. J. L. BROWN. 2000. Molecular evidence for genetic mixing of Arctic and Antarctic subpolar populations of planktonic foraminifers. Nature **405:** 43-47.

DE VARGAS, C., R. NORRIS, L. ZANINETTI, S. W. GIBB, and J. PAWLOWSKI. 1999. Molecular evidence of cryptic speciation in planktonic foraminifers and their relation to oceanic provinces. Proceedings of the National Academy of Sciences of the United States of America **96:** 2864-2868.

DE VARGAS, C., S. RENAUD, H. HILBRECHT, and J. PAWLOWSKI. 2001. Pleistocene adaptive radiation in *Globorotalia truncatulinoides*: genetic, morphologic, and environmental evidence. Paleobiology **27:** 104-125.

DE WIT, R., and T. BOUVIER. 2006. 'Everything is everywhere, but, the environment selects'; what did Baas Becking and Beijerinck really say? Environmental Microbiology **8:** 755-758.

DOLAN, J. R. 2005. An introduction to the biogeography of aquatic microbes. Aquatic Microbial Ecology **41:** 39-48.

EKMAN, S. 1953. Zoogeography of the sea. Sidgwick and Jackson, London.

ELLINGSEN, K. E. 2002. Soft-sediment benthic biodiversity on the continental shelf in relation to environmental variability. Marine Ecology-Progress Series **232:** 15-27.

FABER, W. W., O. R. ANDERSON, and D. A. CARON. 1989. Algal-foraminiferal symbiosis in the planktonic foraminifer *Globigerinella aequilateralis*. 2. Effects of 2 symbiont species on foraminiferal growth and longevity. Journal of Foraminiferal Research **19:** 185-193.

FAGER, E. W., and J. A. MCGOWAN. 1963. Zooplankton species groups in North Pacific. Science **140:** 453-460.

FENCHEL, T., and B. J. FINLAY. 2004. The ubiquity of small species: Patterns of local and global diversity. Bioscience **54:** 777-784.

FERRIS, M. J., and B. PALENIK. 1998. Niche adaptation in ocean cyanobacteria. Nature **396:** 226-228.

FIERER, N., and R. B. JACKSON. 2006. The diversity and biogeography of soil bacterial communities. Proceedings of the National Academy of Sciences of the United States of America **103:** 626-631.

FINLAY, B. J. 2002. Global dispersal of free-living microbial eukaryote species. Science **296:** 1061-1063.

FINLAY, B. J., G. F. ESTEBAN, J. L. OLMO, and P. A. TYLER. 1999. Global distribution of free-living microbial species. Ecography **22:** 138-144.

FONTANETO, D., T. G. BARRACLOUGH, K. CHEN, C. RICCI, and E. A. HERNIOU. 2008. Molecular evidence for broad-scale distributions in bdelloid rotifers: everything is not everywhere but most things are very widespread. Molecular Ecology **17:** 3136-3146.

FREESTONE, A. L., and B. D. INOUYE. 2006. Dispersal limitation and environmental heterogeneity shape scale-dependent diversity patterns in plant communities. Ecology **87:** 2425-2432.

FUHRMAN, J. A., I. HEWSON, M. S. SCHWALBACH, J. A. STEELE, M. V. BROWN, and S. NAEEM. 2006. Annually reoccurring bacterial communities are predictable from ocean conditions. Proceedings of the National Academy of Sciences of the United States of America **103:** 13104-13109.

FUHRMAN, J. A., and J. A. STEELE. 2008. Community structure of marine bacterioplankton: patterns, networks, and relationships to function. Aquatic Microbial Ecology **53:** 69-81.

GARCIA, H. E., R. A. LOCARNINI, T. P. BOYER, and J. I. ANTONOV. 2006a. World ocean atlas 2005. Volume 3: Dissolved oxygen, apparent oxygen utilization, and oxygen saturation. NOAA Atlas NESDIS 63. U.S. Government Printing Office, Washington, D.C.

---. 2006b. World ocean atlas 2005. Volume 4: Nutrients (phosphate, nitrate, silicate). NOAA Atlas NESDIS 64. U.S. Government Printing Office, Washington, D.C.

GIESBRECHT, W. 1892. Systematics and faunistics of the pelagic copepods of the Gulf of Napels and the bordering ocean regions [German]. R. Friedlaender, Berlin.

GOETZE, E. 2003. Cryptic speciation on the high seas; global phylogenetics of the copepod family Eucalanidae. Proceedings of the Royal Society of London Series B-Biological Sciences **270:** 2321-2331.

---. 2005. Global population genetic structure and biogeography of the oceanic copepods *Eucalanus hyalinus* and *E. spinifer*. Evolution **59:** 2378-2398.

GREEN, J., and B. J. M. BOHANNAN. 2006. Spatial scaling of microbial biodiversity. Trends in Ecology & Evolution **21:** 501-507.

GREEN, J. L. and others 2004. Spatial scaling of microbial eukaryote diversity. Nature **432:** 747-750.

GREGR, E. J., and K. M. BODTKER. 2007. Adaptive classification of marine ecosystems: Identifying biologically meaningful regions in the marine environment. Deep Sea Research Part I: Oceanographic Research Papers **54:** 385-402.

HARTIGAN, J. A. 1975. Clustering algorithms. Wiley, New York.

HEWSON, I., J. A. STEELE, D. G. CAPONE, and J. A. FUHRMAN. 2006. Temporal and spatial scales of variation in bacterioplankton assemblages of oligotrophic surface waters. Marine Ecology-Progress Series **311:** 67-77.

HUBBELL, S. P. 2001. The unified neutral theory of biodiversity and biogeography. Princeton University Press, Princeton.

HUBER, B. T., J. BIJMA, and K. DARLING. 1997. Cryptic speciation in the living planktonic foraminifer *Globigerinella siphonifera* (d'Orbigny). Paleobiology **23:** 33-62.

HUNT, B. P. V., and G. W. HOSIE. 2005. Zonal structure of zooplankton communities in the Southern Ocean South of Australia: results from a 2150 km continuous plankton recorder transect. Deep-Sea Research Part I-Oceanographic Research Papers **52:** 1241-1271.

JONES, M. M., H. TUOMISTO, D. B. CLARK, and P. OLIVAS. 2006. Effects of mesoscale environmental heterogeneity and dispersal limitation on floristic variation in rain forest ferns. Journal of Ecology **94:** 181-195.

KANAYA, T., and I. KOIZUMI. 1966. Interpretation of Diatom Thanatocoenoses from the North Pacific Applied to a Study of Core V20-130 (Studies of a Deep-sea Core V20-130). Part IV. Science Reports of the Tohoku University, Second Series (Geology) **37:** 89-130.

KNOWLTON, N. 1993. Sibling species in the sea. Annual Review of Ecology and Systematics **24:** 189-216.

KREBS, C. J. 1999. Ecological methodology, 2nd ed. Benjamin/Cummings, Menlo Park.

LEWIS, J. M., P. M. HULL, K. WEINBERGER, and L. SAUL. 2008. Mapping uncharted waters: exploratory analysis, visualization, and clustering of oceanographic data, Proceedings of the 7th International Conference on Machine Learning and Applications 2008. IEEE Computer Society.

LOCARNINI, R. A., A. V. MISHONOV, J. I. ANTONOV, T. P. BOYER, and H. E. GARCIA. 2006. World ocean atlas 2005. Volume 1: Temperature. U.S. Government Printing Office, Washington, D.C.

LONGHURST, A. R. 1998. Ecological geography of the sea. Academic Press, San Diego.

---. 2007. Ecological geography of the sea, 2nd ed. Academic Press, Amsterdam.

MACARTHUR, R. H., and E. O. WILSON. 1967. The theory of island biogeography. Princeton University Press, Princeton, N.J.

MACQUEEN, J. B. 1967. Some methods for classification and analysis of multivariate observations. Proceedings of 5th Berkeley Symposium on Mathematical Statistics and Probability **1:** 281-297.

MARTINY, J. B. H. and others 2006. Microbial biogeography: putting microorganisms on the map. Nature Reviews Microbiology **4:** 102-112.

MCGOWAN, J. A. 1971. Oceanic biogeography of the Pacific, p. 3-74. *In* B. M. Funnell and W. R. Riedel [eds.], The micropalaeontology of the oceans. Cambridge University Press, Cambridge.

---. 1974. The nature of oceanic ecosystems, p. 9-28. *In* C. B. Miller [ed.], The biology of the oceanic Pacific. Oregon State University Press, Corvallis.

MCGOWAN, J. A., and P. W. WALKER. 1993. Pelagic diversity patterns, p. 203-214. *In* R. E. Ricklefs and D. Schluter [eds.], Species diversity in ecological communities. University of Chicago Press, Chicago.

MONTEGUT, C. D., G. MADEC, A. S. FISCHER, A. LAZAR, and D. IUDICONE. 2004. Mixed layer depth over the global ocean: an examination of profile data and a profile-based climatology. Journal of Geophysical Research-Oceans **109:** 1-20.

MOREY, A. E., A. C. MIX, and N. G. PISIAS. 2005. Planktonic foraminiferal assemblages preserved in surface sediments correspond to multiple environment variables. Quaternary Science Reviews **24:** 925-950.

NEKOLA, J. C., and P. S. WHITE. 1999. The distance decay of similarity in biogeography and ecology. Journal of Biogeography **26:** 867-878.

NG, A., M. JORDAN, and Y. WEISS. 2001. On spectral clustering: Analysis and an algorithm. Advances in Neural Information Processing Systems 14.

NIILER, P. P., N. A. MAXIMENKO, and J. C. MCWILLIAMS. 2003. Dynamically balanced absolute sea level of the global ocean derived from near-surface velocity observations. Geophysical Research Letters **30:** 1-4.

NORRIS, R. D. 2000. Pelagic species diversity, biogeography, and evolution. Paleobiology **26:** 236-258.

NORRIS, R. D., and C. DE VARGAS. 2000. Evolution all at sea. Nature **405:** 23-24.

OLIVER, M. J. and others 2004. Bioinformatic approaches for objective detection of water masses on continental shelves. Journal of Geophysical Research-Oceans **109:** 1-12.

OLIVER, M. J., and A. J. IRWIN. 2008. Objective global ocean biogeographic provinces Geophysical Research Letters **35:** 1-6.

OLSON, D. M. and others 2001. Terrestrial ecoregions of the worlds: a new map of life on Earth. Bioscience **51:** 933-938.

PAPKE, R. T., N. B. RAMSING, M. M. BATESON, and D. M. WARD. 2003. Geographical isolation in hot spring cyanobacteria. Environmental Microbiology **5:** 650-659.

PARMENTIER, I., T. STEVART, and O. J. HARDY. 2005. The inselberg flora of Atlantic Central Africa. I. Determinants of species assemblages. Journal of Biogeography **32:** 685-696.

PASTERNAK, A. F., and S. B. SCHNACK-SCHIEL. 2001. Feeding patterns of dominant Antarctic copepods: an interplay of diapause, selectivity, and availability of food. Hydrobiologia **453:** 25-36.

PELLEG, D., and A. MOORE. 2000. X -means: Extending K-means with efficient estimation of the number of clusters, p. 727–734, Proceedings of the 17th International Conference on Machine Learning. Morgan Kaufmann, San Francisco.

PHLEGER, F. B. 1954. Foraminifera and deep-sea research. Deep-Sea Research **2:** 1-23.

PRELL, W., A. MARTIN, J. CULLEN, and M. TREND. 1999. The Brown University Foraminiferal Data Base. IGBP PAGES/World Data Center-A for

Paleoclimatology, Data Contribution Series # 1999-027. The Brown University Foraminiferal Data Base. NOAA/NGDC Paleoclimatology Program, Boulder.

PROSSER, J. I. and others 2007. The role of ecological theory in microbial ecology. Nature Reviews Microbiology **5:** 384-392.

RECHE, I., E. PULIDO-VILLENA, R. MORALES-BAQUERO, and E. O. CASAMAYOR. 2005. Does ecosystem size determine aquatic bacterial richness? Ecology **86:** 1715-1722.

REDFIELD, A. C. 1958. The biological control of chemical factors in the environment. American Scientist **46:** 205-221.

RUSCH, D. B. and others 2007. The Sorcerer II Global Ocean Sampling expedition: Northwest Atlantic through Eastern Tropical Pacific. Plos Biology **5:** 398-431.

RUTHERFORD, S., S. D'HONDT, and W. PRELL. 1999. Environmental controls on the geographic distribution of zooplankton diversity. Nature **400:** 749-753.

SAEZ, A. G., I. PROBERT, M. GEISEN, P. QUINN, J. R. YOUNG, and L. K. MEDLIN. 2003. Pseudo-cryptic speciation in coccolithophores. Proceedings of the National Academy of Sciences of the United States of America **100:** 7163-7168.

SARMIENTO, J. L. and others 2004. Response of ocean ecosystems to climate warming. Global Biogeochemical Cycles **18:** 1-23.

SOININEN, J. 2007. Environmental and spatial control of freshwater diatoms - A review. Diatom Research **22:** 473-490.

SPALDING, M. D. and others 2007. Marine ecoregions of the world: A bioregionalization of coastal and shelf areas. Bioscience **57:** 573-583.

STEUER, A. 1933. Towards a systematic investigation of the geographic distribution of marine plankton, especially the copepods [German]. Zoogeographica. Internationales archiv fuer vergleichende und kasuale tiergeographie**:** 269-302.

STEWART, I. A., K. F. DARLING, D. KROON, C. M. WADE, and S. R. TROELSTRA. 2001. Genotypic variability in subarctic Atlantic planktic foraminifera. Marine Micropaleontology **43:** 143-153.

TAYLOR, J. W., E. TURNER, J. P. TOWNSEND, J. R. DETTMAN, and D. JACOBSON. 2006. Eukaryotic microbes, species recognition and the geographic limits of species: examples from the kingdom Fungi. Philosophical Transactions of the Royal Society B-Biological Sciences **361:** 1947-1963.

TOBLER, W. R. 1970. A computer movie simulating urban growth in the Detroit region. Economic Geography **46:** 234-240.

TOMCZAK, M., and J. S. GODFREY. 2003. Regional oceanography: an introduction, 2nd ed. Daya Pub. House, Delhi.

TONNIS, B., P. R. GRANT, B. R. GRANT, and K. PETREN. 2005. Habitat selection and ecological speciation in Galapagos warbler finches (*Certhidea olivacea* and *Certhidea fusca*). Proceedings of the Royal Society B-Biological Sciences **272:** 819-826.

TUOMISTO, H., K. RUOKOLAINEN, and M. YLI-HALLA. 2003. Dispersal, environment, and floristic variation of western Amazonian forests. Science **299:** 241-244.

VAN DER GUCHT, K. and others 2007. The power of species sorting: Local factors drive bacterial community composition over a wide range of spatial scales. Proceedings of the National Academy of Sciences of the United States of America **104:** 20404-20409.

VANORMELINGEN, P., E. VERLEYEN, and W. VYVERMAN. 2008. The diversity and distribution of diatoms: from cosmopolitanism to narrow endemism. Biodiversity and Conservation **17:** 393-405.

VINARSKI, M. V., N. P. KORALLO, B. R. KRASNOV, G. I. SHENBROT, and R. POULIN. 2007. Decay of similarity of gamasid mite assemblages parasitic on Palaearctic small mammals: geographic distance, host-species composition or environment. Journal of Biogeography **34:** 1691-1700.

VINCENT, E., and W. H. BERGER. 1981. Planktonic foraminifera and their use in paleoceanography, p. 1025-1119. *In* C. Emiliani [ed.], The Oceanic Lithosphere. The Sea: Ideas and observations on progress in the study of the seas. John Wiley & Sons, Inc., New York.

VYVERMAN, W. and others 2007. Historical processes constrain patterns in global diatom diversity. Ecology **88:** 1924-1931.

WHITAKER, R. J., D. W. GROGAN, and J. W. TAYLOR. 2003. Geographic barriers isolate endemic populations of hyperthermophilic archaea. Science **301:** 976-978.

WIENS, J. J. 2004. Speciation and ecology revisited: phylogenetic niche conservatism and the origin of species. Evolution **58:** 193-197.

WORM, B., M. SANDOW, A. OSCHLIES, H. K. LOTZE, and R. A. MYERS. 2005. Global patterns of predator diversity in the open oceans. Science **309:** 1365-1369.

ZWIRGLMAIER, K. and others 2008. Global phylogeography of marine Synechococcus and Prochlorococcus reveals a distinct partitioning of lineages among oceanic biomes. Environmental Microbiology **10:** 147-161.

Chapter II was submitted for publication as: “The relative importance of environment and dispersal to global pelagic community similarity”. The dissertation author was the primary investigator and author of this paper.

CHAPTER III

Evidence for abrupt speciation in a classic case of gradual evolution

Evidence for abrupt speciation in a classic case of gradual evolution

Pincelli M. Hull[1] and Richard D. Norris

Scripps Institution of Oceanography, University of California at San Diego, La Jolla, CA 92093

Edited by Michal Kucera, University of Tubingen, Germany, and accepted by the Editorial Board October 7, 2009 (received for review March 23, 2009)

In contrast with speciation in terrestrial organisms, marine plankton frequently display gradual morphological change without lineage division (e.g., phyletic gradualism or gradual evolution), which has raised the possibility that a different mode of evolution dominates within pelagic environments. Here, we reexamine a classic case of putative gradual evolution within the *Globorotalia plesiotumida–G. tumida* lineage of planktonic foraminifera, and find both compelling evidence for the existence of a third cryptic species during the speciation event and the abrupt evolution of the descendant *G. tumida*. The third morphotype, not recognized in previous analyses, differs in shape and coiling direction from its ancestor, *G. plesiotumida*. This species dominates the globorotaliid population for 414,000 years just before the appearance of *G. tumida*. The first population of the descendant, *G. tumida*, evolves abruptly within a 44,000-year interval. A combination of morphological data and biostratigraphic evidence suggests that *G. tumida* evolved by cladogenesis. Our findings provide an unexpected twist on one of the best-documented cases of within-lineage phyletic gradualism and, in doing so, revisit the limitations and promise of the study of speciation in the fossil record.

cladogenesis | evolutionary dynamics | foraminifera | fossil record | plankton

The fossil record in marine plankton is characterized by gradual morphological change both with and without apparent cladogenesis (1–10). Phyletic gradualism has been attributed to a lack of barriers to gene flow in species that are both cosmopolitan and phenotypically plastic (11–13). However, a growing number of phylogenetic studies have revealed the presence of multiple cryptic species within named marine morphospecies (14–16). In some cases, within-species morphological clines have subsequently been found to consist of numerous genetically, biogeographically, and ecologically distinct species (17, 18). The presence of cryptic species complexes in the modern ocean suggests a fossil record laden with hidden cladogenetic events (19) potentially affecting the perception and interpretation of evolutionary patterns.

The existence of cryptic species complexes, and the consequent discrepancy between morphological and genetic species, is of general concern because open ocean microfossils provide one of the best records (temporally and spatially) of the last 130 million years of life (20–22). For instance, planktonic foraminifera have been used in global studies of the determinants of species richness (23), body size (24, 25), and speciation (26). For all the utility of open ocean microfossils, there have been relatively few coordinated studies of both the morphologic and genetic similarity of individuals in the modern ocean (although see refs. 17, 18, 27, and 28). There is also evidence that open ocean microfossils may not actually conform to the morphological species concept. A high-resolution study of the *Globorotalia* lineage of planktonic foraminifera in the Early to Middle Miocene failed to find evidence of discrete, nonoverlapping morphological clouds as is expected in the typical morphological species concept (29).

The morphological similarity of foraminiferal species has implications for the detection of cladogenesis. Most past studies have either assumed a priori that cladogenesis occurred (7–9, 30) or, if not, have interpreted evolutionary trends as cases of within-lineage evolution after considering trait distributions (1, 5). Trait variation within a given species is typically normally distributed and, in theory, deviations from normality should occur when two or more species coexist. In practice, this normality test for cladogenesis has little statistical power when two morphologically similar species with high trait variability coexist (as described in ref. 29) and are sampled at the sample sizes typical of past studies (31). Sample variance can also be used to detect the presence of multiple taxa with some of the same statistical limitations (4). The lack of clear correspondences between named morphospecies and discrete morphological clusters increases the difficulty of detecting cladogenesis in fossil planktonic foraminifera. In one instance, reproductive isolation and, putatively, speciation was found to be uncoupled from morphological evolution in the *Fohsella* lineage of globorotaliid foraminifera (32).

Here we test for speciation in the fossil record within a lineage of planktonic foraminifera. In this study, we use the term *speciation* to refer to cladogenetic events (e.g., phyletic splitting), and not within-lineage evolution. We reexamine a classic case of putative gradual evolution in which the ancestor *Globorotalia plesiotumida* is thought to have evolved over ≈500,000 years into the descendant *G. tumida* (1, 33). Both before and after the morphological transition there are several million years of morphological stasis suggesting that this case represents a hybrid of phyletic gradualism and morphological stasis dubbed ''punctuated gradualism'' (33). The *G. tumida* lineage has often been reexamined in studies of evolutionary mode (34–40), due to the compelling results and data availability of Malmgren et al.'s original study (33). In readdressing this widely cited case of within-lineage gradual evolution, we consider the effect of methodology on our perception of evolutionary trends, test for the possibility of phyletic splitting and within-lineage change, and reconsider the morphological species concept in planktonic foraminifera.

Results and Discussion

We analyze morphological change in the *Globorotalia plesiotumida–G. tumida* evolutionary series in a deep-sea sediment core record from the western tropical Pacific [Ocean Drilling Program (ODP) site 806B, Ontong Java Plateau, 0°19.11′N, 159°21.69′E, 2,520 m water depth]. Using eigenshape analysis (a morphometric technique for comparing outlines) (41, 42) and an updated time scale (supporting information (SI) Fig. S1), we

Author contributions: P.M.H. and R.D.N. designed research; R.D.N. performed research; P.M.H. analyzed data; and P.M.H. and R.D.N. wrote the paper.

The authors declare no conflict of interest.

This article is a PNAS Direct Submission. M.K. is a guest editor invited by the Editorial Board.

[1]To whom correspondence should be addressed. E-mail: phull@ucsd.edu.

This article contains supporting information online at www.pnas.org/cgi/content/full/0902887106/DCSupplemental.

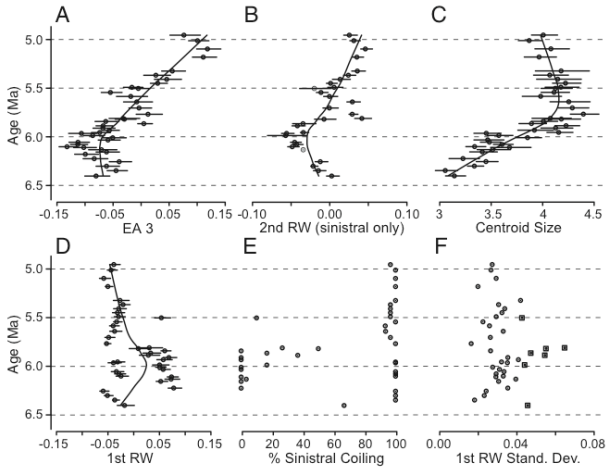

Fig. 1. Morphological trends over time in the *Globorotalia plesiotumida–G. tumida* lineage in the western equatorial Pacific. Mean morphology as a function of time expressed as (*A*) an eigenshape amplitude (EA 3) from eigenshape analysis (all individuals), (*B*) a relative warp score (RW 2) from semilandmark TPS analysis (all individuals analyzed, sinistrally coiled individuals plotted), (*C*) centroid size (all individuals), and (*D*) a relative warp score (RW 1) from semilandmark TPS analysis (all individuals). Error bars in (*A–D*) are parametric 95% CI and mean values are fit with a loess curve. (*E*) Percent sinistral coiling individuals and (*F*) the standard deviation of RW 1 as a function of time. Boxed values in (*F*) indicate samples with 20% or greater overlap in sinistral and dextral coiled individuals. Gray points in (*B*) indicate samples containing three or fewer individuals.

obtained a similar pattern of morphological evolution in the western tropical Pacific as was found in an earlier study in the central Indian Ocean (Fig. 1*A* and Fig. S2). The similarity of both results, despite using materials from widely separated sites, suggests that the evolutionary transition is synchronous across a large stretch of the ocean. Indeed, *G. tumida* displays a near-simultaneous first appearance throughout the tropical Indo-Pacific with a geographic range overlapping that of *G. plesiotumida* at the Miocene/Pliocene boundary (refs. 43–45; see also *SI Materials and Methods* and Fig. S3). Our study design was therefore predicated on the hypothesis that the morphological evolution of *G. tumida* in the western tropical Pacific occurred in situ.

Our analysis departs from previous analyses by controlling for the effects of shell size on morphology, and by using a different morphometric method. In Malmgren et al.'s study (33), a 3-fold increase in mean size accompanies the morphological transition in the *G. tumida–G. plesiotumida* lineage and is strongly correlated with mean morphology along eigenaxis 2 (EA 2, Pearson's $r = 0.89$ and $P < 0.001$). Here we explicitly control for the effect of size on the perceived evolutionary trend by sampling individuals in a narrower size range (250–500 μm in contrast to the ~150-500 μm originally used). Given this greater control for size, the correlation between size and EA 3 is weak (Pearson's $r = 0.23$ and $P < 0.001$). However, we still note a ≈1.4-fold increase in mean centroid size in the equatorial Pacific (Fig. 1*C*).

In an additional departure, we use a second morphometric technique for analyzing outlines, semilandmark thin-plate spline analysis (semilandmark TPS) (46). Methodological aspects of semilandmark TPS techniques suggest advantages of this approach over eigenshape analysis (*SI Materials and Methods*). The second relative warp (RW 2, a morphological eigenaxis capturing 20% of morphological variance) is correlated to EA 3 from eigenshape analysis (Pearson's $r = 0.70$ and $P < 0.001$ for sinistrally coiled individuals; see also Fig. S4) and reveals a comparable shift in mean morphology (Fig. 1*B*). However, our findings also show critical differences between the two methods.

Surprisingly, the first relative warp (RW 1) of the semilandmark TPS analysis indicates that some individuals present during the transition are morphologically more distinct than *Globorotalia plesiotumida* and *G. tumida* are from each other (Fig. 1*D*; RW 1 captures 53% of morphological variance). These divergent individuals are distinctly flattened (see Fig. 3*C Middle* and Movie S1) and are easily differentiated by eye. Furthermore, the flattened morphotype is almost exclusively dextrally coiled (clockwise chamber addition from the spiral perspective) and rarely coexists with sinistral *G. plesiotumida* (Figs. 2 and 3*A*). Grouping individuals by coiling direction reveals a significant difference in the RW 1 scores of sinistral and dextral coiled individuals (Fig. 2; *t* test, $P < 0.001$). A few dextral individuals occur in our oldest sample at 6.403 Ma, but these are more *G. plesiotumida*-like in their outline morphology than any subsequent dextral population. Dextral morphotypes display the typical elongated final chamber often used as a defining characteristic of *G. plesiotumida*. Where dextral and sinistral individuals do co-occur (20% or greater overlap), the populations exhibit higher morphological variance along RW 1 (Fig. 1*F*) than is the case for populations dominated by one coiling morphology. Additionally, we find significant differences in RW 1 scores between coiling groups in each of the seven time periods containing at least three individuals per coiling direction (*t* test, $P < 0.001$). A maximum likelihood analysis of mixture models provides statistical support for the interpretation of two coexisting morphotypes rather than a single morphotype in six time periods (Fig. 3*A*; stars indicate significance at 0.05 and squares at 0.06 significance level; details in *Materials and Methods* and ref. 47).

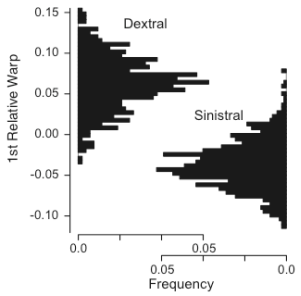

Fig. 2. Distribution of relative warp 1 scores for dextrally and sinistrally coiled individuals. Each histogram is scaled to a unit area. Sinistral and dextral distributions are significantly different (*t* test, $P < 0.001$).

The correspondence between coiling direction and morphology suggests that the flattened, dextral morphotype represents a species fully differentiated from the sinistral *G. plesiotumida*. Our evidence for a cryptic species in the *G. plesiotumida* complex is consistent with evidence in other groups of foraminifera that coiling direction is a heritable trait (48, 49). In two modern planktonic foraminiferal species, *Neogloboquadrina pachyderma* and *Globorotalia truncatulinoides*, coiling direction was found to be indicative of cryptic species (17, 28).

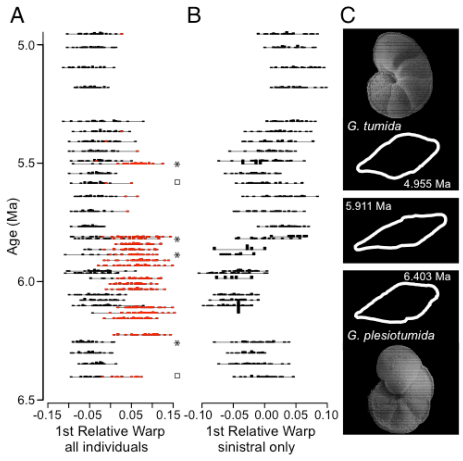

Fig. 3. Morphological change in the *Globorotalia plesiotumida–G. tumida* lineage. (*A*) Morphology viewed as histograms along relative warp 1, with sinistrally coiled individuals in black and dextrally coiled individuals in red, and (*B*) along relative warp 1 as calculated for sinistrally coiled individuals. Stars indicate two overlapping populations supported at a 0.05 significance level and squares at a 0.06 significance level. (*C*) Scanning electron microscopy (umbilical view) and digitized outlines (edge view) of sinistrally coiled *Globorotalia plesiotumida* and *G. tumida* (top two and bottom two panels) and the dextral morphospecies (*Middle*). Individuals panels of morphology with time along RW 1 and RW 2 are shown in Movie S2.

The dextral, flattened morphotype becomes abruptly dominant in our record at 6.225 Ma, and persists for 414,000 years until 5.819 Ma. During this period, which overlaps the start of the gradual evolution of *G. tumida* in eigenshape analyses, the dextrally coiled morphogroup oscillates in dominance with the sinistrally coiled morphogroup. In many oscillations, the abundance of the rare morphotype (sinistral or dextral) is zero. These recorded absences may coincide with time periods during which a given morphotype is globally rare and therefore unsampled. Alternatively, the absences may indicate periods of changing biogeographic distributions, with rare morphotypes found in abundance in other locations. Based on our sampling scheme, we cannot determine which of these two alternatives is more likely.

After the period of oscillating dominance, rare dextrally coiled individuals are present for an additional 444,000 years with a second peak in dextral abundance at 5.503 Ma. Together, these data suggest that the flattened, dextral taxon evolved by cladogenesis and coexisted with its ancestor for at least 850,000 years. If the global first appearance of the dextral species is recorded in our sample set at 6.256 Ma, then its evolution was very rapid, occurring within a 26,000-year window. However, we caution that it is possible that the first appearance of the flattened dextral taxon could reflect immigration or have occurred at or before 6.403 Ma in the equatorial Pacific. Dextral individuals are recorded in the Indian Ocean before 6.4 Ma (33), but whether these have the flattened morphology of the cryptic taxon described here is yet to be determined.

A second cladogenetic event may accompany the first appearance of fully differentiated *Globorotalia tumida* between 5.865 and 5.819 Ma. In this case, both the ancestor, *G. plesiotumida*, and the descendant, *G. tumida*, are sinistrally coiled and therefore differentiated entirely upon a change in outline morphology (Fig. 3*B*). Cladogenesis is indicated by several factors, including (*i*) the abrupt shift in mean morphology toward *G. tumida* within a 44,000-year span (mean shift >1.5 SD), (*ii*) the co-occurrence of pre- and postshift morphologies at 5.819 Ma, a period of elevated population variance (one of the three highest observed), (*iii*) the observation of several reversals in the population morphology toward the *G. plesiotumida* type, and (*iv*) periods of elevated variance between 5.819 and ≈5.5 Ma. Finally, a short interval of co-occurrence (several 100 kya) between *G. plesiotumida* and *G. tumida* is indicated in Indian Ocean records (50). In the Atlantic, *G. plesiotumida* persists well into the middle Pliocene (51, 52).

Throughout the entire time series, maximum likelihood analysis of mixture models provides support for only one sinistral population per time interval (Fig. 3*B*; RW $1_{\text{sinistral}}$ results shown, approximately equivalent to RW 2_{all} as explained in *Materials and Methods* and see Fig. S5), in possible agreement with Malmgren et al.'s (33) interpretation of gradual, within-lineage evolution. However, the high variance in morphology within some samples (particularly between 5.5 and 6.0 Ma) suggests that there could be two coexisting species at several points in the time series. Unfortunately, our maximum likelihood analysis has very low power (0.01–0.48) to detect overlapping populations if they exist, due in part to our small sample size. We conclude that we cannot unambiguously determine whether *G. plesiotumida* co-occurs in the same samples with *G. tumida* during the transition period from approximately 6–5.5 Ma. Both larger sample sizes and more informative traits could help resolve this ambiguity in future studies.

Our conclusions differ from those of Malmgren et al. (1, 33) in two critical ways. First, our methods clearly identify the ecological dominance of a flattened, dextral cryptic species just before the appearance of *G. tumida*, which is inferred to

have arisen cladogenetically from a *G. plesiotumida* ancestor. Malmgren et al. (33) noted the presence of dextral, biconvex forms during the transitional period like the compressed, dextrally coiled individuals we see in the western equatorial Pacific. However, they did not find morphometric evidence that would distinguish these dextral forms as species in their own right. Second, previous work has not detected as rapid an appearance of fully formed *G. tumida* as we observe here at 5.81 Ma. Malmgren et al. (33) did observe a step in both shell size and morphology about this time, but they attributed these morphological shifts to oscillations within a longer evolutionary trend.

Our findings show that morphometric techniques and measurement strategy are key to the interpretation of evolution in the fossil record. It is disturbing that eigenshape analysis (used by previous authors) fails to detect differences in compression of individuals in the equatorial Pacific, where both semilandmark TPS analysis and visual inspection confirm the distinct morphology of dextrally coiled individuals. We hypothesize that eigenshape analysis cannot detect differences in shell compression that are not accompanied by major changes in the angles between many points (see *SI Materials and Methods*). Malmgren et al. (33) also ruled out the possibility of cladogenesis due to the apparent lack of bimodality within populations. This test is less powerful than the mixture models used here, because distributions never appear bimodal along RW 1 even when multiple morphospecies coexist (Fig. 3*A*). Finally, both our outline data and those collected by Malmgren et al. (33) fail to capture essential aspects of shell morphology, such as the shape of the final chamber, that are used by taxonomists to differentiate *Globorotalia plesiotumida* and *G. tumida*. Without examining a larger subset of informative characters, it is difficult to assess whether the perceived mode of evolution and the applicability of the morphological species concept is an artifact of the morphological traits under consideration. Consequently, this and other morphometric studies may lack adequate information to clearly differentiate speciation from within lineage evolution.

A synthesis of past studies of cladogenesis has documented a common pattern of sympatric speciation in open ocean taxa (6), with the gradual divergence of the mean daughter morphotype from a stable ancestral morphotype for ≈500,000 years following speciation in foraminifera (8, 9), radiolarians (30, 53), and diatoms (7). In contrast to instances of sympatric speciation, morphological change associated with allopatric speciation in marine microfossils can be rapid (10 kya) (54).

Our findings add to these observations by showing that, at least in this classic case, the evolution of *G. tumida* from *G. plesiotumida* was not a simple affair. Evolution involved both the cryptic evolution of a dextral, compressed morphotype and the rapid evolution of *G. tumida*, in both cases likely by cladogenesis. The dramatic decrease in abundance of the flattened dextral forms coincides with the abrupt appearance of *G. tumida*. It is clear that the first *G. tumida* appeared very rapidly, in less than 45,000 years, rather than the hundreds of thousands of years inferred from previous work. Furthermore, stratigraphic analysis from other sites has shown that *G. plesiotumida* persists after the evolution of *G. tumida*. Changes in the dominance of coexisting ancestral and descendant morphotypes occur several times and may be due to an oscillation in the environment. Our work underscores the inherent difficulty of inferring evolutionary mechanisms from fossils. At the same time, our study highlights observations unique to the fossil record, including the measurement of evolutionary patterns, species coexistence, and changing population variance through time.

Materials and Methods

Sample Preparation. Within each time interval, we sampled the first 30 individuals encountered from the *Globorotalia plesiotumida–tumida* lineage in the >250-μm size fraction from ODP site 806B on the Ontong Java Plateau (1,140 individuals from 38 depth intervals; Dataset S1). An age model was calculated for the Ontong Java Plateau using 10 biostragraphic markers (55) and assuming constant sedimentation rates between markers (Fig. S1; age model for Atlantic site 959C also shown). The two exceptions to the sampling protocol of 30 individuals occurred in samples at 163.27- and 194.77-meter composite depth (mcd) where 31 and 29 individuals were analyzed, respectively. Individuals were cleaned, taped to glass coverslips, and mounted on a universal stage for the digitization of the edge view using a video capture system. A digitized 2D outline of each individual (100 coordinate points, approximately evenly spaced around the foraminiferal edge view) was initialized at the proloculous for morphometric analyses (41, 42) (Dataset S1).

Morphometric Methods. Semilandmark thin-plate spline analysis is a landmark morphometric technique adapted to assessing similarity among outlines by ignoring differences that arise from the location of coordinates along an outline (46). After an initial consensus form (or mean shape) is calculated, points are allowed to slide along individual outlines to minimize the difference between individual shapes and the consensus form (56, 57). If the semilandmark analysis is recursive, then the postsliding location of points for each outline is used in the next iteration. If the semilandmark analysis is not recursive, then the consensus form is updated for each iteration, but individual outline points always start in same initial location. Eigenshape analysis (41, 42) was also used to compare results between the Pacific and Indian Ocean (see *SI Materials and Methods* for details on this method). Note, the signs of eigenaxes and relative warps can vary between analyses. Signs were reversed along eigenaxes and relative warps when necessary to conform to the orientation of Malmgren et al. (33). For instance, signs were reversed for RW 1_{all} and RW 2_{all} in Figs. 1–3 and related statistics.

Although theoretically preferable, recursive semilandmark TPS was computationally prohibitive given the large number of outlines (1,140) and sliding points (100 per outline) in this study. We assessed the effect of using recursive versus nonrecursive TPS by analyzing a representative subset of individuals with both techniques (304 total outlines, including eight randomly chosen individuals per time interval). Recursive and nonrecursive semilandmark results were highly correlated along the first three relative warps (Pearson's $r > 0.91$, $P < 0.001$), accounting altogether for 73% and 82% of morphological variance, respectively (Table S1). Judging from this subset of outlines, and specifically comparing the relative assignments of dextral and sinistral individuals, the effect of using nonrecursive semilandmark analysis on our interpretation of the large-scale RW 1 displacements is minimal. This was potentially not the case for the subtle trends in sinistrally coiled individuals along relative warp 2. Therefore, sinistral individuals (719 total) were separately analyzed using a recursive semilandmark analysis (three iterations). The first relative warp from sinistral semilandmark TPS analysis was strongly correlated with the second relative warp from the full analysis ($r^2 = 0.94$, $P < 0.001$), and was used in Fig. 3 and in all statistical considerations of the evolution of *G. tumida* from *G. plesiotumida*.

As a preprocessing step to semilandmark TPS analysis, we first performed a Generalized Procrustes alignment (involving translation, rotation, and scaling) to minimize the sum-squared distance between outline points and a consensus shape using the function procGPA in the package ''shapes'' (version 1.0–8) in R (version 2.2.1) (58). This particular function allows shapes to be mirrored, an option that we used to minimize the apparent shape differences between left- and right-coiled individuals (shape outlines and mirroring results visualized in Movie S1).

Here we use relative warps (RWs) to described main patterns of shape change in the *G. plesiotumida–G. tumida* lineage. We used the program tpsRelw (version 1.46, created by F. James Rohlf) for all semilandmark analyses, including the calculation of relative warps. In tpsRelw, we used orthogonal projections and scaling by the cos (rho) for Procrustes alignments; results were unaffected by scaling by a unit centroid size ($r^2 > 0.9999$ for the first 10 relative warps in TPS analysis). Uniform weighting of all partial warps ($\alpha = 0$) was used to include uniform components in the partial warp scores matrix. Uniform components of shape change were estimated as the complement to the nonuniform shape variation (59). Finally, due to computational limitations and the similarity of TPS and semilandmark TPS results (Table S1), semilandmark TPS analysis was run for a maximum of three sliding iterations.

Maximum Likelihood Analysis of Mixture Models. A maximum likelihood analysis of mixture models was used to assess the number of distinct populations along RW 1_{all} and RW $1_{sinstral}$. The maximum likelihood framework allowed us to test the relative support for one or more overlapping populations within a single time period and morphological distribution (specifically, the histograms in Fig. 3). All analyses were performed using the program Mixture Model Analysis (version 1.32, created by G. Hunt) and a previously described approach (47).

In brief, we calculated the likelihood of one to two populations for each time interval along RW 1_{all} and RW $1_{sinistral}$ (roughly equivalent to RW 2_{all}) using 200 random initiations, and assuming equal population variance and a normal distribution. A bootstrap approach was used to determine the relative support for one or more distributions, as increasing parameters generally improves model fit (e.g., the log-likelihood ratio will favor the model with more populations). To compare the relative support for one versus two overlapping populations, we generated 1,000 sample distributions based on the mean and variance calculated for a single population and compared these maximum likelihood estimates with that determined empirically for two overlapping populations. If the two-population log-likelihood ratio was greater than 95% of those generated from a single population ($\alpha = 0.05$), then we considered two overlapping populations more likely than a single population in a given time period. In interpreting negative results (e.g., the failure to reject a single population), we assessed the power of the maximum likelihood test using a second bootstrapped approach (log-likelihood ratio obtained from alpha in the first bootstrap test and assumed population parameters for two populations to generate distributions; see details in ref. 47).

ACKNOWLEDGMENTS. We thank L. Saul and S. Belongie for morphometric advice; M. D. Ohman and P. J. S. Franks for comments on the manuscript; G. Hunt, two anonymous reviewers, and the editor for thorough and insightful suggestions that greatly improved the manuscript; J. M. Lewis for making key contributions to an earlier iteration of this study; and the Ocean Drilling Program for providing samples. This work was supported by a National Science Foundation Division of Earth Sciences (EAR) grant (to R.D.N.) and a National Science Foundation graduate research fellowship (to P.M.H.).

1. Malmgren BA, Berggren WA, Lohmann GP (1984) Species formation through punctuated gradualism in planktonic foraminifera. *Science* 225:317–319.
2. Malmgren BA, Kennett JP (1981) Phyletic gradualism in a Late Cenozoic planktonic foraminiferal lineage: DSDP site 284, southwest Pacific. *Paleobiology* 7:230–240.
3. Malmgren BA, Kucera M, Ekman G (1996) Evolutionary changes in supplementary apertural characteristics of the late Neogene *Sphaeroidinella dehiscens* lineage (planktonic foraminifera). *Palaios* 11:192–206.
4. Arnold AJ (1983) Phyletic evolution in the *Globorotalia crassaformis* (Galloway and Wissler) lineage: A preliminary report. *Paleobiology* 9:390–397.
5. Kucera M, Malmgren BA (1998) Differences between evolution of mean form and evolution of new morphotypes: An example from Late Cretaceous planktonic foraminifera. *Paleobiology* 24:49–63.
6. Benton MJ, Pearson PN (2001) Speciation in the fossil record. *Trends Ecol Evol* 16:405–411.
7. Sorhannus U, Fenster EJ, Burckle LH, Hoffman A (1988) Cladogenetic and anagenetic changes in the morphology of *Rhizosolenia praebergonii* Mukhina. *Hist Biol* 1:185–205.
8. Lazarus D, Hilbrecht H, Spencercervato C, Thierstein H (1995) Sympatric speciation and phyletic change in *Globorotalia truncatulinoides*. *Paleobiology* 21:28–51.
9. Wei KY (1994) Stratophenetic tracing of phylogeny using SIMCA pattern recognition technique: A case study of the late Neogene planktic Foraminifera Globoconella clade. *Paleobiology* 20:52–65.
10. Hunt G (2007) The relative importance of directional change, random walks, and stasis in the evolution of fossil lineages. *Proc Natl Acad Sci USA* 104:18404–18408.
11. Lohmann GP, Malmgren BA (1983) Equatorward migration of *Globorotalia truncatulinoides* ecophenotypes through the Late Pleistocene: Gradual evolution or ocean change? *Paleobiology* 9:414–421.
12. Kucera M, Malmgren BA (1996) Latitudinal variation in the planktic foraminifer *Contusotruncana contusa* in the terminal Cretaceous ocean. *Mar Micropaleontol* 28:31–52.
13. Boltovskoy D, Vrba A (1989) Latitude-related shell patterns in Radiolaria: *Botryostrobus auritus/australis* morphotypes in the equatorial to Antarctic Pacific. *Mar Micropaleontol* 13:309–323.
14. Knowlton N (1993) Sibling species in the sea. *Annu Rev Ecol Syst* 24:189–216.
15. Goetze E (2003) Cryptic speciation on the high seas; global phylogenetics of the copepod family Eucalanidae. *Proc R Soc Lond Ser B* 270:2321–2331.
16. Saez AG, et al. (2003) Pseudo-cryptic speciation in coccolithophores. *Proc Natl Acad Sci USA* 100:7163–7168.
17. de Vargas C, Renaud S, Hilbrecht H, Pawlowski J (2001) Pleistocene adaptive radiation in *Globorotalia truncatulinoides*: Genetic, morphologic, and environmental evidence. *Paleobiology* 27:104–125.
18. de Vargas C, et al. (1999) Molecular evidence of cryptic speciation in planktonic foraminifers and their relation to oceanic provinces. *Proc Natl Acad Sci USA* 96:2864–2868.
19. Alizon S, Kucera M, Jansen VAA (2008) Competition between cryptic species explains variations in rates of lineage evolution. *Proc Natl Acad Sci USA* 105:12382–12386.
20. Phleger FB (1954) Foraminifera and deep-sea research. *Deep Sea Res* 2:1–23.
21. Vincent E, Berger WH (1981) in *The Oceanic Lithosphere*, ed Emiliani C (Wiley, New York), Vol 7, pp 1025–1119.
22. Norris RD, de Vargas C (2000) Evolution all at sea. *Nature* 405:23–24.
23. Rutherford S, D'Hondt S, Prell W (1999) Environmental controls on the geographic distribution of zooplankton diversity. *Nature* 400:749–753.
24. Schmidt DN, Thierstein HR, Bollmann J, Schiebel R (2004) Abiotic forcing of plankton evolution in the Cenozoic. *Science* 303:207–210.
25. Schmidt DN, et al. (2004) Size distribution of Holocene planktic foraminifer assemblages: Biogeography, ecology and adaptation. *Mar Micropaleontol* 50:319–338.
26. Allen AP, Gillooly JF, Savages VM, Brown JH (2006) Kinetic effects of temperature on rates of genetic divergence and speciation. *Proc Natl Acad Sci USA* 103:9130–9135.
27. Huber BT, Bijma J, Darling K (1997) Cryptic speciation in the living planktonic foraminifer *Globigerinella siphonifera* (d'Orbigny). *Paleobiology* 23:33–62.
28. Darling KF, Kucera M, Kroon D, Wade CM (2006) A resolution for the coiling direction paradox in *Neogloboquadrina pachyderma*. *Paleoceanography* 21:PA2011, 10.1029/2005PA001189.
29. Tabachnick RE, Bookstein FL (1990) The structure of individual variation in Miocene *Globorotalia*. *Evolution* 44:416–434.
30. Kellogg DE, Hays JD (1975) Microevolutionary patterns in Late Cenozoic Radiolaria. *Paleobiology* 1:150–160.
31. Cohen J (1988) *Statistical Power Analysis for the Behavioral Sciences* (Erlbaum, Hillsdale, NJ).
32. Norris RD, Corfield RM, Cartlidge J (1996) What is gradualism? Cryptic speciation in globorotaliid foraminifera. *Paleobiology* 22:386–405.
33. Malmgren BA, Berggren WA, Lohmann GP (1983) Evidence for punctuated gradualism in the Late Neogene *Globorotalia tumida* lineage of planktonic foraminifera. *Paleobiology* 9:377–389.
34. Bookstein FL (1987) Random walk and the existence of evolutionary rates. *Paleobiology* 13:446–464.
35. Charlesworth B (1984) Some quantitative methods for studying evolutionary patterns in single characters. *Paleobiology* 10:308–318.
36. Roopnarine PD (2001) The description and classification of evolutionary mode: A computational approach. *Paleobiology* 27:446–465.
37. Kitchell JA, Estabrook G, Macleod N (1987) Testing for equality of rates of evolution. *Paleobiology* 13:272–285.
38. Hunt G (2008) Gradual or pulsed evolution: When should punctuational explanations be preferred? *Paleobiology* 34:360–377.
39. Jackson JBC, Cheetham AH (1999) Tempo and mode of speciation in the sea. *Trends Ecol Evol* 14:72–77.
40. Macleod N (1991) Punctuated anagenesis and the importance of stratigraphy to paleobiology. *Paleobiology* 17:167–188.
41. Lohmann GP (1983) Eigenshape analysis of microfossils: A general morphometric procedure for describing changes in shape. *J Int Assoc Math Geol* 15:659–672.
42. Lohmann GP, Schweitzer PN (1990) in *Proceedings of the Michigan Morphometrics Workshop*, eds Rohlf FJ, Bookstein FL (Univ of Michigan Museum of Zoology, Ann Arbor, MI), pp 147–166.
43. Banner FT, Blow WH (1965) Two new taxa of Globorotaliinae (Globigerinacea Foraminifera) assisting determination of Late Miocene/Middle Miocene boundary. *Nature* 207:1351–1354.
44. Banner FT, Blow WH (1965) Progress in planktonic foraminiferal biostratigraphy of Neogene. *Nature* 208:1164–1166.
45. Kennett JP, Srinivasan MS (1983) *Neogene Planktonic Foraminifera: A Phylogenetic Atlas* (Hutchinson Ross, Stroudsburg, PA).
46. Bookstein FL (1997) Landmark methods for forms without landmarks: Morphometrics of group differences in outline shape. *Med Image Anal* 1:225–243.
47. Hunt G, Chapman RE (2001) Evaluating hypotheses of instar-grouping in arthropods: A maximum likelihood approach. *Paleobiology* 27:466–484.
48. Norris RD, Nishi H (2001) Evolutionary trends in coiling of tropical Paleogene planktic foraminifera. *Paleobiology* 27:327–347.
49. Brummer GJA, Kroon D (1988) in *Planktonic Foraminifers as Tracers of Ocean-Climate History*, eds Brummer GJA, Kroon D (Free Univ Press, Amsterdam), pp 293–298.
50. Srinivasan MS, Chaturvedi SN (1992) in *Centenary of Japanese Micropaleontology*, eds Ishizaki K, Saito T (Terra Scientific, Tokyo), pp 175–188.
51. Norris RD (1998) in *Proceedings of the Ocean Drilling Program, Scientific Results*, eds Mascle J, Lohmann GP, Moullade M (Ocean Drilling Program, College Station, TX), Vol 159, pp 445–479.
52. Chaisson WP, Pearson PN (1997) in *Proceedings of the Ocean Drilling Program, Scientific Results*, eds Shackleton NJ, Curry WB, Richter C, Brawlower TJ (Ocean Drilling Program, College Station, TX), Vol 154, pp 3–31.
53. Lazarus D, Scherer RP, Prothero DR (1985) Evolution of the radiolarian species-complex Pterocanium: A preliminary survey. *J Paleontol* 59:183–220.
54. Wei KY, Kennett JP (1988) Phyletic gradualism and punctuated equilibrium in the late Neogene planktonic foraminiferal clade Globoconella. *Paleobiology* 14:345–363.

55. Berggren WA, Kent DV, Swisher CC, Aubry M-P (1995) *Geochronology, Time Scales and Global Stratigraphic Correlation*. SEPM Special Publication 54 (Society for Sedimentary Geology, Tulsa, OK).
56. Bookstein FL (1997) *Morphometric Tools for Landmark Data: Geometry and Biology* (Cambridge Univ Press, Cambridge, U.K.).
57. Zelditch M (2004) *Geometric Morphometrics for Biologists: A Primer* (Elsevier Academic, Amsterdam).
58. Dryden IL, Mardia KV (1998) *Statistical Shape Analysis* (Wiley, Chichester, U.K.).
59. Rohlf FJ, Bookstein FL (2003) Computing the uniform component of shape variation. *Systematic Biol* 52:66–69.

Supporting Information

Hull and Norris 10.1073/pnas.0902887106

SI Materials and Methods

Stratigraphic Concerns. MacLeod (1) called into question the interpretation of the rate of evolutionary change described by Malmgren et al. (2), noting the potential for small changes in sedimentation rate to have large cascading effects on the perceived rate of evolution. In particular, MacLeod was concerned with the classification of evolution in the *G. plesiotumida–G. tumida* lineage as "punctuated anagenesis" rather than just gradual anagenesis. In our current study we are more concerned with the *type* of evolutionary change (cladogenesis versus within-species evolution) rather than the rate. However, the effect of sedimentation rate on time averaging and population variance is of some importance as an increase in variance coincidences with the abrupt transition to the *G. tumida* morphology. Given the sample spacing (typically over a meter) and the small changes in mean morphology between successive samples, the stratigraphic concerns of MacLeod are unlikely to have a large effect on the contribution of time averaging to perceived patterns of population variance.

Additionally, we sampled at a more consistent interval to minimize the effect of sampling resolution on the perceived rate of change. While our sampling was largely consistent with regards to depth in the core (1.81 +/− 0.99 m), with regards to inferred absolute age, sample spacing varied from 8–143kyr. During the comparable time interval in Site 214, the sampling interval of Malmgren et al. varies between 1- 322kyr with the highest resolution sampling occurring during the transitional interval (2). However, both studies find comparable patterns of morphological evolution using eigenshape analysis (Fig. S2 *A* and *B*).

Biogeography. Our assumption in studying morphological evolution primarily at ODP site 806B in the western tropical Pacific is that evolution occurred in situ and does not represent the immigration of *G. tumida* from a geographically separate location of origination, as has been observed in other lineages (3). With reservations, we justify this assumption based on the following evidence. 1) The appearance of *G. tumida* is tied to the base of magnetochron C3n.4n throughout the tropical Indo-Pacific (4), indicative of a roughly synchronous origination throughout the region. *G. tumida* is know to appear much later and then only sporadically in the Atlantic Ocean (5), largely excluding the Atlantic as a possible location of *G. tumida* origination. Consistent with this observation, we do not find evidence for a morphological transition during the same time interval in the eastern tropical Atlantic (Fig. S3*C*, ODP site 959B 3°37.657′N, 2°44.135′W, 2090 m water depth). 2) There is no indication of localized geographic speciation within the tropical Indo-Pacific. At the time of origination, *G. tumida* is a tropical species with the same geographic range as the ancestral *G. plesiotumida* (Fig. S3 *B* and *C*) (6). Furthermore, a later first occurrence of *G. tumida* is correlated with distance from the equator along a latitudinal transect in the south Pacific (7), the opposite of what might be expected if *G. tumida* arose by geographic isolation across a water mass boundary from a tropical ancestor. Similarly, a latitudinal transect across the tropical Indian Ocean also discounts the possibility of allopatric speciation, with a synchronous first occurrence of *G. tumida* across all sites (6). 3) Environmental change preceding and at the Miocene/Pliocene boundary (detailed in ref. 8) may have provided increased habitat differentiation for sympatric or depth parapatric speciation. Notably, tropical species have elevated speciation rates at the Miocene/Pliocene boundary, a pattern which has been attributed to increased habitat availability due to increased surface water stratification (9).

Morphological Characters. A critical assumption in both Malmgren et al. 's and our study is that an edge view outline captures some aspect of the traits that distinguish species. The relative warp results call this assumption into question by finding relatively weak morphological separation of two recognized species (*Globorotalia plesiotumida* and *G. tumida*) relative to the dextral, previously unrecognized morphospecies.

Globorotalia tumida is distinguished from *G. plesiotumida* by (*i*) being larger relative to the total number of chambers, (*ii*) having a more rapid increase in whorl height, (*iii*) possessing a relatively tumid morphology (more similar dorsal height to ventral depth ratio), (*iv*) having a larger keel, (*v*) thicker walls, (*vi*) more coarse granules on early chambers, and a (*vii*) higher, broader-lipped aperture (10, 11). Of all of the characters used to distinguish between the species, only two will likely be detectable from the edge view outline: the whorl height and keel shape. Of the other characters, size is factored out, and would need to included after controlling for chamber number rather than size fraction (12), and the rest are unmeasured. Therefore, while it is possible to say that some combination of whorl height and keel shape appear to evolve gradually within the *G. plesiotumida–G. tumida* lineage, it is difficult to reject the possibility of cladogenesis during this morphological transition without examining more of the informative characters.

Methodology. We considered two variants of eigenshape analysis: 1) standard eigenshape analysis (13, 14) as applied by Malmgren et al. using a correlation matrix and within-sample normalization and 2) eigenshape analysis using a covariance matrix (e.g., refs. 15–17). For maximal comparability with the original study of Malmgren et al. (2), we display and discuss the results of standard eigenshape analysis in the comparison of trends in the Indian and Pacific Ocean (Fig. S2*B*). Eigenshape analysis requires the conversion of digitized coordinate points for each individual from a Cartesian (*x*,*y*) system to a ϕ^* form using the Zahn and Roskies' shape function (18), a normalized function of net angular change (15). After the conversion to the Zahn and Roskies' shape function, the similarity among shapes is assessed with a principal component analysis. Malmgren et al. used Lohmann's original technique for eigenshape analysis (2, 13). This technique includes 1) the standardization of each ϕ^* function to zero mean and unit variance, 2) the approximate calculation of the correlation matrix of the standardized ϕ^* functions, and 3) a preliminary within sample eigenshape analysis to normalize for any between sample effects (ontogeny and metric error). Over the years there have been a number of discussions on the effect of these normalization procedures and the use of a correlation rather than covariance matrix on eigenshape analysis (14–16). We therefore performed a second eigenshape analysis using the covariance matrix and without standardizing to the angularity of individual ϕ^* functions or within sample morphology. We used Lohmann's original code to perform an eigenshape analysis comparable to Malmgren et al. ($EA_{standard}$) and code modified from that of J. Claude (19) in R (version 2.2.1) to perform the second eigenshape analysis ($EA_{covariance}$). Among the top 10 eigenaxes from both analyses, the most comparable eigenaxes are EA $3_{standard}$ and EA $1_{covariance}$ with an $r^2 = 0.24$ (Fig. S4 *A*, *C*, and *E*, $P < 0.001$).

The eigenshape analysis used by Malmgren et al. is biased against detecting single time-step changes in morphology because each time interval is normalized to the mean morphology and each individual is normalized by angularity, the very characteristic varying in compressed individuals. In the Pacific Ocean sinistral and dextral populations rarely co-occur, so the normalization for angularity and mean sample morphology could effectively subtract out the differences due to coiling direction twice. However, we failed to find morphometric support for the dextral-sinistral morphological difference using the second eigenshape analysis with a covariance matrix and without within sample standardized (Fig. S4 *B*, *D*, and *F*).

We tentatively interpret the results as indicative of the differing methodological strengths of eigenshape and semilandmark TPS analysis. Theoretically, the semilandmark approach will minimize noise arising from the location of points along an outline. We suspected that this aspect of the relative warp analysis led to the detection of the morphological difference between sinistral and dextral individuals. However, in a direct comparison of relative warps based on semilandmark TPS (minimizing along outline error) and standard TPS (not minimizing along outline error), we obtained highly comparable relative warp results along the first 3 RWs ($r^2 > 0.97$, $P < 0.001$). The similarity of the relative warps scores from semilandmark TPS and TPS analyses indicates that the methodological innovation of semilandmark analysis (sliding points along outlines in an iterative alignment) does not account for the marked difference in results obtained from eigenshape analysis and semilandmark TPS analysis.

Instead, we suspect that the relative advantage of the TPS analysis arises from the specific measurement for uniform deformations (compression and shear). In this regards, landmark-based methods may be more sensitive to the visually apparent shape differences that differentiate sinistral and dextral coiled individuals (Fig. 3 *A* and *C*). Eigenshape analysis examines trends in shape angularity, and may miss a uniform shape deformation if the compression is manifested at any one of a number of corner points (diffuse across individuals), affects only a few points (localized within individuals), and/or has a small effect on angularity relative to intraindividual measurement error.

1. Macleod N (1991) Punctuated anagenesis and the importance of stratigraphy to paleobiology. *Paleobiology* 17:167–188.
2. Malmgren BA, Berggren WA, Lohmann GP (1983) Evidence for punctuated gradualism in the Late Neogene *Globorotalia tumida* lineage of planktonic foraminifera. *Paleobiology* 9:377–389.
3. Wei KY, Kennett JP (1988) Phyletic gradualism and punctuated equilibrium in the late Neogene planktonic foraminiferal clade Globoconella. *Paleobiology* 14:345–363.
4. Sinha DK, Singh AK (2008) Late Neogene planktic foraminiferal biochronology of the ODP site 763a, Exmouth Plateau, southeast Indian Ocean. *J Foraminifer Res* 38:251–270.
5. Berggren WA (1977) Late Neogene planktonic foraminiferal biostratigraphy of Rio-Grande Rise (South-Atlantic). *Mar Micropaleontol* 2:265–313.
6. Srinivasan MS, Chaturvedi SN (1992) in *Centenary of Japanese Micropaleontology*, eds Ishizaki K, Saito T (Terra Sci, Tokyo), pp 175–188.
7. Srinivasan MS, Kennett JP (1981) Neogene planktonic foraminiferal biostratigraphy and evolution—Equatorial to Sub-Antarctic, South-Pacific. *Mar Micropaleontol* 6:499–533.
8. Kennett JP, Keller G, Srinivasan MS (1985) Miocene planktonic foraminiferal biogeography and paleoceanographic development of the Indo-Pacific region. *Geol Soc Am Memoir* 163:197–236.
9. Wei KY, Kennett JP (1986) Taxonomic evolution of Neogene planktonic foraminifera and paleoceanographic relations. *Paleoceanography* 1:67–84.
10. Banner FT, Blow WH (1965) Two new taxa of Globorotaliinae (Globigerinacea Foraminifera) assisting determination of Late Miocene/Middle Miocene boundary. *Nature* 207:1351–1354.
11. Kennett JP, Srinivasan MS (1983) *Neogene planktonic Foraminifera: A phylogenetic atlas* (Hutchinson Ross, Stroudsburg).
12. Lohmann GP (1992) Increasing Seasonal Upwelling in the Subtropical South-Atlantic over the Past 700,000 Yrs—Evidence from deep-living planktonic foraminifera. *Mar Micropaleontol* 19:1–12.
13. Lohmann GP (1983) Eigenshape analysis of microfossils: A general morphometric procedure for describing changes in shape. *J Int Assoc Math Geol* 15:659–672.
14. Lohmann GP, Schweitzer PN (1990) in *Proceedings of the Michigan Morphometrics Workshop*, eds Rohlf FJ, Bookstein FL (Univ Michigan Museum Zool, Ann Arbor), pp 147–166.
15. MacLeod N (1999) Generalizing and extending the eigenshape method of shape space visualization and analysis. *Paleobiology* 25:107–138.
16. Rohlf FJ (1986) Relationships among Eigenshape Analysis, Fourier Analysis and Analysis of Coordinates. *Math Geol* 18:845–854.
17. Ray TS (1990) in *Proceedings of the Michigan Morphometrics Workshop*, eds Rohlf FJ, Bookstein FL (Univ Michigan Museum Zool, Ann Arbor), Vol Special Publication Number 2, pp 201–213.
18. Zahn CT, Roskies RZ (1972) Fourier descriptors for plane closed curves. *IEEE T Comput* C 21:269–281.
19. Claude J (2008) *Morphometrics with R* (Springer, New York).

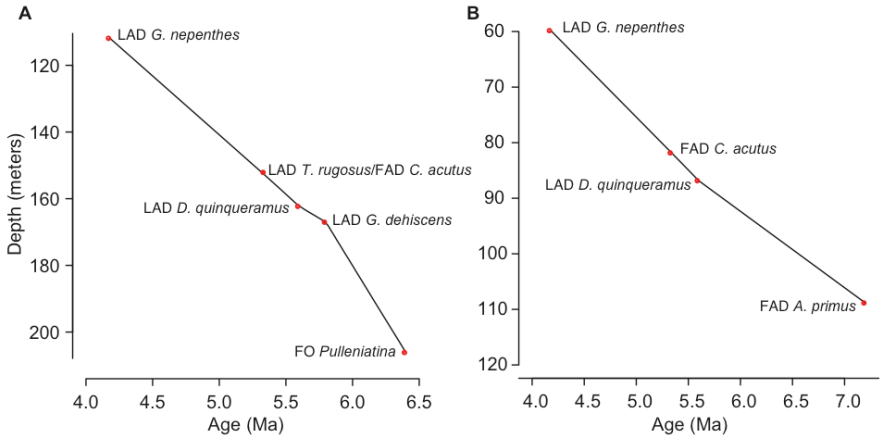

Fig. S1. Age model for ODP site 806B, equatorial Pacific and for ODP site 959C, equatorial Atlantic. Age model for (*A*) ODP site 806B using five stratigraphic markers and (*B*) ODP site 959C using four stratigraphic markers (red dots). Depth, meters composite depth; LAD, last appearance datum; FO, first occurrence.

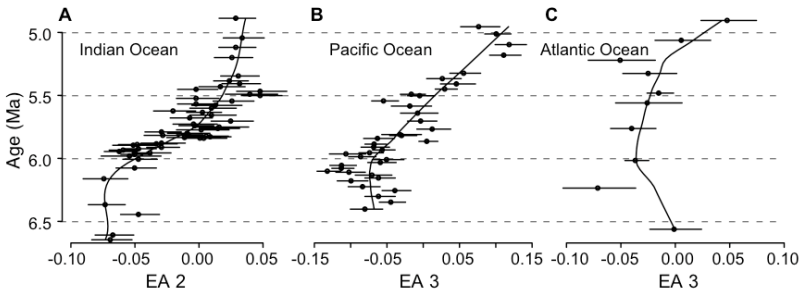

Fig. S2. Morphological trends in the *Globorotalia plesiotumida-G. tumida* lineage in 3-ocean basins. Morphological trends in the *Globorotalia plesiotumida-G.tumida* lineage in (*A*) the Indian Ocean, DSDP Site 214 (data from Malmgren et al. 1983), (*B*) the Pacific Ocean, ODP Site 806B (this study), and (*C*) the Atlantic Ocean, ODP Site 959C (this study). Eigenshape analysis was used at all sites to compare results from the Pacific and Atlantic with Malmgren et al.'s original study in the Indian Ocean.

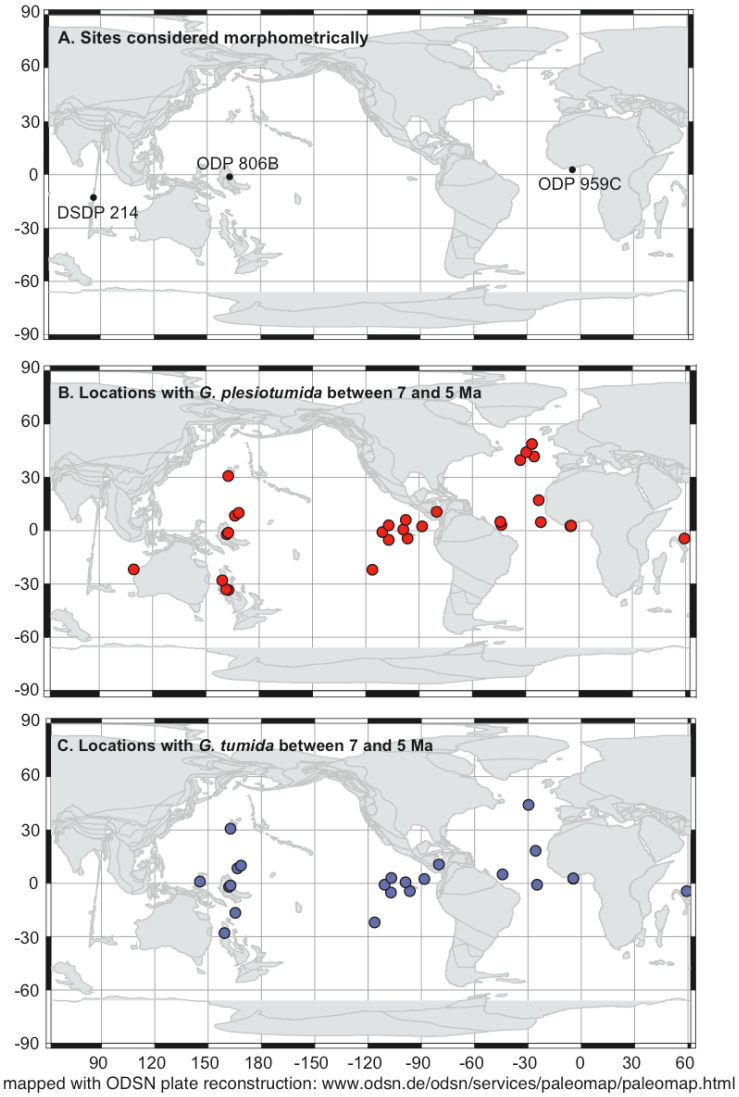

Fig. S3. Paleoreconstruction of 6 Ma with all sites considered and species geographic ranges. (*A*) Morphological trends in the *Globorotalia plesiotumida-G.tumida* lineage were considered in three ocean basins: the Indian Ocean (DSDP Site 214), the Pacific Ocean (ODP Site 806B), and the Atlantic Ocean (ODP Site 959C). These sites span the tropical distribution of both (*B*) *Globorotalia plesiotumida* and (*C*) *G. tumida* as mapped using occurrence data from the Neptune database (http://services.chronos.org/databases/neptune/index.html).

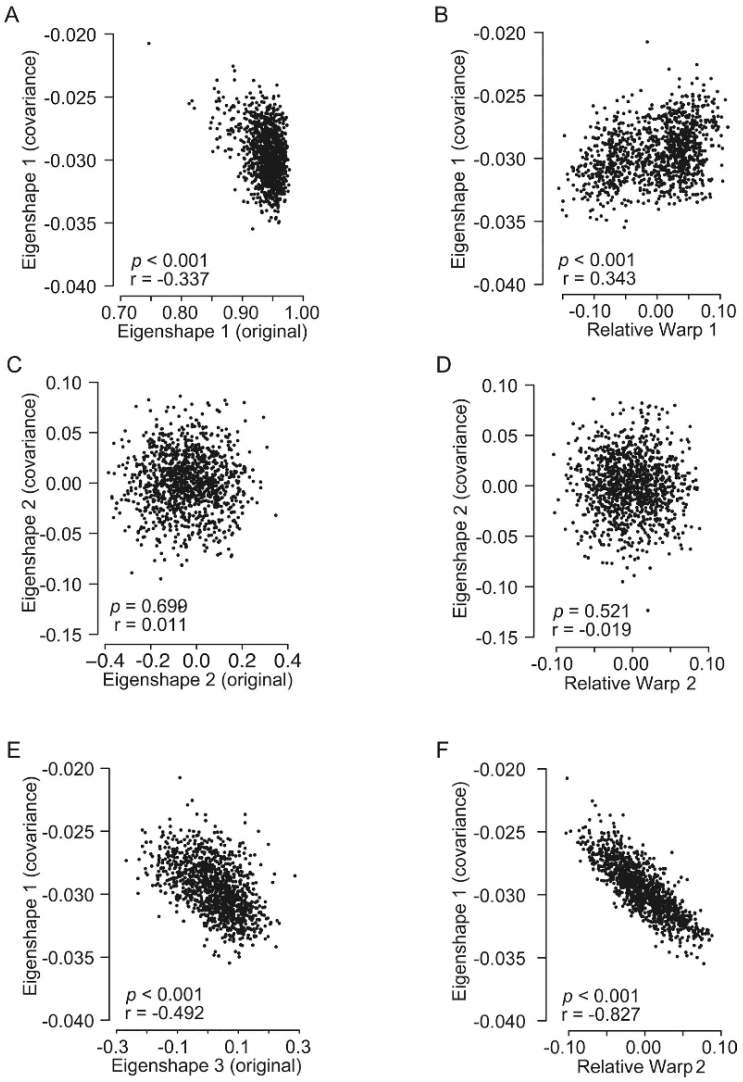

Fig. S4. Methodological comparison of eigenshape and semilandmark TPS results. Morphological trends in the *Globorotalia plesiotumida–G.tumida* lineage compared between eigenshape analysis using Lohmann's original methodology and eigenshape analysis on a covariance matrix (*A*, *C*, and *E*), and between eigenshape analysis on a covariance matrix and relative warps from semilandmark thin-plate spline analysis (*B*, *D*, and *F*). Best correlations shown in *E* and *F*. Eigenaxes and relative warps were not reversed for any of the comparisons in this figure.

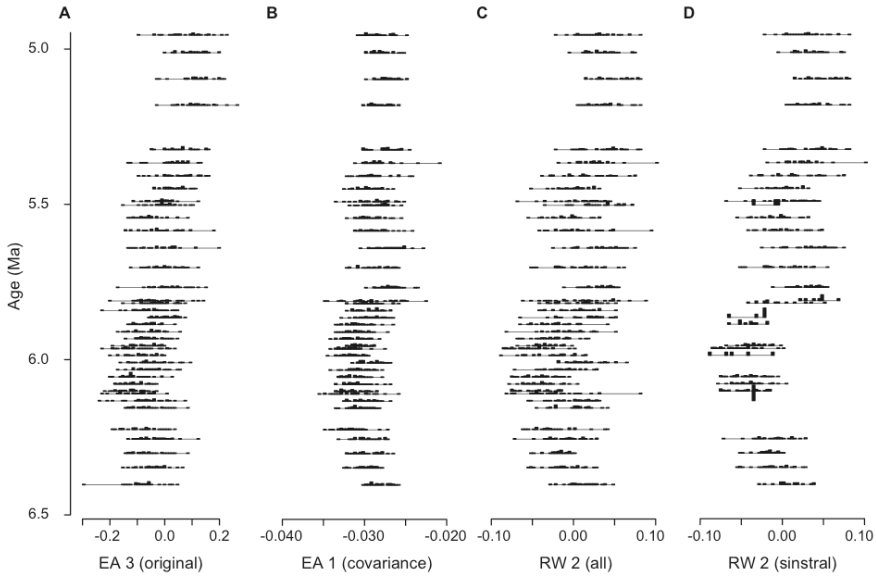

Fig. S5. Multiple perspectives on morphological trends in *Globorotalia plesiotumida-G. tumida*. Morphological trends in the *Globorotalia plesiotumida-G. tumida* lineage in (*A*) eigenshape 3 using the original methodology (*B*) eigenshape 1 using the covariance matrix without intrasample standardization, (*C*) 2nd relative warp (TPS-based methodology) using all individuals, and (*D*) 2nd relative warp (TPS-based methodology) displaying only sinistral individuals.

PNAS PNAS PNAS PNAS

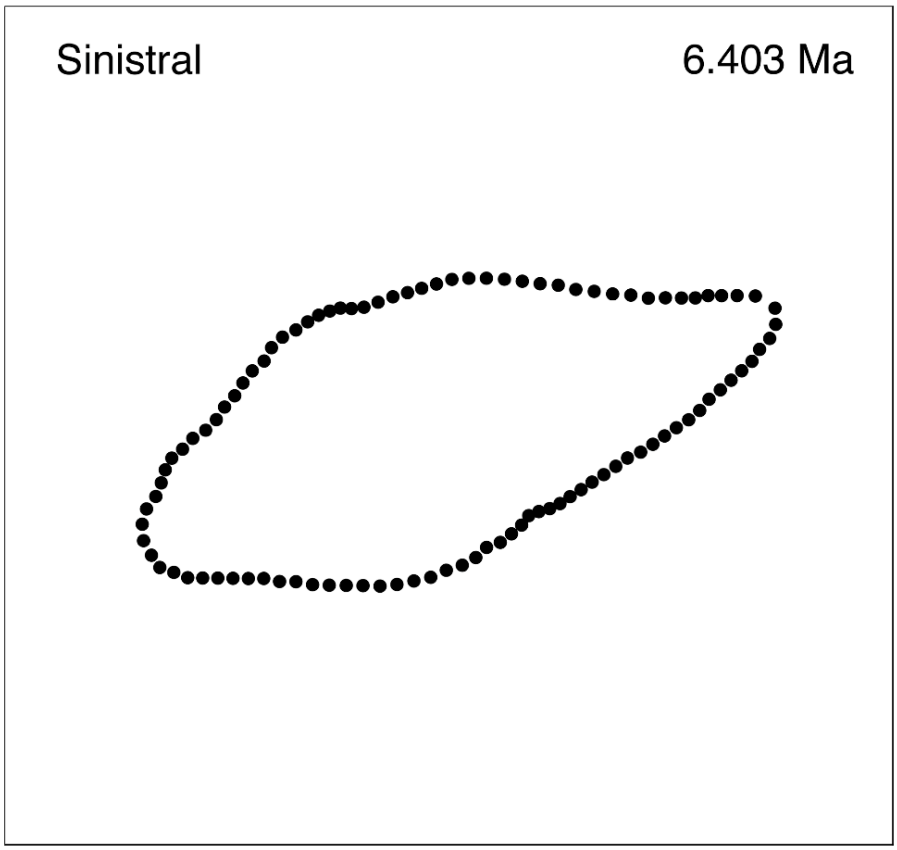

Movie S1. Outlines of all individuals analyzed in the Pacific Ocean at ODP site 806B after Procrustes alignment. Red outlines indicate dextral coiling.

Movie S1 (MOV)

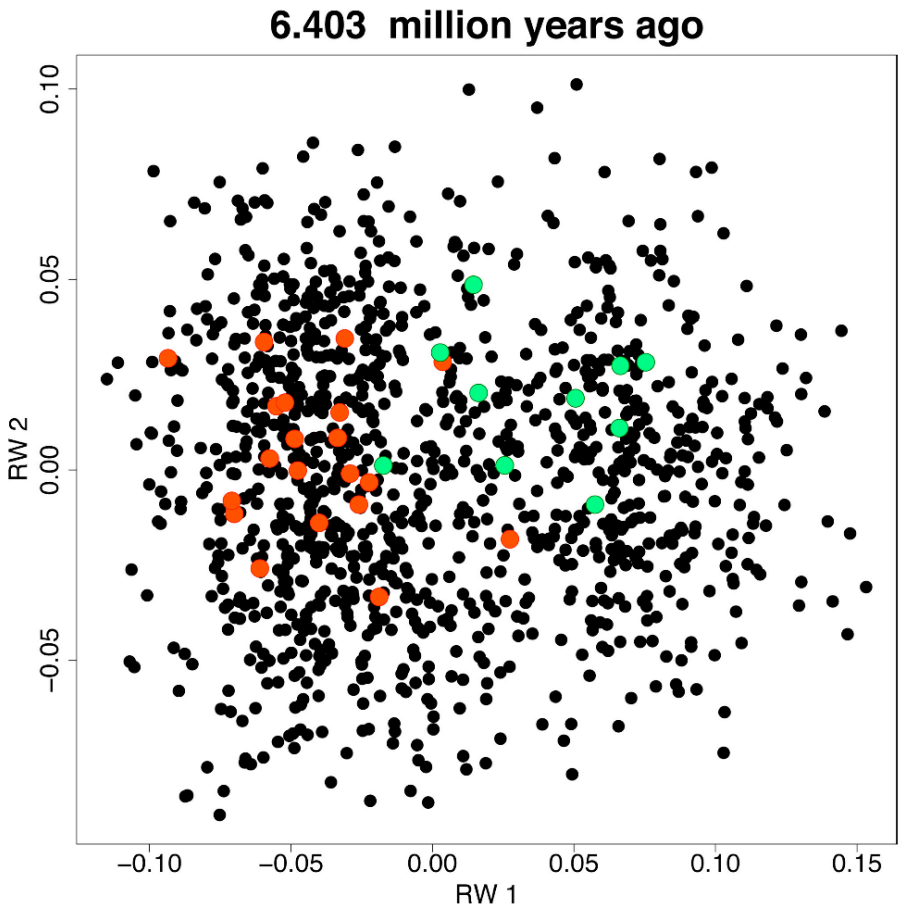

Movie S2. Morphological change through time in the *Globorotalia* lineage. All individuals shown in black along relative warp 1 and relative warp 2. For each time period, individuals from that time are shown in color; orange indicates sinistral coiling and green indicates dextral coiling.

Movie S2 (MOV)

Table S1. Thin-plate spline method comparison

Relative Warp	TPS v. Semi	TPS v. Semi-Rec.	Semi v. Semi-Rec.
1	0.996	0.887	0.911
2	−0.995	−0.905	0.933
3	−0.988	−0.955	0.971
4	−0.983	0.559	−0.656
5	0.943	0.312	0.453

The correlation (Pearson's *r*) of the first five relative warps among three thin-plate spline methods. Methods include traditional thin-plate spline analysis (TPS), semilandmark thin-plate spline analysis without recursion (Semi), and semilandmark thin-plate spline analysis with recursion (Semi-Rec.) All comparisons were computed using a 304-individual subset of the full tropical Pacific dataset (1140 individuals) and were significant at a $P < 0.001$. Relative warps were not reversed for any of the comparisons in this table.

Other Supporting Information Files

Dataset S1 (TXT)

Chapter 3 was published as: Hull, Pincelli; Norris, Richard "Evidence for abrupt speciation in a classic case of gradual evolution" *Proceedings of the National Academy of Sciences USA* 106 (50): 21224-21229. Copyright 2009 National Academy of Sciences, U.S.A. The dissertation author was the primary investigator and author of this paper.

CHAPTER IV

The Cretaceous-Paleogene Mass Extinction

INTRODUCTION

The remaining data chapters of my dissertation focus on the response of open ocean ecosystems to the Cretaceous-Paleogene (KPg) mass extinction. The KPg mass extinction provides an excellent case study for understanding how open ocean ecosystems respond to large, widespread, and rapid disturbance. As the most recent of the five major mass extinction events, the KPg mass extinction has the best fossil record of extinction and recovery and the most similar oceanic boundaries, currents, floras and faunas to the modern ocean. My motivation for studying biotic recovery from the KPg mass extinction was the hope that increased understanding of past global disturbances and recovery might inform both our understanding of and response to the current biotic crisis.

In this chapter that provides background to Chapters V-VII, I introduce the KPg mass extinction and its effects. Detailed descriptions of sites studied in the following chapters are given in Appendix 1.

THE CRETACEOUS-PALEOGENE MASS EXTINCTION

It is now widely agreed that the Cretaceous-Paleogene mass extinction was precipitated by the impact of a 10-14 km wide extraterrestrial bolide into the Yucatan Peninsula approximately 65.5 million years ago (Alvarez et al. 1980; Hildebrand et al. 1991; Morgan et al. 1997). The impactor, possibly a fragment of the carbonaceous-chondrite asteroid Baptistina (Bottke et al. 2007), left a 165-200 km wide crater in the Yucatan (Hildebrand et al. 1991; Morgan et al. 1997) and expelled approximately

50,000 km^3 of ejecta (Morgan et al. 1997). The force of the impact created physical disturbances with earthquakes modeled at magnitudes of 10-13 on the Richter scale causing vertical displacements of 1 m or more within 7000 km of the crater and massive submarine landslides from the Caribbean to Canada (Bralower et al. 1998; Norris et al. 2000; Toon et al. 1997). Tsunamis pounded the shores globally with wave crests estimated at 50-100 m in Texas (Bourgeois et al. 1988; Toon et al. 1997). As the largest pieces of hot ejecta rained out, regional or global wildfires may have been ignited (Kring 2007; Kring and Durda 2002; Wolbach et al. 1988), although new research questions whether the thermal stresses were severe enough to incinerate, rather than just kill, terrestrial flora and fauna (Belcher 2009; Belcher et al. 2003; Goldin and Melosh 2009).

The KPg impact hypothesis, which proposed that a large extraterrestrial impactor precipitated the KPg mass extinction, has been thoroughly examined since it was first proposed by Alvarez and others (Alvarez et al. 1980; Smit and Hertogen 1980; Urey 1973). Evidence for an impact at the KPg boundary is now overwhelming and includes global iridium and other platinum group element anomalies, impact ejecta, and shocked quartz (as reviewed in (as reviewed in [Claeys et al. 2002; Schulte et al. 2010; Smit 1999]). Similarly, there is extensive evidence for synchronous extinction across oceanic and terrestrial taxa with the KPg impact (e.g., D'Hondt et al. 1996; Fastovsky and Sheehan 2005; Labandeira et al. 2002; Pospichal 1996). The scientific evidence supports the consensus that the KPg mass extinction was directly precipitated by an extraterrestrial impact (Fastovsky and Sheehan 2005; Kring 2007; Schulte et al. 2010).

A small, vocal minority maintains that KPg mass extinction was not caused by a single extraterrestrial impact, but has failed to provide any counter-evidence that is free from preservational effects like the Signor-Lipps Effect or stratigraphic complexities of near-impact sites in the Gulf of Mexico (e.g., Keller et al. 2007; Keller et al. 2009; Keller et al. 1993; Keller et al. 2003).

In spite of the consensus surrounding the KPg impact hypothesis, the exact kill mechanism(s) is still debated. Possible global kill mechanisms include global darkness, acid rain, global cooling, global warming, and poisoning (as reviewed in D'Hondt 2005; Kring 2007; Toon et al. 1997). Upon proposing an extraterrestrial impact at the KPg boundary, Alvarez et al. hypothesized that the impact ejecta might have caused a temporary absence of sunlight leading to the collapse of terrestrial and aquatic foodwebs (1980). Ejecta modeling suggests that the period of global darkness was relatively short, 2-months to a year (Toon et al. 1982), but sufficient to cause the pattern and level of extinction (Alvarez et al. 1982; Thierstein 1982; Toon et al. 1997), although see (Pope 2002). Other authors variously invoke death by global cooling or global warming; the first due to decreased incident radiation from ejecta, gases, aerosols, and soot, and the second to adiabatic compression from shock waves and greenhouse gases (Brett 1992; Emiliani et al. 1981; Lewis et al. 1982; Toon et al. 1982). Following the impact, widespread acid rain would likely have resulted from increased atmospheric nitric oxide and carbonic and sulfuric acid (Brett 1992; Kring 2007; Lewis et al. 1982; Zahnle 1990). Modeling suggests that compression heating of the atmosphere may have evolved ~10^{15} mol of nitric acid rain (Zahnle 1990).

Additionally, the impact of the bolide into the anhydrite ($CaSO_4$) rich Yucatan released hundreds of billions of tons of sulfuric acid (Brett 1992; Pierazzo et al. 1998). Sulfuric and nitric acid may have had multifarious negative effects including global cooling, acid rain, acidification of near shore waters, increased weathering, and direct deleterious biological impacts (Kring 2007; Lewis et al. 1982). Finally, chemical and/or heavy metal poisoning may have provided short and longterm kill mechanisms respectively (Erickson and Dickson 1987; Hsu 1980; Toon et al. 1997), in addition to the direct negative effects from nitrous oxide and sulfuric acid.

The Chicxulub impact affected some ecosystems and taxa more than others, possibly reflecting differences in the life histories of pre-extinction species. While some taxa went entirely extinct at the KPg boundary, including ammonites, non-avian dinosaurs, and marine and flying reptiles (Alvarez et al. 1980), other taxa like benthic foraminifera were relatively unaffected (Culver 2003). Surface ocean ecosystems experienced disproportionately large negative effects from KPg boundary impact with large losses in diversity and ecosystem function (Norris 2001). Species richness decreased by nearly 95% in planktonic foraminifera (e.g., D'Hondt et al. 1996; Smit 1982) and 88% in coccolithophorids (Thierstein 1982) in contrast to extinction levels between 40-76% across all environments (Jablonski 1995; Jablonski and Chaloner 1994). Open ocean species that fared well include dinoflagellates, many of which have resting cysts (Thierstein 1982) and benthic foraminifera that rely on sporadic detrital influxes from the surface ocean (Culver 2003). In addition to variation among taxa, the KPg impact had spatially explicit effects on extinction and recovery within taxa. For

example, although near-coastal bivalves may not have suffered spatially-explicit patterns of species extinction (Raup and Jablonski 1993), recovery was more rapid in sites far removed from the Chicxulub impact (Jablonski 1998).

In addition to widespread extinction, the KPg impact appears to have affected global primary productivity with evidence for decreased productivity in terrestrial and open ocean communities (D'Hondt 2005). In the open ocean, a global decline in surface ocean export productivity is primarily indicated by a precipitous decrease in the surface-to-deep water $\delta^{13}C$ gradients, decreased sedimentation rates, and decreased deep water aging (D'Hondt 2005; Hsu et al. 1982; Zachos et al. 1989). Recovery to pre-extinction surface-to-deep water $\delta^{13}C$ gradients and, putatively, export productivity occurred in several steps with a full recovery indicated approximately 2-3 million years after the extinction (Coxall et al. 2006; D'Hondt et al. 1998). Benthic foraminiferal assemblage structure can be used as an independent proxy for changes in productivity (e.g., Gooday 2003; Thomas 2007). In sites throughout the North Atlantic and Tethys, benthic foraminifera proxies provide additional support for a prolonged suppression of export productivity (e.g., Alegret et al. 2004; Alegret et al. 2001; Alegret et al. 2003). Surprisingly, benthic proxies in the Pacific Ocean and South Atlantic appear to contradict evidence from $\delta^{13}C$ and sedimentation rate proxies by recording either no change or increased export productivity in the early Danian (Alegret and Thomas 2007; Alegret and Thomas 2009). The lack of KPg boundary extinction among benthic foraminifera combined with the evidence for high levels of export productivity in some

early Danian locales has fueled a debate on effect of the end-Cretaceous mass extinction on surface ocean ecosystem function.

On land, plant and sedimentary $\delta^{13}C$ also indicate suppressed productivity in the earliest Danian (Arens and Jahren 2000; Beerling et al. 2001). In contrast to open ocean $\delta^{13}C$ gradients, terrestrial proxies suggests a more rapid recovery to pre-extinction primary productivity levels (Arens and Jahren 2000; Beerling et al. 2001). A similar contrast is apparent in the rate of recovery of species richness between terrestrial and open ocean ecosystems. Highly diverse floral assemblages approximately 1.4 million years post-impact in Castle Rock, Denver suggest that some terrestrial ecosystems recovered to pre-extinction diversity levels more quickly than the 2-3 million years observed in open ocean ecosystems (Coxall et al. 2006; Johnson and Ellis 2002). However, it is notable that most terrestrial plant assemblages studied to date did not recover until the late Paleocene to early Eocene (Johnson and Ellis 2002; McElwain and Punyasena 2007).

In the context of mass extinctions, the idea of recovery can refer to the recovery of pre-extinction levels of species richness and diversity, or to the re-establishment of community structure or ecosystem functions like primary or export production and biogeochemical cycling. In general, biotic recoveries from mass extinctions share several of the following features, including i) low diversity assemblages dominated by eurytopic taxa (e.g., taxa able to thrive in a wide range of environments), ii) reduced guild structure (e.g., loss of specific life history strategies) iii) early dominance of opportunistic, “bloom” taxa, and iv) reappearance of Lazarus taxa at the end of the

recovery (Erwin 1998; Erwin 2001). Early Paleocene communities on land and in the sea are characterized by the dominance of a small number of eurytopic, bloom taxa that thrive in the wake of the extinction. On land, a global fungal spore spike followed by a fern spike precedes the recovery of diverse floral assemblages (McElwain and Punyasena 2007; Tschudy et al. 1984; Vajda and McLoughlin 2004). In the open ocean, opportunistic taxa of previously coastal planktonic foraminifera, e.g., the triserial *Guembelitria*, briefly dominate planktonic assemblages (D'Hondt et al. 1996; MacLeod 1993). Disaster fauna are replaced by recovery fauna within ~500 kyr in planktonic foraminifera (D'Hondt and Keller 1991), although the recovery to full species diversity takes around 2-3 My (Coxall et al. 2006). In addition, guild structure in planktonic foraminifera is reduced, with some life histories, like photosymbiosis, requiring several million years to re-evolve (Berggren and Norris 1997; Coxall et al. 2006). Finally, a theoretical expectation of recoveries from mass extinctions is a delayed onset and stepped pattern of recovery (Sole et al. 2002). Recovery of both export productivity and species richness appear to conform to this model, with recovery occurring in several steps over 2-3 million years (Coxall et al. 2006; D'Hondt et al. 1998).

REFERENCES

ALEGRET, L., M. A. KAMINSKI, and E. MOLINA. 2004. Paleoenvironmental recovery after the Cretaceous/Paleogene boundary crisis: evidence from the marine bidart section (SW France). Palaios **19:** 574-586.

ALEGRET, L., E. MOLINA, and E. THOMAS. 2001. Benthic foraminifera at the Cretaceous-Tertiary boundary around the Gulf of Mexico. Geology **29:** 891-894.

---. 2003. Benthic foraminiferal turnover across the Cretaceous/Paleogene boundary at Agost (southeastern Spain): paleoenvironmental inferences. Marine Micropaleontology **48:** 251-279.

ALEGRET, L., and E. THOMAS. 2007. Deep-sea environments across the Cretaceous/Paleogene boundary in the eastern South Atlantic Ocean (ODP leg 208, Walvis ridge). Marine Micropaleontology **64:** 1-17.

---. 2009. Food supply to the seafloor in the Pacific Ocean after the Cretaceous/Paleogene boundary event. Marine Micropaleontology **73:** 105-116.

ALVAREZ, L. W., W. ALVAREZ, F. ASARO, and H. V. MICHEL. 1980. Extraterrestrial cause for the Cretaceous-Tertiary extinction - experimental results and theoretical interpretation. Science **208:** 1095-1108.

ALVAREZ, W., L. W. ALVAREZ, F. ASARO, and H. V. MICHEL. 1982. Current status of the impact theory for the terminal Cretaceous extinction. *In* L. T. Silver and P. H. Schultz [eds.], Geological implications of impacts of large asteroids and comets on the Earth: Geological Society of America Special Paper 190.

ARENS, N. C., and A. H. JAHREN. 2000. Carbon isotope excursion in atmospheric CO2 at the Cretaceous-Tertiary boundary: evidence from terrestrial sediments. Palaios **15:** 314-322.

BEERLING, D. J. and others 2001. Evidence for the recovery of terrestrial ecosystems ahead of marine primary production following a biotic crisis at the Cretaceous-Tertiary boundary. Journal of the Geological Society **158:** 737-740.

BELCHER, C. M. 2009. Reigniting the Cretaceous-Palaeogene firestorm debate. Geology **37:** 1147-1148.

BELCHER, C. M., M. E. COLLINSON, A. R. SWEET, A. R. HILDEBRAND, and A. C. SCOTT. 2003. Fireball passes and nothing burns - the role of thermal radiation in the Cretaceous-Tertiary event: Evidence from the charcoal record of North America. Geology **31:** 1061-1064.

BERGGREN, W. A., and R. D. NORRIS. 1997. Biostratigraphy, phylogeny and systematics of Paleocene trochospiral planktic foraminifera. Micropaleontology **43:** 1-116.

BOTTKE, W. F., D. VOKROUHLICKY, and D. NESVORNY. 2007. An asteroid breakup 160 Myr ago as the probable source of the K/T impactor. Nature **449:** 48-53.

BOURGEOIS, J., T. A. HANSEN, P. L. WIBERG, and E. G. KAUFFMAN. 1988. A tsunami deposit at the Cretaceous-Tertiary boundary in Texas. Science **241:** 567-570.

BRALOWER, T. J., C. K. PAULL, and R. M. LECKIE. 1998. The Cretaceous-Tertiary boundary cocktail: Chicxulub impact triggers margin collapse and extensive sediment gravity flows. Geology **26:** 331-334.

BRETT, R. 1992. The Cretaceous-Tertiary extinction - a lethal mechanism involving anhydrite target rocks. Geochimica Et Cosmochimica Acta **56:** 3603-3606.

CLAEYS, P., W. KIESSLING, and W. ALVAREZ. 2002. Distribution of Chicxulub ejecta at the Cretaceous-Tertiary boundary, p. 55 - 69. *In* C. Koeberl and K. G. MacLeod [eds.], Catastrophic events and mass extinctions: impacts and beyond: Geological Society of America Special Paper 356.

COXALL, H. K., S. D'HONDT, and J. C. ZACHOS. 2006. Pelagic evolution and environmental recovery after the Cretaceous-Paleogene mass extinction. Geology **34:** 297-300.

CULVER, S. J. 2003. Benthic foraminifera across the Cretaceous-Tertiary (K-T) boundary: a review. Marine Micropaleontology **47:** 177-226.

D'HONDT, S. 2005. Consequences of the Cretaceous/Paleogene mass extinction for marine ecosystems. Annual Review of Ecology Evolution and Systematics **36:** 295-317.

D'HONDT, S., P. DONAGHAY, J. C. ZACHOS, D. LUTTENBERG, and M. LINDINGER. 1998. Organic carbon fluxes and ecological recovery from the Cretaceous-Tertiary mass extinction. Science **282:** 276-279.

D'HONDT, S., and G. KELLER. 1991. Some patterns of planktic foraminiferal assemblage turnover at the Cretaceous Tertiary boundary. Marine Micropaleontology **17:** 77-118.

D'HONDT, S. L., T. D. HERBERT, J. KING, and C. GIBSON. 1996. Planktic foraminifera, asteroids and marine production: death and recovery at the Cretaceous-Tertiary boundary, p. 303–317. *In* G. Ryder, D. Fastovsky and S. Gartner [eds.], The Cretaceous-Tertiary event and other catastrophes in Earth history: Geological Society of America Special Paper 307.

EMILIANI, C., E. B. KRAUS, and E. M. SHOEMAKER. 1981. Sudden death at the end of the Mesozoic. Earth and Planetary Science Letters **55:** 317-334.

ERICKSON, D. J., and S. M. DICKSON. 1987. Global trace-element biogeochemistry at the K/T boundary - oceanic and biotic response to a hypothetical meteorite impact. Geology **15:** 1014-1017.

ERWIN, D. H. 1998. The end and the beginning: recoveries from mass extinctions. Trends in Ecology & Evolution **13:** 344-349.

---. 2001. Lessons from the past: biotic recoveries from mass extinctions. Proceedings of the National Academy of Sciences of the United States of America **98:** 5399-5403.

FASTOVSKY, D. E., and P. M. SHEEHAN. 2005. The extinction of the dinosaurs in North America. GSA Today **15:** 4-10.

GOLDIN, T. J., and H. J. MELOSH. 2009. Self-shielding of thermal radiation by Chicxulub impact ejecta: Firestorm or fizzle? Geology **37:** 1135-1138.

GOODAY, A. J. 2003. Benthic foraminifera (protista) as tools in deep-water palaeoceanography: Environmental influences on faunal characteristics. Advances in Marine Biology **46:** 1-90.

HILDEBRAND, A. R. and others 1991. Chicxulub crater - a possible Cretaceous Tertiary Boundary impact crater on the Yucatan Peninsula, Mexico. Geology **19:** 867-871.

HSU, K. J. 1980. Terrestrial catastrophe caused by cometary impact at the end of Cretaceous. Nature **285:** 201-203.

HSU, K. J., Q. X. HE, and A. MCKENZIE. 1982. Terminal Cretaceous environmental and evolutionary changes, p. 317–328. *In* L. T. Silver and P. H. Schultz [eds.], Geological implications of impacts of large asteroid and comets on the Earth: Geological Society of America Special Paper 190.

JABLONSKI, D. 1995. Extinctions in the fossil record, p. 25-44 *In* J. H. Lawton and R. M. May [eds.], Extinction rates. Oxford University Press.

---. 1998. Geographic variation in the molluscan recovery from the end-Cretaceous extinction. Science **279:** 1327-1330.

JABLONSKI, D., and W. G. CHALONER. 1994. Extinctions in the fossil record. Philosophical Transactions of the Royal Society of London Series B-Biological Sciences **344:** 11-16.

JOHNSON, K. R., and B. ELLIS. 2002. A tropical rainforest in Colorado 1.4 million years after the Cretaceous-Tertiary boundary. Science **296:** 2379-2383.

KELLER, G. and others 2007. Chicxulub impact predates K-T boundary: new evidence from Brazos, Texas. Earth and Planetary Science Letters **255:** 339-356.

KELLER, G., T. ADATTE, A. P. JUEZ, and J. G. LOPEZ-OLIVA. 2009. New evidence concering the age and biotic effects of the Chicxulub impact in NE Mexico. Journal of the Geological Society **166:** 393-411.

KELLER, G., E. BARRERA, B. SCHMITZ, and E. MATTSON. 1993. Gradual mass extinction, species survivorship, and long-term environmental changes across the Cretaceous-Tertiary boundary in high latitudes. Geological Society Of America Bulletin **105:** 979-997.

KELLER, G., W. STINNESBECK, T. ADATTE, and D. STUBEN. 2003. Multiple impacts across the Cretaceous-Tertiary boundary. Earth-Science Reviews **62:** 327-363.

KRING, D. A. 2007. The Chicxulub impact event and its environmental consequences at the Cretaceous-Tertiary boundary. Palaeogeography Palaeoclimatology Palaeoecology **255:** 4-21.

KRING, D. A., and D. D. DURDA. 2002. Trajectories and distribution of material ejected from the Chicxulub impact crater: implications for postimpact wildfires. Journal of Geophysical Research-Planets **107**.

LABANDEIRA, C. C., K. R. JOHNSON, and P. WILF. 2002. Impact of the terminal Cretaceous event on plant-insect associations. Proceedings of the National Academy of Sciences of the United States of America **99:** 2061-2066.

LEWIS, J. S., G. H. WATKINS, H. HARTMAN, and R. G. PRINN. 1982. Chemical consequences of major impact events on earth, p. 215-221. *In* L. T. Silver and P. H. Schultz [eds.], Geological implications of impacts of large asteroids and comets on the Earth: Geological Society of America Special Paper 190.

MACLEOD, N. 1993. The Maastrichtian-Danian radiation of triserial and biserial planktic foraminifera - testing phylogenetic and adaptational hypotheses in the (micro) fossil record. Marine Micropaleontology **21:** 47-100.

MCELWAIN, J. C., and S. W. PUNYASENA. 2007. Mass extinction events and the plant fossil record. Trends in Ecology & Evolution **22:** 548-557.

MORGAN, J. and others 1997. Size and morphology of the Chicxulub impact crater. Nature **390:** 472-476.

NORRIS, R. D. 2001. Impact of K-T Boundary events on marine life p. 229-231. *In* D. E. G. Briggs and P. G. Crowther [eds.], Palaeobiology II. Blackwell Science Ltd.

NORRIS, R. D., J. FIRTH, J. S. BLUSZTAJN, and G. RAVIZZA. 2000. Mass failure of the North Atlantic margin triggered by the Cretaceous-Paleogene bolide impact. Geology **28:** 1119-1122.

PIERAZZO, E., D. A. KRING, and H. J. MELOSH. 1998. Hydrocode simulation of the Chicxulub impact event and the production of climatically active gases. Journal of Geophysical Research-Planets **103:** 28607-28625.

POPE, K. O. 2002. Impact dust not the cause of the Cretaceous-Tertiary mass extinction. Geology **30:** 99-102.

POSPICHAL, J. J. 1996. Calcareous nannoplankton mass extinction at the Cretaceous/Tertiary boundary: An update, p. 335-360. *In* G. Ryder, D. Fastovsky and S. Gartner [eds.], The Cretaceous-Tertiary event and other catastrophes in Earth history: Geological Society of America Special Paper 307.

RAUP, D. M., and D. JABLONSKI. 1993. Geography of End-Cretaceous marine bivalve extinctions. Science **260:** 971-973.

SCHULTE, P. and others 2010. The Chicxulub Asteroid Impact and Mass Extinction at the Cretaceous-Paleogene Boundary. Science **327:** 1214-1218.

SMIT, J. 1982. Extinction and evolution of planktonic foraminifera at the Cretaceous/Tertiary boundary after a major impact, p. 329 –352. *In* L. T. Silver and P. H. Schultz [eds.], Geological implications of impacts of large asteroids and comets on the Earth: Geological Society of America Special Paper 190.

---. 1999. The global stratigraphy of the Cretaceous-Tertiary boundary impact ejecta. Annual Review of Earth and Planetary Sciences **27:** 75-113.

SMIT, J., and J. HERTOGEN. 1980. An extraterrestrial event at the Cretaceous-Tertiary boundary. Nature **285:** 198-200.

SOLE, R. V., J. M. MONTOYA, and D. H. ERWIN. 2002. Recovery after mass extinction: evolutionary assembly in large-scale biosphere dynamics. Philosophical Transactions of the Royal Society of London Series B-Biological Sciences **357:** 697-707.

THIERSTEIN, H. R. 1982. Terminal Cretaceous plankton extinctions: A critical assessment, p. 385–399. *In* L. T. Silver and P. H. Schultz [eds.], Geological implications of impacts of large asteroids and comets on the Earth: Geological Society of America Special Paper 190.

THOMAS, E. 2007. Cenozoic mass extinctions in the deep sea: what perturbs the largest habitat on Earth?, p. 1–23. *In* S. Monechi, R. Coccioni and M. R. Rampino [eds.], Large ecosystem perturbations: causes and consequences: Geological Society of America Special Paper 424.

TOON, O. B., J. B. POLLACK, T. P. ACKERMAN, R. P. TURCO, C. P. MCKAY, and M. S. LIU. 1982. Evolution of an impact-generated dust cloud and its effects on the atmosphere, p. 187-200. *In* L. T. Silver and P. H. Schultz [eds.], Geological implications of impacts of large asteroids and comets on the Earth: Geological Society of America Special Paper 190.

TOON, O. B., K. ZAHNLE, D. MORRISON, R. P. TURCO, and C. COVEY. 1997. Environmental perturbations caused by the impacts of asteroids and comets. Reviews of Geophysics **35:** 41-78.

TSCHUDY, R. H., C. L. PILLMORE, C. J. ORTH, J. S. GILMORE, and J. D. KNIGHT. 1984. Disruption of the terrestrial plant ecosystem at the Cretaceous-Tertiary boundary, western interior. Science **225:** 1030-1032.

UREY, H. C. 1973. Cometary collisions and geological periods. Nature **242:** 32-33.

VAJDA, V., and S. MCLOUGHLIN. 2004. Fungal proliferation at the Cretaceous-Tertiary boundary. Science **303:** 1489-1489.

WOLBACH, W. S., I. GILMOUR, E. ANDERS, C. J. ORTH, and R. R. BROOKS. 1988. Global fire at the Cretaceous-Tertiary boundary. Nature **334:** 665-669.

ZACHOS, J. C., M. A. ARTHUR, and W. E. DEAN. 1989. Geochemical evidence for suppression of pelagic marine productivity at the Cretaceous/Tertiary boundary. Nature **337:** 61-64.

ZAHNLE, K. J. 1990. Atmospheric chemistry by large impacts, p. 271-288. *In* V. L. Sharpton and P. D. Ward [eds.], Global catastrophes in eaerth history: an interdisciplinary conference on impacts, volcanism and mass mortality: Geological Society of America Special Paper 247.

CHAPTER V

Using mixing models and iridium anomalies to quantify sediment mixing at the Cretaceous-Paleogene boundary

ABSTRACT

Sediment mixing models can provide a means to quantify and account for the effect of sediment mixing on the geological record. Here, we introduce a Lagrangian mixing model that differs from typical one-dimensional advection-diffusion models in modeling mixing as a non-deterministic process. We use this model to explore the theoretical effects of sediment mixing on records of rapid events and to investigate the effect of mixing on a Cretaceous-Paleogene (KPg) boundary record from the North Pacific. A site-specific tracer of sediment mixing is needed to fit mixing models to empirical records. We suggest that iridium, an elemental impact marker, can provide a good tracer of sediment mixing at the KPg boundary in oxic pelagic sites after a review of the potential determinants of anomaly shape. The correspondence in mixing extent between iridium and micro- to nannofossils suggests that iridium may provide a better tracer of the sedimentary constituents of interest to many researchers than previously proposed mixing tracers such as Ni-spinels. Our discussion of theoretical mixing effects and review of the processes determining iridium anomaly shape provides a needed revision of the expectations for and interpretation of the effect of sediment mixing at the KPg boundary.

INTRODUCTION

An extraterrestrial impact like that at the Cretaceous-Paleogene (KPg) boundary results in the rapid deposition of a number of physical and chemical markers of the event (Kyte 2002), including iridium (Ir) and other platinum group elements (PGEs),

shocked quartz, nickel-spinels, microtektites, and microkrystites (as reviewed in Alvarez 1996; Claeys et al. 2002; Smit 1999). Impact markers like iridium are primarily deposited in narrow, <<1 cm thick, event horizons at distal sites (Claeys et al. 2002; Smit 1999) before being remobilized by sedimentary processes like bioturbation, diagenesis or slumping. As a result, geologically instantaneous markers like impact ejecta and volcanic ashes have long been used to quantitatively understand deep-sea sediment mixing (e.g., Glass 1969; Guinasso and Schink 1975; Ruddiman and Glover 1972; Ruddiman et al. 1980). Mixing profiles can be used to quantify the magnitude and duration of the initial, unmixed record of both the impact marker and other sedimentary constituents like foraminifera, diatoms, and other nannofossils (Ruddiman and Glover 1972). At the KPg boundary a number of questions exist about the ecological, evolutionary, and biogeochemical response in the decades to millennia following the impact, as most records are well mixed over these time scales. However, despite an abundance of impact markers and the potential utility of sediment mixing models, we are unaware of any previous attempt to quantitatively describe sediment mixing profiles across the KPg boundary. In this study, we use one impact marker, elemental iridium, as a tracer of deep-sea sediment mixing in oxic, pelagic sites in the early Danian. Iridium anomalies at the KPg boundary have the potential to be useful tracers of sedimentary mixing as they were deposited in a geological brief interval and have been measured at more sites and at a higher resolution than other KPg impact markers (Claeys et al. 2002).

Here, we introduce and use a Lagrangian particle-tracking model of sediment mixing, which has the advantage of allowing for non-deterministic sediment mixing within a one-dimensional advection-diffusion model. The simplest and most widely used sediment mixing models are advection-diffusion models. In an advection-diffusion model, the record of a sedimentary event is mixed within a mixed layer according to a mixing coefficient (e.g., diffusion coefficient), before being advected into a historic layer of sediment that predates the event (Goldberg and Koide 1962; Guinasso and Schink 1975). Numerical simulations of time-dependent mixing (e.g., models involving multiple time steps rather than the integration of all mixing in a single step), typically model the sedimentary column as a stack of discrete layers with a constant mixing coefficient within each layer (e.g., Peng et al. 1979; Ridgwell 2007; Ridgwell and Hargreaves 2007). Basic advection-diffusion approaches generally do not model non-local mixing like the lumpy mixing of large burrowers that occasionally carry surface sediment to great depths. While non-local sediment mixing models do exist (e.g., Boudreau and Imboden 1987; Shull 2001; Trauth 1998), they are hard to parameterize from tracer profiles alone (Boudreau 1986a; Boudreau 1986b; Boudreau and Imboden 1987) and do not necessarily outperform advection-diffusion models (Meysman et al. 2003). Notably, simple one-dimensional advection-diffusion mixing models have been used to understand or describe mixing in the deep sea (e.g., Guinasso and Schink 1975; Peng et al. 1979), the effect of sediment mixing on the record of past events (e.g., Charbit et al. 2002; Ridgwell 2007), and to account for sediment buffering effects in future climate projections (e.g, Archer et al. 1998; Ridgwell and Hargreaves 2007).

We address two questions in this study. First, does the shape of iridium anomalies primarily reflect sediment mixing in oxic, pelagic sites distal to the impact or does it primarily reflect other processes, like diagenetic remobilization? In order to be a useful tracer of sediment mixing, the shape of iridium anomalies must be primarily determined by sedimentary mixing and should be representative of the sedimentary constituents of interest. However, the two-tailed peaked shape of the iridium anomaly has been attributed to a number of sedimentary processes (e.g., Smit 1999; Stueben et al. 2002) including i) bioturbation and other physical mixing (Alvarez et al. 1990; Kyte et al. 1985), ii) diagenetic remobilization and diffusion (Kyte et al. 1985; Schmitz 1985; Wallace et al. 1990), iii) prolonged deposition due to oceanic residence times (Anbar et al. 1996), iv) volcanism (Crocket et al. 1988; Officer and Drake 1985; Rocchia et al. 1990), and v) redeposition from primary deposits (Preisinger et al. 1986). Of these mechanisms, only the first four provide a global mechanism for shaping iridium anomalies.

Second, we then test the ability of our Lagrangian advection-diffusion sediment mixing model to fit the shape of a highly resolved iridium anomaly at the Shatsky Rise in the North Pacific. We compare the sediment mixing model fits with evidence for the other two mechanisms, including tracers of diagenetic remobilization and modeled effects of prolonged iridium deposition. A good fit between profiles obtained from the mixing model and the measured iridium anomaly indicates that highly resolved iridium anomalies may provide a site-specific means of estimating sediment mixing in early Danian oceans. We also explore the sensitivity of theoretical mixing profiles to different

model parameters, discuss the range in possible mixing profile shapes, and list a number theoretical expectations for mixed KPg boundary sections.

MIXING MODEL

Our model is a one-dimensional Lagrangian particle-tracking model with a depth-dependent eddy diffusivity modified from Tanaka and Franks (Tanaka and Franks 2008). Sediment mixing was driven by vertical diffusivity (K_v), which we modeled as a decreasing hyperbolic tangent (tanh) function (Figure 5-1). The tanh function captures a fundamental feature of sediment mixing, namely, the existence of a superficial well-mixed layer underlain by increasingly unmixed sediments. The tanh function generates

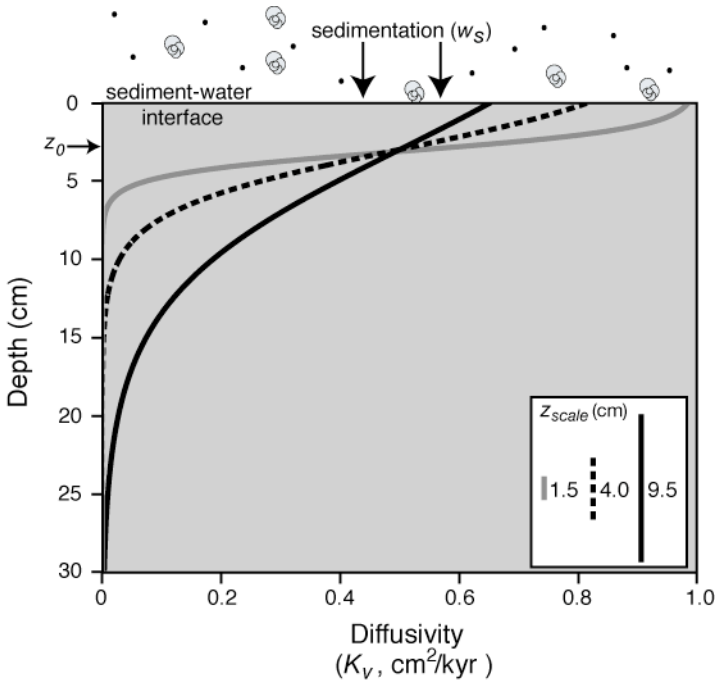

Figure 5-1. The Lagrangian sediment mixing model. Three mixing curves highlight the effect of z_{scale} on depth-dependent diffusivity (K_v). All curves are parameterized with the same z_0, indicated on the depth axis, and the same K_0. Larger values for z_{scale} (black) increase the depth range over which K_v asymptotes to zero relative to a smaller z_{scale} values (grey).

a vertical diffusivity profile that is continuously differentiable with depth (Ross and Sharples 2004). The depth of sediment mixing and diffusivity are expected to primarily be a function of the flux of organic matter to the deep sea (e.g., Smith and Rabouille 2002; Trauth et al. 1997), and are used here as free parameters for tuning the mixing model to fit measured iridium anomalies.

Three parameters define sediment mixing: i) z_0 is the depth of the inflection point in the tanh profile, delineating the bottom of the well-mixed layer of sediment, ii) z_{scale} is the *e*-folding scale for the tanh profile and determines the depth over which mixing asymptotes to zero, and iii) K_0 is the maximum vertical diffusivity. K_v, or depth-dependent diffusivity, decreases with depth according to:

$$K_v(z) = \frac{K_0}{2}\left[1 - \tanh\left(\frac{z - z_0}{z_{scale}}\right)\right]$$

Unlike many mixing models, K_0 defines the upper limit of mixing in the tanh profile, and not diffusivity at the sediment-water interface. As z_{scale} approaches zero, the diffusivity at the sediment-water-interface ($K_{surface}$) will approach K_0 (Fig. 1a versus Fig. 1b).

Modeled iridium was moved vertically by vertical diffusivity after the algorithms of Visser (Visser 1997) and Ross and Sharples (Ross and Sharples 2004), as a Markov process where the depth $z_{t+\Delta t}$ of a particle at time $t+\Delta t$ was a function of the depth (z_t) in the previous time step (t):

$$z_{t+\Delta t} = z_t + \frac{\partial K_v(z_t)}{\partial z}\Delta t + R\left[\frac{2K_v\left(z_t + \frac{1}{2}\frac{\partial K_v}{\partial z}\Delta t\right)\Delta t}{r}\right]^{1/2} + w_s \Delta t$$

where R is a random process with a zero mean and a variance of r. We set $r = 1/3$, and drew R from a uniform distribution ranging from -1 to 1 (Ross and Sharples 2004; Tanaka and Franks 2008). Sedimentation (w_s) drives the continual sinking of sediment out of the mixed layers. The mixing model time step Δt was 10 years, representing a compromise between model run-time and an accurate depiction of mixing.

Iridium deposition was simulated by the introduction of "particles" into the model at the sedimentary surface, with each particle representing an equal amount of iridium. 10,000 and 100,000 particles were injected into the model and mixed according to the model parameterization in order to fit empirical iridium profiles and explore mixing model sensitivity respectively. Particle numbers were binned over 0.2 cm deep increments to obtain concentrations; the magnitude of the iridium anomaly was matched by multiplying the modeled profile by a constant multiplier. Model simulations were repeated 20 times during empirical model fitting, as individual model runs can vary due to the non-deterministic nature of our approach. Model fit is reported as the r^2 between the scaled median model and measured iridium. We included 27 data points in the calculation of r^2, truncating the long tail of background measurements as our model does not include any background iridium.

We approximate a one-layer model to contrast with the tanh-profile model by setting z_{scale} equal to 1.5cm. This truncates the mixing model to approximately one, well-mixed layer, but allows the simulation to model the bottom boundary without a large boundary artifact (e.g., Ross and Sharples 2004). In general, model artifacts are

introduced when:

$$\Delta t \lesssim \frac{(z_{scale})^2}{2K_0}$$

When Δt is equal to or larger than this ratio, the model will generate artificial accumulations of particles along boundaries (Ross and Sharples 2004).

We model the sediment-sea water interface as a reflecting boundary to handle instances where modeled sediment would be moved above the sea floor. The values of K_0, z_0, and z_{scale} were fit through an iterative procedure. In practice, we explored the model parameter space to identify promising parameter combinations. K_0, z_0, and z_{scale} were then optimized by randomly combining parameters drawn from uniform distributions in parameter space centered around initial K_0, z_0, and z_{scale} values. The best parameter combination was selected as the one that minimized the absolute average model error.

MODELING EXPERIMENTS

Model sensitivity was explored using a standard theoretical model with defaults of K_0= 1.0 cm^2/kyr, z_0= 5 cm, z_{scale}= 1.5 cm, sedimentation rate (w_s)= 0.5 cm/kyr and a single input of 100,000 tracer particles at time zero (Figure 5-2). In all cases, modeled concentrations were scaled to match the peak tracer count, to mimic the scaling of models to a given iridium profile.

The first three modeling experiments explored the effect of varying a single model parameter on modeled profile shape. K_0 was explored from 1-100 cm^2/kyr in the

mixing rate experiment (Figure 5-2a), w_s from 0.5-15 cm/kyr in the sedimentation rate experiment (Figure 5-2b), and z_0 from 2-15 cm in the mixing depth experiment (Figure 5-2c), while holding all other parameters constant.

A no mixing experiment investigated the contribution of iridium dissolved in seawater to the shape of KPg boundary iridium anomalies. On impact, part of the KPg bolide was vaporized, delivering a portion of the original iridium in a dissolved rather than particulate state (Paquay et al. 2008). As dissolved iridium has an oceanic residence time of 2000 – 20,000 years (Anbar et al. 1996), the vaporization of a portion of the KPg impactor resulted in a prolonged input of iridium to pelagic sediments. This prolonged iridium deposition has been hypothesized to be sufficient to account for the shape of deep-sea boundary anomalies. We modeled multiple impactor vaporization scenarios with the assumption of no sedimentary mixing in order to visualize the sensitivity of the iridium peak to the large uncertainties in both the portion of the impactor vaporized, 10-70% vaporization tested, and the residence time of oceanic iridium (Figure 5-2d).

In mixing scenario 1, we tested the relative effect of including versus excluding impactor dissolution on the resulting iridium anomaly shape given sediment mixing. We quantified the similarity between the resulting two profiles using a subsample of 22 evenly spaced points along the anomaly to calculate r^2.

In mixing scenario 2, we explored the possible complexity of iridium profiles that could be obtained given assumptions of temporally heterogeneous mixing depths and intensities and the prolonged deposition of iridium following the KPg impact.

Specifically, we modeled a large increase in mixing depth and intensity for 50 years following the KPg impact. This boundary mixing spike model was parameterized with base parameters of K_0= 1.0 cm^2/kyr, z_0= 5 cm, z_{scale}= 1.5 cm, w_s= 0.5 cm/kyr, and a 50 year period of enhanced mixing beginning with the iridium injection with parameters of K_0= 1000 cm^2/kyr, z_0= 100 cm, z_{scale}= 1.5 cm, w_s= 0.5 cm/kyr. Iridium deposition assumptions included the 30% dissolution of the impactor, a 6,300 year oceanic residence time for dissolved iridium, and a 60 year residence time for particulate iridium.

SAMPLE MATERIALS

We fit a highly resolved iridium anomaly measured by Michel *et al.* (1985) at the Deep Sea Drilling Program (DSDP) Site 577B, Shatsky Rise, North Pacific (32°26.48'N, 157°43.39'E) (Heath et al. 1985). The biostratigraphically-complete KPg boundary section is described as "a slightly mottled nannofossil ooze", with mottling of the boundary reflecting the bioturbation of the very pale brown Danian sediments into the white upper Maastrichtian nannofossil ooze (Heath et al. 1985). Relatively shallow sediment mixing is indicated by mixing of rare thoracosphaerids down to 5 cm below the nannofossil KPg boundary and the near-complete replacement of Mesozoic nannofossils (90-95%) at 10 cm above the boundary (Wright et al. 1985). Relatively deeper mixing is indicated by the mixing of Paleocene foraminifera more than 1 m into the Mesozoic (D'Hondt and Keller 1991).

We inferred sedimentation rates for DSDP Site 577B by tuning an x-ray florescence (XRF) record of Fe to a nearby astronomically calibrated site, Ocean Drilling Program (ODP) Site 1211. ODP Site 1211 was astronomically calibrated through the Paleocene to a number of sites by Westerhold *et al.* (Westerhold et al. 2008), and thus provides the most reliable set of relative ages for calculating sedimentation rates at Site 577B (see Table 5-1 and 5-2 for age model and age model tie points). In addition to fitting sediment mixing models to measured iridium anomalies, we also considered the distributions of three additional elements measured by Michel *et al.* (1985), Fe, Ni, and Al, as additional proxies for diagenetic remobilization.

RESULTS

Modeling Experiments

Varying mixing rate (K_0) while keeping all other parameters constant resulted in profiles with varying up-core slopes, in contrast to similar down-core profiles (Figure 5-2a). The highest diffusivities corresponded to the widest spread in boundary iridium and the most gradual up-core slope. Varying sedimentation rate (w_s, Figure 5-2b) effected iridium profile symmetry in addition to up-core and down-core iridium anomaly width and slope. Relatively high sedimentation rates, 5 and 15 cm/kyr, resulted in relatively symmetrical and narrow iridium anomalies as compared to profiles obtained with sedimentation rates of 0.5 and 1 cm/kyr. The extent of down-core mixing was most sensitive to the relative mixing depth (z_0) (Figure 5-2c). Deep mixing

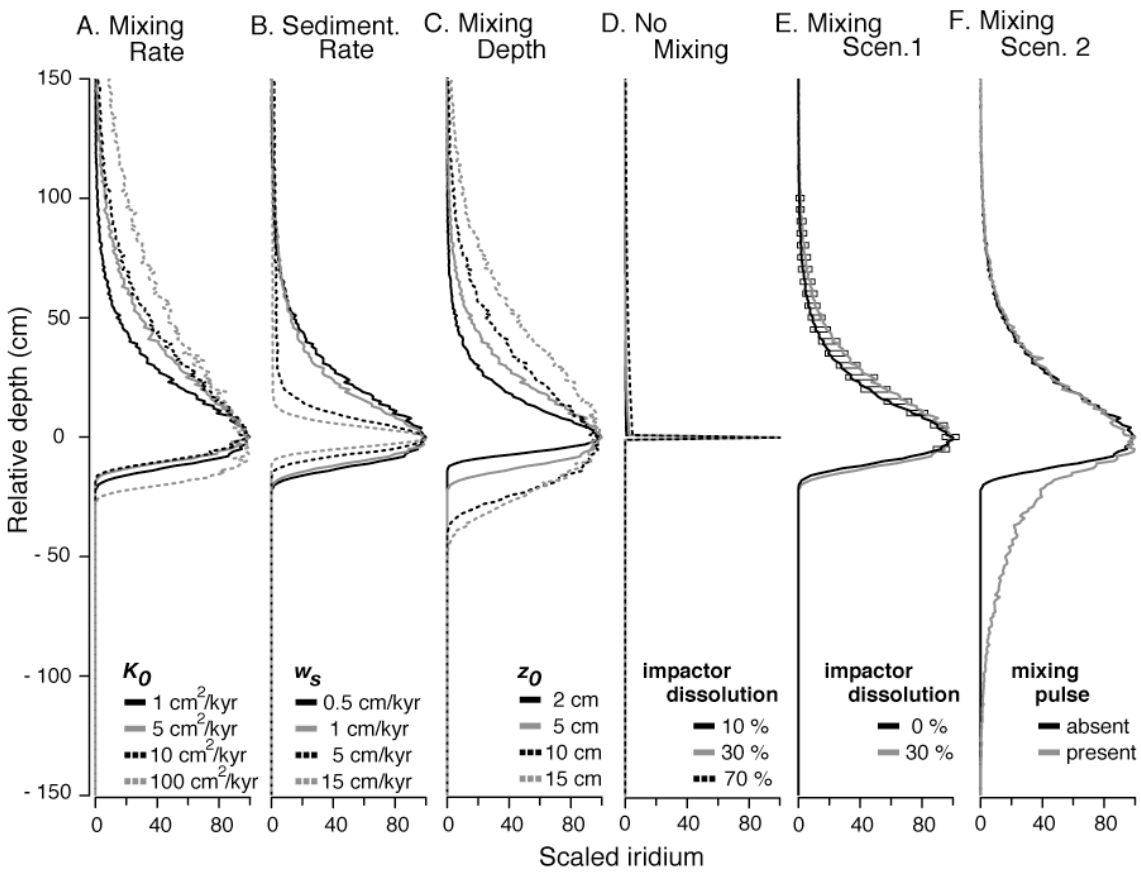

Figure 5-2. Theoretical examples of the effect of mixing parameters on model iridium profile shape. A standard mixing model was used to illustrate the model sensitivity to changes in (A) sediment diffusivity, K_0, (B) sedimentation rate, w_s, and (C) the depth of the well-mixed zone, (z_0). (D) Three scenarios for a prolonged iridium injection are shown assuming no sediment mixing and an iridium oceanic residence time of 6.3 kyr (10 and 30% impactor dissolution) or 20 kyr (70% dissolution). (E) Mixing scenario 1 contrasts the standard mixing model with and without a prolonged input of iridium from an assumed 30% impactor dissolution and 6.3 kyr residence time. Rectangles indicate samples used to calculate r^2. (F) Mixing scenario 2 contrasts the standard mixing model against a scenario assuming prolonged iridium deposition and elevated sediment mixing (depth and rate) for a short period following the KPg impact.

increased the depth of the down-core tail, while increasing overall profile symmetry.

Relative to the effect of sediment mixing on the modeled iridium anomaly, the inclusion or exclusion of impactor dissolution and ocean residence time had little effect on anomaly shape (Figure 5-2d, r^2 between profiles of 0.99 and $p< 0.001$).

Figure 5-2f demonstrates that it is possible to obtain complex, down-core sloping profiles with an advection-diffusion model given assumptions of temporally heterogeneous mixing and prolonged iridium deposition. The modeled boundary spike in sedimentary during part of an initial prolonged iridium injection period generated a down-core mixing profiles like that sometimes observed in heavily bioturbated sites such as Maud Rise (Figure 5-3a).

Shatsky Rise Iridium Anomaly

At Shatsky Rise DSDP Site 577B, the peak position and width of the iridium anomaly coincide with the peak position and width of elements with a range in redox sensitivities, from Al, which is relatively resistant to diagenetic remobilization, to Ni and Fe, which are remobilized under reducing conditions (Figure 5-4a). We fit three models to the iridium anomaly at Shatsky Rise. The first model was a no-mixing model that assumed no sediment mixing but incorporated the oceanic residence time of dissolved iridium. The no-mixing model failed to explain much of the anomaly shape (Figure 5-4c, r^2=0.12, p=0.07).

For the two subsequent models, both of which included sediment mixing, we assume that 90% of iridium was deposited instantaneously and 10% was impact vaporized with an oceanic residence time of 6,300 years. At the sedimentation rates typical at Shatsky Rise (0.5 - 1 cm/1000 years), the prolonged input of iridium has a minimal effect on profile shape after sediment mixing (Figure 5-2e), as well as on model parameterization and fit.

In contrast to the no-mixing model, both the one-layer and tanh mixing models explained most of the iridium anomaly shape, with r^2 of 0.81 and 0.87 respectively ($p<$ 0.001). The one-layer model was parameterized with K_0=0.5 cm^2/kyr, z_0=13 cm, and z_{scale}=1.5 cm. The tanh model was parameterized with K_0= 1 cm^2/kyr, z_0= 2.5 cm, and z_{scale}= 9.5 cm.

DETERMINANTS OF KPg IRIDIUM ANOMALY SHAPE IN OPEN OCEAN SEDIMENTS

Evidence for the diagenetic remobilization of iridium

Among the siderophilic elements enriched in KPg boundary sediments, iridium is the best candidate for a tracer of mixing as it is the least likely to be diagenetically remobilized (Colodner et al. 1992; Evans et al. 1993), and unlikely to be confounded by other iridium sources (Kyte 2002). Although relatively immobile, recent work has shown that iridium like other PGEs can be mobilized in reducing, low-temperature pore fluids (Colodner et al. 1992; Evans et al. 1993; Sawlowicz 1993). For example, remobilization of iridium in recent pelagic sediments under changes in redox conditions has been studied in an abyssal plain periodically influenced by distal turbidite flows (Colodner et al. 1992). Iridium becomes mobile by the reduction of oxic sediments below a newly deposited turbidite, resulting in a depletion of iridium at the oxic/suboxic transition (Colodner et al. 1992). This mechanism cannot account for the larger iridium anomalies at the KPg boundary, but has been evoked to explain iridium anomalies in other intervals marked by a large change in sedimentary environments and redox

conditions (Colodner et al. 1992; Sawlowicz 1993; Wallace et al. 1990; Wang et al. 1993). There is evidence, however, for the remobilization of the KPg boundary iridium anomaly in reducing environments, including terrestrial coal deposits (Evans et al. 1993; Izett 1990) and, possibly, reducing marine settings (Martinez-Ruiz et al. 1999). Remobilization of iridium in reducing KPg sediments is not a universal feature, as iridium can lack evidence of remobilization in reducing sites where other PGEs are remobilized (Evans et al. 1993; Kyte 2002) and PGE ratios often differ from expected values given their relative diagenetic mobility (e.g., Lee et al. 2003; Stueben et al. 2002).

Pelagic sections have relatively low organic carbon content and, outside of the Tethys and other neritic sites, appear to have been largely oxic in the early Danian (e.g., Barker et al. 1988; Heath et al. 1985; Perch-Nielsen et al. 1977). Oxic bottom waters and low organic fluxes are both characteristics which theoretically reduce the likelihood of iridium remobilization (e.g., Colodner et al. 1992).

Evidence for prolonged deposition shaping deep sea iridium profiles

The spread in the iridium anomaly at the KPg boundary has also been attributed to prolonged iridium input from the partial dissolution of the impactor (Anbar et al. 1996, although see Smit 1999). We were unable to simulate a comparable spread in the iridium anomaly from simply assuming a prolonged iridium input (Figure 5-2d) with very permissive assumptions including a higher impactor dissolution than has previously been hypothesized (70% in contrast to the 5-30% typically considered,

[Paquay et al. 2008]), the uppermost bound for iridium residence times (20 kyr, [Anbar et al. 1996]), and low sedimentation rates (0.5 cm/kyr).

Evidence of volcanism in deep sea iridium profiles

Many KPg iridium profiles have low, wide shoulders bracketing the steep boundary anomaly with Ir concentrations above background levels (e.g., Officer and Drake 1983; Robin et al. 1991; Rocchia et al. 1990). This enrichment above background iridium, readily apparent only on a log scale, has been variously attributed to volcanism (Officer and Drake 1985; Rocchia et al. 1990), multiple impacts (Rocchia et al. 1990), prolonged iridium input (Anbar et al. 1996), a change in sedimentary dilution (Robinson et al. 2009), and diagenetic remobilization of iridium (Robin et al. 1991; Rocchia et al. 1990). Growing evidence suggests that Deccan volcanism may provide the most parsimonious explanation for this increase in background iridium.

The time period of the main phase of Deccan volcanism generally coincides with a pre- and post- boundary elevation in background iridium. Peak Deccan emplacement occurred during C29r which lasted ~800 kyr (Courtillot et al. 1986), with the main volcanic phase beginning ~340 kyr prior to the impact (Robinson et al. 2009) and possibly ending at the KPg boundary with a subsequent eruption in late C29r to early C29n (Chenet et al. 2007; Keller et al. 2009). The increase in background iridium spans a comparable time interval at some sites (e.g., Robin et al. 1991; Robinson et al. 2009; Rocchia et al. 1990), although is considerably shorter at others (Officer and Drake 1985; Robin et al. 1991). Osmium isotopes and Os and iridium levels at multiple

sites indicate a distinct pre-boundary shift coincident with the onset of Deccan volcanism (Ravizza and Peucker-Ehrenbrink 2003; Robinson et al. 2009), with PGE ratios (Pt/Ir) ruling out an influence of extensive diagenetic remobilization. Deccan volcanism may influence Ir, Os and other PGEs directly by the addition of new PGEs to the ocean or indirectly via a change in sedimentary dilution (e.g., decreased sedimentation rates due to volcanogenic CO_2/acidification; Robinson et al. 2009).

Alternative mechanisms for the increase in background iridium fail to fully explain the observed patterns: i) slow deposition of dissolved impact iridium cannot account for the pre-impact elevation in background concentrations, ii) diagenetic explanations have been rejected in a recent investigation on the basis of Pt/Ir ratios (Robinson et al. 2009); evidence which also precludes a sediment mixing mechanism, and iii) evidence for multiple impacts driving the elevation is lacking as small extra-KPg peaks occur at different stratigraphic intervals between cores and correspond with burrows within cores (e.g., Pospichal et al. 1990). Thus, the relative timing and explanatory power suggests that Deccan volcanism provides the most likely explanation for the increase in background iridium.

Evidence for sediment mixing in boundary anomaly shapes

From the earliest discussions of the distribution of boundary ejecta and microfossils, bioturbation and other sedimentary processes have been used to explain the apparent temporal spread of impact markers and the faunal mixing of the late Cretaceous and early Paleocene species (e.g., Kyte et al. 1985; Robin et al. 1991;

Thierstein 1981). Pervasive burrowing of complete distal KPg boundary sections is readily apparent due to a distinct color change between light Maastrichtian and dark

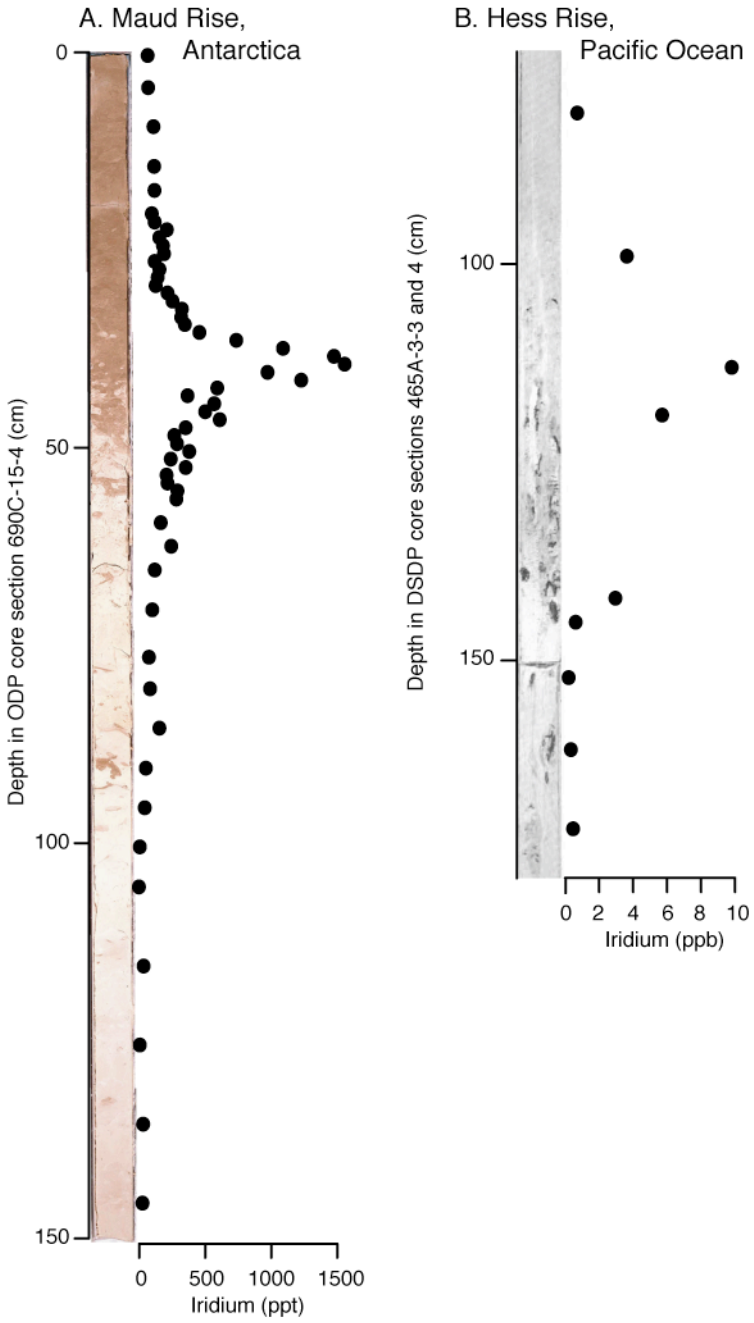

Figure 5-3. Core photographs illustrate physical mixing of sediment at Maud Rise and Hess Rise. Iridium anomalies are plotted adjacent to photographs of cores for (A) the heavily bioturbated Maud Rise KPg boundary, and (B) the coring-disturbed KPg boundary at Hess Rise.

Danian sediments (Smit 1999). Among the visibly bioturbated boundary sections are sites like Agost (Rodriguez-Tovar 2005), Caravaca (Rodriguez-Tovar and Uchman 2008), and Maud (Pospichal et al. 1990), to name just a few. Burrowing by early Danian benthic communities into Masstrichtian sediments is confirmed by the presence of impact ejecta (Rodriguez-Tovar 2005) and Danian fossils (e.g., Pospichal et al. 1990; Premoli Silva et al. 2005) in the boundary-crossing burrows. The correspondence between the extent of visible burrows, fossil reworking, and the iridium anomalies at sites like Maud Rise (Figure 5-3a, [Barker et al. 1988; Michel et al. 1990]) and El Kef (Pospichal 1994; Robin et al. 1991), and the extent of coring disturbance and the iridium anomaly at Hess Rise (Figure 5-3b, [Michel et al. 1981; Vallier et al. 1981]), provides some support for the hypothesis that physical mixing is the primary determinant of iridium anomaly shape in oxic, pelagic sites distal to the impact.

The correspondence in mixing extent between iridium and micro- to nannofossils suggests that iridium has a key characteristic of a useful tracer, namely, it tracks the sedimentary constituent of interest. Sediment mixing is generally biased by size, with smaller particles being transported over greater distances than larger particles (e.g., Thomson et al. 1995; Wheatcroft 1992). In a comparison between boundary profiles of iridium and Ni-spinels, iridium anomalies had greater peak widths than Ni-spinels in the three sites analyzed (Robin et al. 1991). Ni-spinels are much larger (Robin et al. only quantified spinels >1 mm) and denser than the main constituents of carbonate oozes (foraminifera, nannoplankton, and clay). In contrast iridium is thought to likely be bound to the clay or fine fraction of sediments (Claeys et al. 2002; Rocchia et al.

1990). A comparison between nannofossil reworking (Pospichal 1994) and the up-core tail of iridium at El Kef (Robin et al. 1991), indicates that iridium provides a better tracer than Ni-spinels of the sedimentary mixing of nannofossils. The Ni-spinel peak at all sites studied by Robin et al. is narrow compared to typical burrowing depth and fossil reworking as well as iridium anomaly width, suggesting that iridium may behave more like the carbonate fossils that comprise most of the sediment.

In some pelagic sites, a sediment mixing driver of iridium anomaly shape has been disregarded in favor chemical remobilization on the grounds of an overly symmetrical anomaly shape (e.g., Lee et al. 2003; Officer and Drake 1985) and a width (uncompacted thickness of 61 cm) requiring an unrealistically large mixing depth (Officer and Drake 1983). However, our results show that realistic mixing depths and rates can readily generate anomalies with comparable dimensions (Figure 5-2).

MODELING SEDIMENT MIXING AT THE CRETACEOUS-PALEOGENE BOUNDARY

Sediment mixing at Shatksy Rise (DSDP 577B), North Pacific

Diagenetic remobilization and prolonged iridium inputs do not appear to explain much of the shape in KPg boundary iridium at Shatsky Rise. Fe, Ni, and Al anomalies match the iridium anomaly shape (Figure 5-4a) despite the diversity of diagenetic mobility of these elements in reducing environments. We would expect diagenetic remobilization to cause the divergence of elemental profiles from one another; this is not observed. Similarly, modeled prolonged iridium input from impact vaporization

alone poorly fits the observed iridium shape (Figure 5-4b). Without mixing, 70% of the iridium input is contained in 3cm spanning the KPg boundary as compared with the approximately 20 cm spanned by 70% of the boundary iridium at DSDP Site 577B.

In contrast to diagenesis and prolonged iridium input, Lagrangian advection-

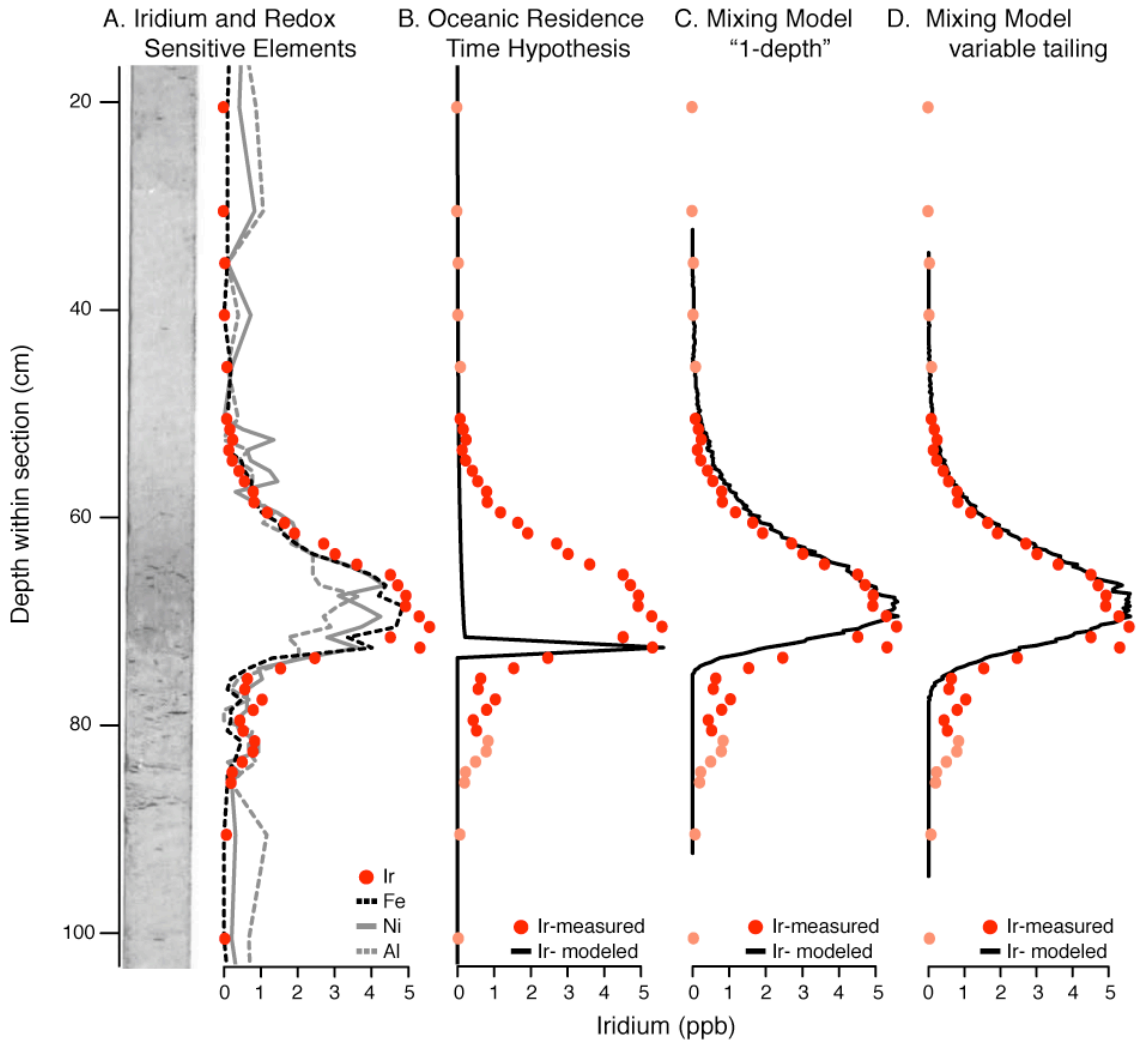

Figure 5-4. Investigation of potential mechanisms leading to iridium anomaly shape at DSDP 577B, Shatsky Rise. The 577B iridium anomaly is plotted against (A) elements ranging in redox sensitivity, (B) a model of prolonged iridium deposition assuming no mixing, (C) a model of iridium mixing assuming a near one-layer mixing profile, and (D) a model of iridium mixing assuming an asymptotic decrease in sediment mixing with depth. In all panels iridium is plotted with red or pink circles; in panels B-D the pink circles indicate samples that were excluded from the calculation of r^2.

diffusion mixing models explain most of the observed iridium anomaly shape. We test a one-layer model against a more complex, tahn mixing model (Figure 5-4c and 4d, one-layer approximated with the smallest z_{scale} possible given model conditions, z_{scale}=1.5 cm) and find that both models perform nearly as well (0.81 and 0.87 respectively, $p<$ 0.001). As the one-layer model is effectively the simpler model, we choose this as the best model of sediment mixing at DSDP Site 577B. Iridium anomalies reported from other sites can have more complex shapes than the anomalies at Shatsky Rise in the North Pacific. In these more complex profiles, the independent manipulation of z_0 and z_{scale} may be of greater import.

Both models failed to fit two Maastrichtian peaks between 75 and 85 cm. Given the distinct mottled appearance of boundary mixing, we suspect that both peaks are due to lumpy mixing rather than pre-boundary events. These pre-boundary peaks highlight a general limitation of basic advection-diffusion models; namely, they are not designed to model non-local mixing like the rare transport of surface sediment to great depths by large burrowers. Notably, the Lagrangian mixing model used in this study can be readily modified to include non-local mixing like lumpy mixing.

General expectations for mixed records of rapid events

The model sensitivity analysis, literature review, and analysis at the Shatsky Rise, North Pacific suggest a number of general expectations for mixed records of geologically instantaneous events like the impact at the KPg boundary.

1) **Strict tests of relative symmetry cannot be used to test for sediment mixing.** Sediment mixing can mix a point event into a wide-range of profile shapes

from relatively symmetrical to down-core tailing under assumptions of no-change in mixing depth or rate, to up-core tailing with assumptions of decreased mixing rates with the time (Figure 5-2).

2) For any event, small sedimentary constituents may be transported farther than large ones. The differential reworking of nannofossils and foraminifera across the KPg boundary, and different KPg boundary placement on the basis of iridium, nannofossil and foraminiferal biostratigraphy have all been the subject of some debate in the past. Such offsets are expected given sediment mixing; the relative depth of sediment mixing can range from effectively the same across size classes to increasing with decreasing size from foraminifera to nannofossils to iridium. The largest sedimentary constituents (Ni-spinels and other large ejecta at the KPg boundary) will typically have narrow distributions as compared to all common sedimentary constituents.

3) Sediment mixing tends to move the peak depth of a mixing tracer into stratigraphically older sediments. The relative magnitude of the peak offset from the depth of initial emplacement is controlled by the combination of mixing parameters used to generate a given mixing profile. As two similar profiles can be obtained from different combinations of mixing parameters (Figure 5-2), it will be difficult to accurately estimate the depth of peak shift from fitting profiles alone. It may be possible to better estimate this movement by a comparison of relatively immobile particles like large ejecta and relatively mobile particles like sediment-associated iridium. Such comparisons may help constrain possible mixing parameter combinations to better approximate the mixing conditions that generated any given profile.

4) Lumpy or non-local mixing can result in secondary peaks in the abundance of an event marker; peaks may not occur at all locales, will be diachronous when present, and may visibly correspond with displaced sediment. Advection-diffusion models, including the model used in this study, typically do not model non-local, lumpy mixing. However, at the KPg boundary

secondary peak characteristics fit the description above suggesting that lumpy mixing provides a reasonable explanation for secondary peaks in KPg iridium anomalies when present.

5) **If a chemical marker is transported to depths equal to or less than the depth of visible burrowing, then sediment mixing may provide the most parsimonious determinant of profile shape.** Although diagenesis and diffusion are commonly evoked to explain KPg iridium profiles in the presence of visible burrowing, it is difficult to imagine conditions whereby mixing would move sediment but not iridium, with diagenetic remobilization of iridium only occurring once sediment sinks below the depth of active mixing. Sediment mixing is not always visible, so the converse of this statement is not valid.

CONCLUSIONS

The shape of the KPg iridium anomaly in oxic, pelagic sites appears to be primarily determined by sediment mixing. Evidence supporting sediment mixing includes: (1) the correspondence of iridium profiles with sedimentary burrows and boundary material, (2) the low mobility of iridium in oxic sediments, and (3) the similarity of element profiles despite differences in susceptibility to diagenetic remobilization. Many existing studies attribute the shape of the iridium anomaly to diagenesis by default despite the extensive documentation of burrowing and evidence for assemblage mixing across the boundary. We find more evidence supporting diagenetic remobilization of iridium in reducing sites and advise against the use of iridium as a mixing tracer in these instances.

We directly model sediment mixing at Shatsky Rise by fitting a Lagrangian advection-diffusion model to measured iridium and find that our simplest model

provides the best fit relative to model complexity. Thus, parameterizing sediment mixing models to KPg boundary iridium anomalies offers a powerful approach for quantitatively defining and accounting for the extent of mixing effects in KPg boundary records. It remains to be tested whether mixing models can fit highly resolved iridium anomalies from other pelagic environments with more complicated mixing histories. If sediment mixing models can be fit to a range of pelagic boundary sections, it may be possible to statistically increase the temporal resolution of our interpretation of boundary impacts and recovery in the earliest Danian.

REFERENCES

ALVAREZ, W. 1996. Trajectories of ballistic ejecta from the Chicxulub Crater, p. 141-150. *In* G. Ryder, D. Fastovsky and S. Gartner [eds.], The Cretaceous-Tertiary event and other catastrophes in earth history: Geological Society of America Special Paper 307.

ALVAREZ, W., F. ASARO, and A. MONTANARI. 1990. Iridium profile for 10-million years across the Cretaceous-Tertiary boundary at Gubbio (Italy). Science **250:** 1700-1702.

ANBAR, A. D., G. J. WASSERBURG, D. A. PAPANASTASSIOU, and P. S. ANDERSSON. 1996. Iridium in natural waters. Science **273:** 1524-1528.

ARCHER, D., H. KHESHGI, and E. MAIER-REIMER. 1998. Dynamics of fossil fuel CO2 neutralization by marine CaCO3. Global Biogeochemical Cycles **12:** 259-276.

BARKER, P. F., J. P. KENNETT, and E. AL. 1988. Site 690, p. 183-292. *In* P. F. Barker, J. P. Kennett and e. al. [eds.], Proc. ODP, Init. Repts., 113. Ocean Drilling Program, College Station, TX.

BOUDREAU, B. P. 1986a. Mathematics of tracer mixing in sediments: 1. Spatially-dependent, diffusive mixing. American Journal of Science **286:** 161-198.

---. 1986b. Mathematics of tracer mixing in sediments: 2. Nonlocal mixing and biological conveyor-belt phenomena. American Journal of Science **286:** 199-238.

BOUDREAU, B. P., and D. M. IMBODEN. 1987. Mathematics of tracer mixing in sediments: 3. The theory of nonlocal mixing within sediments. American Journal of Science **287:** 693-719.

CHARBIT, S., C. RABOUILLE, and G. SIANI. 2002. Effects of benthic transport processes on abrupt climatic changes recorded in deep-sea sediments: A time-dependent modeling approach. Journal of Geophysical Research-Oceans **107**.

CHENET, A. L., X. QUIDELLEUR, F. FLUTEAU, V. COURTILLOT, and S. BAJPAI. 2007. K-40-Ar-40 dating of the Main Deccan large igneous province: Further evidence of KTB age and short duration. Earth and Planetary Science Letters **263:** 1-15.

CLAEYS, P., W. KIESSLING, and W. ALVAREZ. 2002. Distribution of Chicxulub ejecta at the Cretaceous-Tertiary boundary, p. 55 - 69. *In* C. Koeberl and K. G. MacLeod [eds.], Catastrophic events and mass extinctions: impacts and beyond: Geological Society of America Special Paper 356.

COLODNER, D. C., E. A. BOYLE, J. M. EDMOND, and J. THOMSON. 1992. Postdepositional mobility of platinum, iridium and rhenium in marine-sediments. Nature **358:** 402-404.

COURTILLOT, V., J. BESSE, D. VANDAMME, R. MONTIGNY, J. J. JAEGER, and H. CAPPETTA. 1986. Deccan flood basalts at the Cretaceous-Tertiary boundary. Earth and Planetary Science Letters **80:** 361-374.

CROCKET, J. H., C. B. OFFICER, F. C. WEZEL, and G. D. JOHNSON. 1988. Distribution of noble-metals across the Cretaceous/Tertiary boundary at Gubbio, Italy - iridium variation as a constraint on the duration and nature of Cretaceous/Tertiary boundary events. Geology **16:** 77-80.

D'HONDT, S., and G. KELLER. 1991. Some patterns of planktic foraminiferal assemblage turnover at the Cretaceous Tertiary boundary. Marine Micropaleontology **17:** 77-118.

EVANS, N. J., D. C. GREGOIRE, W. D. GOODFELLOW, B. I. MCINNES, N. MILES, and J. VEIZER. 1993. Ru/Ir Ratios at the Cretaceous-Tertiary boundary - Implications for PGE source and fractionation within the ejecta cloud. Geochimica Et Cosmochimica Acta **57:** 3149-3158.

GLASS, B. P. 1969. Reworking of deep-sea sediments as indicated by vertical dispersion of Australasian and Ivory Coast microtektite horizons. Earth and Planetary Science Letters **6:** 409-&.

GOLDBERG, E. D., and M. KOIDE. 1962. Geochronological Studies of Deep Sea Sediments by the Ionium-Thorium Method. Geochimica Et Cosmochimica Acta **26:** 417-450.

GUINASSO, N. L., and D. R. SCHINK. 1975. Quantitative estimates of biological mixing rates in abyssal sediments. Journal of Geophysical Research-Oceans and Atmospheres **80:** 3032-3043.

HEATH, G. R., L. H. BURCKLE, and E. AL. 1985. Site 577, p. 91-137. *In* G. R. Heath, L. H. Burckle and e. al. [eds.], Init. Repts. DSDPP, 86. U.S. Govt. Printing Office, Washington.

IZETT, G. A. 1990. The Cretaceous/Tertiary boundary interval, Raton Basin, Colorado, and New Mexico, and its content of shock-metamorphosed minerals: evidence relevant to the K/T boundary impact-extinction theory. GSA Spec. Paper 249**:** 100.

KELLER, G. and others 2009. K-T transition in Deccan Traps of central India marks major marine seaway across India. Earth and Planetary Science Letters **282:** 10-23.

KYTE, F. T. 2002. Tracers of the extraterrestrial component in sediments and inferences for Earth's accretion history, p. 21-38. *In* C. Koeberl and N. MacLeod [eds.], Catastrophic events and mass extinctions: impacts and beyond: Geological Society of America Special Paper 356.

KYTE, F. T., J. SMIT, and J. T. WASSON. 1985. Siderophile interelement variations in the Cretaceous-Tertiary boundary sediments from Caravaca, Spain. Earth and Planetary Science Letters **73:** 183-195.

LEE, C. T. A., G. J. WASSERBURG, and F. T. KYTE. 2003. Platinum-group elements (PGE) and rhenium in marine sediments across the Cretaceous-Tertiary boundary: constraints on Re-PGE transport in the marine environment. Geochimica Et Cosmochimica Acta **67:** 655-670.

MARTINEZ-RUIZ, F., M. ORTEGA-HUERTAS, and I. PALOMO. 1999. Positive Eu anomaly development during diagenesis of the K/T boundary ejecta layer in the Agost section (SE Spain): implications for trace-element remobilization. Terra Nova **11:** 290-296.

MEYSMAN, F. J. R., B. P. BOUDREAU, and J. J. MIDDELBURG. 2003. Relations between local, nonlocal, discrete and continuous models of bioturbation. Journal of Marine Research **61:** 391-410.

MICHEL, H. V., F. ASARO, W. ALVAREZ, and L. W. ALVAREZ. 1981. Distribution of iridium and other elements near the Cretaceous/Tertiary boundary in Hole 465A: Preliminary results, p. 847-849. *In* J. Thiede and T. L. Vallier [eds.], Init. Repts. DSDP, 62. U.S. Govt. Printing Office, Washington.

---. 1985. Elemental profile of iridium and other elements near the Cretaceous/Tertiary boundary in Hole 577B, p. 533-538. *In* G. R. Heath, L. H. Burckle and e. al. [eds.], Init. Repts. DSDPP, 86. U. S. Govt. Printing Office, Washington.

---. 1990. Geochemical studies of the Cretaceous-Tertiary boundary in ODP holes 689B and 690C. *In* P. F. Barker and J. P. Kennett [eds.], Proc. ODP, Sci. Results, 113. Ocean Drilling Program, College, Station, TX.

OFFICER, C. B., and C. L. DRAKE. 1983. The Cretaceous-Tertiary transition. Science **219:** 1383-1390.

---. 1985. Terminal Cretaceous environmental events. Science **227:** 1161-1167.

PAQUAY, F. S., G. E. RAVIZZA, T. K. DALAI, and B. PEUCKER-EHRENBRINK. 2008. Determining chondritic impactor size from the marine osmium isotope record. Science **320:** 214-218.

PENG, T. H., W. S. BROECKER, and W. H. BERGER. 1979. Rates of benthic mixing in deep-sea sediment as determined by radioactive-tracers. Quaternary Research **11:** 141-149.

PERCH-NIELSEN, K., P. R. SUPKO, and E. AL. 1977. Site 356: São Paulo Plateau, p. 141-230. *In* P. R. Supko, K. Perch-Nielsen and e. al [eds.], Init. Repts. DSDP, 39. U.S. Govt. Printing Office, Washington.

POSPICHAL, J. J. 1994. Calcareous nannofossils at the K-T Boundary, El Kef - no evidence for stepwise, gradual, or sequential extinctions. Geology **22:** 99-102.

POSPICHAL, J. J., S. W. WISE JR., F. ASARO, and N. HAMILTON. 1990. The effects of bioturbation across a biostratigraphically complete high southern latitude Cretaceous/Tertiary boundary, p. 497-507. *In* V. L. Sharpton and P. D. Ward [eds.], Global catastrophes in earth history: an interdisciplinary conference on impacts, volcanism, and mass mortality: Geological Society of America Special Paper 247.

PREISINGER, A. and others 1986. The Cretaceous Tertiary Boundary in the Gosau Basin, Austria. Nature **322:** 794-799.

PREMOLI SILVA, I., M. R. PETRIZZO, and D. MELLONI. 2005. Data Report: Planktonic foraminiferal biostratigraphy across the Cretaceous/Paleocene boundary at

Shatsky Rise (ODP Leg 198, Northwest Pacific), p. 1-16. *In* T. Bralower, I. Premoli Silva and M. J. Malone [eds.], Proc. ODP, Sci. Results, 198.

RAVIZZA, G., and B. PEUCKER-EHRENBRINK. 2003. Chemostratigraphic evidence of Deccan volcanism from the marine osmium isotope record. Science **302:** 1392-1395.

RIDGWELL, A. 2007. Interpreting transient carbonate compensation depth changes by marine sediment core modeling. Paleoceanography **22:** -.

RIDGWELL, A., and J. C. HARGREAVES. 2007. Regulation of atmospheric CO2 by deep-sea sediments in an Earth system model. Global Biogeochemical Cycles **21:** -.

ROBIN, E., D. BOCLET, P. BONTE, L. FROGET, C. JEHANNO, and R. ROCCHIA. 1991. The Stratigraphic distribution of Ni-rich spinels in Cretaceous-Tertiary boundary rocks at El-Kef (Tunisia), Caravaca (Spain) and Hole-761c (Leg-122). Earth and Planetary Science Letters **107:** 715-721.

ROBINSON, N., G. RAVIZZA, R. COCCIONI, B. PEUCKER-EHRENBRINK, and R. NORRIS. 2009. A high-resolution marine Os-187/Os-188 record for the late Maastrichtian: distinguishing the chemical fingerprints of Deccan volcanism and the KP impact event. Earth and Planetary Science Letters **281:** 159-168.

ROCCHIA, R. and others 1990. The Cretaceous Tertiary boundary at Gubbio revisited - vertical extent of the Ir anomaly. Earth and Planetary Science Letters **99:** 206-219.

RODRIGUEZ-TOVAR, F., and A. UCHMAN. 2008. Bioturbational disturbance of the Cretaceous-Palaeogene (K-Pg) boundary layer: implications for the interpretation of the K-Pg boundary impact event. Geobios **41:** 661-667.

RODRIGUEZ-TOVAR, F. J. 2005. Fe-oxide spherules infilling Thalassinoides burrows at the Cretaceous-Paleogene (K-P) boundary: evidence of a near-contemporaneous macrobenthic colonization during the K-P event. Geology **33:** 585-588.

ROSS, O. N., and J. SHARPLES. 2004. Recipe for 1-D Lagrangian particle tracking models in space-varying diffusivity. Limnology and Oceanography-Methods **2:** 289-302.

RUDDIMAN, W. F., and L. K. GLOVER. 1972. Vertical mixing of ice-rafted volcanic ash in North Atlantic sediments. Geological Society of America Bulletin **83:** 2817-&.

RUDDIMAN, W. F., G. A. JONES, T. H. PENG, L. K. GLOVER, B. P. GLASS, and P. J. LIEBERTZ. 1980. Tests for size and shape dependency in deep-sea mixing. Sedimentary Geology **25:** 257-276.

SAWLOWICZ, Z. 1993. Iridium and other Platinum-Group Elements as geochemical markers in sedimentary environments. Palaeogeography Palaeoclimatology Palaeoecology **104:** 253-270.

SCHMITZ, B. 1985. Metal precipitation in the Cretaceous-Tertiary boundary clay at Stevns Klint, Denmark. Geochimica Et Cosmochimica Acta **49:** 2361-2370.

SHULL, D. H. 2001. Transition-matrix model of bioturbation and radionuclide diagenesis. Limnology and Oceanography **46:** 905-916.

SMIT, J. 1999. The global stratigraphy of the Cretaceous-Tertiary boundary impact ejecta. Annual Review of Earth and Planetary Sciences **27:** 75-113.

SMITH, C. R., and C. RABOUILLE. 2002. What controls the mixed-layer depth in deep-sea sediments? The importance of POC flux. Limnology and Oceanography **47:** 418-426.

STUEBEN, D. and others 2002. Two anomalies of platinum group elements above the Cretaceous-Tertiary boundary at Beloc, Haiti: Geochemical context and consequences for the impact scenario, p. 55-68. *In* C. Koeberl and K. G. MacLeod [eds.], Catastrophic events and mass extinctions: impacts and beyond: Geological Society of America Special Paper 356.

TANAKA, Y., and P. J. S. FRANKS. 2008. Vertical distributions of Japanese sardine (Sardinops melanostictus) eggs: comparison of observations and a wind-forced Lagrangian mixing model. Fisheries Oceanography **17:** 89-100.

THIERSTEIN, H. R. 1981. Late Cretaceous calcareous nannoplankton and the change at the Cretaceous-Tertiary boundary, p. 355-394, Society of Economic Paleontologists and Mineralogists Special Publications no. 32.

THOMSON, J., G. T. COOK, R. ANDERSON, A. B. MACKENZIE, D. D. HARKNESS, and I. N. MCCAVE. 1995. Radiocarbon age offsets in different-sized carbonate components of deep-sea sediments. Radiocarbon **37:** 91-101.

TRAUTH, M. H. 1998. TURBO: A dynamic-probabilistic simulation to study the effects of bioturbation on paleoceanographic time series. Computers & Geosciences **24:** 433-441.

TRAUTH, M. H., M. SARNTHEIN, and M. ARNOLD. 1997. Bioturbational mixing depth and carbon flux at the seafloor. Paleoceanography **12:** 517-526.

VALLIER, T. L., J. THIEDE, and E. AL. 1981. Site 465: Southern Hess Rise. *In* J. Thiede and T. L. Vallier [eds.], Init. Repts. DSDP, 62. U.S. Govt. Printing Office, Washington.

VISSER, A. W. 1997. Using random walk models to simulate the vertical distribution of particles in a turbulent water column. Marine Ecology-Progress Series **158:** 275-281.

WALLACE, M. W., V. A. GOSTIN, and R. R. KEAYS. 1990. Acraman impact ejecta and host shales - evidence for low-temperature mobilization of iridium and other platinoids. Geology **18:** 132-135.

WANG, K., M. ATTREP, and C. J. ORTH. 1993. Global iridium anomaly, mass extinction, and redox change at the Devonian-Carboniferous boundary. Geology **21:** 1071-1074.

WESTERHOLD, T. and others 2008. Astronomical calibration of the Paleocene time. Palaeogeography Palaeoclimatology Palaeoecology **257:** 377-403.

WHEATCROFT, R. A. 1992. Experimental tests for particle size-dependent bioturbation in the deep ocean. Limnology and Oceanography **37:** 90-104.

WRIGHT, A. A. and others 1985. Summary of the Cretaceous/Tertiary Boundary studies, Deep Sea Drilling Project Site 577, Shatsky Rise, p. 799-804. *In* G. R. Heath, L. H. Burckle and e. al. [eds.], Init. Repts. DSDPP, 86. U. S. Govt. Printing Office, Washington.

Chapter 5 is in preparation for publication as: Hull, Pincelli; Franks, Peter; Norris, Richard "Using mixing models and iridium anomalies to quantify sediment mixing at the Cretaceous-Paleogene boundary". The dissertation author was the primary investigator and author of this paper.

Table 5-1. **Iridium measurements from DSDP Site 577B (Michel et al. 1985), Shatsky Rise, with revised age model based on current model for ODP Site 1211 (Westerhold et al. 2008).** mbsf= meters below sea floor.

Site-Hole-Core-Section	Depth (cm)	mbsf (m)	Age (my)	Ir (ppb)	Ir error (+/-)
577B-1-4	1-2	108.915	65.178	0.019	0.006
	10-11	109.005	65.195	0.019	0.006
	20-21	109.105	65.214	0.019	0.006
	30-31	109.205	65.232	0.019	0.006
	35-36	109.255	65.241	0.058	0.014
	40-41	109.305	65.251	0.048	0.007
	45-46	109.355	65.260	0.117	0.016
	50-51	109.405	65.264	0.11	0.014
	51-52	109.415	65.265	0.194	0.033
	52-53	109.425	65.266	0.272	0.029
	53-54	109.435	65.266	0.166	0.025
	54-55	109.445	65.267	0.261	0.023
	55-56	109.455	65.268	0.443	0.044
	56-57	109.465	65.268	0.59	0.05
	57-58	109.475	65.269	0.83	0.05
	58-59	109.485	65.270	0.85	0.04
	59-60	109.495	65.271	1.21	0.06
	60-61	109.505	65.271	1.68	0.07
	61-62	109.515	65.272	1.95	0.1
	62-63	109.525	65.273	2.74	0.12
	63-64	109.535	65.274	3.05	0.13
	64-65	109.545	65.274	3.64	0.16
	65-66	109.555	65.275	4.55	0.2
	66-67	109.565	65.276	4.75	0.19
	67-68	109.575	65.277	4.97	0.21
	68-69	109.585	65.277	4.96	0.21
	69-70	109.595	65.278	5.33	0.21
	70-71	109.605	65.279	5.61	0.22
	71-72	109.615	65.280	4.55	0.18
KPg boundary	72-73	109.625	65.281	5.35	0.21
	73-74	109.635	65.282	2.5	0.08
	74-75	109.645	65.284	1.57	0.05
	75-76	109.655	65.285	0.67	0.034
	76-77	109.665	65.287	0.601	0.036
	77-78	109.675	65.288	1.07	0.08
	78-79	109.685	65.290	0.83	0.08
	79-80	109.695	65.292	0.465	0.044
	80-81	109.705	65.293	0.557	0.05
	81-82	109.715	65.295	0.87	0.06

Table 5-1. Continued from previous page

Site-Hole-Core-Section	Depth (cm)	mbsf (m)	Age (my)	Ir (ppb)	Ir error (+/-)
	82-83	109.725	65.296	0.82	0.06
	83-84	109.735	65.298	0.53	0.04
	84-85	109.745	65.299	0.257	0.03
	85-86	109.755	65.301	0.229	0.02
	90-91	109.805	65.308	0.102	0.013
	100-101	109.905	65.324	0.059	0.011
	110-111	110.005	65.339	0.297	0.025
	120-121	110.105	65.355	0.019	0.003
	130-131	110.205	65.370	0.019	0.003
	140-141	110.305	65.385	0.019	0.003
	150-151	110.405	65.401	0.019	0.003

Table 5-2. DSDP Site 577B, Shatsky Rise, mbsf tie points to ODP Site 1211 age model (Westerhold et al. 2008) based on matching features in x-ray florescence models of iron from both sites.

mbsf (m)	Age (my)
107.460	64.872
107.629	64.981
107.672	64.990
107.754	65.001
108.155	65.083
108.311	65.103
108.795	65.160
108.853	65.167
109.358	65.261
109.620	65.280
111.313	65.541
111.449	65.558
111.539	65.575
111.672	65.625

CHAPTER VI

Geographically and temporally heterogeneous changes in ocean export productivity at the Cretaceous-Paleogene boundary

ABSTRACT

The impact at the Cretaceous-Paleogene boundary led to a mass extinction in the open sea and reduced export of organic matter from the surface to deep ocean. Here, we consider barium, along with other proxies for oceanic export productivity, and find evidence for geographically and temporally heterogeneous changes following the Cretaceous-Paleogene event. These patterns suggest the possible existence of spatial refugia with relatively unaltered or a rapid recovery in total organic fluxes for benthic communities in the earliest Danian, and may help explain the paradoxical lack of extinction in the deep sea.

INTRODUCTION

The Cretaceous-Paleogene (KPg) mass extinction provides a valuable natural experiment for understanding processes of extinction and recovery, as it is the most recent and well studied of the five major mass extinctions. In addition to widespread extinction (Jablonski and Chaloner 1994), the KPg impact is thought to have precipitated a sudden decrease in global export productivity. Decreased export of organic matter from the surface ocean is indicated by evidence for a precipitous decrease in the surface-to-deep water $\delta^{13}C$ gradient, sedimentation rates, and interocean basin deep water aging (D'Hondt 2005; Hsu et al. 1982; Zachos et al. 1989). During the recovery interval, the stepped pattern in the reestablishment of pre-impact surface-to-deep gradients in $\delta^{13}C$ coincides with the recovery of planktonic foraminiferal species richness (Coxall et al. 2006). This diversity-productivity correlation is striking, and

suggests that stable, species-rich ocean ecosystems are either necessary for and/or dependent on high export production (Coxall et al. 2006; D'Hondt et al. 1998).

In contrast to the plankton, benthic foraminifera did not suffer a mass extinction at the KPg boundary (e.g., Culver 2003, and references therein). This presents a paradox (Thomas 2007), as most benthic communities are largely dependent on the flux of organic matter from the pelagic realm (e.g., Gooday 2003). While extinctions were rare, many benthic foraminiferal communities do experience a period of altered community composition across the KPg boundary, suggestive of a decrease in the local food supply (e.g., Alegret and Thomas 2005; Culver 2003; Widmark and Malmgren 1992). Surprisingly, this is not true throughout the ocean, contradicting evidence from carbonate proxies. At some early Paleocene sites, benthic proxies suggest a robust or even increased organic flux across the KPg boundary (Alegret and Thomas 2009).

Here, we seek to resolve the paradox of conflicting effects of the KPg boundary in the plankton and benthos by investigating the magnitude and change in primary productivity in multiple ocean basins using barium proxies like biogenic barium (Ba_{bio}). Ba_{bio} is a productivity proxy that correlates well with modern export production (e.g., Dymond et al. 1992; Francois et al. 1995) and has been used to trace changes in Cenozoic productivity (e.g., Bains et al. 2000; Paytan et al. 1996; Thompson and Schmitz 1997). We conclude by considering the new records of biogenic barium and Ba/Al (Ba/Ti) together with results from studies involving benthic foraminiferal proxies and from other studies of non-carbonate geochemical productivity proxies. These approaches provide a largely coherent picture of a post-extinction ocean in which

changes in primary productivity are synchronous with the KPg boundary, but vary geographically in magnitude and duration.

MATERIALS AND METHODS

We examined biogenic barium, Ba/Al, Ba/Ti, and/or Ba/Fe at five sites (Figure 6-2): i) the Vigo Seamount, North Atlantic, Deep Sea Drilling Project (DSDP) Site 398D, ii) São Paulo Plateau, South Atlantic, DSDP Site 356, iii) Maud Rise, Antarctica, Ocean Drilling Program (ODP) Site 690C, iv) Shatsky Rise, North Pacific, DSDP Site 577B and ODP Site 1209, and v) Wombat Plateau, Indian Ocean, ODP Site 761C. Bio- and magnetostratigraphic markers from shipboard stratigraphy were used to infer relative age using a consistent relative time scale (Berggren et al. 1995), except for Shatsky Rise where we used the age model of Westerhold et al. for ODP Site 1209 and tied DSDP Site 577B to Westerhold et al.'s age model for ODP Site 1211 using XRF Fe measurements (Westerhold et al. 2008).

Biogenic barium (Ba_{bio}) can be infered by normalizing the total barium content of sediment (Ba_{total}) to the non-biogenic component ($Ba_{detrital}$) by use of a conserved tracer such as aluminum (Al) or titanium (Ti) (e.g., Dymond et al. 1992). Alternatively, barite ($BaSO_4$), the primary form of biogenic barium in marine sediments (e.g., Dymond et al. 1992; Paytan and Griffith 2007), can be directly enumerated after extraction, by scanning electron microscopy (e.g., Paytan 1996; Paytan and Griffith 2007). In pure carbonate oozes, calculated Ba_{bio} and direct barite enumeration can yield comparable results (Eagle et al. 2003; Gonneea and Paytan 2006). Both methods

require accurate mass accumulation rates (MAR) to interpret barite and/or Ba_{bio} in terms of relative or absolute export productivity, which introduces a large source of potential error in productivity calculations (e.g., Dymond et al. 1992). Ba/Al or Ba/Ti ratios provide an alternate means of inferring export productivity and are not dependent on accurate MAR (e.g., Calvert and Pedersen 2007; Goldberg and Arrhenius 1958; Murray et al. 2000). However, concerns exist for Ba/Al (or, Ba/Ti) as well, as different sources contain varying amounts of Ba relative to Ti and Al (Paytan and Griffith 2007). Given the differing strengths of each approach, here we include and compare both Ba_{bio} and Ba/Al (or Ba/Ti) ratios when possible. We also consider Ba/Fe ratios, as Fe is better measured by XRF core scanning than Ti and, in certain environments, should mirror trends in Ti. Al is too poorly detected by XRF in our deep sea sediments to calculate Ba/Al.

General site characteristics suggest that biogenic barium may be well preserved: all sites are biostratigraphically complete within the boundary sections examined here, are comprised of nannofossil oozes to chalks with minor amounts of biogenic silica, and have evidence of oxic depositional environments including well bioturbated KPg boundaries (e.g., Barker et al. 1988; Bralower et al. 2002; Heath et al. 1985; Moore et al. 1984; Perch-Nielsen et al. 1977; Ryan and al. 1979, additional site information in the initial and scientific results volumes of DSDP and ODP). We considered, but did not include, barium proxies at DSDP Site 527, Walvis Ridge, South Atlantic as this site had a relatively high proportion of detrital to biogenic barium (20-100% detrital). In cores with high detrital barium, small changes in source Ba and Al composition can

dramatically affect the calculated Ba_{bio} or Ba/Al, thereby precluding the use of Ba_{bio} or Ba/Al for inferences about productivity (e.g., Dymond et al. 1992; Reitz et al. 2004).

We used X-ray fluorescence (XRF) measurements at 10 kV and 50 kV to obtain high resolution records of barium (Ba), iron (Fe) and titanium (Ti) in total counts from four sites: Vigo, Sao Paulo, Maud and Shatsky. Ba/Ti records are shown with a three-point and seven-point running median at Maud and Shatsky respectively to reduce the noise associated with poor Ti detection at low abundances. We also use existing Ba, Fe, and aluminum (Al) records from Shatsky Rise (DSDP Site 577, Michel et al. 1985) and the Wombat Plateau (Rocchia et al. 1992) to calculate Ba/Al, Ba/Fe and Ba_{bio}. Ba_{bio} was calculated according to Dymond (1992) with the detrital barium ratio of 0.0037 determined empirically rather than the crustal average of 0.0075 used by Dymond (Reitz et al. 2004).

We compare our results with published accounts of early Paleocene primary productivity from studies of benthic foraminifera and non-carbonate geochemical proxies. We restrict our comparison to a small subset of the available benthic foraminifera proxy record, choosing the taxonomic and stratigraphic stability of a single research group over the extensive coverage offered by considering studies from the entire community. Our map represents the dominant conclusion pertaining to the relative organic flux based on benthic foraminiferal proxies reached by Alegret, Thomas, and others at 16 sites (Figure 6-1, sites and references in figure caption). We also consider the results and interpretations of three geochemical studies (Figure 6-1).

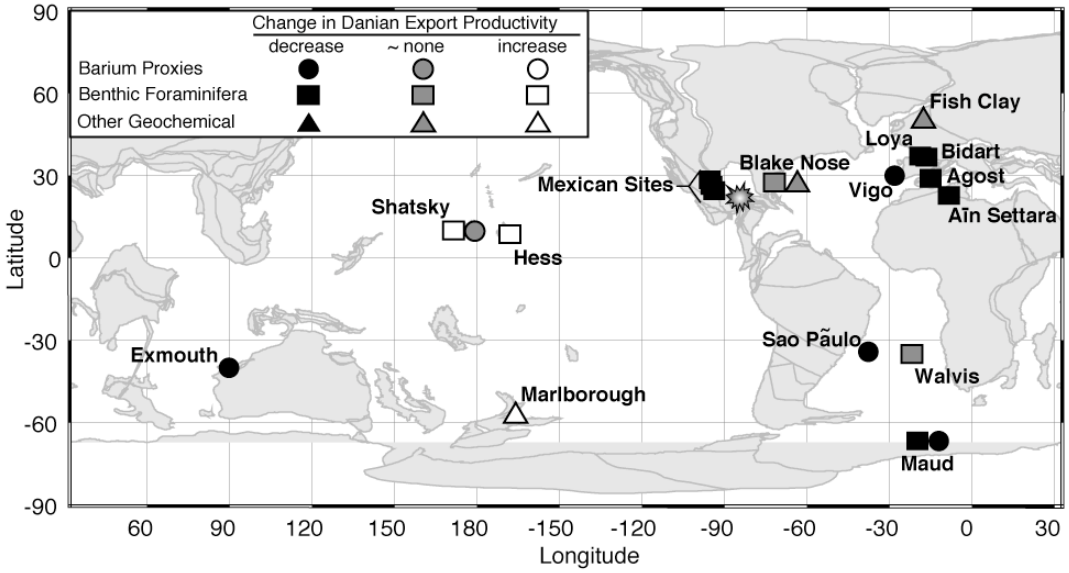

Figure 6-1. Map of change in export production across the KPg boundary as inferred from multiple, independent proxies. Paleoreconstruction of continental configuration 65Mya generated using ODSN plate reconstruction (www.odsn.de/odsn/services/paleomap/paleomap.html). Benthic foraminiferal sites include Mexican Sites (eight locals: Los Ramones, El Penon, El Tecolote, La Ceiba, El Mulato, La Lajila, El Mimbral, and Coxquihui) (Alegret et al. 2002; Alegret et al. 2001; Alegret and Thomas 2001); Blake Nose, east of Florida (Alegret and Thomas 2005); Agost, Spain (Alegret et al. 2003); Loya, Spain (Alegret 2007); Bidart, France (Alegret et al. 2004); Ain Settara, Tunisia (Peryt et al. 2002); Walvis Ridge, eastern South Atlantic (Alegret and Thomas 2007); Maud Rise, Antarctica (Thomas 1990); Hess Rise, North Pacific (Algeret and Thomas 2009); and Shatsky Rise, North Pacific (Algeret and Thomas 2009). Geochemical sites and proxies include Blake Nose, east of Florida, using reactive P and organic C (Faul et al. 2003); Marlborough, New Zealand, using biogenic barium, excess silica, and diatom/radiolarian ratio proxies (Hollis et al. 1995; Hollis et al. 2003); and the Fish Clay, Denmark, using sterane and hopane biomarkers, and $\delta^{13}C_{organic}$ and $\delta^{15}N_{organic}$ (Sepulveda et al. 2009).

RESULTS AND DISCUSSION

Results from biogenic barium, benthic foraminifera, and other geochemical proxies suggest geographically heterogeneous effects of the KPg extinction on inferred early Paleocene export productivity (Figure 6-1; heterogeneous benthic patterns previously discussed in Alegret and Thomas 2005; Alegret and Thomas 2007; Alegret and Thomas 2009 among others). The barium proxies (Ba_{bio}, Ba/Al, Ba/Ti, and Ba/Fe)

indicate a decrease in export productivity coincident with the KPg boundary in the Atlantic (Vigo and Sao Paulo), Antarctic (Maud), and Indian (Wombat) Oceans (Figure 6-2). At Maud Rise, Ba/Ti and Ba/Al ratios recover to pre-impact levels within ~350 kyr, supporting the rapid resurgence in export productivity previously hypothesized on the basis of surface to deep $\delta^{13}C$ gradients (e.g., Stott and Kennett 1989). In contrast, barium proxies and inferred organic fluxes fail to recover in the interval scanned at Sao Paulo, Wombat, and Vigo, a period of more than 600 kyr at Sao Paulo and Wombat (Figure 6-2) and more than 2 million years at Vigo (Figure 6-3).

At Shatsky Rise, the barium proxies are somewhat ambiguous due to differences between Ba/Al, Ba/Fe, and Ba_{bio} at DSDP 577B and Ba/Ti and Ba/Fe at 1209 (Figure 6-2e-f), but provide no evidence for a distinct KPg-associated decline in export productivity. At Site 577B, Ba/Al ratios and Ba_{bio} actually increase sharply in the very earliest Danian, supporting inferences of increased export production based on benthic foraminifera proxies at Shatsky and Hess Rise (Alegret and Thomas 2009). XRF Ba/Ti measurements also increase sharply at 577B, matching Ba/Al results in expressing a longer duration excursion than revealed by Ba_{bio} (Figure 6-4). At both 577B and 1209, Ba/Fe ratios are unchanged or increase slightly across the KPg boundary but diverge from coinciding measurements of Ba/Ti or Ba/Al. At 1209, Ba/Ti decreases slightly across the boundary but is well within the range of pre-boundary oscillations, exceeds pre-boundary organic fluxes within ~300 kyr, and is analytically suspect given XRF limitations measuring the very low Ti concentrations of this interval. When considered together, the best proxies at each site support either roughly

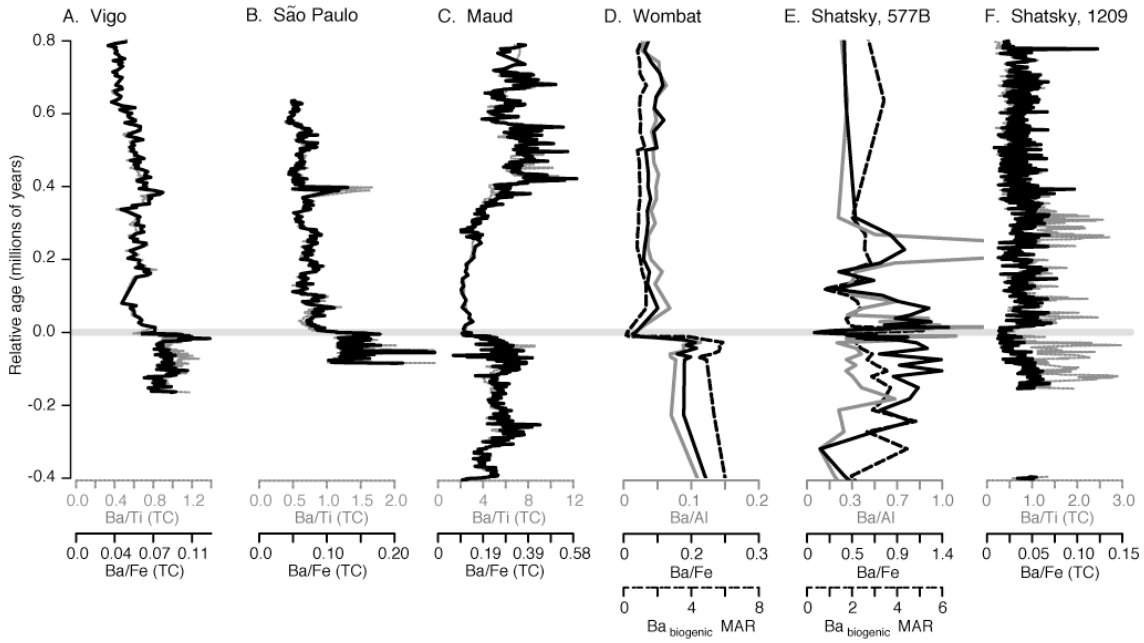

Figure 6-2. Barium proxies of export production in the latest Maastrichtian to early Danian. Ba/Ti and Ba/Fe ratios of total counts from XRF core scanning in dotted grey and solid black respectively at (A) the Vigo Seamount, North Atlantic, (B) Sao Paulo, South Atlantic, (C) Maud Rise, Antarctica, and (F) Shatsky Rise, ODP Site 1209, North Pacific. Ba/Al, Ba/Fe, and Ba_{bio} in solid grey, solid black and dotted black respectively and calculated from existing records of Ba (ppm), Al (ppm) and Fe (ppm) for (D) Wombat Plateau (Rocchia et al. 1992), and (E) Shatsky Rise 577B (Michel et al. 1985). The KPg boundary is placed at 0 million years in relative age.

no change (1209) or a short, ~100 kyr burst (557B) in export production at Shatsky Rise.

The sites investigated to date using barium, benthic foraminifera, and other geochemical proxies indicate differences in biotic responses by geography and habitat. At the largest scale, organic fluxes at sites in the Pacific appear to be maintained or increased in the earliest Danian, while most sites in the North Atlantic show large, persistent declines in export production (Figure 6-1). This does not appear to be a proxy artifact. Benthic foraminifera and barium proxies in sites near Vigo (e.g., Loya, Bidart,

Agost and Ain Settara) show boundary declines, while benthic foraminifera and barium at Shatsky and Hess Rise support maintained to increased organic fluxes in the very earliest Danian.

The pattern in the South Atlantic is more complex. Sao Paulo shows distinct boundary declines in Ba/Ti beyond the range of pre-boundary oscillations. In contrast, Maud Rise, the highest latitude site, shows boundary declines in export in both benthic foraminifer and barium proxies, but these declines are within the scope of pre-boundary oscillations (Figure 6-2c) and are reversed and surpassed by ~350 kyr post-KPg. At Walvis, benthic foraminifera proxies indicate approximately similar levels of export production across the boundary. From this limited sample size, it is unclear whether South Atlantic sites are generally less affected by boundary events or if this pattern merely reflects the chance sampling of a few relatively unaffected sites in a region characterized by KPg-related declines in export production.

The two North Atlantic sites with relatively unaffected export productivity, Blake Nose and the Fish Clay, are generally more productive than the other North Atlantic sites during the time in question. Blake Nose, with roughly no boundary decline in benthic and geochemical proxies (Alegret and Thomas 2005; Faul et al. 2003), is hypothesized to have been located in a productive coastal upwelling region. Similarly, the Fish Clay is a neritic rather than oceanic site. The boundary effects at Blake Nose and Fish Clay together with the unchanged to increased export production described at the neritic Marlborough sites, support the suggestion that the KPg impact

may have had heterogeneous ecological effects dependent upon habitat. It is possible that communities in highly productive regions, with pre-boundary communities more-

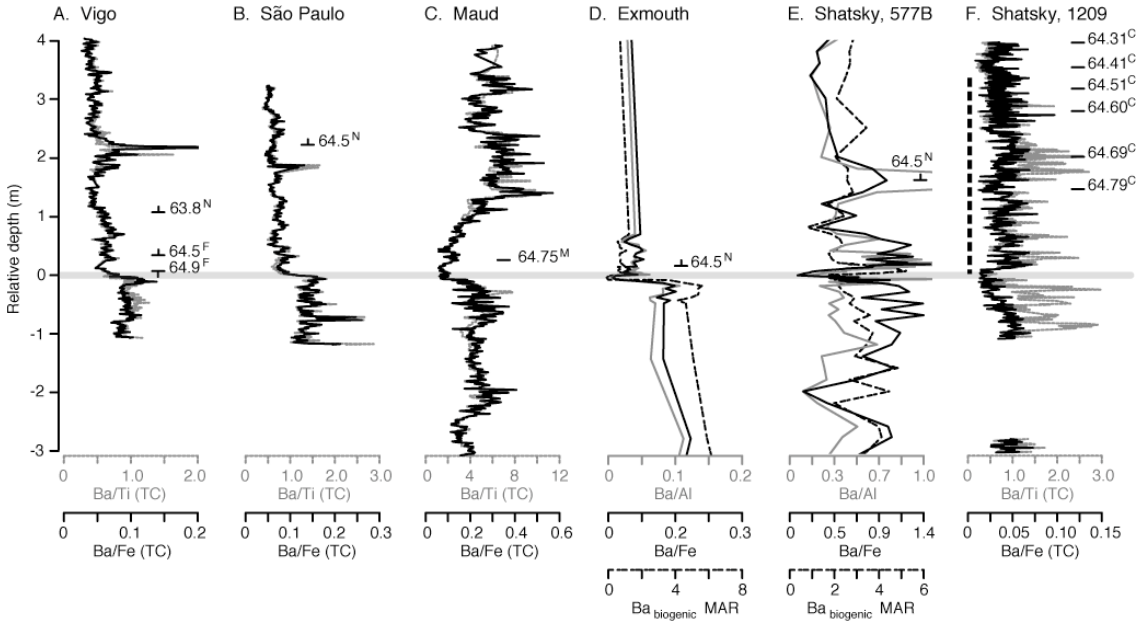

Figure 6-3. Full-length barium proxy records of export production in the latest Maastrichtian to early Danian plotted against core depth. Ba/Ti and Ba/Fe ratios of total counts from XRF core scanning in dotted grey and solid black respectively at (A) the Vigo Seamount, North Atlantic, (B) Sao Paulo, South Atlantic, (C) Maud Rise, Antarctica, and (F) Shatsky Rise, ODP Site 1209, North Pacific. Ba/Al, Ba/Fe, and Babio in solid grey, solid black and dotted black respectively and calculated from existing records of Ba (ppm), Al (ppm) and Fe (ppm) for (D) Exmouth Plateau (Rocchia et al., 1992), and (E) Shatsky Rise 577B (Michel et al., 1985). The KPg boundary is placed at 0 m relative depth and 65 Mya. First (⊥) and last (⊤) occurrence of nannofossils (N) and foraminifera (F) and magnetostratigraphy (M) indicate relative age in panels A-E. In panel F, relative ages were obtained from a high resolution study of cyclostratigraphy (C), although age model uncertainties characterize the period indicated by the thick dashed line.

like those that flourished in the Danian, rebounded much more rapidly from the KPg impact. Indeed, early Paleocene bloom taxa in planktonic foraminifera are descendants of coastal taxa in the late Maastrichtian and therefore may have been adapted to the generally high productivity of coastal waters (D'Hondt et al. 1996; MacLeod 1993). Unexplained is why foraminiferal faunas and export proxies take so long to recover in

North Atlantic and Indian Ocean sites (>2 million years for Vigo) and why the North Pacific sites fared relatively well in the Danian.

CONCLUSIONS

The results of this study provide independent support for the geographically heterogeneous changes in export productivity indicated by community structure in benthic foraminifera across the KPg boundary. The existence of spatial and temporal heterogeneity suggests a solution to the paradoxical lack of mass extinction in deep sea benthic foraminifera. Oceanic regions with relatively unaffected export production or very rapid recovery of pre-extinction organic fluxes, such as neritic regions, Pacific sites, and Maud Rise, may have provided refugia for benthic species temporally extirpated from more affected regions.

While some geographic differences in organic flux may be attributed to habitat type, it is unclear how geographical differences were maintained between similar oceanic environments. Furthermore, if some regions did rapidly recover to pre-extinction levels of export productivity then this would decouple the recovery of ecosystem diversity from the recovery of export production. Our data clearly indicate that export recovery sometimes preceeded the full recovery of species-rich ecosystems in the open ocean.

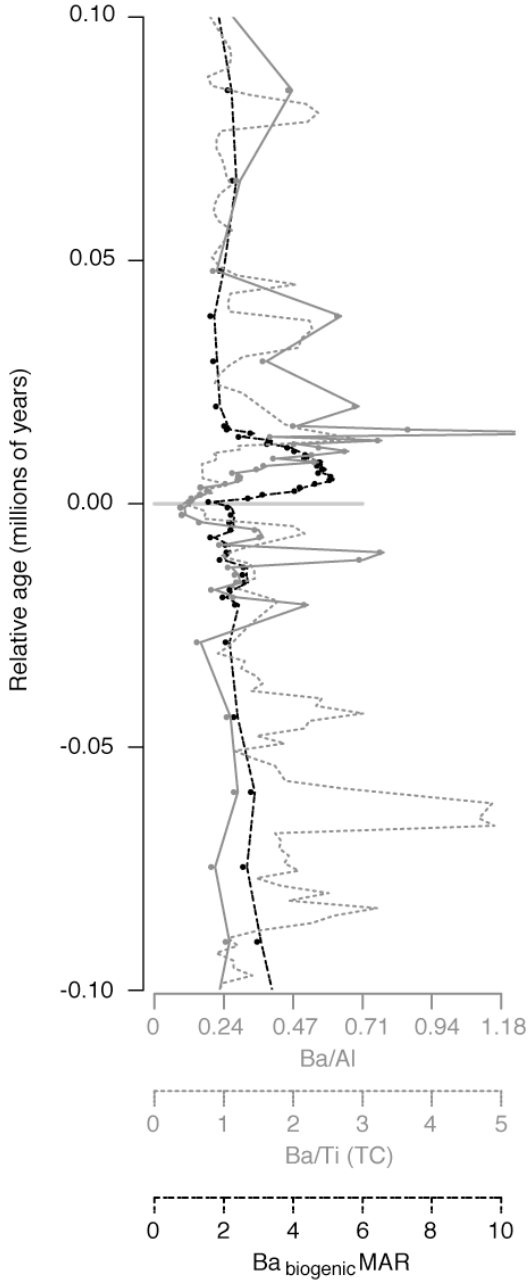

Figure 6-4. Barium proxies of export production in the latest Maastrichtian to early Danian at DSDP Site 577B, Shatsky Rise, North Pacific. Ba/Ti ratios of total counts from XRF core scanning in dotted grey against Ba/Al and Ba measured with neutron-activation analysis (Michel et al., 1985) in solid grey and dotted black respectively. The KPg boundary is placed at 0 million years relative age.

REFERENCES

ALEGRET, L. 2007. Recovery of the deep-sea floor after the Cretaceous-Paleogene boundary event: The benthic foraminiferal record in the Basque-Cantabrian basin and in South-eastern Spain. Palaeogeography Palaeoclimatology Palaeoecology **255:** 181-194.

ALEGRET, L., I. ARENILLAS, J. A. ARZ, and E. MOLINA. 2002. Environmental changes triggered by the K/T impact event at Coxquihui (Mexico) based on foraminifera. Neues Jahrbuch Fur Geologie Und Palaontologie-Monatshefte**:** 295-309.

ALEGRET, L., M. A. KAMINSKI, and E. MOLINA. 2004. Paleoenvironmental recovery after the Cretaceous/Paleogene boundary crisis: evidence from the marine bidart section (SW France). Palaios **19:** 574-586.

ALEGRET, L., E. MOLINA, and E. THOMAS. 2001. Benthic foraminifera at the Cretaceous-Tertiary boundary around the Gulf of Mexico. Geology **29:** 891-894.

---. 2003. Benthic foraminiferal turnover across the Cretaceous/Paleogene boundary at Agost (southeastern Spain): paleoenvironmental inferences. Marine Micropaleontology **48:** 251-279.

ALEGRET, L., and E. THOMAS. 2001. Upper Cretaceous and lower Paleogene benthic foraminifera from northeastern Mexico. Micropaleontology **47:** 269-316.

---. 2005. Cretaceous/Paleogene boundary bathyal paleo-environments in the central North Pacific (DSDP Site 465), the Northwestern Atlantic (ODP Site 1049), the Gulf of Mexico and the Tethys: the benthic foraminiferal record. Palaeogeography Palaeoclimatology Palaeoecology **224:** 53-82.

---. 2007. Deep-sea environments across the Cretaceous/Paleogene boundary in the eastern South Atlantic Ocean (ODP leg 208, Walvis ridge). Marine Micropaleontology **64:** 1-17.

---. 2009. Food supply to the seafloor in the Pacific Ocean after the Cretaceous/Paleogene boundary event. Marine Micropaleontology **73:** 105-116.

BAINS, S., R. D. NORRIS, R. M. CORFIELD, and K. L. FAUL. 2000. Termination of global warmth at the Palaeocene/Eocene boundary through productivity feedback. Nature **407:** 171-174.

BARKER, P. F., J. P. KENNETT, and E. AL. 1988. Site 690, p. 183-292. *In* P. F. Barker, J. P. Kennett and e. al. [eds.], Proc. ODP, Init. Repts., 113. Ocean Drilling Program, College Station, TX.

BERGGREN, W. A., D. V. KENT, C. C. SWISHER, and M.-P. AUBRY. 1995. Geochronology, time scales and global stratigraphic correlation, SEPM Special Publication 54. SEPM, Tulsa.

BRALOWER, T., I. PREMOLI SILVA, M. J. MALONE, and E. AL. 2002. Site 1209, p. 1-102. *In* T. Bralower, I. Premoli Silva and M. J. Malone [eds.], Proc. ODP, Initial Reports, 198. Ocean Drilling Program, College Station, TX.

CALVERT, S. E., and T. F. PEDERSEN. 2007. Elemental proxies for palaeoclimatic and palaeoceanographic variability in marine sediments: interpretation and application, p. 567-644. *In* C. Hillaire-Marcel and A. de Vernal [eds.], Proxies in late Cenozoic paleoceanography. Developments in marine geology. Elsevier, Oxford.

COXALL, H. K., S. D'HONDT, and J. C. ZACHOS. 2006. Pelagic evolution and environmental recovery after the Cretaceous-Paleogene mass extinction. Geology **34:** 297-300.

CULVER, S. J. 2003. Benthic foraminifera across the Cretaceous-Tertiary (K-T) boundary: a review. Marine Micropaleontology **47:** 177-226.

D'HONDT, S. 2005. Consequences of the Cretaceous/Paleogene mass extinction for marine ecosystems. Annual Review of Ecology Evolution and Systematics **36:** 295-317.

D'HONDT, S., P. DONAGHAY, J. C. ZACHOS, D. LUTTENBERG, and M. LINDINGER. 1998. Organic carbon fluxes and ecological recovery from the Cretaceous-Tertiary mass extinction. Science **282:** 276-279.

D'HONDT, S. L., T. D. HERBERT, J. KING, and C. GIBSON. 1996. Planktic foraminifera, asteroids and marine production: death and recovery at the Cretaceous-Tertiary boundary, p. 303–317. *In* G. Ryder, D. Fastovsky and S. Gartner [eds.], The Cretaceous-Tertiary event and other catastrophes in Earth history: Geological Society of America Special Paper 307.

DYMOND, J., E. SUESS, and M. LYLE. 1992. Barium in deep-sea sediment: a geochemical proxy for paleoproductivity. Paleoceanography **7:** 163-181.

EAGLE, M., A. PAYTAN, K. R. ARRIGO, G. VAN DIJKEN, and R. W. MURRAY. 2003. A comparison between excess barium and barite as indicators of carbon export. Paleoceanography **18:** 1-13.

FAUL, K. L., L. D. ANDERSON, and M. L. DELANEY. 2003. Late Cretaceous and early Paleogene nutrient and paleoproductivity records from Blake Nose, western North Atlantic Ocean. Paleoceanography **18:** 1-16.

FRANCOIS, R., S. HONJO, S. J. MANGANINI, and G. E. RAVIZZA. 1995. Biogenic barium fluxes to the deep-sea - implications for paleoproductivity reconstruction. Global Biogeochemical Cycles **9:** 289-303.

GOLDBERG, E. D., and G. O. S. ARRHENIUS. 1958. Chemistry of pacific pelagic sediments. Geochimica Et Cosmochimica Acta **13:** 153-212.

GONNEEA, M. E., and A. PAYTAN. 2006. Phase associations of barium in marine sediments. Marine Chemistry **100:** 124-135.

GOODAY, A. J. 2003. Benthic foraminifera (protista) as tools in deep-water palaeoceanography: Environmental influences on faunal characteristics. Advances in Marine Biology **46:** 1-90.

HEATH, G. R., L. H. BURCKLE, and E. AL. 1985. Site 577, p. 91-137. *In* G. R. Heath, L. H. Burckle and e. al. [eds.], Init. Repts. DSDPP, 86. U.S. Govt. Printing Office, Washington.

HOLLIS, C. J., K. A. RODGERS, and R. J. PARKER. 1995. Siliceous plankton bloom in the earliest tertiary of Marlborough, New-Zealand. Geology **23:** 835-838.

HOLLIS, C. J., C. P. STRONG, K. A. RODGERS, and K. M. ROGERS. 2003. Paleoenvironmental changes across the Cretaceous/Tertiary boundary at Flaxbourne River and Woodside Creek, eastern Marlborough, New Zealand. New Zealand Journal of Geology and Geophysics **46:** 177-197.

HSU, K. J., Q. X. HE, and A. MCKENZIE. 1982. Terminal Cretaceous environmental and evolutionary changes, p. 317–328. *In* L. T. Silver and P. H. Schultz [eds.], Geological implications of impacts of large asteroid and comets on the Earth: Geological Society of America Special Paper 190.

JABLONSKI, D., and W. G. CHALONER. 1994. Extinctions in the fossil record. Philosophical Transactions of the Royal Society of London Series B-Biological Sciences **344:** 11-16.

MACLEOD, N. 1993. The Maastrichtian-Danian radiation of triserial and biserial planktic foraminifera - testing phylogenetic and adaptational hypotheses in the (micro) fossil record. Marine Micropaleontology **21:** 47-100.

MICHEL, H. V., F. ASARO, W. ALVAREZ, and L. W. ALVAREZ. 1985. Elemental profile of iridium and other elements near the Cretaceous/Tertiary boundary in Hole 577B, p. 533-538. *In* G. R. Heath, L. H. Burckle and e. al. [eds.], Init. Repts. DSDPP, 86. U. S. Govt. Printing Office, Washington.

MOORE, T. C., JR., P. D. RABINOWITZ, and E. AL. 1984. Site 527. *In* T. C. Moore, Jr., P. D. Rabinowitz and e. al. [eds.], Init. Repts. DSDP, 74. U.S. Govt. Printing Office, Washington.

MURRAY, R. W., C. KNOWLTON, M. LEINEN, A. C. MIX, and C. H. POLSKY. 2000. Export production and carbonate dissolution in the central equatorial Pacific Ocean over the past 1 Myr. Paleoceanography **15:** 570-592.

PAYTAN, A. 1996. Marine barite: A recorder of oceanic chemistry, productivity and circulation, Scripps Institution of Oceanography. University of California, San Diego.

PAYTAN, A., and E. M. GRIFFITH. 2007. Marine barite: Recorder of variations in ocean export productivity. Deep-Sea Research Part II-Topical Studies in Oceanography **54:** 687-705.

PAYTAN, A., M. KASTNER, and F. P. CHAVEZ. 1996. Glacial to interglacial fluctuations in productivity in the equatorial Pacific as indicated by marine barite. Science **274:** 1355-1357.

PERCH-NIELSEN, K., P. R. SUPKO, and E. AL. 1977. Site 356: São Paulo Plateau, p. 141-230. *In* P. R. Supko, K. Perch-Nielsen and e. al [eds.], Init. Repts. DSDP, 39. U.S. Govt. Printing Office, Washington.

PERYT, D., L. ALEGRET, and E. MOLINA. 2002. The Cretaceous/Palaeogene (K/P) boundary at Ain Settara, Tunisia: restructuring of benthic foraminiferal assemblages. Terra Nova **14:** 101-107.

REITZ, A., K. PFEIFER, G. J. DE LANGE, and J. KLUMP. 2004. Biogenic barium and the detrital Ba/Al ratio: a comparison of their direct and indirect determination. Marine Geology **204:** 289-300.

ROCCHIA, R. and others 1992. Iridium and other element distributions, mineralogy, and magnetostratigraphy near the Cretaceous/Tertiary Boundary in Hole 761C, p. 753-762. *In* U. von Rad, B. U. Haq and e. al. [eds.], Proc. ODP, Sci. Results, 122. Ocean Drilling Program, College Station, TX.

RYAN, W. B. F., and E. AL. 1979. Site 398. *In* J. Sibuet, -C., W. B. F. Ryan and e. al. [eds.], Init. Repts. DSDP, 47 part 2. U.S. Govt. Printing Office, Washington.

SEPULVEDA, J., J. E. WENDLER, R. E. SUMMONS, and K. U. HINRICHS. 2009. Rapid resurgence of marine productivity after the Cretaceous-Paleogene mass extinction. Science **326:** 129-132.

STOTT, L. D., and J. P. KENNETT. 1989. New constraints on early Tertiary paleoproductivity from carbon isotopes in foraminifera. Nature **342:** 526-529.

THOMAS, E. 1990. Late Cretaceous through Neogene deep-sea benthic foraminifers (Maud Rise, Weddell Sea, Antarctica), p. 571-594. *In* P. F. Barker, J. P. Kennett and e. al. [eds.], Proc. ODP, Sci. Repts., 113. Ocean Drilling Program, College Station, TX.

---. 2007. Cenozoic mass extinctions in the deep sea: what perturbs the largest habitat on Earth?, p. 1–23. *In* S. Monechi, R. Coccioni and M. R. Rampino [eds.], Large ecosystem perturbations: causes and consequences: Geological Society of America Special Paper 424.

THOMPSON, E. I., and B. SCHMITZ. 1997. Barium and the late Paleocene delta C-13 maximum: Evidence of increased marine surface productivity. Paleoceanography **12:** 239-254.

WESTERHOLD, T. and others 2008. Astronomical calibration of the Paleocene time. Palaeogeography Palaeoclimatology Palaeoecology **257:** 377-403.

WIDMARK, J. G. V., and B. MALMGREN. 1992. Benthic foraminiferal changes across the Cretaceous-Tertiary boundary in the deep sea - DSDP Site 525, Site 527, and Site 465. Journal of Foraminiferal Research **22:** 81-113.

ZACHOS, J. C., M. A. ARTHUR, and W. E. DEAN. 1989. Geochemical evidence for suppression of pelagic marine productivity at the Cretaceous/Tertiary boundary. Nature **337:** 61-64.

Chapter 6 is in preparation for publication as: Hull, Pincelli; Norris, Richard "Geographically and temporally heterogeneous changes in ocean export productivity at the Cretaceous-Paleogene boundary". The dissertation author was the primary investigator and author of this paper.

CHAPTER VII

Rapid recovery of pelagic ecosystem function following the end-Cretaceous extinction

ABSTRACT

Mass extinctions provide case studies into the mechanisms and speed of ecosystem recovery from global biotic crises (Erwin 2008). In contrast to a link between diversity and function in extant ecosystems (e.g., Tilman et al. 2001), species richness can be decoupled from ecological structure and function during the recovery from mass extinctions (Droser et al. 2000; Sahney and Benton 2008; Wilf et al. 2006; Yedid et al. 2009). Here we show a similar decoupling between the evolution of ecosystems and species richness in open ocean communities after the Cretaceous-Paleogene (KPg) mass extinction. Although the diversification of planktonic foraminifera was nearly instantaneous (Coxall et al. 2006; D'Hondt and Keller 1991; D'Hondt 1991), early pelagic ecosystems existed in an alternative state characterized by the dominance of microperforate planktonic foraminifera, high foraminiferal fluxes relative to export productivity, high species dominance, and rapid dominance turnovers within the microperforate foraminifera for 100,000 - 350,000 years. The reestablishment of typical planktonic foraminiferal communities occurred independently of a change in species richness. The initial recovery of pelagic ecosystems to an alternative ecosystem state provides empirical support for a similar pattern recently described in freely evolving digital communities (Yedid et al. 2009), and may also reflect the importance of contingency in the ecology and evolution of depauperate ecosystems. These results suggest that open ocean ecosystems comprised of the same list of species can function in fundamentally different ways over geological time scales, with important

implications for the loss of ecologically meaningful densities of many species from the modern ocean.

INTRODUCTION

Similar trends in species richness and some export productivity proxies suggest that the recovery of species richness, ecosystem structure, and ecosystem function were coupled in pelagic ecosystems during the ~3-4 million year recovery from the KPg mass extinction (Coxall et al. 2006; D'Hondt 2005; Fuqua et al. 2008). Open ocean ecosystems experienced disproportionately large negative effects from KPg boundary impact with species extinction levels of nearly 95% in planktonic foraminifera (D'Hondt et al. 1996; Smit 1982) and 88% in calcareous nannofossils (Thierstein 1982), and with a precipitous decrease in surface ocean export productivity indicated by reduced surface-to-deep water $\delta^{13}C$ gradients, sedimentation rates, and interocean basin deep water aging (D'Hondt 2005; Hsu et al. 1982; Zachos et al. 1989). The recovery of surface-to-deep water $\delta^{13}C$ gradients, an export productivity proxy, occurred in two steps at ~1 and 3-4 million years post-KPg (D'Hondt et al. 1998; a pattern supported by new records in Figure 7-1a), and was accompanied by concurrent steps in species richness of planktonic foraminifera (Coxall et al. 2006). However, other work has shown that the initial diversification of planktonic foraminifera does not coincide with the initial recovery of community structure; instead early communities were dominated by a succession of disaster faunas (D'Hondt and Keller 1991). Here we seek to understand the linkage between ecosystem and species recovery in post-extinction

pelagic communities by synthesizing evidence described independently in past studies (e.g., D'Hondt and Keller 1991; Zachos et al. 1989), together with new, high resolution multiproxy records from the North Pacific and South Atlantic. We also propose a single hypothesis to unify previously conflicting or unexplained patterns including productivity proxies (Alegret and Thomas 2009; Zachos et al. 1989) and grain size change (D'Hondt 2005; Zachos et al. 1989) respectively.

RESULTS AND DISCUSSION

High resolution grain size analyses (Brawlower et al. in review) reveals a large increase in the relative abundance of planktonic foraminifera to nannofossils during the earliest recovery interval, ranging from the KPg boundary through Carbon Isotope (CI) Recovery I (Figure 7-1a-b). Here we find that the flux of planktonic foraminifera actually *increased* by more than 8-fold in the North Pacific during the earliest Danian (Figure 7-1c). This large flux increase does not appear to be an artifact of the method used to calculate the mass accumulation rate (MAR) of foraminifera; foraminiferal MARs calculated with helium isotopes yield similar results (A. Bhattacharya unpublished results). Early Paleocene planktonic foraminifera communities at Shatsky Rise, North Pacific supported a far larger standing stock of individuals than pre-extinction or later-Danian communities.

The period of high foraminiferal flux is coincident with the dominance of 3 successive microperforate foraminiferal species (*Parvularugoglobigerina eugibina*, *Guembelitria cretacea*, and *Woodringina hornerstownensis*, Figure 7-2a-b).

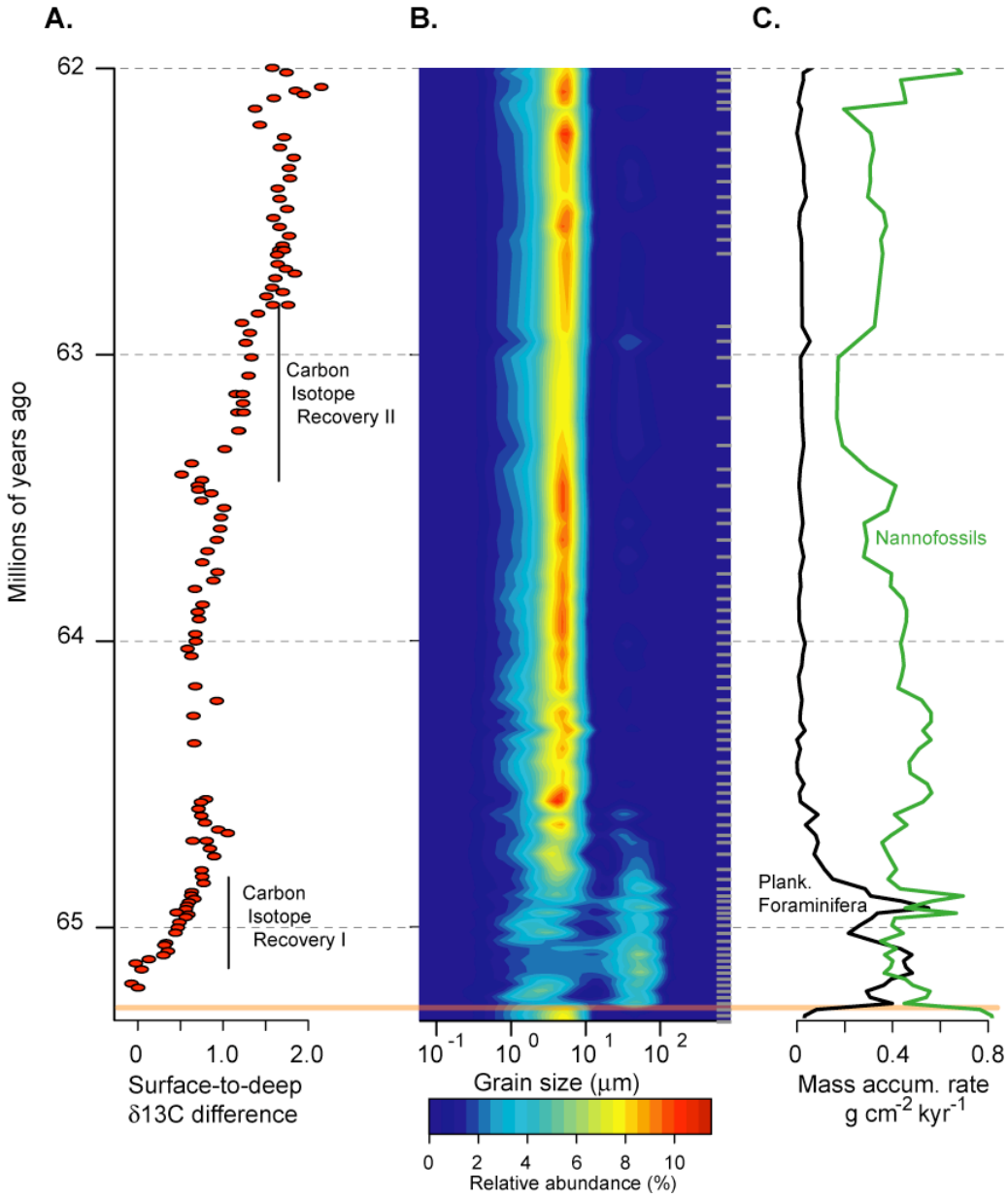

Figure 7-1. An overview of >3 million years of recovery from the Cretaceous-Paleogene mass extinction at the North Pacific. Three proxies for ecological recovery throughout the main pelagic recovery interval at Shatsky Rise, North Pacific, including (A) the difference in $\delta^{13}C$ ratios between planktonic and benthic foraminifera, (B) grain size distributions with a peak in the nannofossil size range (1-10 µm) and a briefly visible peak in the foraminiferal size range (~60 µm), and (C) the mass accumulation rate of planktonic foraminiferal and nannofossil-sized carbonates. Data are plotted against the Westerhold et al. age model (Westerhold et al. 2008) and the KPg boundary (at 65.28 mya) is indicated across all panels in orange.

Microperforate foraminiferal taxa are often considered “disaster” or “bloom” species. *Guembelitria cretacea*, the founding Danian microperforate species, primarily inhabited eutrophic, coastal environments and stressed habitats in the Maastrichtian before expanding in both range and relative dominance following the end-Cretaceous extinction (Keller and Pardo 2004). In the initial post-extinction diversification, *G. cretacea* is hypothesized to have given rise to four genera in less than 30 kyrs (*Globoconusa*, *Parvularugoglobigerina*, *Woodringina*, and *Chiloguembelina*, the last of which founds a separate family) with 8 recognized species and 19 clearly distinguishable morphotypes (D'Hondt and Keller 1991; Macleod 1993; Olsson et al. 1999). This explosive diversification coincides with the initial diversification of the normal perforate foraminiferal taxa that gave rise to the fully recovered species and communities of the Paleocene (Olsson et al. 1999), and is consistent with models of adaptive radiation (Gavrilets and Vose 2005) and increased evolutionary rates during periods of environmental stress (e.g., Kashtan et al. 2007; Matic et al. 1995). The correspondence between the period of high foraminiferal to nannofossil fluxes and the dominance of microperforate species may be a general feature of early Danian pelagic communities, with similar patterns in the South Atlantic site at Walvis Ridge (Figure 7-3). Microperforate dominated communities, with rapid turnovers in the dominant microperforate species, have also been described for the first 100 to >500 kyr of the Danian in the Tethys and Gulf of Mexico (D'Hondt and Keller 1991) and may also characterize the >20 additional sites with known *G. cretacea* blooms (Keller and Pardo 2004).

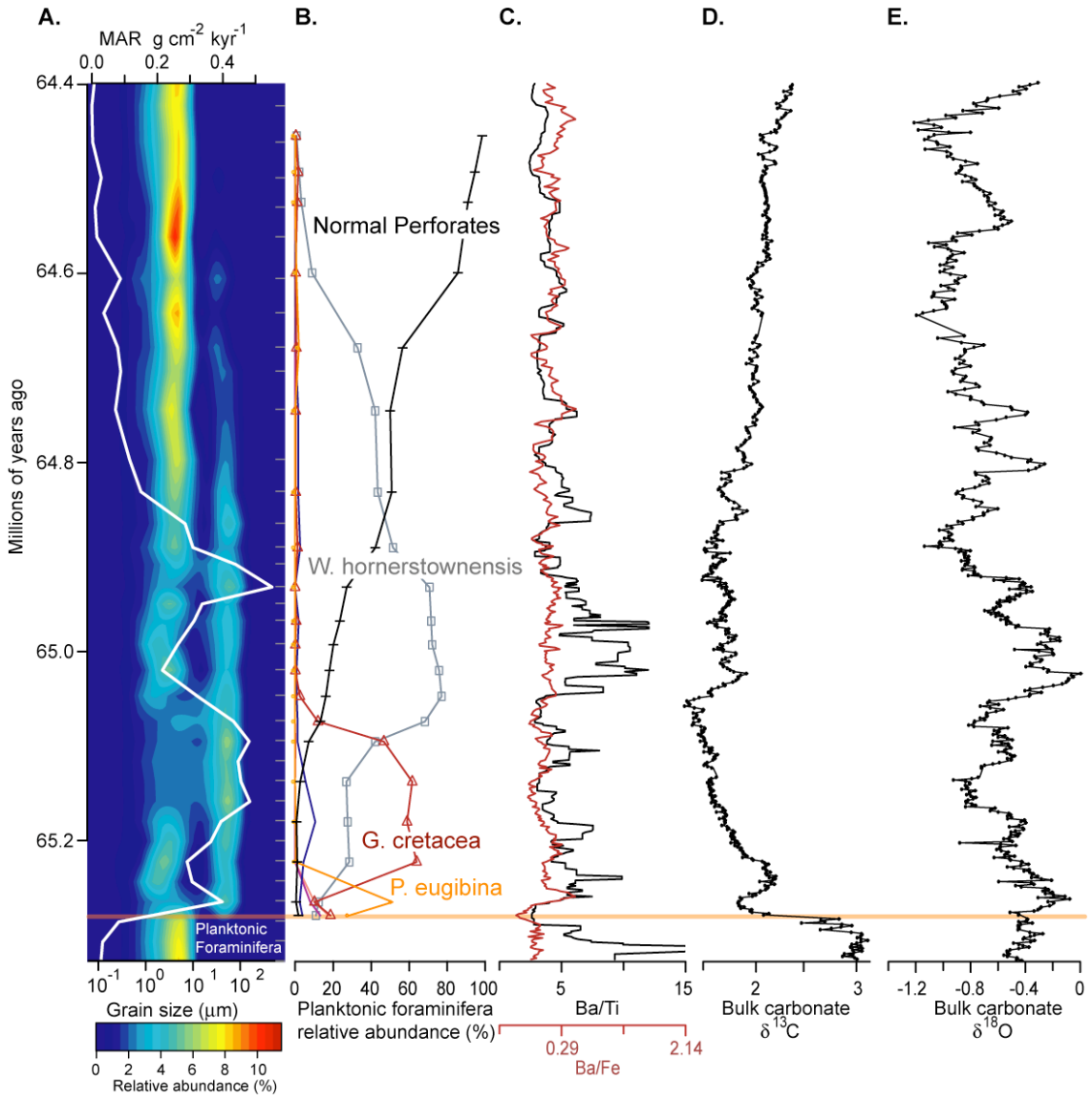

Figure 7-2. Early ecological recovery in the North Pacific. Ecological and environmental change in the earliest Danian at Shatsky Rise, North Pacific as revealed by (A) grain size distributions with overlain planktonic foraminiferal fluxes (white line), (B) the dominant foraminiferal species or taxa (*Guembelitria cretacea*, *Parvularugoglobigerina eugibina*, and *Woodringina hornerstownensis)*, (C) Ba/Ti (black) and Ba/Fe (red) ratios, and bulk carbonate (D) $d^{13}C$ and (E) $d^{18}O$. Data are plotted against the Westerhold et al. age model(Westerhold et al. 2008) and the KPg boundary (at 65.28 mya) is indicated across all panels in orange.

We propose that the interval between the KPg boundary and the turnover from micro- to normal perforate dominance represents an alternative state in early Danian pelagic ecosystems. We propose an alternative, rather than disaster, ecosystem for this time because the presence of high foraminiferal fluxes and unaffected export productivity at some sites suggest that pelagic ecosystems i) had a different food web structure and ii) may have maintained pre-extinction levels of some ecosystem functions. During this microperforate-dominated period, foraminiferal MARs are high relative to export productivity, indicating that planktonic foraminifera comprise a relatively larger proportion of these ecosystems by biomass than is found in later recovery communities. Pacific foraminiferal MARs increase 8-fold over pre-KPg and later recovery communities and export productivity was generally unaffected by the KPg mass extinction (Figure 7-2c), with evidence for a post-boundary 10-30 kyr bloom in export production (Alegret and Thomas 2009). At Walvis Ridge, South Atlantic the evidence for a boundary decline in export production is mixed, with $\delta^{13}C$ suggesting a precipitous drop (Zachos and Arthur 1986) and benthic foraminifera indicating roughly equivalent total fluxes (Alegret and Thomas 2007). At Walvis, fluxes of foraminifera may have decreased by about half across the KPg boundary, but were on average 3 times larger in the alternative, microperforate communities than in later recovery communities (results not shown). Thus, regardless of the site-specific export productivity changes, foraminiferal biomass was greater in recovery communities characterized by microperforate dominance than in later recovery communities.

Intriguingly, Pacific coccolithophorid communities have the greatest delay in recovery (Jiang et al. *in press*). We propose that this delay in the Pacific may reflect the relative success a non-calcifying community of early Danian primary producers, which could have prevented the regional reestablishment of coccolithophorid abundances. The relative success of unfossilized primary producers in the North Pacific is reflected both in the maintained levels of export production across the KPg boundary and in the high standing stocks of grazers like the microperforate foraminifera.

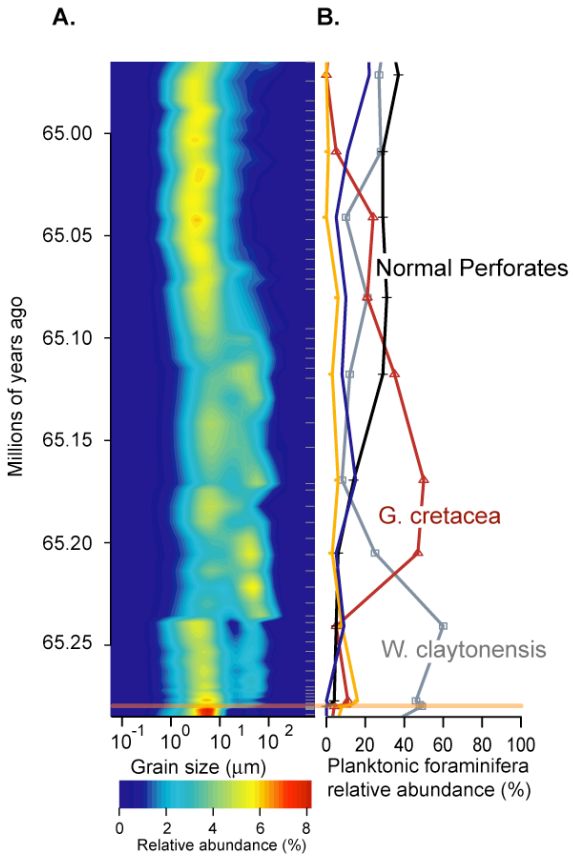

Figure 7-3. Early ecological recovery in the South Atlantic. Ecological and environmental change in the earliest Danian at Walvis Ridge, South Atlantic as revealed by (A) grain size distributions at ODP Site 1262, and (B) the dominant foraminiferal species or taxa as determined by D'Hondt and Keller at DSDP Site 528 (D'Hondt and Keller 1991).

The pattern of microperforate dominance is not the same at all sites; inter-site variation exists in the relative order and timing of the community turnovers (Figure 7-2b and 3). Faunal changes between microperforate communities in different ocean basins are characterized by differing orders of faunal succession; in the North Pacific communities change from *P. eugibina* to *G. cretacea* to *W. hornerstownensis* while in the South Atlantic they change from *W. claytonensis* to *G. cretacea*. Within a given time period the ecologically dominant species may differ between sites. For instance, *P. eugibina* dominates in the North Pacific while *W. claytonensis* dominates in the South Pacific. The timing (but not order) of the two faunal turnovers in the South Atlantic coincide with the first two faunal changes in the North Pacific, providing support for the hypothesis that environmental perturbations can provide ecological opportunities for different species to gain dominance (Keller and Pardo 2004). This perturbation-dominance change hypothesis may be impossible to fully test in the fossil record given that the environmental perturbation and ecological response would have to occur on ecological time scales (years), rather than over the thousands of years averaged by deep sea sediments.

While turnovers in microperforate relative dominance within a site may be linked to environmental perturbations, we hypothesize that the recovery of normal perforate planktonic foraminiferal communities required an additional biotic change. First, once normal perforate communities gain dominance, communities do not return to the mono-dominance of single microperforate species (D'Hondt and Keller 1991). If chance turnover following an environmental perturbation alone led to the establishment

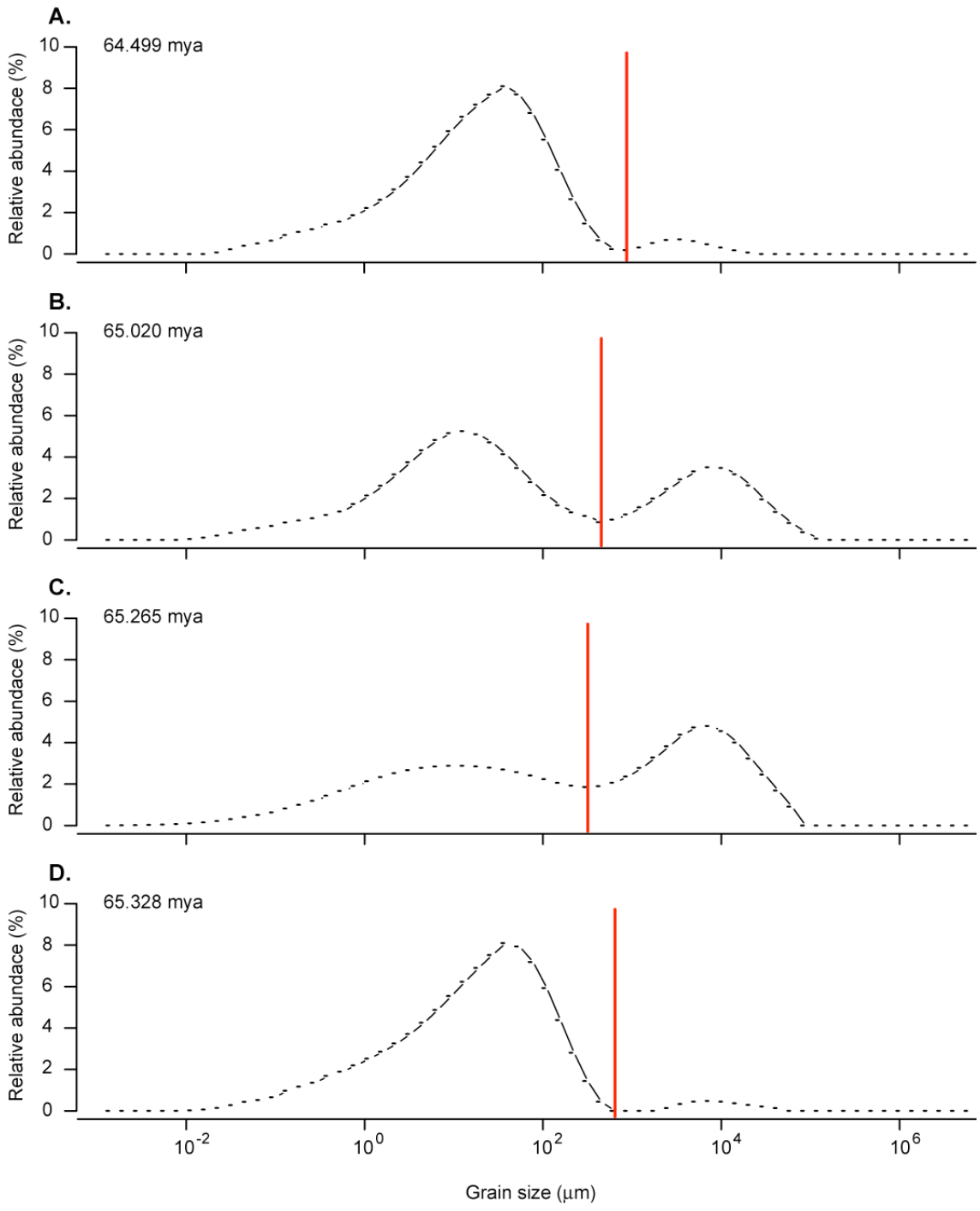

Figure 7-4. Selected size spectra at Shatsky Rise, ODP 1209. Size distributions were split between foraminiferal and nannofossil sized individuals at the minima between the two size peaks

of normal perforate communities, then we would expect to see occasional reversals to microperforate-dominated communities. Second, the change from microperforate to normal perforate dominance is characterized by at least two ecological changes, including a change in depth habitat (surface to thermocline) and foraminiferal populations sizes (large to modest). Third, long-term changes in environmental conditions do not correlate with faunal turnover. In the Pacific, variation in environmental indicators of ocean temperature, productivity and carbon are unremarkable during transition from the disaster fauna to later Paleocene normal-perforate faunas and fall within the normal range of variation preceding and following the transition. Similarly, export production in the South Atlantic does not recover from its KPg boundary-related drop on the recovery of normal perforate communities. This ecosystem state change may have been top-down, due to ecological rise of grazers, predators, or parasites, or bottom-up, due to a change in the dominant primary producers.

Species richness, ecosystem structure and ecosystem function were decoupled during the very early stage evolutionary recovery of pelagic ecosystems (D'Hondt and Keller 1991), spanning from the KPg boundary up to the recovery of normal perforate foraminiferal communities. Notably, ecosystem function as measured by export productivity was as high in some microperforate communities as before the mass extinction, suggesting that export production is not tightly linked to community structure or species dominance. The recovery of more typical foraminiferal

communities occurred independently of any evolutionary turnover within planktonic foraminifera or any apparent change in ecosystem function as measured by Ba/Ti ratios and $\delta^{13}C$ of bulk carbonates. The ecological recovery of pelagic ecosystems from the last mass extinction is not a simple function of the accumulation of species. Instead, it is the fundamental change in the composition of foraminiferal communities that correlates with the recovery of sediments once again dominated by nannofossils and, perhaps, with open ocean ecosystems more like those of the latest Maastrichtian.

REFERENCES

ALEGRET, L., and E. THOMAS. 2007. Deep-sea environments across the Cretaceous/Paleogene boundary in the eastern South Atlantic Ocean (ODP leg 208, Walvis ridge). Marine Micropaleontology **64:** 1-17.

---. 2009. Food supply to the seafloor in the Pacific Ocean after the Cretaceous/Paleogene boundary event. Marine Micropaleontology **73:** 105-116.

BRALOWER, T., I. PREMOLI SILVA, M. J. MALONE, and E. AL. 2002. Site 1209, p. 1-102. *In* T. Bralower, I. Premoli Silva and M. J. Malone [eds.], Proc. ODP, Initial Reports, 198. Ocean Drilling Program, College Station, TX.

BRAWLOWER, T. J. and others in review. Grain size of Cretaceous-Paleogene boundary sediments from Chicxulub to the open ocean: implications for interpretation of the mass extinction event. Geology.

COXALL, H. K., S. D'HONDT, and J. C. ZACHOS. 2006. Pelagic evolution and environmental recovery after the Cretaceous-Paleogene mass extinction. Geology **34:** 297-300.

D'HONDT, S. 2005. Consequences of the Cretaceous/Paleogene mass extinction for marine ecosystems. Annual Review of Ecology Evolution and Systematics **36:** 295-317.

D'HONDT, S., P. DONAGHAY, J. C. ZACHOS, D. LUTTENBERG, and M. LINDINGER. 1998. Organic carbon fluxes and ecological recovery from the Cretaceous-Tertiary mass extinction. Science **282:** 276-279.

D'HONDT, S., and G. KELLER. 1991. Some patterns of planktic foraminiferal assemblage turnover at the Cretaceous Tertiary boundary. Marine Micropaleontology **17:** 77-118.

D'HONDT, S. L. 1991. Phylogenetic and stratigraphic analysis of earliest Paleocene biserial and triserial planktonic foraminifera. Journal of Foraminiferal Research **21:** 168-181.

D'HONDT, S. L., T. D. HERBERT, J. KING, and C. GIBSON. 1996. Planktic foraminifera, asteroids and marine production: death and recovery at the Cretaceous-Tertiary boundary, p. 303–317. *In* G. Ryder, D. Fastovsky and S. Gartner [eds.], The Cretaceous-Tertiary event and other catastrophes in Earth history: Geological Society of America Special Paper 307.

DROSER, M. L., D. J. BOTTJER, P. M. SHEEHAN, and G. R. MCGHEE. 2000. Decoupling of taxonomic and ecologic severity of Phanerozoic marine mass extinctions. Geology **28:** 675-678.

ERWIN, D. H. 2008. Extinction as the loss of evolutionary history. Proceedings of the National Academy of Sciences of the United States of America **105:** 11520-11527.

FUQUA, L. M., T. J. BRALOWER, M. A. ARTHUR, and M. E. PATZKOWSKY. 2008. Evolution of calcareous nannoplankton and the recovery of marine food webs after the cretaceous-paleocene mass extinction. Palaios **23:** 185-194.

GAVRILETS, S., and A. VOSE. 2005. Dynamic patterns of adaptive radiation. Proceedings of the National Academy of Sciences of the United States of America **102:** 18040-18045.

HSU, K. J., Q. X. HE, and A. MCKENZIE. 1982. Terminal Cretaceous environmental and evolutionary changes, p. 317–328. *In* L. T. Silver and P. H. Schultz [eds.], Geological implications of impacts of large asteroid and comets on the Earth: Geological Society of America Special Paper 190.

HULL, P. M., and R. D. NORRIS. in prep. Geographically and temporally heterogeneous changes in ocean export productivity at the Cretaceous-Paleogene boundary.

JIANG, S., T. BRALOWER, M. E. PATZKOWSKY, L. R. KUMP, and J. D. SCHUETH. *in press*. Geographic controls on nannoplankton extinction across the Cretaceous-Paleogene boundary. Nature Geoscience.

KASHTAN, N., E. NOOR, and U. ALON. 2007. Varying environments can speed up evolution. Proceedings of the National Academy of Sciences of the United States of America **104:** 13711-13716.

KELLER, G., and A. PARDO. 2004. Disaster opportunists Guembelitrinidae: index for environmental catastrophes. Marine Micropaleontology **53:** 83-116.

MACLEOD, N. 1993. The Maastrichtian-Danian radiation of triserial and biserial planktic foraminifera - testing phylogenetic and adaptational hypotheses in the (micro) fossil record. Marine Micropaleontology **21:** 47-100.

MATIC, I., C. RAYSSIGUIER, and M. RADMAN. 1995. Interspecies gene exchange in bacteria - the role of SOS and mismatch repair systems in evolution of species. Cell **80:** 507-515.

MOORE, T. C., JR., P. D. RABINOWITZ, and E. AL. 1984. Site 528, p. 307-405. *In* T. C. Moore, Jr., P. D. Rabinowitz and e. al. [eds.], Init. Repts. DSDP, 74. U.S. Govt. Printing Office, Washington.

OLSSON, R. K., C. HEMLEBEN, W. A. BERGGREN, and L. K. HUBER [eds.] 1999. Atlas of Paleocene planktonic foraminifera. Smithsonian Institution Press, Washington, D.C.

PERCH-NIELSEN, K., P. R. SUPKO, and E. AL. 1977. Site 356: São Paulo Plateau, p. 141-230. *In* P. R. Supko, K. Perch-Nielsen and e. al [eds.], Init. Repts. DSDP, 39. U.S. Govt. Printing Office, Washington.

SAHNEY, S., and M. J. BENTON. 2008. Recovery from the most profound mass extinction of all time. Proceedings of the Royal Society B-Biological Sciences **275:** 759-765.

SHIPBOARD, S. P. 2004. Leg 208 Summary, p. 1-112. *In* J. C. Zachos, D. Kroon, P. Blum and e. al. [eds.], Proc. ODP, Initial Reports, 208. Ocean Drilling Program, College Station, TX.

SMIT, J. 1982. Extinction and evolution of planktonic foraminifera at the Cretaceous/Tertiary boundary after a major impact, p. 329 –352. *In* L. T. Silver and P. H. Schultz [eds.], Geological implications of impacts of large asteroids and comets on the Earth: Geological Society of America Special Paper 190.

THIERSTEIN, H. R. 1982. Terminal Cretaceous plankton extinctions: A critical assessment, p. 385–399. *In* L. T. Silver and P. H. Schultz [eds.], Geological implications of impacts of large asteroids and comets on the Earth: Geological Society of America Special Paper 190.

TILMAN, D., P. B. REICH, J. KNOPS, D. WEDIN, T. MIELKE, and C. LEHMAN. 2001. Diversity and productivity in a long-term grassland experiment. Science **294:** 843-845.

WESTERHOLD, T. and others 2008. Astronomical calibration of the Paleocene time. Palaeogeography Palaeoclimatology Palaeoecology **257:** 377-403.

WILF, P., C. C. LABANDEIRA, K. R. JOHNSON, and B. ELLIS. 2006. Decoupled plant and insect diversity after the end-Cretaceous extinction. Science **313:** 1112-1115.

YEDID, G., C. A. OFRIA, and R. E. LENSKI. 2009. Selective press extinctions, but not random pulse extinction cause delayed ecological recovery in communities of digital organims. American Naturalist **173**.

ZACHOS, J. C., and M. A. ARTHUR. 1986. Paleoceanography of the Cretaceous/Tertiary Boundary event: inferences from stable isotopic and other data. Paleoceanography **1:** 5-26.

ZACHOS, J. C., M. A. ARTHUR, and W. E. DEAN. 1989. Geochemical evidence for suppression of pelagic marine productivity at the Cretaceous/Tertiary boundary. Nature **337:** 61-64.

Chapter 7 is in preparation for publication as: Hull, Pincelli; Norris, Richard; Bralower, Timothy and Bhattacharya, Atreyee "Rapid recovery of pelagic ecosystem function following the end-Cretaceous extinction". The dissertation author was the primary investigator and author of this paper.

SUPPLEMENTARY METHODS

Our study primarily focuses on ecological recovery at Shatsky Rise in the equatorial North Pacific (paleolatitude ~10ºN [D'Hondt and Keller 1991], Ocean Drilling Program (ODP) Site 1209, currently 32°39.102'N by 158°30.359'E [Bralower et al. 2002]) , but also considers a high resolution record from Walvis Ridge in the South Atlantic (paleolatitude ~38ºS [D'Hondt and Keller 1991], ODP Site 1262 and Deep Sea Drilling Site 528, located at 27°11.15'S by 1°34.62'E [Shipboard 2004] and

28°31.49'S by 2°19.44'E [Moore et al. 1984], respectively), a low resolution record from São Paulo Plateau (DSDP Site 356, 28°17.22'S by 41°05.28'W [Perch-Nielsen et al. 1977]), and supporting faunal data from a number of additional sites studied by D'Hondt and Keller (D'Hondt and Keller 1991). At Shatsky Rise, the highly calcareous (>90%) latest Maastrichtian- earliest Danian sediments are comprised primarily of nannofossils (~1-30µm, primary producers) and planktonic foraminifera (~30-300µm, 1^{st}-2^{nd} consumers [Bralower et al. 2002]), with nannofossils generally occupying > 90% of sediments by volume.

For each faunal sample, we identified 300-1000 planktonic foraminifera in the 63-102µm size fraction at ODP Site 1209 Shatsky Rise and DSDP 356, São Paulo Plateau. Foraminifera were identified using the taxonomic concepts of the *Atlas of Paleocene Planktonic Foraminifera* (Olsson and Smithsonian Institution. Press 1999), with subspecific designations according to the species concepts of D'Hondt and Keller (D'Hondt and Keller 1991) and MacLeod (Macleod 1993). *G. cretacea* as plotted for both Shatsky Rise and Walvis Ridge combines the abundance counts of *G. cretacea*, *G. trifolia*, and *G. danica*. *G. trifolia*, and *G. danica* are not recognized species in the *Atlas of Paleocene Planktonic Foraminifera*, but are recognized by some taxonomists (e.g., D'Hondt and Keller 1991 and Macleod 1993). Separating *G. cretacea* into finer taxonomic subdivisions has little effect on relative dominance at Shastky Rise as assemblages are highly dominated by the *G. cretacea* morphotype, but changes the picture at Walvis Ridge where *G. cretacea* and *G. trifolia* are roughly equally dominate with *G. trifolia* populations increasing over time.

All samples analyzed at Shatsky Rise Site 1209 follow the main spline, except at the KPg boundary where our sampling remained in the A rather than C hole. Similarly, grain size analysis at Walvis Ridge Site 1262 occurred along the main spline as well. Both sites are plotted using the Westerhold et al. age model solution 1, with the KPg boundary at 65.28 Mya (Westerhold et al. 2008). We investigated the effect of using alternative age models on the diachroneity of the size structure change between Sites 1209 and 1262, but found that all age models result in an offset in timing of at least 100kyr. Faunal counts of D'Hondt and Keller for Walvis Ridge Site 528 (D'Hondt and Keller 1991) were aligned to the Site 1262 size structure data using the KPg boundary and C29R magnetochron as tie points.

We used the Malvern Mastersizer in the Materials Research Laboratory at Pennsylvania State University for high resolution grain size analyses (Brawlower et al. in review). The relatively fine binning of grain sizes allowed us to reliably discriminate foraminiferal and nannofossil sized fossils. While a relative increase in the large grain size bin (>63 or >38μm) has been detected in a number of sites previously including Shatsky Rise (D'Hondt 2005; Zachos and Arthur 1986; Zachos et al. 1989), the fine subdivisions allowed us to more accurately calculate the relative flux of foraminifera and nannofossils leading to the surprising find of an 8-fold increase in foraminiferal accumulation at Shatsky Rise.

The carbonate mass accumulation rate at Site 1209 was calculated using sedimentation rates from the Westerhold *et al.* age model, a dry bulk density of 1.2 g/cm^3, and a constant assumption of 90% carbonate in sediments. These age-model

MARs were spot checked with 8 He-derived MARs, which provided an independent, instantaneous MAR estimate robust to age model uncertainties. The relative percent of foraminiferal and nannofossil sized individuals was estimated by dividing the bimodal grain size distribution data at the abundance trough. At Shatsky Rise the trough between foraminifera and nannofossils had a medium size of 16.5μm and an interquartile range from 14.2-16.5μm (see example distributions in Supplementary Fig. 1). At Walvis Ridge the high degree of overlap between foraminiferal and nannofossil size distributions precluded the automated subdivision of distribution data and introduced a large source of uncertainty into group-specific estimates of MAR. Thus, inferences about the MAR of foraminifera at Walvis Ridge are suggestive rather than conclusive and should be interpreted with caution. Ba, Ti, and Fe, were measured using XRF core scanning at the Scripps Institution of Oceanography at 10 and 50kV (additional scanning details in [Hull and Norris in prep]). Bulk carbonate $\delta^{13}C$ and $\delta^{18}O$ were run on homogenized sediments in the Stable Isotope Laboratory at the University of California, Santa Cruz (UCSC). The surface-to-deep $\delta^{13}C$ difference was calculated between benthic foraminifera (*Nuttalides truempyi* and *Stensioeina beccariiformis*) and planktonic foraminifera (the *Pramurica taurica-Morozovella angulata* evolutionary series) picked from the 150-180 μm and >250 μm size fractions, respectively, and analyzed at UCSC and Scripps Institution of Oceanography.

CHAPTER VIII

Summary of the dissertation

INTRODUCTION

> Recently in the course of preparation of chapters on the zooplankton for a forthcoming comprehensive work on all aspects of limnology, it has been necessary to study in detail a considerable number of papers on the freshwater copepoda, particularly the Calanoida and planktonic Cyclopoida. During the course of this study it became apparent that the literature contained a number of disconnected facts of considerable evolutionary significance.
>
> - G. E. Hutchinson, 1951

The unifying goal of the research presented in this dissertation was to provide new insights into the long-term dynamical behavior of open ocean species and ecosystems. My research follows in a tradition of process-based and exploratory research in marine micropaleontology (e.g, Phleger 1954; Vincent and Berger 1981) that long ago began to ask and address the largest scale issues in the evolution of the open ocean. While some aspects of my thesis work primarily resulted in the development of new analytical approaches, like **Chapter V** on sediment mixing, most chapters provide new insights into some aspect of pelagic evolution. Like Hutchinson, I too have found myself compiling "disconnected facts" of evolutionary significance, and it is within a comparable context that I summarize both the contributions of my individual chapters as well as insights that arise from a cross-chapter synthesis. My summary focuses on the three main issues to which my thesis work pertains : i) speciation in the plankton, ii) pelagic community assembly, and iii) ecosystem recovery from massive disturbances.

SPECIATION IN THE PLANKTON

Environmental differences may be relatively more important than geographic distance in isolating pelagic populations. Pelagic biogeographers have long described the relatively large and disjunct ranges of many planktonic species (e.g., Bradshaw 1959; Ekman 1953; McGowan 1974). The discovery of cryptic, genetic species within classic morphospecies has not changed this basic feature of planktonic foraminiferal species distributions. In two cryptic complexes of planktonic foraminifera studied throughout the Atlantic, *Orbulina universa* and *Globorotalia truncatulinoides*, cryptic species had disjunct distributions and reoccurred in oceanographic regions with similar environmental conditions regardless of geographic separation (de Vargas et al. 1999; de Vargas et al. 2001). Similarly, two morphospecies of polar to upwelling foraminifera, *Globigerina bulloides* and *Neogloboquadrina pachyderma*, contain morphologically cryptic, genetic species with disjunct ranges (Darling et al. 2004; Darling et al. 2007; Darling et al. 2003; Darling et al. 2000). In **Chapter II**, I directly test the relative importance of geography and environment in driving genetic isolation by examining existing genetic and distribution data for *G. bulloides* and *N. pachyderma*. Here, I found that the genetic distance between cryptic species was more related to the environmental than the geographic distance between them. In past studies of morphological evolution in fossil planktonic foraminifera, some authors have attributed speciation events across currents to vicariance (e.g., Wei and Kennett 1988). However, given the large, disparate geographic ranges of modern and fossil foraminifera and fossil evidence for repeated

long-distance dispersal events (Sexton and Norris 2008), an ecological rather than geographic isolating mechanism may be more common.

It is unclear whether geographic speciation may be relatively more important in other pelagic organisms. While large, disjunct species ranges are known in a variety of plankton and nekton (McGowan 1974; McGowan and Walker 1993; Norris 2000), there is suggestive evidence that some taxa may be relatively more dispersal limited. For instance, while many species of euphausiids have geographically disjunct distributions, there are no truly bipolar species and many Atlantic species are endemic (Brinton 1962). In contrast, geographically disjunct distributions of genetic species or genotypes have been observed in copepods (Goetze 2005), coccolithophores (Saez et al. 2003) and cyanobacteria (Ferris and Palenik 1998), providing some evidence for relatively high dispersal in pelagic taxa other than planktonic foraminifera. The near-ubiquitous presence of cryptic species complexes in marine taxa (e.g., Knowlton 1993) makes molecular phylogenetic approaches critical in fully evaluating this question in future research.

Short lived cryptic species within fossil taxa may lead to an underestimation of the frequency of speciation and extinction, in addition to confounding estimates of tempo and mode. In **Chapter III**, I use a different ensemble of morphometric techniques to revisit a classic case of gradual evolution in fossil planktonic foraminifera. Here, I find the presence of a cryptic species during the evolution of *Globorotalia tumida* from *G. plesiotumida*. This research provides one concrete example of the effect of cryptic species in interpreting the fossil record of speciation.

Namely, it results in the underestimation of the frequency of speciation and extinction and of the tempo of speciation. These characteristics define key aspects of speciation in the fossil record, as mode is generally quite difficult to identify due to spatial and stratigraphic limitations.

If this case study is representative of other speciation events in planktonic foraminifera, then the implications of these results may be far reaching. For instance, past studies have indicated that simpler organisms like foraminifera and corals have long species durations as compared to more complex taxa like mammals, birds and fishes (Stanley 1979; Stanley 1998). However, if short-lived cryptic species, like that identified during the evolution of *Globorotalia tumida* from *G. plesiotumida*, are common, than we may have underestimated the frequency of speciation and extinction in planktonic foraminifera and, thereby, overestimated the average duration of species. My results provide an indication that the perceived trend in species duration may simply reflect a comparable trend in our taxonomic and morphometric acuity.

Rapid evolution of species richness and morphological disparity following the KPg mass extinction suggests a fundamental difference in the establishment versus maintenance of pelagic diversity. The initial diversification following the KPg mass extinction is unlike the morphological evolution detailed in **Chapter III** or in other investigations of speciation in planktonic foraminifera (e.g., Kucera and Malmgren 1998; Wei 1987; Wei and Kennett 1988). Although I argue that speciation in the *G. plesiotumida – G. tumida* lineage is rapid relative to what was previously described (45 kyr rather than >100 kyr (Malmgren et al. 1983)), it pales in comparison to the

explosive radiation following the KPg mass extinction when at least 8 species with 3 different coiling types arose from a common ancestor in less than 30 kyr (Olsson et al. 1999). This is not due to uncharacteristically slow rates of evolution in the *G. plesiotumida – G. tumida* lineage, as the evolution of *G. tumida* is relatively rapid and abrupt as compared to evolution in other lineages (Kucera and Malmgren 1998; Wei 1987; Wei and Kennett 1988; but see also Malmgren et al. 1996). The explosive diversification at the KPg boundary is consistent with models of adaptive radiation (Gavrilets and Vose 2005) and with models of increased rates of evolution during times of environmental stress (e.g., Kashtan et al. 2007; Matic et al. 1995).

The rapid radiation of planktonic foraminifera following the KPg mass extinction raises the question: what is the relative contribution of large, infrequent disturbances to the establishment and maintenance of pelagic diversity? Rapid increases in disparity relative to species richness are generally characteristic of evolutionary recoveries from mass extinctions (e.g., Erwin 2007), but have yet to be studied in planktonic foraminifera. Planktonic foraminifera provide an interesting contrast to other groups studied to date in that both the rate of speciation and the rate of morphological innovation appear relatively high during the early recovery from the KPg mass extinction. Comparative studies across multiple types of oceanic disturbance regimes could help elucidate the importance of rare events in driving changes in morphological and species richness and potential differences in the dominant mode of speciation during these times.

PELAGIC COMMUNITY ASSEMBLY

Community similarity in planktonic foraminifera is primarily related to environmental similarity, not geographic proximity. The dominant conclusion of **Chapter II** is the ecological correlate of a general lack of dispersal limitation in planktonic foraminiferal species. The use of a community similarity metric that accounts for relative abundance as well as the species present indicates that not only are individual morphospecies capable of long distance dispersal, species can reassemble similar communities in terms of relative species abundance throughout their ranges. The similarity of relative species composition in geographically isolated communities suggests that the relative niches occupied and exploited by species may be similar throughout the core of a given species' range, and implies that species differ in their ecological adaptations even though we have yet to understand what these adaptive differences may be.

Relative patterns among taxa are not maintained following massive disturbances; different taxa may follow very different recovery trajectories. When I first considered biogeography in planktonic foraminifera (**Chapter II)**, I was quite impressed by the similarity in faunal distribution patterns across a number of zooplankton taxa and nekton (Bé and Tolderlund 1971; Bieri 1959; Bradshaw 1959; Brinton 1962; McGowan 1971; Worm et al. 2005). I was similarly stuck by the difference in the ecological response of planktonic foraminifera and coccolithophorids to the KPg mass extinction (**Chapter VII**). While both groups suffer similarly high levels of extinction, the fluxes and inferred standing stock of planktonic foraminifera

rebound immediately during a period in which coccolithophorid fluxes are a small fraction of their normal levels. Modern studies of coccolithophorids suggest that they can be out competed by diatoms in unstable or fluctuating environmental conditions, and that dinoflagellates may also be relatively superior during times of environmental stress (Lichtman 2007, and references therein). Hence, following massive disturbances, coccolithophorids may simply be poorly adapted to thrive, while certain groups of coastal foraminifera may be pre-adapted to such an existence. Similar differences are likely to exist across zooplankton taxa as well, although it is difficult to predict which groups would be post-extinction winners and losers. Thus, while foraminifera may provide a good proxy for distribution patterns in zooplankton today, the fidelity of this relationship during times of acute perturbations or even under different oceanic configurations and/or states is unclear. If taxa respond individualistically to sea changes, than extrapolating from planktonic foraminifera to zooplankton in general may not be advisable. An increased understanding of the relative importance of different mechanisms in structuring modern communities and increased understanding of unfossilized organisms through the use of biomarkers could provide important insights into the relative responses of multiple, ecological disparate taxa to large-scale environmental change.

ECOSYSTEM RECOVERY FROM MASSIVE DISTURBANCES

The recovery of some ecosystem functions following biotic crises may be quite rapid and disconnected from the recovery of species richness. As the most recent and

well understood mass extinction, the KPg mass extinction and recovery have been the subject of intensive study over the nearly 3 decades since the impact-extinction mechanism was first hypothesized (Alvarez et al. 1980; Claeys et al. 2002; D'Hondt 2005; Smit 1999). Pelagic ecosystems have long represented the extreme end of the destruction potential of this event. Pelagic taxa generally suffered much greater losses of species (Norris 2001) and the recovery of normal export productivity appeared to lag far behind the recovery of primary productivity on land (~3-4 million years [D'Hondt et al. 1998; Zachos et al. 1989] versus 10,000 years or less [Arens and Jahren 2000; Beerling et al. 2001]).

In contrast to the slow recovery in species richness and some export productivity proxies, I found that barium productivity proxies support inferences from benthic foraminifera in indicating spatially and temporally heterogeneous declines in organic fluxes to the deep sea. Indeed, barium proxies, benthic foraminifera, and other non-carbonate productivity proxies indicate that some coastal and open ocean ecosystems actually thrived in the earliest recovery stage long before the recovery of pre-extinction levels of diversity (**Chapter VI**). Considered together, environmental, ecological, and faunal records from the North Pacific and South Atlantic present an unusual combination of conditions in the earliest recovery interval, and suggest an alternative ecosystem, rather than an utterly devastated one, during the earliest recovery (**Chapter VII**).

This hypothesis has the advantage of reconciling contradictory evidence and explaining previously unexplained phenomena including a lack of mass extinction in

benthic foraminifera (Culver 2003), unaffected or increased fluxes of organic matter in some sites (benthic foraminiferal proxies: Alegret and Thomas 2005; Alegret and Thomas 2007; Alegret and Thomas 2009; geochemical proxies: Faul et al. 2003; Hollis et al. 2003; Sepulveda et al. 2009; Stott and Kennett 1990), a large increase in the relative abundance of large size fraction fossils (e.g., foraminifera relative to nannofossils; D'Hondt 2005; Zachos and Arthur 1986; Zachos et al. 1989), and the dominance of a typically coastal dwelling group of planktonic foraminifera, the microperforates (D'Hondt and Keller 1991; Keller and Pardo 2004). **Chapter VII** provides new insight into how pelagic ecosystems respond to massive perturbations by suggesting that open ocean communities can exist in alternative states on geological time-scales. These alternative ecosystems may function similarly when measured by some ecosystem metrics, like the total amount of export productivity, but may differ in others, like the long-term stability of primary production (Alegret and Thomas 2005; Alegret and Thomas 2007; Alegret and Thomas 2009)

REFERENCES

ALEGRET, L., and E. THOMAS. 2005. Cretaceous/Paleogene boundary bathyal paleo-environments in the central North Pacific (DSDP Site 465), the Northwestern Atlantic (ODP Site 1049), the Gulf of Mexico and the Tethys: the benthic foraminiferal record. Palaeogeography Palaeoclimatology Palaeoecology **224:** 53-82.

---. 2007. Deep-sea environments across the Cretaceous/Paleogene boundary in the eastern South Atlantic Ocean (ODP leg 208, Walvis ridge). Marine Micropaleontology **64:** 1-17.

---. 2009. Food supply to the seafloor in the Pacific Ocean after the Cretaceous/Paleogene boundary event. Marine Micropaleontology **73:** 105-116.

ALVAREZ, L. W., W. ALVAREZ, F. ASARO, and H. V. MICHEL. 1980. Extraterrestrial cause for the Cretaceous-Tertiary extinction - experimental results and theoretical interpretation. Science **208:** 1095-1108.

ARENS, N. C., and A. H. JAHREN. 2000. Carbon isotope excursion in atmospheric CO2 at the Cretaceous-Tertiary boundary: evidence from terrestrial sediments. Palaios **15:** 314-322.

BÉ, A. W. H., and D. S. TOLDERLUND. 1971. Distribution and ecology of living planktonic foraminifera in surface waters of the Atlantic and Indian Oceans, p. 105-149. *In* B. M. Funnell and W. K. Riedel [eds.], Micropaleontology of marine bottom sediments. Cambridge University Press, Cambridge.

BEERLING, D. J. and others 2001. Evidence for the recovery of terrestrial ecosystems ahead of marine primary production following a biotic crisis at the Cretaceous-Tertiary boundary. Journal of the Geological Society **158:** 737-740.

BIERI, R. 1959. The distribution of the planktonic Chaetognatha in the Pacific and their relationship to the mater masses. Limnology and Oceanography **4:** 1-28.

BRADSHAW, J. S. 1959. Ecology of living planktonic foraminifera in the North and Equatorial Pacific Ocean. Contributions to the Cushman Foundation for Foraminiferal Research **10:** 25-64.

BRINTON, E. 1962. The distribution of Pacific euphausiids. Bulletin of the Scripps Institution of Oceanography **8:** 51-269.

CLAEYS, P., W. KIESSLING, and W. ALVAREZ. 2002. Distribution of Chicxulub ejecta at the Cretaceous-Tertiary boundary, p. 55 - 69. *In* C. Koeberl and K. G. MacLeod [eds.], Catastrophic events and mass extinctions: impacts and beyond: Geological Society of America Special Paper 356.

CULVER, S. J. 2003. Benthic foraminifera across the Cretaceous-Tertiary (K-T) boundary: a review. Marine Micropaleontology **47:** 177-226.

D'HONDT, S. 2005. Consequences of the Cretaceous/Paleogene mass extinction for marine ecosystems. Annual Review of Ecology Evolution and Systematics **36:** 295-317.

D'HONDT, S., P. DONAGHAY, J. C. ZACHOS, D. LUTTENBERG, and M. LINDINGER. 1998. Organic carbon fluxes and ecological recovery from the Cretaceous-Tertiary mass extinction. Science **282:** 276-279.

D'HONDT, S., and G. KELLER. 1991. Some patterns of planktic foraminiferal assemblage turnover at the Cretaceous Tertiary boundary. Marine Micropaleontology **17:** 77-118.

DARLING, K. F., M. KUCERA, C. J. PUDSEY, and C. M. WADE. 2004. Molecular evidence links cryptic diversification in polar planktonic protists to quaternary climate dynamics. Proceedings of the National Academy of Sciences of the United States of America **101:** 7657-7662.

DARLING, K. F., M. KUCERA, and C. M. WADE. 2007. Global molecular phylogeography reveals persistent Arctic circumpolar isolation in a marine planktonic protist. Proceedings of the National Academy of Sciences of the United States of America **104:** 5002-5007.

DARLING, K. F., M. KUCERA, C. M. WADE, P. VON LANGEN, and D. PAK. 2003. Seasonal distribution of genetic types of planktonic foraminifer morphospecies in the Santa Barbara Channel and its paleoceanographic implications. Paleoceanography **18:** 1-11.

DARLING, K. F., C. M. WADE, I. A. STEWART, D. KROON, R. DINGLE, and A. J. L. BROWN. 2000. Molecular evidence for genetic mixing of Arctic and Antarctic subpolar populations of planktonic foraminifers. Nature **405:** 43-47.

DE VARGAS, C., R. NORRIS, L. ZANINETTI, S. W. GIBB, and J. PAWLOWSKI. 1999. Molecular evidence of cryptic speciation in planktonic foraminifers and their relation to oceanic provinces. Proceedings of the National Academy of Sciences of the United States of America **96:** 2864-2868.

DE VARGAS, C., S. RENAUD, H. HILBRECHT, and J. PAWLOWSKI. 2001. Pleistocene adaptive radiation in *Globorotalia truncatulinoides*: genetic, morphologic, and environmental evidence. Paleobiology **27:** 104-125.

EKMAN, S. 1953. Zoogeography of the sea. Sidgwick and Jackson, London.

ERWIN, D. H. 2007. Disparity: Morphological pattern and developmental context. Palaeontology **50:** 57-73.

FAUL, K. L., L. D. ANDERSON, and M. L. DELANEY. 2003. Late Cretaceous and early Paleogene nutrient and paleoproductivity records from Blake Nose, western North Atlantic Ocean. Paleoceanography **18:** 1-16.

FERRIS, M. J., and B. PALENIK. 1998. Niche adaptation in ocean cyanobacteria. Nature **396:** 226-228.

GAVRILETS, S., and A. VOSE. 2005. Dynamic patterns of adaptive radiation. Proceedings of the National Academy of Sciences of the United States of America **102:** 18040-18045.

GOETZE, E. 2005. Global population genetic structure and biogeography of the oceanic copepods *Eucalanus hyalinus* and *E. spinifer*. Evolution **59:** 2378-2398.

HOLLIS, C. J., C. P. STRONG, K. A. RODGERS, and K. M. ROGERS. 2003. Paleoenvironmental changes across the Cretaceous/Tertiary boundary at Flaxbourne River and Woodside Creek, eastern Marlborough, New Zealand. New Zealand Journal of Geology and Geophysics **46:** 177-197.

KASHTAN, N., E. NOOR, and U. ALON. 2007. Varying environments can speed up evolution. Proceedings of the National Academy of Sciences of the United States of America **104:** 13711-13716.

KELLER, G., and A. PARDO. 2004. Disaster opportunists Guembelitrinidae: index for environmental catastrophes. Marine Micropaleontology **53:** 83-116.

KNOWLTON, N. 1993. Sibling species in the sea. Annual Review of Ecology and Systematics **24:** 189-216.

KUCERA, M., and B. A. MALMGREN. 1998. Differences between evolution of mean form and evolution of new morphotypes: an example from Late Cretaceous planktonic foraminifera. Paleobiology **24:** 49-63.

LICHTMAN, E. 2007. Resource competition and the ecological success of phytoplankton. *In* P. G. Falkowski and A. H. Knoll [eds.], Evolution of primary producers in the sea. Elsevier.

MALMGREN, B. A., W. A. BERGGREN, and G. P. LOHMANN. 1983. Evidence for punctuated gradualism in the Late Neogene *Globorotalia tumida* lineage of planktonic foraminifera. Paleobiology **9:** 377-389.

MALMGREN, B. A., M. KUCERA, and G. EKMAN. 1996. Evolutionary changes in supplementary apertural characteristics of the late Neogene *Sphaeroidinella dehiscens* lineage (planktonic foraminifera). Palaios **11:** 192-206.

MATIC, I., C. RAYSSIGUIER, and M. RADMAN. 1995. Interspecies gene exchange in bacteria - the role of SOS and mismatch repair systems in evolution of species. Cell **80:** 507-515.

MCGOWAN, J. A. 1971. Oceanic biogeography of the Pacific, p. 3-74. *In* B. M. Funnell and W. R. Riedel [eds.], The micropalaeontology of the oceans. Cambridge University Press, Cambridge.

---. 1974. The nature of oceanic ecosystems, p. 9-28. *In* C. B. Miller [ed.], The biology of the oceanic Pacific. Oregon State University Press, Corvallis.

MCGOWAN, J. A., and P. W. WALKER. 1993. Pelagic diversity patterns, p. 203-214. *In* R. E. Ricklefs and D. Schluter [eds.], Species diversity in ecological communities. University of Chicago Press, Chicago.

NORRIS, R. D. 2000. Pelagic species diversity, biogeography, and evolution. Paleobiology **26:** 236-258.

---. 2001. Impact of K-T Boundary events on marine life p. 229-231. *In* D. E. G. Briggs and P. G. Crowther [eds.], Palaeobiology II. Blackwell Science Ltd., Oxford.

OLSSON, R. K., C. HEMLEBEN, W. A. BERGGREN, and L. K. HUBER [eds.] 1999. Atlas of Paleocene planktonic foraminifera. Smithsonian Institution Press, Washington, D.C.

PHLEGER, F. B. 1954. Foraminifera and deep-sea research. Deep-Sea Research **2:** 1-23.

SAEZ, A. G., I. PROBERT, M. GEISEN, P. QUINN, J. R. YOUNG, and L. K. MEDLIN. 2003. Pseudo-cryptic speciation in coccolithophores. Proceedings of the National Academy of Sciences of the United States of America **100:** 7163-7168.

SEPULVEDA, J., J. E. WENDLER, R. E. SUMMONS, and K. U. HINRICHS. 2009. Rapid resurgence of marine productivity after the Cretaceous-Paleogene mass extinction. Science **326:** 129-132.

SEXTON, P. F., and R. D. NORRIS. 2008. Dispersal and biogeography of marine plankton: Long-distance dispersal of the foraminifer *Truncorotalia truncatulinoides*. Geology **36:** 899-902.

SMIT, J. 1999. The global stratigraphy of the Cretaceous-Tertiary boundary impact ejecta. Annual Review of Earth and Planetary Sciences **27:** 75-113.

STANLEY, S. M. 1979. Macroevolution, pattern and process. W. H. Freeman, San Francisco.

---. 1998. Macroevolution, pattern and process, Johns Hopkins paperbacks ed. Johns Hopkins University Press, Baltimore.

STOTT, L. D., and J. P. KENNETT. 1990. The paleoceanographic and paleoclimatic signature of the Cretaceous/Paleogene boundary in the Antarctic: stable isotopic results from ODP Leg 113, p. 829-848. *In* P. F. Barker, J. P. Kennett and e. al. [eds.], Proc. ODP, Sci. Repts., 113. Ocean Drilling Program, College Station, TX.

VINCENT, E., and W. H. BERGER. 1981. Planktonic foraminifera and their use in paleoceanography, p. 1025-1119. *In* C. Emiliani [ed.], The Oceanic Lithosphere. The Sea: Ideas and observations on progress in the study of the seas. John Wiley & Sons, Inc., New York.

WEI, K. Y. 1987. Multivariate morphometric differentiation of chronospecies in the Late Neogene planktonic foraminiferal lineage *Globoconella*. Marine Micropaleontology **12:** 183-202.

WEI, K. Y., and J. P. KENNETT. 1988. Phyletic gradualism and punctuated equilibrium in the late Neogene planktonic foraminiferal clade *Globoconella*. Paleobiology **14:** 345-363.

WORM, B., M. SANDOW, A. OSCHLIES, H. K. LOTZE, and R. A. MYERS. 2005. Global patterns of predator diversity in the open oceans. Science **309:** 1365-1369.

ZACHOS, J. C., and M. A. ARTHUR. 1986. Paleoceanography of the Cretaceous/Tertiary Boundary event: inferences from stable isotopic and other data. Paleoceanography **1:** 5-26.

ZACHOS, J. C., M. A. ARTHUR, and W. E. DEAN. 1989. Geochemical evidence for suppression of pelagic marine productivity at the Cretaceous/Tertiary boundary. Nature **337:** 61-64.

Appendix 1

Primary KPg Study Sites

PRIMARY STUDY SITES

I consider KPg boundary sections from six primary sites in the Chapters V-VIII (Figure A-1). Chapter V investigates iridium anomalies at two sites, Shatsky and Maud Rise. In Chapter VI, I consider barium proxies (biogenic barium, Ba/Al, and Ba/Ti) at all six sites described below: i) the Vigo Seamount, North Atlantic, ii) São Paulo Plateau, South Atlantic, iii) Walvis Ridge, South Atlantic, iv) Maud Rise, Antarctica, v) Shatsky Rise, North Pacific, and vi) and Wombat Plateau, Indian Ocean. In Chapter VII, I consider early ecological recovery at Walvis and Shatsky Rise.

I generally used biostratigraphic markers from shipboard biostratigraphy to infer relative age using a consistent relative time scale (Berggren et al. 1995). Brief site descriptions follow:

i) The Vigo Seamount Deep Sea Drilling Project (DSDP) Site 398D is located at 40°57.6'N by 10°43.1'W (Ryan and al. 1979), with a paleodepth of 2500m based on subsidence curves (Zachos and Arthur 1986). Early Paleocene to late Maastrichtian sediments at the Vigo Seamount are bioturbated marly nannofossil chalks with periodic thin silt or sand layers and laminations. Slumped sediments underlay the KPg boundary, which also coincides with a sharp change in sediment color between the light grey late Maastrichtian and red-brown Paleocene sediments (Ryan and al. 1979). No hiatus is described during the boundary interval, and all biozones are identified in the early Paleocene. Sediments range in carbonate content from ~34-61% carbonate in the

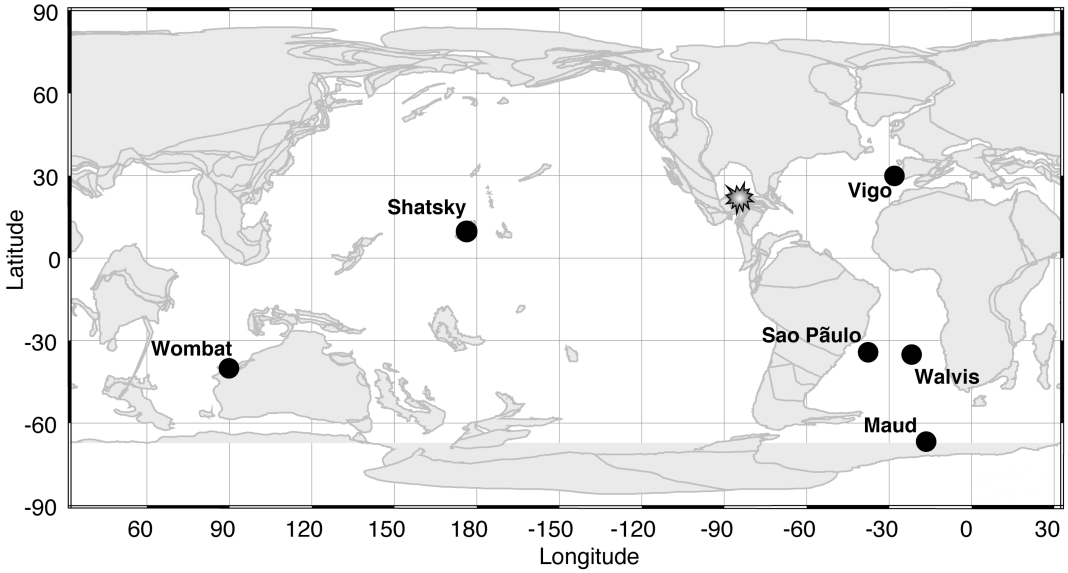

Figure A-1. Paleomap of primary study sites. Continental configuration reconstructed to 65 million years ago using ODSN plate reconstruction services (www.odsn.de/odsn/services/). Impact site indicated with starburst, sites with black circles.

sections examined in my dissertation (Ryan and al. 1979). Petrographic evidence suggests oxidizing conditions at Site 398 in the Maastrichtian and Paleocene (Bourbon 1979), and gains additional supported by the presences of extensively bioturbated sediments.

ii) DSDP Site 356 at the Sao Paulo Plateau is located at 28°17.22'S by 41°05.28'W (Perch-Nielsen et al. 1977), and has a paleodepth of 2200m based on subsidence curves (Zachos and Arthur 1986). Early Paleocene to late Maastrichtian sediments are marly nannofossils chalks, with a distinct color change at the KPg boundary from brown to grey sediments and clear evidence of bioturbation. A hiatus spans foraminiferal zone P1b but does not affect my short record (Perch-Nielsen et al. 1977), and is not indicated in the higher resolution nannofossil biostratigraphy.

Sediments are ~55-70% carbonates in the late Maastrichtian with a drop in percent carbonate to 18-40% in the early Danian (Emelyanov 1977; Perch-Nielsen et al. 1977). Site 356 is thought to be oxygenated at the KPg boundary (Kumar et al. 1977), with the last period of low-oxygen waters indicated in Campanian by benthic foraminifera and laminated sediments (Sliter 1977).

iii) DSDP Site 527 at Walvis Ridge, 28°02.49'S by 01°45.80'E (Moore et al. 1984a), has a paleodepth of 2700m based on subsidence curves (Moore et al. 1984b). KPg boundary sediments are marly nannofossil chalks with a distinct color change from light brown Maastrichtian to pale yellow brown early Danian sediments (Moore et al. 1984a). The boundary is mixed by planolites and zoophycos burrows and is thought to be complete (Moore et al. 1984a). Sediments are comprised of roughly 60-70% carbonate in the late Maastrichtian and earliest Danian, falling to 30% carbonate by the end of our study interval (Huffman et al. 1990). Low oxic bottom conditions are supported by the bulk geochemistry and clay mineralogy (Chamley et al. 1984; Maillot and Robert 1984), in addition to the presence of vigorous bioturbation.

iv) Maud Rise, Antarctica Site 690C was drilled by the Ocean Drilling Program (ODP) at 65°09.621'S by 1°12.285'E (Barker et al. 1988), and has a paleodepth between 1500 and ~2000m based on benthic foraminifera and subsidence curves (Kennett and Stott 1988; Thomas 1990). KPg boundary sediments are predominately nannofossil ooze with minor amounts of foraminifera, clay and minerals; siliceous plankton are effectively absent. Extensive bioturbation of the boundary, predominately chondrites, planolites and zoophycos burrows, are clearly evident due to the color

change from white sediments in the latest Maastrichtian to brown in the early Danian (Barker et al. 1988). Clays during this interval are 100% smectite and are likely eolian deposits from the East Antarctic. The KPg boundary interval is biostratigraphically complete; however, magnetochron C29R appears relatively short. Using sedimentation rates of 7.4 m/my above the boundary, Hamilton calculated that the KPg boundary was approximately 35,000 years below the C29R/ boundary (Hamilton 1990), or approximately 617.5 kyr shorter than expected (Smit 1999). Thus, Hamilton hypothesizes a reduced sedimentation rates in C29R or a stratigraphically unrecognized hiatus. Site 690 is an open ocean site with sediments comprised of roughly 77-90% carbonate in the latest Maastrichtian and earliest Danian, falling to between 43-63% carbonate for the first 50cm of the Danian (Stott and Kennett 1990). Oxic bottom conditions in the latest Cretaceous to early Paleocene are suggested by clay composition (Robert and Maillot 1990), relatively high proportions of infaunal benthics (Thomas 1988), pore water sulfate concentrations (Ereberg and Abdullah 1990), and extensive bioturbation of the KPg boundary (Barker et al. 1988).

v) I consider two sites on the Southern High of the Shatsky Rise, DSDP 577B (32°26.48'N, 157°43.39'E) and ODP Site 1209 (32°39.102'N, 158°30.359'E) , with paleodepths of 2400 and 2000-2500m respectively (Bralower et al. 2002b; Heath et al. 1985; Zachos and Arthur 1986). At DSDP 577B, the KPg boundary lies within the lithological Unit II, a white to pale brow nannofossil ooze with foraminifera comprising up to 35% of the sample, minerals and ash typically less than 10%, and an absence of diatoms and radiolarians (Heath et al. 1985). The KPg boundary section is described as

"a slightly mottle nannofossil ooze", with mottling of the boundary reflecting the bioturbation of the very pale brown Danian sediments into the white upper Maastrichtian nannofossil ooze (Heath et al. 1985). The boundary is thought to be complete and is recognized by a very minor color change. Relatively shallow sediment mixing is indicated by mixing of rare Thoracosphaerids down to 5cm below the nannofossil KPg boundary and the near-complete replacement of Mesozoic nannofossils (90-95%) at 10cm above the boundary (Wright et al. 1985). At Site 577B, the KPg boundary falls relatively high in magnetochron C29R (Monechi 1985) suggesting relatively large declines in sedimentation rates or an unrecognized hiatus. However, the relative position of the KPg boundary to C29R is quite variable globally (Bleil 1985), and continuous deposition at Shatsky Rise is suggestion by the presence of all Paleocene nannofossil zones between 577 and 577A (Monechi 1985).

Similarly, at Site 1209 the KPg boundary falls at the base of the lithological Unit II and separates light orange foraminiferal nannofossil Paleocene oozes from the white nannofossil oozes of the latest Maastrichtian, with burrows containing P0 fauna crossing the boundary by up to 10cm (Bralower et al. 2002a). The basal Paleocene ooze is speckled by pyrite, with the lowermost 2-3 cm containing spherules of diagenetically altered tektites. Nannofossil biostratigraphy indicates that the boundary sections drilled at 1209 are also complete (Bralower et al. 2002b), although a coring and splitting disturbance disrupts ~7cm of the latest Maastrichtian at 1209A. Sediment accumulation rates at 1209 are estimated to fall from 1.0 g/cm2/ky in the latest Maastrichtian to 0.5g/cm2/ky in the earliest Paleocene (Bralower et al. 2002b)

Late Maastrichtian through Early Paleocene sediments at DSDP 577B are generally comprised of 87-97% carbonates with lower percent carbonate values following the KPg boundary (Heath et al. 1985); comparable trends characterize Site 1209. The initial 577 reports vary in the description of relative carbonate preservation across the KPg boundary. While several authors described decreased nannofossil preservation in the very early Paleocene (Monechi 1985; Wright et al. 1985), Zachos presents evidence for stable to improved carbonate preservation at DSDP 577 on the basis of Sr/Ca ratios, Mg, Mn, and SEMs of calcareous nannofossils (Zachos et al. 1985). Furthermore, KPg sediment hydrocarbons at Site 577 suggest organic carbon deposition in oxic environments with extensive microbial reworking (Meyers and Simoneit 1990). Additional support for oxic deposition is gained from the ratio of the alkanes pristane (Pr) to phytane (Ph) and the absence of elemental sulfur (Simoneit and Beller 1985). Supporting Zachos' interpretation at Site 577, preservation of nannofossils improves across the KPg boundary at Site 1209 (Bralower et al. 2002a). Red/blue reflectance ratios and Fe variation at Site 1209 during the Paleocene also suggest relatively oxidizing conditions (Bralower et al. 2002b).

vi) ODP Site 761C was drilled on the Wombat Plateau, Indian Ocean at 16°44.23'S by 115°32.10'E and has a paleodepth of roughly 1500m based on subsidence curves and a paleolatitude of approximately ~36°(Haq et al. 1990; Pospichal and Bralower 1992; von Rad et al. 1992). Site 761C is thought to have the most complete boundary section drilled at the Wombat and Exmouth Plateaus, although several unusual features accompany the boundary (Haq et al. 1990). Based on

nannofossil stratigraphy, the KPg boundary is place 8cm above a distinct color change in the nannofossil chalk separating upper Maastrichtian white chalk from highly burrowed pale-brown, clay rich chalk (Pospichal and Bralower 1992). In contrast, the peak iridium anomaly is only 1cm above the color change (Rocchia et al. 1992). The nannofossil KPg boundary is located at the contact of a drilling disturbance and appears to contain a thin layer of white, late-Maastrichtian colored chalk (Fig. 4 in Pospichal and Bralower 1992). This 8cm interval is suspect and could represent slumped early Danian sediments (R. Norris, per. comm.). Given the stratigraphic complexities, I do not attempt to make inferences about the Ba/Al in this interval, and instead compare Ba/Al from the late Maastrichtian white chalks to Ba/Al levels after the nannofossil KPg boundary. Oxic conditions are suggested by the presence of burrowing, stable downcore sulfate concentrations, and poor preservation of organic carbon (de Carlo 1992; Haq et al. 1990; Snowdon and Meyers 1992).

REFERENCES

BARKER, P. F., J. P. KENNETT, and E. AL. 1988. Site 690, p. 183-292. *In* P. F. Barker, J. P. Kennett and e. al. [eds.], Proc. ODP, Init. Repts., 113. Ocean Drilling Program, College Station, TX.

BERGGREN, W. A., D. V. KENT, C. C. SWISHER, and M.-P. AUBRY. 1995. Geochronology, time scales and global stratigraphic correlation, SEPM Special Publication 54. SEPM, Tulsa.

BLEIL, U. 1985. The magnetostratigraohy of Northwest Pacific sediments, Deep Sea Drilling Project Leg 86, p. 441-458. *In* G. R. Heath, L. H. Burckle and e. al. [eds.], Init. Repts. DSDP, 86. U.S. Govt. Printing Office, Washington.

BOURBON, M. 1979. Petrographic and sedimentological study of the Cretaceous-Paleocene sequence of Hole 398D. *In* J. Sibuet, -C., W. B. F. Ryan and e. al. [eds.], Init. Repts. DSDP, 47 part 2. U.S. Govt. Printing Office, Washington.

BRALOWER, T., I. PREMOLI SILVA, M. J. MALONE, and E. AL. 2002a. Leg 198 Summary, p. 1-148. *In* T. Bralower, I. Premoli Silva and M. J. Malone [eds.], Proc. ODP, Initial Reports, 198. Ocean Drilling Program, College Station, TX.

---. 2002b. Site 1209, p. 1-102. *In* T. Bralower, I. Premoli Silva and M. J. Malone [eds.], Proc. ODP, Initial Reports, 198. Ocean Drilling Program, College Station, TX.

CHAMLEY, H., H. MAILLOT, and C. ROBERT. 1984. Paleoenvironmental history of the Walvis Ridge at the Cretaceous-Tertiary transition, from mineralogical and geochemical investigations, p. 685-690. *In* T. C. Moore, Jr., P. D. Rabinowitz and e. al. [eds.], Init. Repts. DSDP, 74. U.S. Govt. Printing Office, Washington.

DE CARLO, E. H. 1992. Geochemistry of pore water and sediments recovered from the Exmouth Plateau, p. 295-308. *In* U. von Rad, B. U. Haq and e. al. [eds.], Proc. ODP, Sci. Results, 122. Ocean Drilling Program, College Station, TX.

EMELYANOV, E. M. 1977. Geochemistry of sediments in the western central Atlantic, DSDP Leg 39. *In* P. R. Supko, K. Perch-Nielsen and e. al [eds.], Init. Repts. DSDP, 39. U.S. Govt. Printing Office, Washington.

EREBERG, P. K., and M. I. ABDULLAH. 1990. The diagenetic factors controlling the dissolved organic carbon (DOC) in pore water from deep sea sediments (ODP Leg 113, Weddell Sea). *In* P. F. Barker, J. P. Kennett and e. al. [eds.], Proc. ODP, Sci. Repts., 113. Ocean Drilling Program, College Station, TX.

HAMILTON, N. 1990. Mesozoic magnetostratigraphy of Maud Rise, Antarctica. *In* P. F. Barker, J. P. Kennett and e. al. [eds.], Proc. ODP, Sci. Repts., 113. Ocean Drilling Program, College Station, TX.

HAQ, B. U., U. VON RAD, and E. AL. 1990. Site 761, p. 161-211. *In* B. U. Haq, U. von Rad and e. al. [eds.], Proc. ODP, Initial Reports, 122. Ocean Drilling Program, College Station, TX.

HEATH, G. R., L. H. BURCKLE, and E. AL. 1985. Site 577, p. 91-137. *In* G. R. Heath, L. H. Burckle and e. al. [eds.], Init. Repts. DSDPP, 86. U.S. Govt. Printing Office, Washington.

HUFFMAN, A. R., J. H. CROCKET, N. L. CARTER, P. E. BORELLA, and C. B. OFFICER. 1990. Chemistry and mineralogy across the Cretaceous/Tertiary boundary at DSDP Site 527, Walvis Ridge, South Atlantic Ocean, p. 319–334. *In* V. L. Sharpton and P. D. Ward [eds.], Global catastrophes in earth history: An

interdisciplinary conference on impacts, volcanism and mass mortality. GSA Special Paper 247.

KENNETT, J. P., and L. D. STOTT. 1988. Proteus and Proto-Oceanus: ancestral Paleogene oceans as revealed from Antarctic stable isotopic results, ODP Leg 113. *In* P. F. Barker, J. P. Kennett and e. al. [eds.], Proc. ODP, Sci. Repts., 113. Ocean Drilling Program, College Station, TX.

KUMAR, N., L. A. P. GAMBOA, B. C. SCHREIBER, and J. MASCLE. 1977. Geological history and origin of São Paulo Plateau (Southeastern Brazillian Margin), comparison with the Angolan Margin and the early evolution of the Northern South Atlantic, p. 927-945. *In* P. R. Supko, K. Perch-Nielsen and e. al [eds.], Init. Repts. DSDP, 39. U.S. Govt. Printing Office, Washington.

MAILLOT, H., and C. ROBERT. 1984. Paleoenvironmental evolution of the Walvis Ridge deduced from inorganic geochemical and clay mineralogical data, Deep Sea Drilling Project Leg 74, Southeast Atlantic, p. 663-683. *In* T. C. Moore, Jr., P. D. Rabinowitz and e. al. [eds.], Init. Repts. DSDP, 74. U.S. Govt. Printing Office, Washington.

MEYERS, P. A., and B. R. T. SIMONEIT. 1990. Global comparisons of organic matter in sediments across the Cretaceous-Tertiary boundary. Organic Geochemistry **16:** 641-648.

MONECHI, S. 1985. Campanian to Pleistopcene calcareous nannofossil stratigraphy from the Northwest Pacific Ocean, Deep Sea Drilling Project Leg 86, p. 301-336. *In* G. R. Heath, L. H. Burckle and e. al. [eds.], Init. Repts. DSDP, 86. U.S. Govt. Printing Office, Washington.

MOORE, T. C., JR., P. D. RABINOWITZ, and E. AL. 1984a. Site 527. *In* T. C. Moore, Jr., P. D. Rabinowitz and e. al. [eds.], Init. Repts. DSDP, 74. U.S. Govt. Printing Office, Washington.

MOORE, T. C., JR., P. D. RABINOWITZ, P. E. BORELLA, N. J. SHACKLETON, and A. BOERSMA. 1984b. History of the Walvis Ridge. *In* T. C. Moore, Jr., P. D. Rabinowitz and e. al. [eds.], Init. Repts. DSDP, 74. U.S. Govt. Printing Office, Washington.

PERCH-NIELSEN, K., P. R. SUPKO, and E. AL. 1977. Site 356: São Paulo Plateau, p. 141-230. *In* P. R. Supko, K. Perch-Nielsen and e. al [eds.], Init. Repts. DSDP, 39. U.S. Govt. Printing Office, Washington.

POSPICHAL, J. J., and T. BRALOWER. 1992. Calcareous nannofossils across the Cretaceous/Tertiary boundary, Site 761, Northwest Australian margin. *In* U. von

Rad, B. U. Haq and e. al. [eds.], Proc. ODP, Sci. Results, 122. Ocean Drilling Program, College Station, TX.

ROBERT, C., and H. MAILLOT. 1990. Paleoenvironments in the Weddell Sea area and Antarctic climates, as deduced from clay mineral associations and geochemical data, ODP Leg 113, p. 51-70. *In* P. F. Barker, J. P. Kennett and e. al. [eds.], Proc. ODP, Sci. Repts., 113. Ocean Drilling Program, College Station, TX.

ROCCHIA, R. and others 1992. Iridium and other element distributions, mineralogy, and magnetostratigraphy near the Cretaceous/Tertiary Boundary in Hole 761C, p. 753-762. *In* U. von Rad, B. U. Haq and e. al. [eds.], Proc. ODP, Sci. Results, 122. Ocean Drilling Program, College Station, TX.

RYAN, W. B. F., and E. AL. 1979. Site 398. *In* J. Sibuet, -C., W. B. F. Ryan and e. al. [eds.], Init. Repts. DSDP, 47 part 2. U.S. Govt. Printing Office, Washington.

SIMONEIT, B. R. T., and H. R. BELLER. 1985. Lipid geochemistry of the Cretaceous/Tertiary boundary sediments, Hole 577, Deep Sea Drilling Project Leg 86, p. 671-674. *In* G. R. Heath, L. H. Burckle and e. al. [eds.], Init. Repts. DSDP, 86. U.S. Govt. Printing Office, Washington.

SLITER, W. V. 1977. Cretaceous benthic foraminifers from the western South Atlantic Leg 39, Deep Sea Drilling Project, p. 657-697. *In* P. R. Supko, K. Perch-Nielsen and e. al [eds.], Init. Repts. DSDP, 39. U.S. Govt. Printing Office, Washington.

SMIT, J. 1999. The global stratigraphy of the Cretaceous-Tertiary boundary impact ejecta. Annual Review of Earth and Planetary Sciences **27:** 75-113.

SNOWDON, L. R., and P. A. MEYERS. 1992. Source and maturity of organic matter in sediments and rocks from sites 759, 760, 761, and 764 (Wombat Plateau) and sites 762 and 763 (Exmouth Plateau), p. 309-315. *In* U. von Rad, B. U. Haq and e. al. [eds.], Proc. ODP, Sci. Results, 122. Ocean Drilling Program, College Station, TX.

STOTT, L. D., and J. P. KENNETT. 1990. The paleoceanographic and paleoclimatic signature of the Cretaceous/Paleogene boundary in the Antarctic: stable isotopic results from ODP Leg 113, p. 829-848. *In* P. F. Barker, J. P. Kennett and e. al. [eds.], Proc. ODP, Sci. Repts., 113. Ocean Drilling Program, College Station, TX.

THOMAS, E. 1988. Late Cretaceous through Neogene deep-sea benthic foraminifers (Maud Rise, Weddell Sea, Antarctica). *In* P. F. Barker, J. P. Kennett and e. al. [eds.], Proc. ODP, Init. Repts., 113. Ocean Drilling Program, College Station, TX.

---. 1990. Late Cretaceous through Neogene deep-sea benthic foraminifers (Maud Rise, Weddell Sea, Antarctica), p. 571-594. *In* P. F. Barker, J. P. Kennett and e. al. [eds.], Proc. ODP, Sci. Repts., 113. Ocean Drilling Program, College Station, TX.

VON RAD, U., N. F. EXON, and B. U. HAQ. 1992. Rift-to-drift history of the Wombat Plateau, Northwest Australia: Triassic to Tertiary Leg 122 results, p. 765-800. *In* U. von Rad, B. U. Haq and e. al. [eds.], Proc. ODP, Sci. Results, 122. Ocean Drilling Program, College Station, TX.

WRIGHT, A. A. and others 1985. Summary of the Cretaceous/Tertiary Boundary studies, Deep Sea Drilling Project Site 577, Shatsky Rise, p. 799-804. *In* G. R. Heath, L. H. Burckle and e. al. [eds.], Init. Repts. DSDPP, 86. U. S. Govt. Printing Office, Washington.

ZACHOS, J. C., and M. A. ARTHUR. 1986. Paleoceanography of the Cretaceous/Tertiary Boundary event: inferences from stable isotopic and other data. Paleoceanography **1:** 5-26.

ZACHOS, J. C., M. A. ARTHUR, R. THUNELL, D. F. WILLIAMS, and E. J. TAPPA. 1985. Stable isotope and trace element geochemistry of carbonate sediments across the Cretaceous/Tertiary Boundary at Deep Sea Drilling Project Hole 577, Leg 86, p. 513 - 532. *In* G. R. Heath, L. H. Burckle and e. al. [eds.], Init. Repts. DSDPP, 86. U.S. Govt. Printing Office, Washington.